5-2003

Oxygen Delignification Kinetics and Selectivity Improvement

Steven M. Violette

OXYGEN DELIGNIFICATION KINETICS AND SELECTIVITY IMPROVEMENT

By

Steven M. Violette

B.S. University of Maine, 1994

A THESIS

Submitted in Partial Fulfillment of the

Requirements for the Degree of

Doctor of Philosophy

(in Chemical Engineering)

The Graduate School

The University of Maine

May, 2003

Advisory Committee:

Adriaan van Heiningen, Professor of Chemical Engineering, Advisor

Barbara Cole, Professor of Chemistry

Raymond Fort, Professor of Chemistry

Joseph Genco, Professor of Chemical Engineering

John Hassler, Professor of Chemical Engineering

LIBRARY RIGHTS STATEMENT

In presenting this thesis in partial fulfillment of the requirements for an advanced degree at The University of Maine, I agree that the Library shall make it freely available for inspection. I further agree that permission for "fair use" copying of this thesis for scholarly purposes may be granted by the Librarian. It is understood that any copying or publication of this thesis for financial gain shall not be allowed without my written permission.

Signature: Sara M. Vale

Date: 5-1-2003

OXYGEN DELIGNIFICATION KINETICS AND SELECTIVITY IMPROVEMENT

By

Steven M. Violette

Thesis Advisor: Dr. Adriaan van Heiningen

An Abstract of the Thesis Presented
in Partial Fulfillment of the
Requirements for the Degree of
Doctor of Philosophy
(in Chemical Engineering)
May, 2003

Pulp strength loss during oxygen delignification is caused by cellulose chain cleavage resulting from attack by oxygen-based radicals generated through reactions with lignin. The objective of this research was to improve the lignin-to-cellulose selectivity during oxygen delignification by using radical-scavenging polymeric additives that adsorb on the cellulose surfaces where protection from radicals is needed. Among the polymers evaluated were starch, carboxymethyl-cellulose, galactomannan, xylan, and glucomannan.

Oxygen delignification experiments were conducted on Northeast softwood Kraft pulps at different temperatures, sodium hydroxide charges, reaction times, and pretreatments. The effect of polymer additives on the selectivity and kinetics was studied. Polymer adsorption on pulp was measured by sugar analysis using high performance anionic exchange chromatography.

It was determined that increasing alkali charge between 1.5 % and 5.0 % sodium hydroxide decreases the selectivity of oxygen delignification, and that an increase in temperature from 90 °C to 120 °C does not significantly affect the selectivity. The observed Kappa number changes were corrected for alkali extraction in the absence of oxygen. The corrected Kappa number change was shown to be proportional to the number of cellulose chain scissions, confirming that the cellulose degradation is directly related to oxygen-mediated reactions. Kinetic equations were developed for the rate of change of Kappa number and cellulose chain scission. The alkali consumption was found to be linearly related to the change in Kappa number.

Significant increases in lignin-cellulose selectivity were observed for galactomannan and glucomannan as the adsorbed additives, with significant improvements at charges as low as 0.3 % added on pulp. At 2.0 % galactomannan or glucomannan on pulp, the selectivity improvement was about 30 % to 40 %. None of the other polymers tested gave results as favorable. The selectivity improvements were found to increase linearly with the amount of adsorbed polymer additive. This supports the hypothesis that the adsorbed additives on cellulose provide a protective barrier.

Lastly, extended delignification up to 65 % Kappa number reduction was successfully achieved by using high temperature, extended reaction time, and split NaOH addition to keep the alkali concentration low throughout two- and multi-stage delignification experiments.

ACKNOWLEDGEMENTS

Dr. van Heiningen: Thank you for your support, guidance, and patience.

Thesis advisory committee:
Dr. Cole
Dr. Fort
Dr. Genco
Dr. Hassler

Financial Support and Donations:
University of Maine Pulp and Paper Foundation
Praxair, Inc.
International Paper

For your help: Guo Jun Kang, Yang Gao, Denilson da Silva Parez, Shawn Kelley, Amos Cline, Albert Co, Angel Hildreth, Cathy Dunn, Dan Jolicoeur, and Keith Hodgins.

All Graduate students, Faculty, and Staff.

Special thanks to my family and friends for their support and encouragement, especially Mom, Dad, and Anne Marie.

TABLE OF CONTENTS

LIST OF TABLES

LIST OF FIGURES

Chapter 1

INTRODUCTION

1.1. PULPING AND BLEACHING

Wood fibers consist of four major chemical components: cellulose, lignin, hemicellulose, and extractives. In pulp manufacture, it is necessary to remove the lignin and extractives from the wood, leaving primarily the fiber's polymer carbohydrates, cellulose and hemicellulose. The pulping process is used to break down wood or other cellulosic materials into the individual fibers. The majority of pulps manufactured throughout the world are produced by chemical means, of which the most predominant method is the Kraft pulping process. Kraft pulping uses a cooking liquor containing sodium hydroxide and sodium sulfide, and it has become a favorable process because it produces relatively strong fibers and because pulping chemicals and energy are recycled from the byproducts. During the Kraft process and other methods of chemical pulping, extractives are removed and the lignin content of the wood is also reduced considerably. The product of the pulping process is known as brown stock, because of the color of the fibers.

Following pulping, the bleaching process is used to remove from the brown stock the majority of the remaining lignin and other trace compounds called chromophores, which cause coloration of the fibers. Fully bleached, or "white", pulps are then produced. Chemicals that have been used for bleaching include, but are not limited to, chlorine dioxide, sodium hydroxide, hydrogen peroxide, oxygen, and ozone. In recent

decades, environmental concerns have heightened interest in non-chlorine bleaching processes, among which is oxygen delignification.

1.2. OXYGEN DELIGNIFICATION

Oxygen delignification is the process by which the pulp, suspended in an alkaline solution, is pressurized with oxygen in a vessel wherein the lignin will react with various oxygen species until it dissolves and can be removed from the pulp with the spent liquor solution. This process has become predominant in modern pulp bleaching plants over the last few decades, and it will continue its growth as an essential part of most elementally and totally chlorine-free bleaching sequences. The growth of this process is illustrated in Figure 1.1, which shows the world-wide production of oxygen–delignified pulp growing from less than 10,000 tons per day in 1975 to over 120,000 tons per day by 1995 (Dence and Reeve, 1996). Used to remove a significant portion of lignin (40-70%) remaining in brown stock pulp, the major advantage of oxygen delignification is the chemical cost savings realized by displacing the use of chlorine dioxide, hydrogen peroxide, or ozone by the cheaper oxygen and caustic (Dence and Reeve, 1996). Other benefits of replacing these traditional bleaching chemicals with an oxygen stage include lower emissions of chlorinated waste and the ability to recycle the filtrate to the recovery furnace. The disadvantages of oxygen delignification are the capital cost and its lower selectivity of lignin removal versus cellulose degradation compared to chlorine dioxide bleaching. The cellulose degradation leads to weaker pulp fibers and thus has limited commercial single stage delignification to about 50%. When used to replace the later part of Kraft pulping, oxygen delignification has the advantage of higher yield and

selectivity, and reduction in the output of odorous sulfur compounds. If the selectivity of oxygen delignification bleaching is improved, then it may be used even more extensively to replace the other means of lignin removal. Presently, most mills have the oxygen delignification system follow directly after the washing sequence of the brown stock and before the pulp goes to the bleaching operation.

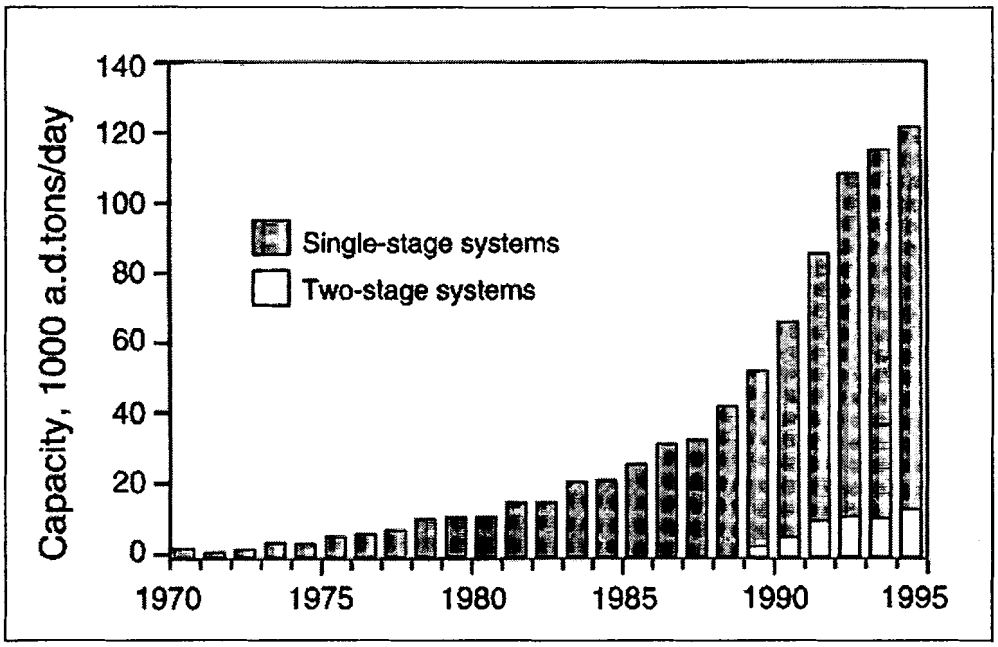

Figure 1.1. Growth of oxygen delignification (Dence and Reeve, 1996)

1.3. OBJECTIVE AND SCOPE OF THESIS

Many researchers have reported on the basic kinetics of oxygen delignification and have improved the selectivity by manipulation of process variables or by affecting the chemistry. Several different chemical groups have been studied as additives in the oxygen delignification process, as discussed in chapter 2 of the thesis, which summarizes the literature. However, there has been very little work done with polymeric additives,

the area of focus for this thesis. The objective of this investigation is to improve the selectivity of oxygen delignification as much as possible, by any new or combination with existing technologies, so that this can be implemented in the industrial setting. It is also important to explore the effects of important process conditions on the kinetics and selectivity of oxygen delignification. This preliminary work is detailed in chapters 4 and 5, following the description or our experimental methods in chapter 3. Chapter 6 details the results of our investigation with polymeric additives. Chapter 7 outlines the statistical treatment of experimental data, determination of mathematical models to formulate results, and evaluates our ability to predict oxygen delignification behavior from these models. Extended and multi-stage oxygen delignification results are presented in Chapter 8, in which findings of the previous chapters are incorporated to achieve selective process options for extended delignification. Chapter 9 summarizes the conclusions and recommendations of this research.

Chapter 2

LITERATURE REVIEW

2.1. OXYGEN DELIGNIFICATION PROCESS

Medium consistency oxygen delignification is typically carried out with either softwood or hardwood pulps using sodium hydroxide as an alkali source (1 to 4 percent NaOH on pulp, or 0.025 to 0.1 N at 10 % pulp consistency) and pressurized with 400 kPa to 1000 kPa oxygen. Three phases are present in the reaction vessel: the solid pulp fibers, the aqueous phase around the fibers and within the fiber pores, and the gas phase of oxygen bubbles distributed throughout the mixture. The pulp, at 8 to 12 % solids, is heated to 80 °C to 120 °C, and retention times of 15 to 90 minutes are usually achieved by the use of an up-flow tower.

Key parameters in the commercial process are the temperature, caustic charge, and the degree of mixing for efficient mass transfer of the oxygen (McDonough, 1986; Bennington and Pineault, 1999). In a typical laboratory reactor, the mixing is applied constantly and there is a large excess volume of gaseous oxygen surrounding the pulp. In contrast, commercial reactors have only dispersed gas bubbles of varying size distributed throughout the reactor, so the pre-mixing is much more important in the mill. With adequate oxygen contact, the extent of delignification is mostly dependent on the alkali charge, temperature, and time of reaction. Oxygen concentrations are usually sufficient with partial pressures of only few atmospheres (300 kPa), but delignification may be hindered if the bubbles are not distributed well.

The selectivity of lignin reactions to cellulose-degrading reactions is of utmost importance in the oxygen process, and it is mostly affected by the temperature and alkali charge, although it becomes lower when extending the reaction time to achieve very low lignin contents. High temperatures (above 100 °C) and increasing alkali charge have a negative impact on the selectivity, particularly towards the end of the delignification (McDonough, 1986; Irabarne and Schroeder, 1997). The degradation of the cellulose within the fibers is caused by oxygen radicals generated through lignin reactions and the reduction of oxygen species during the process (Gratzl, et al., 1992; Gierer, et al., 1989; Guay, et al., 1999).

2.2. OXYGEN SPECIES CHEMISTRY

Several oxygen-containing species are present during oxygen delignification. Figure 2.1 shows the step-wise reduction of oxygen as described by Gratzl and coworkers (1992). Furthest to the left is diatomic oxygen, which is reduced into the hydroperoxide radical ($HOO^{\bullet}$). During this reduction, oxygen reacts as an electrophile and extracts an electron, as it does from the phenoxy-anion on the lignin molecule, for example. The hydroperoxide radical can be dissociated into a proton and the superoxide anion radical ($^{\bullet}O_2^-$), shown beneath the hydroperoxide radical. The next step in the reduction is the formation of hydrogen peroxide, which dissociates into a proton and the hydroperoxide anion (HOO^-). When further reduced, water and the hydroxyl radical ($HO^{\bullet}$) are formed. The last step in the reduction is the formation of another water molecule.

According to the pKa values given in the diagram, at a typical oxygen delignification pH around 12, the superoxide anion radical, the peroxide molecule and its

conjugate base, and the hydroxyl radical and its conjugate base are all present in appreciable concentrations when this reduction reaction take place. It is widely believed that radicals are responsible for carbohydrate degradation, and studies have shown that the hydroxyl radical cleaves the glycosidic linkage (Gierer, et al., 1996; Guay, et al., 1999).

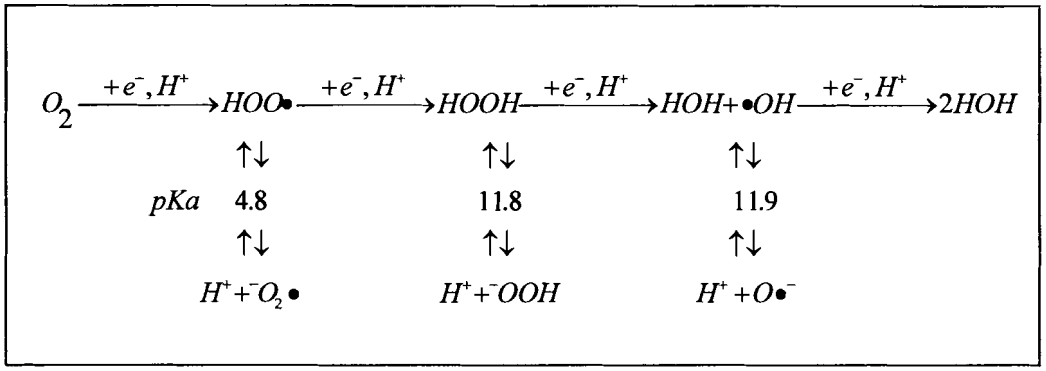

Figure 2.1. Step-wise reduction of oxygen (Gratzl, et al., 1992)

2.3. CHEMISTRY OF LIGNIN REACTIONS

Lignin is a large and complex polymer that is difficult to analyze because it must be broken down to remove it from wood, so the structure is mostly theorized from the analysis of the products. At the stage of lignin removal during oxygen delignification, many of the original structures and bonds are still present in the residual lignin. Researchers use phenolic rings, biphenolic structures, and compounds like guaiacol, syringaldehyde, and veratraldehyde as model compounds to represent the lignin (Argyropoulos and Liu, 2000; Hausman, 1999). A typical lignin component is shown in Figure 2.2 under electrophilic attack. This may be achieved with the oxygen compounds shown in the top row of Figure 2.1. Once the radical is produced on the phenolic hydroxyl oxygen, resonance structures may shift the radical to the ortho- and para-

positions relative to the carbon containing the hydroxyl group. These radicals have now become new sites available for electrophilic attack of an oxygen molecule, which results in bridging, ring opening, and then formation of carboxylic acid and ester groups. Eventually, when the lignin undergoes a few of these steps, its aromatic structure breaks down and the number of hydrophilic oxidized groups increases; so the lignin fragments become water-soluble and can be removed from the pulp. Also, when the initial resonance structure moves to a carbon on an alkene side chain, oxygen will attack the radical, bridge to the adjacent carbon, and cleave the carbon-carbon linkage, leaving two carbonyl groups and eliminating part of the side chain. These reactions happen in succession as long as there are available electron-rich sites on the lignin.

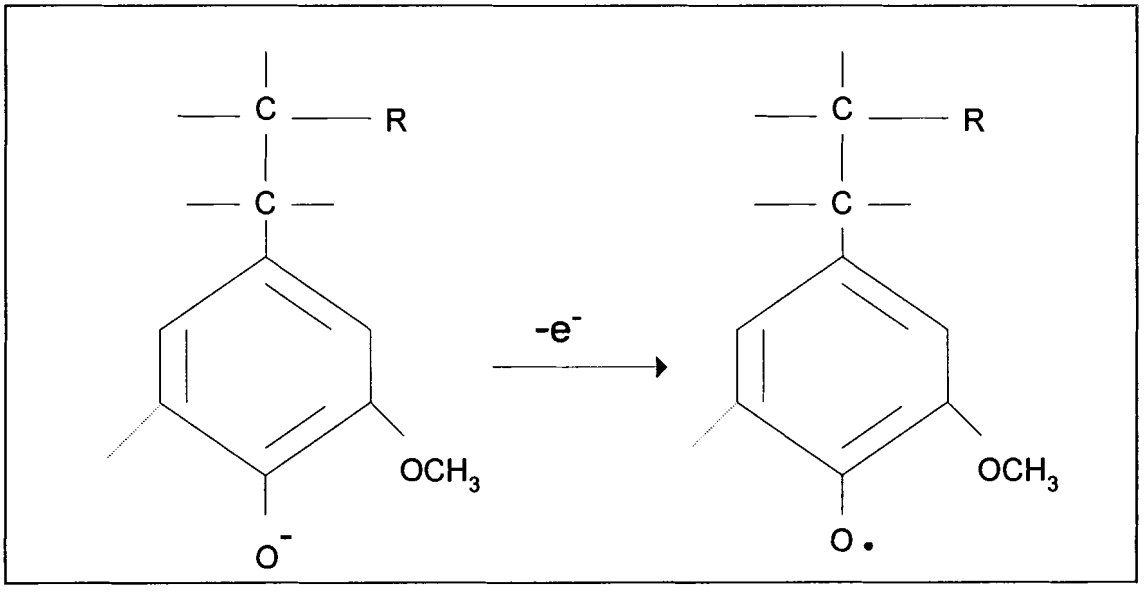

Figure 2.2. Electrophilic attack on a model lignin compound (McDonough, 1992)

2.4. CHEMISTRY OF CELLULOSE DEGRADATION

While the oxygen species undergo the reactions with lignin mentioned above, the reduction path in Figure 2.1 is followed and the various radicals are formed, such as the

highly reactive and non-selective hydroxyl radical. Another mechanism for forming the hydroxyl radical is via hydrogen peroxide and the Fenton Mechanism (Fenton, 1894), as shown below. The first half of this reduction-oxidation reaction forms the hydroxyl radical, which is induced by the presence of transition metals (M) native to the pulp, such as manganese, iron, or copper.

$$H_2O_2 + M^{n+} \rightarrow HO^- + HO^\bullet + M^{n+1}$$

$$^\bullet O_2^- + M^{n+1} \rightarrow M^n + O_2$$

(Fenton, 1894)

Transition metals with lower oxidation states are more likely to undergo this reaction. Once the radicals are formed, they may react with the carbohydrates and cleave the glycosidic linkages of the carbohydrates. Figure 2.3, outlined by Guay and coworkers (Guay et al., 1999), proposes one mechanism for the degradation of methyl-β-D-glucose. According to this study, the electrophilic attack is on the anomeric carbon, and the presence of methanol and β-D-glucose in the product mixture confirmed that the glycosidic linkage was cleaved.

Another mechanism for the glycosidic cleavage of cellulose models by hydroxyl radicals was proposed by Geirer and coworkers (1989). Regardless of the mechanism involved, the model compound studies show that the hydroxyl radical is a likely contributor to the degradation of the cellulose in the pulp during oxygen delignification.

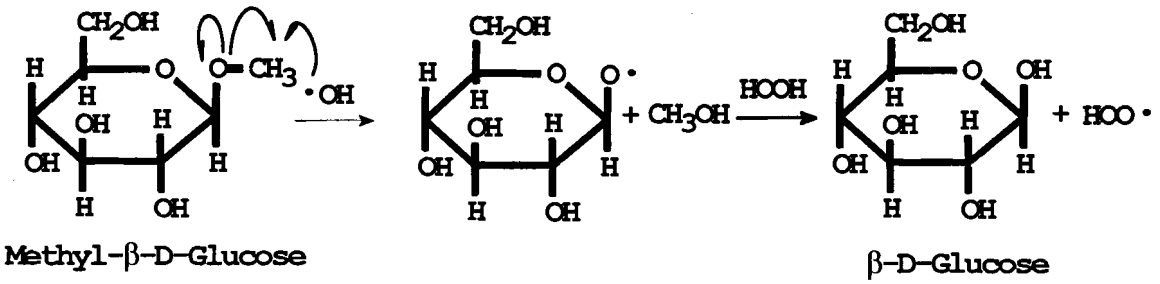

Figure 2.3. Proposed mechanism for the cleavage of a model cellulose compound (Guay, et al., 1999)

2.5. SELECTIVITY OF OXYGEN DELIGNIFICATION

The selectivity of oxygen delignification at a specific moment may be defined as the ratio of the rate of lignin reactions to the rate of carbohydrate reactions, dL/dM, where L is the lignin concentration remaining in the pulp and M is the molecular weight of the cellulose. Since this is difficult to measure experimentally, it is more common to express a ratio over a longer reaction time and with more practical measures such as the Kappa number decrease replacing the decrease in lignin content, and the viscosity change or degree of polymerization (DP) change for the cellulose degradation. One such expression is $\Delta K/\Delta V$ (Kang et al., 1998), where K is the Kappa number and V is the Tappi viscosity.

Since there is a more direct correlation between intrinsic viscosity, $[\eta]$, and the DP of cellulose, it is more beneficial to measure the intrinsic viscosity and then to convert it to DP. The correlation between intrinsic viscosity and DP is typically expressed by the Mark-Houwink-Sakurada equation (Evans and Wallis, 1989), given in the chapter on experimental methods. For this study, we will use the following expression for selectivity:

$$S = \text{Selectivity Parameter} = \frac{\Delta K}{\left(\frac{1}{DP_t} - \frac{1}{DP_0}\right)} \qquad (2\text{-}1)$$

where DP_t is the calculated cellulose DP at time t and DP_0 is the calculated cellulose DP of the untreated pulp. It is not too difficult to show that the numerator of this expression is a weight-based estimate of the lignin content change, while the denominator is the number of chain scissions per glucose unit, another weight based estimate. Exact definitions of these commonly used measurements are given in the chapter on experimental methods. This is the best measure of cellulose degradation we have since it gives a measure of the number of cleavages of the glycosidic linkages per monomer unit of cellulose. Another advantage of this measurement is that S can be measured as the slope of a selectivity plot of ΔK versus $(1/DP_t - 1/DP_0)$. A second variation of this selectivity parameter is obtained by using the chain scission number (CSN) as described by Gendron and coworkers (2002):

$$\text{Chain scission number} = \text{CSN} = \left(\frac{1}{DP_t} - \frac{1}{DP_0}\right) \cdot DP_0 \qquad (2\text{-}2)$$

To express selectivity based on chain scission number, Equation 2-1 then would contain CSN in the denominator instead of $(1/DP_t - 1/DP_0)$. The only difference between these two measurements is that $1/DP_t - 1/DP_0$ is based on the number of linkages in the cellulose polymers, and the CSN is based on the number of cellulose polymer chains.

2.6. KINETICS AND PROCESS VARIABLES

In an effort to optimize the effectiveness and selectivity of oxygen delignification, many kinetic studies have been documented (Irabarne and Shroeder, 1997; Olm and Teder, 1979 and 1981; Hsu and Hsieh, 1988; Perng and Oloman, 1994; Agarwal, et al., 1996). Both one and two region mathematical models have been proposed. The general expressions for the reaction rates are shown in Figure 2.4. Included here are the rates for lignin concentration, L, and molecular weight of the cellulose, M. The major variables are temperature, oxygen pressure, and alkali charge. The exponents found in each investigation are listed in Table 2.1. In this table, five studies are outlined. The exponents for the cellulose degradation were not all determined (Olm and Teder, 1981; Agarwal, et al., 1996; Hsu and Hsieh, 1988), and a couple of studies describe the delignification in two phases, initial and final delignification. Also, it should be noted that the lignin reaction orders listed as 1.0 in the table (Irabarne and Shroeder, 1997; Olm and Teder, 1979) were assumed for the models and not experimentally determined.

$$\frac{dL}{dt} = k_0 \cdot \exp\left(\frac{E_1}{RT}\right) \cdot Po_2^{\alpha} \cdot \left[OH^-\right]^{\beta} \cdot L^{\psi}$$

$$\frac{dM}{dt} = k_1 \cdot \exp\left(\frac{E_2}{RT}\right) \cdot Po_2^{\kappa} \cdot \left[OH^-\right]^{\chi} \cdot M^{\theta}$$

Figure 2.4. Kinetic expressions for oxygen delignification

Table 2.1. Summary of kinetic studies, listing determined exponents

	Lignin Removal Reaction				Cellulose Cleavage Reaction			
	$[OH^-]$ exponent	$[O_2]$ exp.	Kappa Exp.	Activation energy, kJ/mol	$[OH^-]$ exp.	$[O_2]$ exp.	M(MW) exp.	Activation Energy, kJ/mol
Olm and Teder (1979)	I 0.1 F 0.3	0.1 0.2	1 1	10 45	0.2 0.6	0.8 0.1	0 0	40 53
Olm and Teder (1981)	0.6	0.5	3.2					
Hsu and Hsieh (1988)	I 0.8 F 0.7	0.4 0.7	3.1 3.1	36 71				
Perng and Oloman (1994)	0.4	0.5	4.8	60	0.7	2.1	-5.3	94
Iribarne and Schroeder, (1997)	I 1.2 F 0.3	1.3 0.2	1 1	67 40	0.3	0.4	0	78
Agarwal, et al., (1999)	0.92	0.53	7.7	107.2				

Although many discrepancies exist in these results, some commonalities are evident. All the studies listing activation energies for the lignin and cellulose reactions show larger values for the cellulose reactions, suggesting that as temperature is increased the relative degree of cellulose degradation increases. Secondly, with the exception of the initial phase of delignification in the study by Irabarne and Shroeder (Iribarne and Shroeder, 1997), the hydroxyl exponent is higher for the cellulose cleavage reaction than the lignin reaction. This supports the general idea that selectivity decreases with increasing alkali concentration. The discrepancy of the finding of Iribarne and Shroeder may be caused by the initial extraction of some soluble lignin rather than by oxygen reactions. This phenomenon, which is the principle of the alkaline extraction stage in a bleach plant, will be discussed along with the presentation of results in the current investigation. Another interesting question which will be pursued in the present work is whether temperature or alkali charge is more crucial to selectivity, because both the lignin and cellulose reactions increase with these variables.

The exponent for the lignin content, or Kappa number, is of particular interest because its observed value may indicate more than just reaction order. Some studies listed here found reaction orders higher than one for the Kappa number term (Hsu and Hsieh, 1988; Perng and Oloman, 1994, Olm and Teder, 1981). When Olm and Teder modeled their data with only one kinetic equation, the reaction order was determined as 3.2 (Olm and Teder, 1981), similarly to the order of 3.1 determined by Hsu and Hsieh (1988). In a paper published by Schoon, very high reaction orders with respect to lignin were found for several pulping and bleaching reactions of hardwood pulps (Schoon, 1982). The explanation proposed for this was that several different lignin species were reacting in parallel first-order reactions. The Schoon model was tested also in the study by Agarwal, and here a reaction order of 7.7 was found (Agarwal, et al., 1996). This is a more descriptive type of postulation in kinetic modeling, as opposed to assigning a reaction order to the model then determining coefficients, because the physical explanation is supported by the fact lignin does exist in several varying moieties (McDonough, 1986; Olm and Teder, 1979). Also, these studies support that hardwood pulps may have more lignin moieties and hexeneuronic acids (Zou, 2002) than softwood pulps, since the results from experimenting with hardwoods rendered the highest reaction orders (Schoon, 1982; Agarwal, et al., 1996).

2.7. TWO STAGE DELIGNIFICATION

The kinetic data can be used when optimizing a commercial operation, first by controlling the temperature and alkali charge, and also by designing two separate physical stages of delignification at different conditions in succession. To take advantage

of the postulated changes in kinetics observed in different phases of the delignification, such configurations have been tested in mills. One example of two-stage delignification being employed to extend lignin removal and to maximize selectivity was the Oxy-Trac process described by some researchers for softwood pulp (Brewster and Justason, 1999), and based on the results by Iribarne and Schroeder (1997). The best results were observed using a short 20-minute first stage at a high oxygen pressure and a low temperature followed by a longer 60-minute second stage under a lower pressure and higher temperature. The temperature was adjusted from 83 °C to 98 °C between stages, and the pressure was lowered from 116 psig to 61 psig oxygen. This was done because the kinetics showed a higher temperature dependence for the cellulose reactions than the lignin reaction in the initial phase, and because the exponent for the oxygen concentration in the kinetic expressions of Irabarne and Shroeder (1997) in Table 2.1 for the cellulose reaction was smaller than that for the lignin reaction in the initial phase, but not in the final phase. All the alkali was charged before the first stage.

Not all two-phase concepts employ the same conditions as this configuration, because some are based on contradicting results and some are just installed for extending the delignification without much optimization of variables to maximize selectivity. Another example of a two-stage delignification system was installed in a mill to extend the oxygen delignification to realize savings on chlorine dioxide (Miller et al., 1999). Although the primary purpose of this work was not to maximize selectivity, the practice of split caustic addition was used and found to be beneficial to Kappa number reduction. Over the last several decades, similar control strategies for pulping chemicals have led to the so-called modified cooking processes.

2.8. INFLUENCE OF METALS CONTENT ON SELECTIVITY

The effects of transition metals on the selectivity during hydrogen peroxide bleaching have been documented by several sources (Bouchard et al., 1995; Li et al., 2000; Gullichsen et al., 1997; Presley et al., 1996). Removal of manganese and iron from the pulp by chelation with DPTA (diethylene triamine pentaacetic acid) or EDTA (ethylene diamine tetraacetic acid) or by acid washing have resulted in better selectivity during the subsequent peroxide bleaching. Since oxygen delignification also produces hydrogen peroxide and the same oxygen radicals, the same effect on the selectivity would be expected.

It is unclear whether both iron and manganese have the same effect of promoting radical formation and cellulose degradation, because some sources have actually found higher selectivity with the presence of manganese (Abrahamsson and Samuelson, 1975; Manouchehri and Samuelson, 1977), particularly when interacting with magnesium added to the pulp (Gevert et al., 1997; Samuelson and Ojteg, 1995). One reason for the addition of magnesium is that the metals removal techniques decrease the presence of all the metals in the pulp, not just the manganese or the iron. The efficiency of these techniques varies widely depending on the amount of metals found in the original pulp and the conditions used, such as pH, temperature, and washing techniques. But in general, manganese is more easily removed via chelation with DPTA or EDTA at a pH of 5 to 6 than is iron (Bouchard et al., 1995; Li et al., 2000). While it is difficult to remove more than 50 % of the iron with chelation, manganese levels will decrease anywhere from 30 % to 90 % under the same conditions.

Studies have also shown that both iron and manganese levels can be brought to much lower levels using acid washing (1.5 to 3 pH) and displacement techniques. For example, pulps at 50 to 150 ppm iron may only be chelated to 30 to 50 ppm iron, but a subsequent acid wash may bring levels to around 15 to 20 ppm. And pulps with manganese levels of 140 to 250 ppm may be brought to 10 to 30 ppm by chelation, but they may also be brought to levels below 3 ppm using acid washing (Bouchard et al., 1995; Li et al., 2000). Although very low pH levels (1.5 to 3) were used in these lab studies, typically mills do not go lower than 3 pH during acid washing.

In oxygen delignification, selectivity improvements have also been observed following metals removal (Gevert, et al., 1997; Sjogren and Hook, 2000; Brown and Dawe, 1996). In one paper (Sjogren and Hook, 2000), pretreatment with DPTA at 90°C and 5.5 pH led to a viscosity improvement of 40 mL/g intrinsic viscosity (940 mL/g versus 900 mL/g), which corresponds to a Tappi viscosity improvement around 3.5 cp; but the Kappa number reduction was 41.5 % versus 45 % for the control under the same conditions. In the same paper, the chelation stage (Q) was followed by an acid wash stage at 1.5 pH (QA). This resulted in a viscosity improvement of 50 mL/g and also at a higher Kappa number reduction of 49 %. But it should be noted that the pretreatments alone reduced the Kappa number and the viscosity by 6 % and 30 to 50 mL/g respectively. Acid washing was mostly responsible for the viscosity decrease during pretreatments, as the chelation stage has very little effect on the cellulose. This is because acid hydrolysis becomes appreciable at a pH lower than 3 and temperatures above 80 to 90 °C. Considering this and the physical equipment and chemicals required to do the pretreatments, the improvements seem quite modest. Most studies employing

chelation and acid washing show similar improvements in the delignification, as do preliminary results in the current investigation. Presently, there are not many commercial processes using chelation and acid treatments prior to oxygen delignification, but chelation has been used extensively in peroxide bleaching.

Commercially, the most common additive to oxygen delignification is magnesium sulfate (Robert et al., 1968). Although this additive's effectiveness is attributed to interactions with metals as well, it is discussed in the next section because it is added to the oxygen reactor and not as a pretreatment.

One other metal control strategy of significance is pretreatment with nitrogen dioxide (Yethon et al., 1980). Dozens of other papers have been published detailing the work in this area. The use of about 2 % NO_2 at 80 °C for 20 minutes followed by washing resulted in a manganese and magnesium removal of up to 95 % and also modified the lignin so that it was removed more rapidly (Gevert et al., 1997). Then following oxygen delignification, the viscosity was improved as much as 100 mL/g from the control, while the pulp was delignified from 30 to 5 Kappa number. However, in order to achieve the improvement of the pretreated pulp, higher temperatures (110 to 135 °C) and alkali charges (7 %) were used; and the process also resulted in significant formation of methanol and yield loss. Further modification of these pretreated pulps was achieved by adding manganese sulfate (up to 1000 ppm manganese), which also resulted in viscosity improvements up to 100 mL/g under milder conditions (Gevert et al., 1997). As mentioned earlier, this also suggests that the presence of manganese may be beneficial for pulp quality following oxygen delignification under certain conditions.

2.9. SELECTIVITY IMPROVEMENT WITH CHEMICAL ADDITIVES

Magnesium is the most common additive to oxygen delignification, and was patented in 1968 by Robert and others using magnesium carbonate (Robert et al., 1968). Today, many processes employ the use of Epsom salt ($MgSO_4$) to increase the levels of magnesium in the pulp, because it is cheap and equally effective. It has been published that the charge of magnesium needed is based on the magnesium/manganese ratio (Samuelson and Ojteg, 1994), and should be at least 10:1. For example, a pulp with 100 ppm manganese should contain 1000 ppm magnesium, or roughly 0.2 % magnesium sulfate. It should also be noted that not all manganese in pulp is considered harmful, as discussed earlier, and this may depend upon its oxidation number, i.e. Mn^{2+} or Mn^{4+}.

While some pulps show only modest improvements by the addition of magnesium during oxygen delignification, other studies have shown more significant improvements (Brown and Dawe, 1996; Samuelson and Ojteg, 1994). Brown and Dawe (Brown and Dawe, 1996) found improvements in the percent Tappi viscosity loss to be as high as 10 % out of 34 % with a charge of 0.5 % $MgSO_4$. Samuelson and Ojteg (1994) found a viscosity improvement of 70 to 80 mL/g by varying the Mg:Mn ratio from 8:1 to 16:1, or 0.4 % addition of magnesium, which roughly corresponds to 0.9 % magnesium sulfate. The mechanism of selectivity improvement by the addition of magnesium is believed to be an ion exchange in the magnesium hydroxide precipitate formed under alkaline conditions (Liden and Ohman, 1997). The transition metal in the 2+ redox state is shown undergoing such a transition below:

$$\mathbf{xMg(OH)_2 + yMn^{2+} + 2yH_2O \longrightarrow}$$

$$\mathbf{xMg(OH)_2 + yMn(OH)_2 + 2yH^+}$$

This conversion renders the metal less available to catalyze the degradation of hydrogen peroxide by the Fenton mechanism.

Another additive for oxygen delignification is hydrogen peroxide (Sjogren and Hook, 2000; Parthasarathy et al., 1989). Hydrogen peroxide accelerates the breakdown of lignin, just as it does in peroxide bleaching. And depending on the metals present in the pulp, a selectivity improvement has also been noticed. Parthasarathy and others (Parthasarathy et al., 1989) observed an increase in lignin removal from 61 % to 73 %, accompanied by a decrease in Tappi viscosity loss of 1.5 cp, or about 18 to 20 mL/g while adding 0.5 % H_2O_2. Since most cellulose protecting mechanisms also inhibit the lignin removal, this was considered a significant selectivity improvement. Similar results were observed by Sjogren and Hook (Sjogren and Hook, 2000). When hydrogen peroxide was added to pulp which had been chelated and acid-washed, and they saw a viscosity improvement of 40 to 50 mL/g with the addition 1.5 % H_2O_2 and 0.2 % $MgSO_4$. But without the addition of the magnesium, they noticed a greater viscosity loss of 20 to 50 mL/g. This further confirms the belief that the addition of peroxide to oxygen delignification is ineffective without metals control.

The next group of chemical additives for improved selectivity is radical scavengers, compounds whose reactivity towards the oxygen radicals is higher than that of the oxygen radicals towards the carbohydrates. This group includes alcohols, poly-alcohols, aldehydes, and organic acids. Colodette and Santos de Campos (1993) found that when added to the delignification, ethanol increased the final viscosity and the percent delignification. At a 10 % ethanol charge on pulp and 1.5 % sodium hydroxide, the viscosity was improved 1.5 cp (20 mL/g) over the control experiment while the

delignification increased from 45.5 % to 47.9 %. And at 80 % ethanol on pulp and 2.5 % NaOH, the viscosity was improved 2 cp (25 mL/g) while the delignification increased from 45.5 % to 47.3 %. At a lower NaOH charge (1.5 %), the viscosity improvement was higher by 2 to 3 cp, but the delignification remained the same or decreased half a percent.

A similar group of radical scavengers tested for oxygen selectivity are poly-alcohols (e.g. ethylene glycol). Solinas and Proust (1997) found that when added to oxygen delignification, a charge of 10 % ethylene glycol on pulp gave a viscosity improvement of 3 cp (38 mL/g) at a Kappa number of 10. And at the same Kappa number and a 70 % ethylene glycol charge, the viscosity increase was 6 cp (75 mL/g). Similar results were reported for propylene glycol. It is unlikely, however, that these compounds would be compatible with the oxygen process, and the charges are prohibitively large for profit without some recovery scheme.

The next group of radical scavengers that has been investigated is aldehydes. Swan and Gustavsson (Swan and Gustavsson, 1977) patented the addition of formaldehyde using very high viscosity pulps (originally 146 cp). When a charge of 0.9 % formaldehyde was added to delignification with 4 % NaOH, a viscosity of 59 cp was observed, compared to the control batch with a viscosity of 40 cp; but the delignification was reduced from 57 % lignin removal to 50 % lignin removal. When a higher charge of formaldehyde (2.4 %) was used with the same conditions, the viscosity was improved from 40 cp to 88 cp; but the delignification was hindered from 57 % to 45 %. Still, these results are appreciable. The same investigators tested methanol at 1 % under the same conditions for comparison. This experiment led to a viscosity of 43 cp,

but with a delignification of 71 %. No other results have been published using these two compounds.

The last group of radical scavengers included in this summary is the organic acid group. Young first patented sodium gluconate, the sodium salt of gluconic acid in 1960 (Young, 1960), for use in hydrogen peroxide bleaching. Other organic acids used in oxygen delignification are sodium sulfamate and polyaminocarboxylic acids (Payton et al., 1997). In this patent, no viscosity improvements were reported.

2.10. SODIUM GLUCONATE AS AN ADDITIVE

One paper published prior to this investigation deals with the addition of chemicals found in the oxygen delignification filtrate (Kang et al., 1998), such as muconic acid, glucose, methyl-β-D-glucopyranoside, sodium carbonate, and sodium gluconate. Some results from this investigation are summarized in Table 2.2. The most favorable results were found for sodium gluconate. The selectivity measurement, $\Delta K/\Delta V$, was reported as follows when a pulp with original viscosity of 30 cp and 30 Kappa number was delignified with 4 % NaOH, 0.2 % $MgSO_4$, 90 °C, and under 100 psig oxygen pressure for 2 hours.

The sodium gluconate results showed a significant viscosity improvement (4 cp) with very little effect on the degree of delignification (11.3 Kappa number compared to 11.1) using a relatively modest additive charge, 2.2 % on pulp. This compound is also compatible with the process and may potentially be obtained from black liquor, where it is present in abundance.

Table 2.2. Results of oxygen delignification recycling filtrate chemicals (Kang et al., 1998)

	Kappa	Viscosity(MPa·s)	ΔK/ΔV
Original Pulp	32.6	32.5	----
H_2O (control)	11.1	15.8	1.28
10% Glucose	26.5	27.3	1.17
10% MeOH	11.8	17.6	1.40
10% Ethylene glycol	12.4	18.3	1.42
10% Methyl-β-D-glucopyranoside	11.8	17.3	1.27
10% Muconic Acid	19.2	23.4	1.47
10% Gluconate	**11.8**	**21.2**	**1.84**
2.2% Gluconate	11.3	19.7	1.66
10% Gluconate	11.8	21.2	1.84
50% Gluconate	13.3	23.6	2.17
100% Gluconate	13.3	26.1	3.01
200% Gluconate	16.8	27.3	3.03

The reason why sodium gluconate gave such good results is probably because it works by two separate mechanisms, radical scavenging and the formation of metal complexes, thus lowering the catalytic effect of harmful transition metals such as iron (Sawyer, 1964). These two possible mechanisms are shown below in Figure 2.5. The first drawing shows the complexing between the iron and the electrons on the oxygen atoms in the gluconate. The second drawing shows the resonance stabilization for the radical after it is transferred to the gluconate carboxylic acid salt, which is why it is a good radical scavenger.

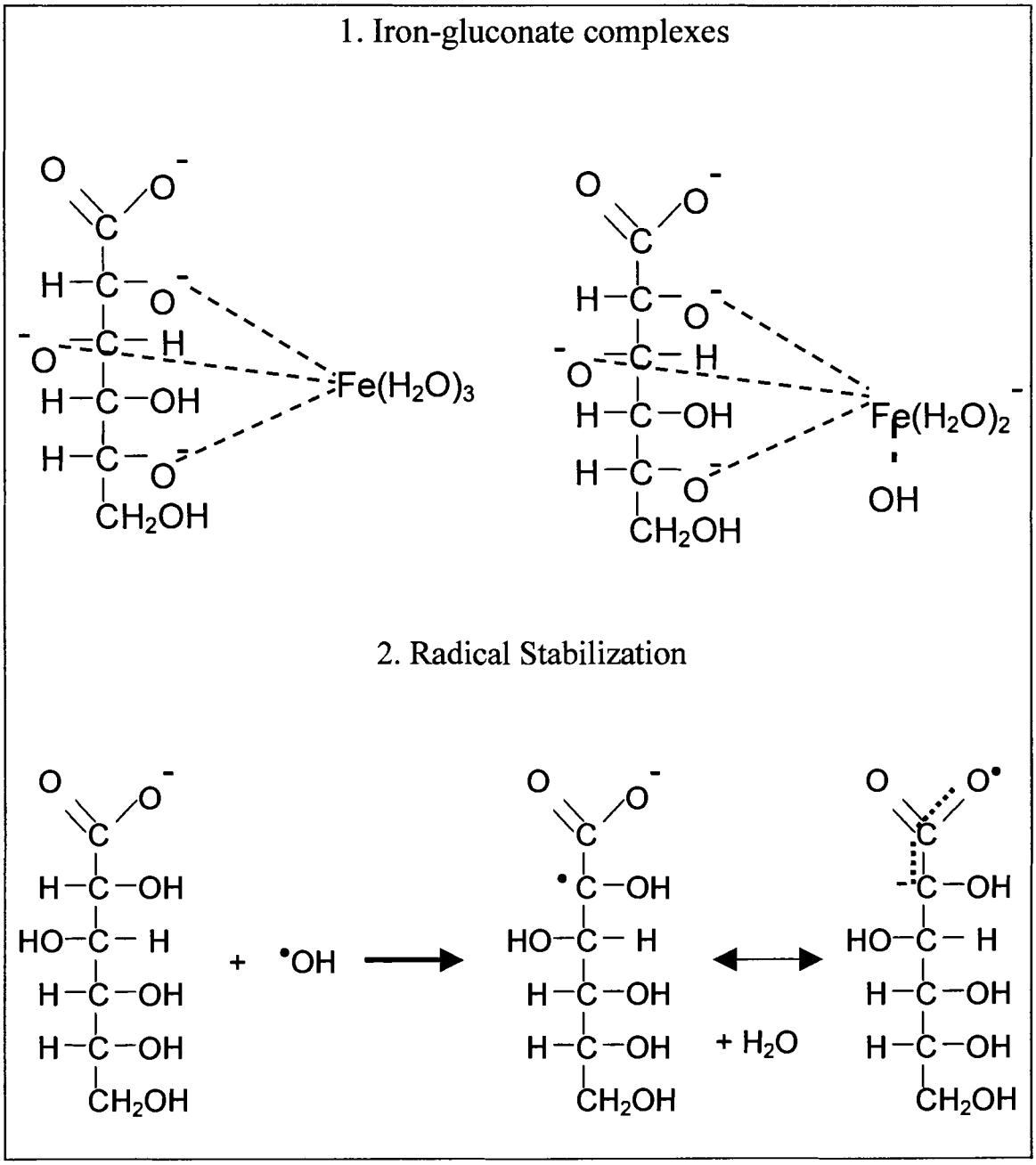

Figure 2.5. Mechanisms for sodium gluconate (Sawyer, 1964)

2.11. HYPOTHESIS OF THE INVESTIGATION

Even though sodium gluconate is an effective and compatible oxygen delignification additive, the benefits realized still may not be economically feasible because dosages of the additive needed are too high. The additive is soluble, and is therefore found everywhere in the aqueous media. However, the harmful radicals are created in the solid lignin near the cellulosic surfaces within the micro-pores and amorphous regions of the pulp. These radicals are very reactive, and therefore exist for a very short time and thus can diffuse only very short distances within the pulp or solution. Therefore, the radicals do not interact with the vast majority of the additive molecules, because most are not close to the pulp surface.

Hypothesis statement:

The hypothesis of the present investigation is that oxygen radicals may be trapped with relatively low amounts of additive radical scavengers if they are concentrated at the cellulosic surfaces, thereby acting as protective barriers for the cellulose.

Figure 2.6 depicts a physical representation of this scenario. The top picture represents a non-adsorbing additive and the bottom picture represents a polymeric additive adsorbed at the surface of the pulp. This may be achieved with polymeric carbohydrate polymers that adsorb on the cellulose and scavenge radicals, similarly to the gluconic acid salt. It would also be advantageous if these additives have the ability to form complexes with the metals. Furthermore, they should be resistant to oxidative chemistry, effective at a high pH, and have an appropriate molecular size to penetrate fiber pores, and be economical and compatible with the delignification and recovery processes.

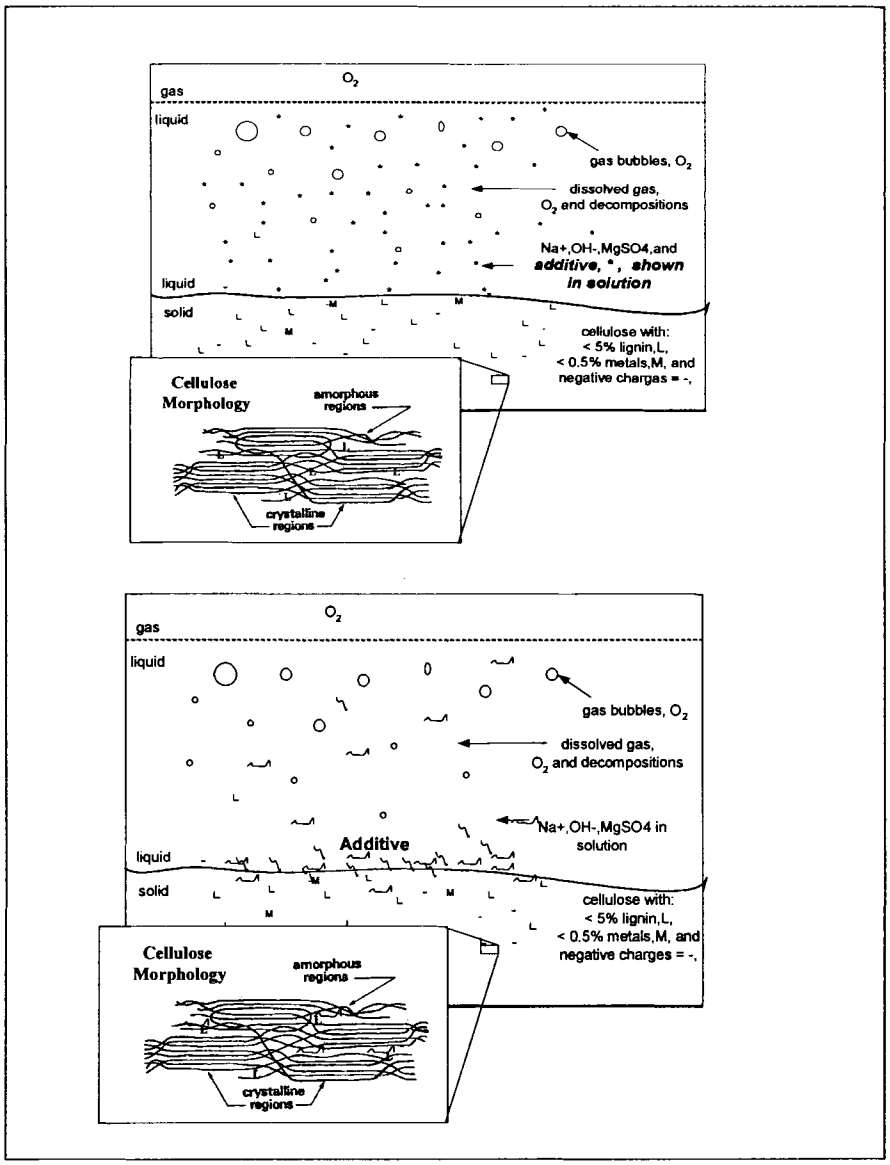

Figure 2.6. Representation of dissolved (top) versus adsorbed (bottom) additive on the pulp surface

2.12. CARBOHYDRATE POLYMERS WHICH ADSORB ON CELLULOSE

Our objective has been to determine if some polymers that both adsorb on pulp and scavenge oxygen radicals may be used in small amounts as additives to oxygen delignification. The advantage would come from the polymer's ability to concentrate at the pulp surface where the protection is needed, and therefore not much additive would be wasted in the bulk of the liquid solution. Although many criteria for the selection of these compounds were considered, the following introduction will focus primarily on the basic chemistry of the molecules, their solubility in alkaline aqueous media, and their ability to adsorb on cellulosic fibers. The basic chemistry of a polymer includes its repeat unit chemical structure, any other functional groups, and the molecular weight.

2.12.1. Starch

Starch comes from several abundant sources and is used extensively in papermaking, both as a wet-end additive and also for surface sizing. Being comprised of amylose and amylopectin, the linear and branched polymers of alpha-D-glucose, it adsorbs on pulp in the wet state and hydrogen bonds with cellulose when dried in a paper sheet as well. Starch's ability to interact with pulp fibers is enhanced by the addition of an alkyl amine, particularly a quaternary amine, etherified to the starch molecule. The cationic characteristic of the substituted group improves bonding to the anionic pulp surface in pulp slurry. Starch is not fully soluble in water, so it forms a viscous, cloudy suspension. The components, amylose and amylopectin, range up to 500,000 and above 5 million Daltons, respectively (Swinkels, 1985).

2.12.2. Carboxymethyl Cellulose

Carboxymethyl cellulose (CMC) is another carbohydrate polymer that adsorbs on pulp. Derived typically from spruce wood pulp, CMC is alkaline-steeped cellulose substituted with an ether linkage at any of the three available hydroxyls on the glucose ring, connected to a carboxy-methyl group (Gelman, 1987). This compound is usually sold as sodium carboxymethyl cellulose and is used extensively as a thickener industrially and also in foods. The degree of substitution, DS, of carboxymethyl groups on the CMC polymer is measured as the average number per glucose unit, so it can be as high as 3. The water solubility of CMC increases with increasing DS and solution pH. CMC with a DS less than 0.5 is only slightly water-soluble but may be dissolved in strong alkali (above 0.1 N NaOH). CMC's with a DS greater than 0.5 are water-soluble at room temperature, but they are viscous at very low solids content. Only the CMC's with a very high DS (>1.2) can be dissolved more than 2.0 % in water or alkali (Ullmann, 1989). The ability of CMC to adsorb on pulp decreases directly with its solubility in the aqueous phase.

2.12.3. Carbohydrate Gums

Other sugar-based gums such as hemicellulose and closely related polymers may also be readily adsorbed on pulp. Guar gum (galactomannan), xylan, and glucomannan are common examples of this class of branched polysaccharides. They are lower in molecular weight than cellulose and dissolve in water quite readily. Galactomannan, for example, dissolves slightly in water (less than 0.2 %) at room temperature, but it may be dissolved at 1 to 2 % in 0.5N NaOH. Similarly to the other polysaccharide polymers, the

gums' ability to adsorb on pulp increases with molecular weight and decreases with solubility (Rojas and Neuman, 1999). Galactomannan is a linear chain of β-linked mannan with one side unit of galactan, which is α-linked at the number 6 carbon of the mannan ring. The molecular weight of galactomannan may be 100,000 to 1,000,000 g/mole, and the ratio of mannan to galactan is roughly 2 (Rojas and Neuman, 1999). The major source for guar galactomannan is the guar bean, and it has been used as a wet-end papermaking additive for sheet drainage and internal bonding for decades, similarly to starch. Industrially, galactomannan is much more abundant than the other gums.

Glucomannan is extracted from the Konjac plant and is used as a dietary fiber supplement. It has the same structure as guar galactomannan, but with side units of Glucan. The adsorption of mannans such as galactomannan (GM) and galactoglucomannan (GGM) was studied by Hannuksela and Holmbom (2002). They found that the adsorption may be achieved to a high extent (1.5 % to 2 % by weight of substrate absorbed on softwood Kraft pulp), and that this adsorption is mostly in a monolayer. Xylan, the primary component of hardwood hemicellulose, may be extracted from birch wood.

Chapter 3

EXPERIMENTAL METHODS

3.1 OXYGEN DELIGNIFICATION REACTOR

Oxygen delignification experiments were carried out in a two-liter stainless steel Parr batch reactor (model 4530), equipped with back-to-back anchor stirrers and a 115 volt external electric mantle heater. The temperature control was achieved with a PID controller unit (Parr model 4843), also supplied by the Parr Instrument Company but manufactured by Watlow (model 982). A type J thermocouple located in the center and middle of the reactor was also supplied and calibrated by Parr instruments, which was removed and re-tested regularly throughout the experimentation. The temperature can be controlled to within 1 to 2 °C after reaching the operation temperature, but rarely deviates more than one degree C longer than 30 seconds. The time required to raise the temperature to 90 °C from room temperature was 1 to 4 minutes, depending on the timely loading of the pulp into the reactor during the heating period. This procedure was determined through trial-and-error, since the thermocouple reading cannot determine the mixture temperature prior to loading due to elevated wall temperatures. Typical experiments were at 90 °C and 780 kPa (100 psig) oxygen, but the temperature control worked effectively through the range 70 to 120 °C.

3.2. BASIC PULP MEASUREMENTS

Mixed northeast softwood Kraft brown stock pulps were obtained from Miramichi Ltd., Irving Ltd., and the International Paper (IP) Company. The consistency of the pulp,

or dry solids percentage, was measured gravimetrically using high consistency (about 33 % solids) samples that were above the saturation point of the fibers. The high consistency was used to minimize the effect of water within the pulp settling under gravity and causing moisture gradients during the sampling procedure. Following equilibration of the pulp overnight (minimum of 12 hours) in a sealed container, three samples weighing 10 to 15 grams were taken and weighed to the nearest ten thousandths of a gram. The weight measurements were repeated following drying overnight in an oven at 105 °C. The tolerance for the range of consistency measurement was 0.30 % consistency. Repeat measurements were conducted when the span from low to high values was more than 0.30 %. The standard deviation of the consistency measurement was determined at 0.07 %.

3.3. DELIGNIFICATION BATCHES AND WASHING

Oxygen delignification batches were conducted on pulp samples of weighing 30 grams oven dry as determined by sampling using the above consistency procedure and weighing the pulp mass. Then the pulp was made up to 10 % consistency with distilled, de-ionized water and appropriate chemicals or additives. The make-up water and chemicals were thoroughly kneaded into the pulp after each one was added. After oxygen delignification, the pulps were washed with the same water that has been distilled, de-ionized, and filtered, at about 1 % consistency. This was done twice subsequently and drained over a 200 mesh (79 micron hole diameter) polypropylene screen in a Buchner funnel. Each time the filtrate was poured back over the pulp mat to re-capture any fines in the filtrate.

3.4. PULP YIELD

The yield was determined by weighing the entire contents of the batch after it was mixed, pressed to high consistency, and equilibrated overnight (minimum 12 hours) as before. Another consistency determination was then performed exactly as before the delignification, the yield percent was equal to the mass before divided by the mass after times one hundred.

3.5. KAPPA NUMBER

The Kappa number of the pulp was used to estimate the lignin content, and was determined according to Tappi standard method T-236. This test measures the capacity of the pulp to be oxidized using a solution of potassium permanganate ($KMnO_4$); its units are milli-equivalents $KMnO_4$ consumed per 10 grams pulp. The lignin content of the softwood pulp ranging from 10 to 30 Kappa number may be estimated as follows: percent lignin in the pulp equals the Kappa number times 0.15 (Gendron, et al., 2002). The standard deviation of Kappa number has been determined at 0.13.

3.6. VISCOSITY AND DEGREE OF POLYMERIZATION

The viscosity of the pulp was used to estimate the molecular size or degree of polymerization (DP) of the cellulose within the pulp fiber. It is important since the fiber strength characteristics depend highly upon the cellulose DP. Both Tappi standard viscosity method and intrinsic viscosity were used in this investigation. Both measurements were determined by dissolving the pulp in cupriethylene diamine solution, and then measuring the elution times in a capillary viscometer at constant temperature. Tappi standard method T-230 was used to estimate the viscosity in centipoise. ASTM

designation D1795-62 was used to determine the intrinsic viscosity in mL/g. The standard deviation of the intrinsic viscosity measured was determined to be 16 mL/g.

Equations have been published to express the relation between Tappi and intrinsic viscosity. One such equation for wood pulp was reported by Sihtola and coworkers (1963) as follows: $[\eta] = 954 \log (\text{Tappi viscosity/cp}) - 325$ (in mL/g). In the present investigation, only the Tappi viscosity was measured initially. Later when converting to intrinsic viscosity, data were taken on the same pulp samples for both methods for a few months. Then a correlation of Tappi versus intrinsic viscosity was developed based on these results. Figure 3.1 shows these results when the intrinsic viscosity was plotted against the log of the Tappi viscosity for the IP mixed softwood brown stock pulp from the Androscoggin Mill in Jay, Maine. The equation for converting between Tappi and intrinsic viscosity for this pulp would therefore be:

$$[\eta] = 848 \log (\text{Tappi viscosity/cp}) - 265 \quad (\text{in mL/g}). \qquad (3\text{-}1)$$

For comparison, the graph also displays the previously mentioned correlation (Sihtola et al., 1963). From the data, a linear relationship was estimated over the range 700 to 1200 mL/g between an incremental change of Tappi and intrinsic viscosity by using: $\Delta([\eta], \text{mL/g}) = 12.5 \cdot \Delta(\text{Tappi viscosity, cp})$. This was measured by taking the slope of a line regressed through the plot of intrinsic versus Tappi viscosity, before the logarithm was taken. It was used only for estimations when evaluating viscosity changes.

The degree of polymerization of the pulp was estimated using the Mark-Houwink-Sakurada equation: $[\eta] = K_m \cdot M^a$. For the softwood pulp, the form published by Evans and Wallis (Evans and Wallis, 1989) was used. This was reported as follows:

$$[\eta] = 0.6061 \cdot DP^{0.90} \qquad (3\text{-}2)$$

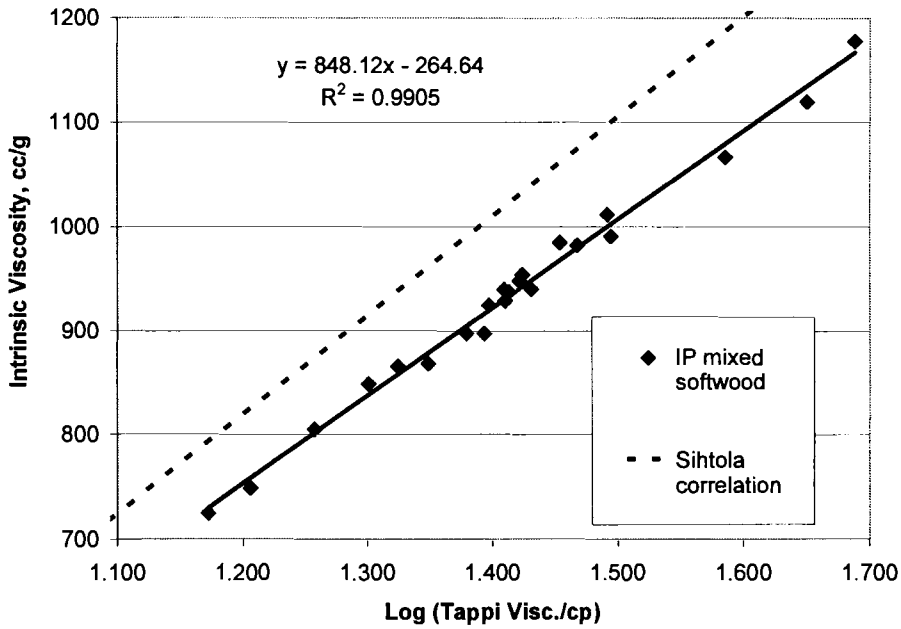

Figure 3.1. Correlation for the conversion between intrinsic and Tappi viscosity for IP softwood pulp

3.7. SELECTIVITY

Following the degree of polymerization, the selectivity parameter (S) was calculated as described in the literature review:

$$S = \frac{\Delta K}{\left(\frac{1}{DP_t} - \frac{1}{DP_0}\right)} \qquad (3\text{-}3)$$

The slope of the graph of ΔKappa versus the quantity $(1/DP_t - 1/DP_0)$, the chain scissions per monomer unit of the carbohydrate chain, was the selectivity parameter.

When plotting ($1/DP_t - 1/DP_0$) versus ΔKappa, the slope was the reciprocal of the selectivity parameter. The value of S was usually quite large, in the order of 10^4 or 10^5, because there are so many glucose units in a cellulose chain, making the denominator very small. An alternate form of S is the corrected selectivity parameter, S_C , in which the value ΔK_C is used instead of ΔK. As discussed in later chapters, ΔK_C is the corrected Kappa number change when it is corrected to include only the Kappa number change by oxygen mediated reactions rather than by alkali extraction.

3.8. ALKALI CHARGE

The alkalinity of a delignification batch was measured by filtering the liquor through a coarse paper filter to remove suspended particles, and then by titrating with the appropriate concentration of standard normality hydrochloric acid (HCl) to a pH of 7.0. An appropriate titration for this study was 30 mL filtered liquor titrated with 0.1 N HCl, since the alkalinity of the liquor was usually 0.03 N to 0.11 N. This was done so that the titrant volume was about 10 to 30 mL, a range accurately measured in a standard 50 mL burette. The sodium hydroxide charge remaining may be calculated with this result by converting normality to grams NaOH per grams water, and then multiplying by the liquid weight fraction of the slurry.

3.9. WET ZERO SPAN TENSILE STRENGTH

The wet zero span tensile strength test was a measure of individual fiber strength of paper, which was not affected by hydrogen bonding and fiber-to-fiber interactions present in dried paper. Tappi standard hand sheets were prepared according to standard preparation procedures, stored in a constant humidity and temperature room, and then

tested in accordance with TAPPI T273 pm-95 to determine the wet zero span tensile breaking length, Z. This test measures the load-bearing capability of wet fibers clamped with a zero gap length in a standard Pulmac tester at the moment of tensile failure. The test gives a good measurement of fiber strength loss when comparing the wet zero span measured before and after the bleaching process. Although refining was not expected to increase the wet zero span, some initial increase has been reported (Seth, 1999). It was found that some fibers contain crimps and kinks that were straightened during refining, thus increasing the wet zero span as much as 2 to 3 km.

The pulp delignified in this investigation was refined in a CPPA PFR mill with a 0.2 mm gap width at different number of revolutions, and the wet zero span was measured as shown in Figure 3.2. The refining did not appreciably increase the results at 4000 revolutions. Because of this and the demand for 24 grams of pulp for the refining procedure, any level of refining was considered unnecessary.

3.10. METALS CONTENT IN PULP

The metals content in the pulp was measured by inductively-coupled plasma atomic emissions spectroscopy (I.C.P.-A.E.S.) at Deering Hall in the Department of Soil and Environmental Sciences at the University of Maine. Measurements in milligrams of metal per kilogram dry pulp, or parts per million, were obtained for Mn, Fe, Cu, Mg, and Ca. Those were the metals contained in the pulp considered to have a potential impact on the experiments.

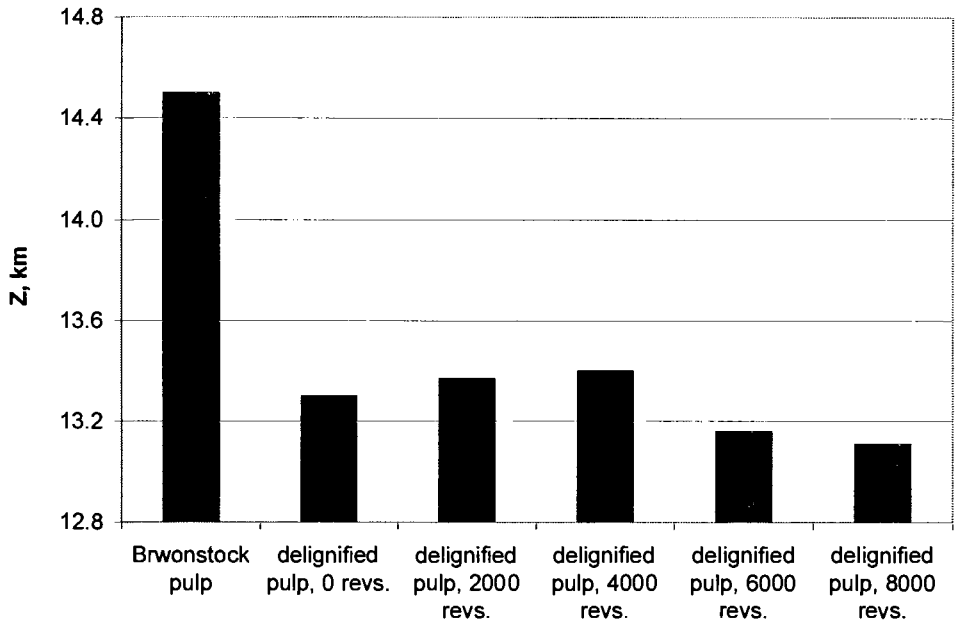

Figure 3.2. Effect of refining on wet zero span tensile strength (Z)

3.11. POLYMER MOLECULAR WEIGHT

Carbohydrate polymer molecular weight was estimated by gel permeation chromatography, a size exclusion technique. Samples of polymer additives were analyzed using this technique at the Limerick Pulp and Paper Centre at U.N.B. in Fredericton, New Brunswick. The analysis was done using pullulan standards ranging from 5900 to 788,000 Daltons. Pullulan, or polymaltotriose, is a linear polymer resembling cellulose that contains a known narrow molecular weight distribution. Although there are some differences in structure between the various polymers measured, such as degree of branching and repeat unit bond angles, the results are indicative of relative changes in molecular weight and degree of polymerization of such carbohydrate polymers.

3.12. POLYMER ADSORPTION ON PULP

3.12.1. Gravimetric Measurements

Polymer adsorption has been measured gravimetrically. Known amounts of the polymers to be adsorbed were added to pulp suspensions at different levels of addition while varying conditions like pH and consistency. The samples were sealed and equilibrated over time, then they were drained and the liquor was separated from the solid mass fraction. Determinations have been made based on the solids in the liquor compared with blank liquor samples without additives under identical conditions. The results have been verified by mass balance on the remaining solids. The objective was to measure the adsorption at high pH, as were the conditions during oxygen delignification. To obtain this with a minimum amount of reaction with the pulp, the equilibration was conducted without air or elevated oxygen pressure and at a moderate temperature of 60 °C. Since lignin and other materials were also partially extracted from the pulp at these conditions, results were subject to significant errors. At low levels of solutions solids, the extracted material weight was comparable to the weight of the polymer in the liquor. Moreover, the determination of equilibration times necessary was confounded by the increasing mass of extracted material from the pulp.

3.12.2. Ion Exchange Chromatography

The preferred method to measure the adsorption of the polymers on pulp was to analyze the composition after it underwent oxygen delignification. This was far better than simulating the oxygen delignification. The pulp was drained, washed, and processed in the same way as described previously, and then the sugar content of the solid pulp was

analyzed by hydrolyzing the carbohydrates and measuring the monosugars using High Performance Anion Exchange Chromatography (H.P.A.E.C.). The adsorption on pulp was calculated by comparing the appropriate monosugar concentrations in samples containing the adsorbed material with that of the control samples without the adsorbed materials. The adsorbed polymer was also analyzed separately. This method gave the permanently adsorbed amount of these carbohydrate polymers on pulp. Experiments were conducted under 100 psig oxygen pressure and under 100 psig nitrogen pressure. This was done to correct for lignin removal solely by alkaline extraction in oxygen delignification and to give adsorption data not influenced by the oxygen reactions.

In preparation for H.P.A.E.C., duplicate pulp samples were prepared by grinding air-dried pulp in a Wiley mill. Then the samples were extracted for 5 hours with 1-2-dichloromethane using 15 minute cycles through porous ceramic crucibles. Primary hydrolysis of 100 mg pulp samples in 1.50 mL of 72 % sulfuric acid was carried out at 30 °C for 1 hour. For the secondary hydrolysis, samples were diluted with 41 mL water and 1 mL solution containing the internal standard, 50 mg/mL fucose, then autoclaved at 120 °C for 2 hours. Following filtration through a 0.45 micron membrane, samples were made up to 50 mL in preparation for ion chromatography.

Duplicate samples were run in the chromatograph in accordance with the detailed operation procedures described in Appendix A. Six calibration solutions with known increasing monosugar concentrations encompassing the appropriate range needed for the pulp samples were run directly before and after the samples. These tests determined the relation between the internal standard and monosugar response for each sugar of interest. Plots and equations were determined for the monosugar-to-standard peak area ratio

versus monosugar-to-standard concentration ratio. Those calibrations were used to calculate the concentration of each monosugar present in the samples. Sample calibration graphs and equations are given in Appendix D (Figures D.1 to D.5). A reference pulp sample was also analyzed with each series as a further check on the operation of the instrument.

Chapter 4

EFFECT OF PULP ORIGIN AND COMPOSITION

In the initial part of this investigation, the basic response of the pulp to oxygen delignification under a standard set of process conditions was of primary interest. It was also important to determine how oxygen delignification is affected by the origin and composition of the pulp. Since the metal profile of the pulp and the use of chemical additives influences the response to oxygen delignification, these effects were also evaluated in this chapter. Chapter 5 focuses on the major process variables and how they affect oxygen delignification performed on pulp at a given composition.

4.1. STANDARD OXYGEN DELIGNIFICATION CONDITIONS

Initially, oxygen delignification batches were conducted at standard conditions chosen for this investigation. These conditions were selected to resemble typical conditions for a mill operation of oxygen delignification on softwood pulp. These standard conditions for the initial experiments were as follows: temperature of 90 °C held constant, oxygen pressure of 100 psig, 60 minutes reaction time, 10 % pulp consistency, sodium hydroxide charge of 4.0 % on pulp, and a magnesium sulfate charge of 0.2 % on pulp. Although the alkali charge of 4.0 % sodium hydroxide on pulp is somewhat higher than most mill operations, this charge was chosen to achieve a higher degree of lignin removal so that differences in results may be more noticeable.

In this chapter, basic experiments at 60 minutes reaction time were conducted on different pulps to compare results for lignin removal, cellulose degradation, and the

overall selectivity of treatments. An experiment conducted without chemical additives other than magnesium sulfate is referred to as a control reaction. In the few cases where the use of the magnesium sulfate was tested, the experiments in the absence of magnesium sulfate is referred to as the control experiment. Following the experiments comparing the basic control reactions with different pulps, experiments were evaluated using known chemical additives and pretreatments which were discussed in the literature review. The Kappa number reduction and calculated selectivity (S) are the two most important measurements used to evaluate the effectiveness of these treatments during typical 60-minute experiments. The following sections present the results of this initial phase of experimentation.

4.2. PULP ORIGIN

Initially, three different softwood pulps were evaluated. These pulps originated from Miramichi Ltd. and Irving Ltd. in New Brunswick (Canada), and from International Paper (IP) in Jay, Maine. The pulp properties are briefly described in Table 4.1. The pulp from IP is denoted "A" because it was the first of two similar pulps from that mill.

Table 4.1. Comparison of three softwood pulps (metals content by I.C.P.-A.E.S.)

	Kappa number	Tappi Viscosity, cp	Intrinsic Viscosity, mL/g	Mn (ppm)	Fe (ppm)	Cu (ppm)	Mg (ppm)
Miramichi	32.5	32.6	1120	219	10	0.5	240
Irving	24.6	29.4	1088	123	27.8	27.3	454
IP pulp A	26.7	44.7	1250	23.8	30.5	27.4	370

4.3. BASIC EXPERIMENTS WITH THREE SOFTWOOD PULPS

The pulps summarized in Table 4.1 were tested under standard conditions of oxygen delignification. The results are shown in Figures 4.1 to 4.4. Figure 4.1 shows the Kappa number reduction, which ranged from 50 % to 56 % lignin removal. The Miramichi pulp had the highest degree of lignin removal and the IP pulp had the lowest; but these responses were similar at same conditions as expected.

Figure 4.2 shows the loss of Tappi viscosity these pulps sustained during the delignification. Although the IP pulp had the highest viscosity loss (more than 20 centipoise), this may be expected because it had a very high initial viscosity compared to the other pulps. The Miramichi pulp lost the least viscosity, which indicates that pulp is the most selective of the three, since it also had the greatest Kappa number reduction.

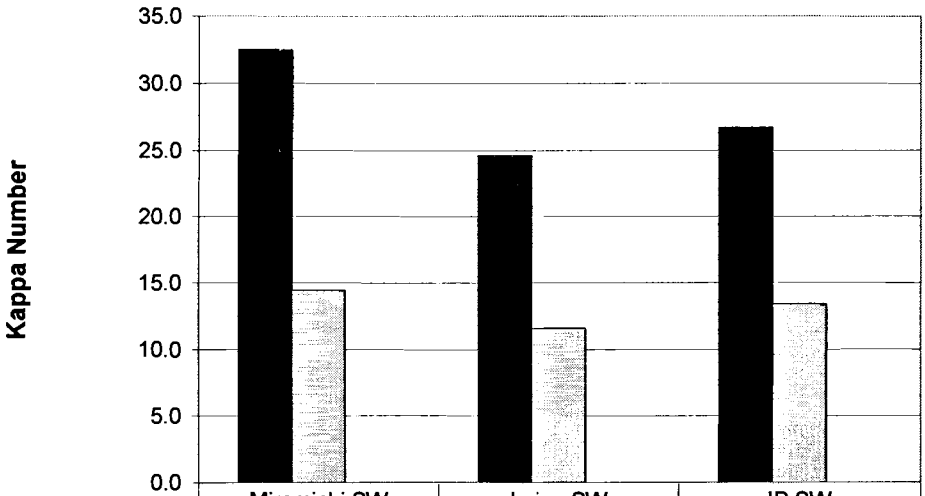

	Miramichi SW	Irving SW	IP SW
Initial	32.5	24.6	26.7
Final	14.4	11.6	13.4
% Reduction	55.7	52.8	49.8

Figure 4.1. Initial and final Kappa number of three softwood pulps undergoing 60 minutes oxygen delignification (standard conditions: 10 % consistency, 90 °C, 780 kPa oxygen pressure, 4.0 % NaOH on pulp, 0.2 % $MgSO_4$ on pulp)

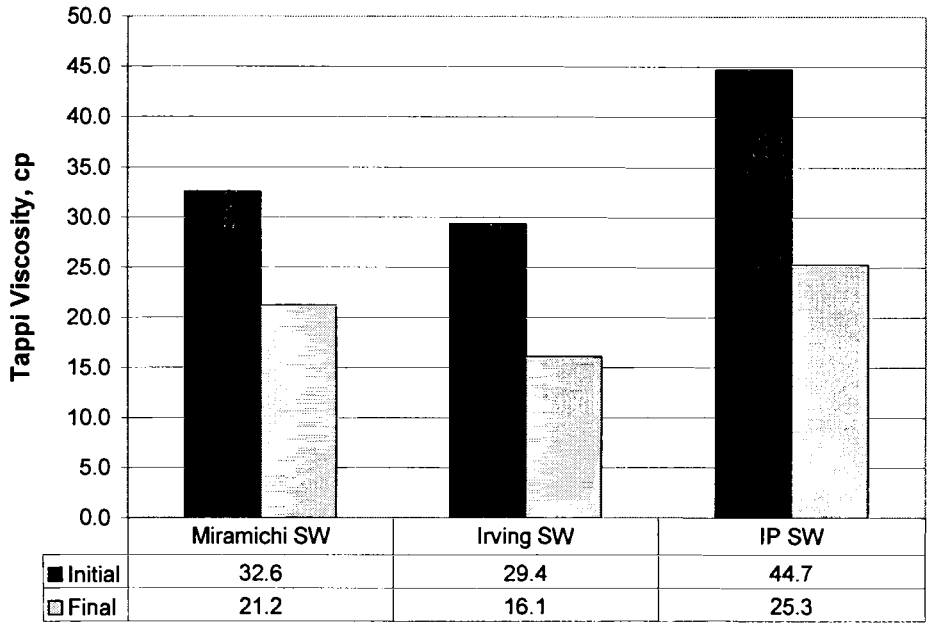

Figure 4.2. Initial and final Tappi viscosity of three softwood pulps undergoing 60 minutes of oxygen delignification (standard conditions)

Figure 4.3 shows the yield for these three experiments, plotted next to the maximum possible yield based on lignin removal. The difference between these two values is the undesirable yield loss, which only varies from 2.0 % to 2.5 % of the overall initial mass. This shows that although these pulps underwent varying degrees of cellulose degradation (evident from viscosity losses), it had little effect on the yield. This is because very little cellulose is lost from the fiber, due to random scission followed by peeling.

Figure 4.4 shows the selectivity as defined by equation 3-1 for these three experiments, compared to three experiments in which a charge of 2 % sodium gluconate on pulp was added to the delignification batches. These results show a higher selectivity for the Miramichi pulp under the control conditions as before. The difference in

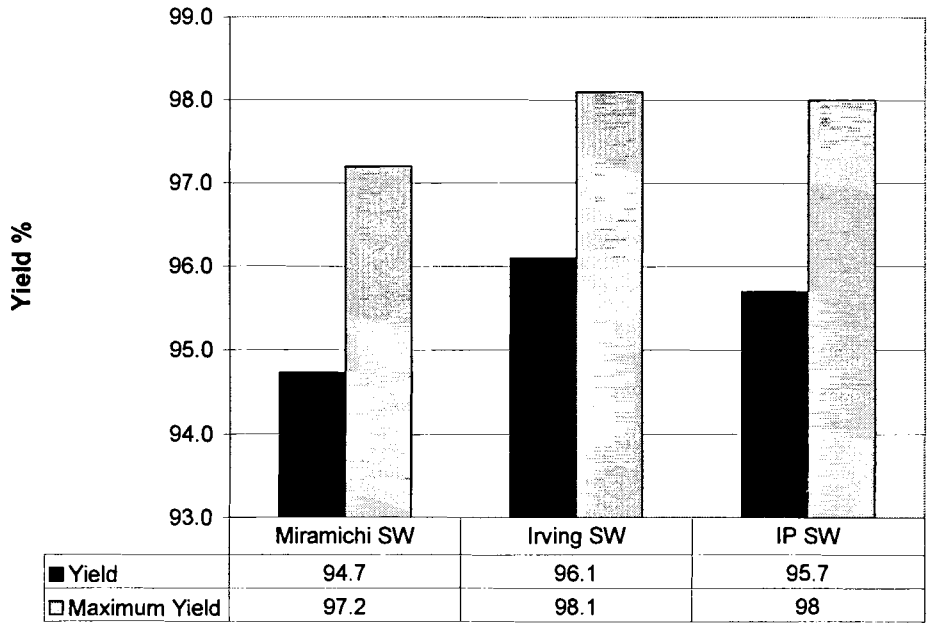

Figure 4.3. Yield percent of three softwood pulps undergoing 60 minutes oxygen delignification (standard conditions)

selectivity may be explained by the metals content in the pulps. Referring to table 4.1, the Miramichi pulp has high levels of manganese, but is much lower in iron and copper than the other two pulps. It is well known that iron is a promoter of hydroxyl radical formation (Fenton, 1894) and the viscosity loss during oxygen delignification has been shown to increase with iron content (Sjogren and Hook, 1999; Gevert, et al. 1997).

4.4. EFFECT OF SODIUM GLUCONATE ON SELECTIVITY

The benefit in selectivity from adding 2.0 % sodium gluconate to oxygen delignification may also be seen in Figure 4.4. This treatment appears to have a much larger impact with the Miramichi pulp, as the selectivity increased from 32 to 48 (x 10^4) for a 50 % increase. The gluconate only improved the selectivity of the other two pulps by 25 %. The over-abundance of iron and copper in these two pulps makes this additive

less effective. Since gluconate is also a complexing agent which forms weak bonds with metals (Sawyer, 1964), it may be more effective for low metal content pulps.

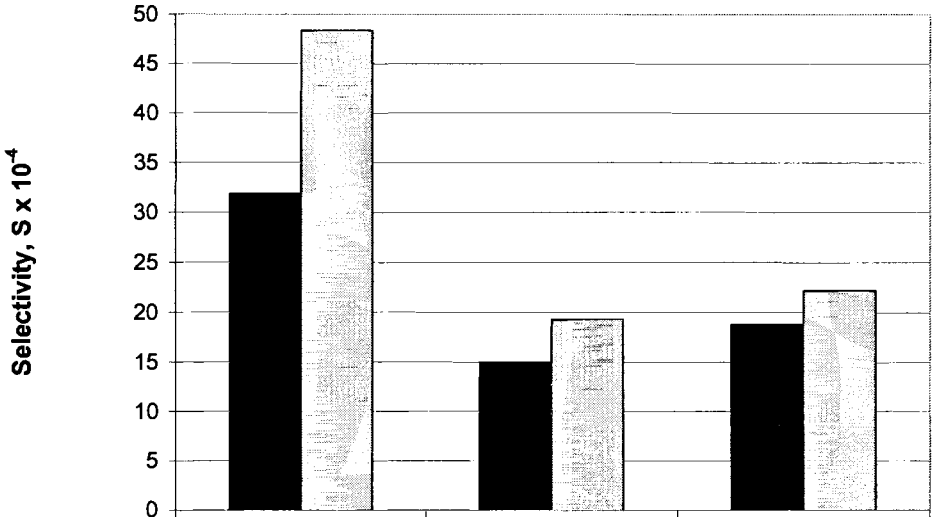

Figure 4.4. Selectivity (S x 10^{-4}) of three softwood pulps undergoing 60 minutes oxygen delignification, control and 2 % sodium gluconate (standard conditions)

4.5. EFFECT OF METALS REMOVAL BY CHELATION

It has already been shown that metals likely affect cellulose degradation and thus the oxygen delignification selectivity. In this section, experiments were conducted on pulps from which metals have been removed by chelation. Table 4.2 summarizes the chelation results on two of the previously mentioned pulps, Irving and IP pulp A. These two pulps were chelated under standard conditions which are given in the bottom of the table. Pulps that have undergone this treatment will be denoted "Q", as the typical pulp chelated with DTPA (diethylene triamine pentaacetic acid). The metals content before and after chelation pretreatment are given for both these pulps. It can be seen in Table 4.2 that at least 80 % of manganese and almost all the copper was removed, but

still more than half of the iron remains in the chelated pulp. The difficulty in removing iron by chelation compared to removing manganese and copper has also been previously documented (Bouchard, et al., 1995; Li, et al. 2000).

Table 4.2. Chelated pulp metals analysis (by I.C.P.-A.E.S.)

	Mn (ppm)	Fe (ppm)	Cu (ppm)	Mg (ppm)
Irving (untreated)	123	27.8	27.3	454
Irving (chelated)	13.1	16.1	< 3.0	280
IP (untreated)	23.8	30.5	27.4	370
IP A (chelated)	< 1.0	17.2	< 2.0	10 to 29
Conditions of chelation: 0.5 % D.T.P.A. on pulp, pH 5.0, 70 °C, 3.0 % consistency for 30 min., then washed twice with distilled, de-ionized water at 1 % consistency				

Figure 4.5 shows the selectivity of the original Irving pulp and the chelated Irving pulp (described in Table 4.2) undergoing different treatments followed by oxygen delignification. The chelated pulp is denoted with the "Q" again at the bottom of the graph. These results show appreciable increases in selectivity for chelation and gluconate addition, and modest improvements from $MgSO_4$. Combining the chelation and gluconate did increase the selectivity, but the increase is not as high as for the Miramichi pulp with the low metal content. These results clearly show that the removal of metals from the pulp leads to selectivity improvements. However, there are still unexplained influences on the selectivity related to the origin, and thus the composition, of the pulp.

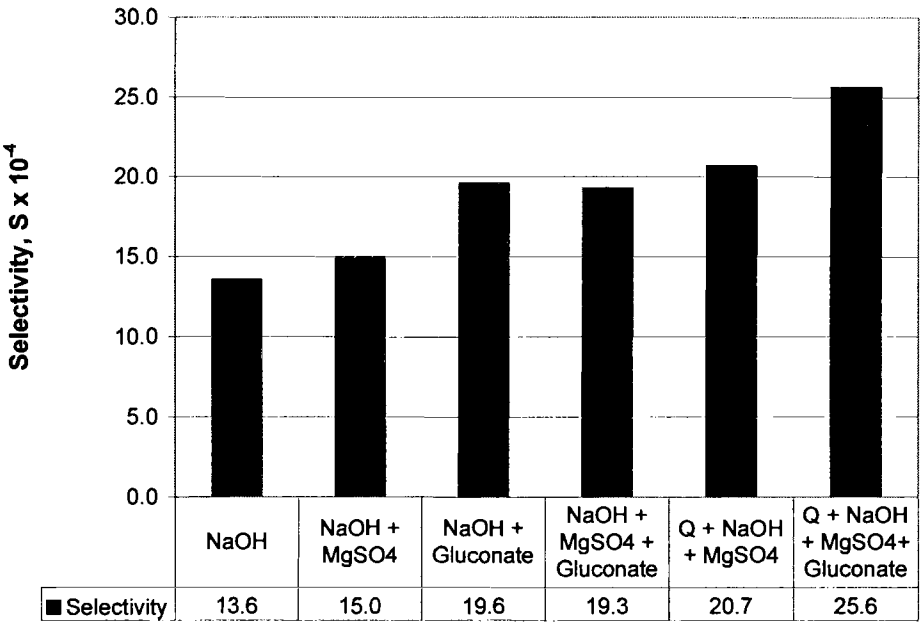

Figure 4.5. Selectivity results on Irving pulp after oxygen delignification for 60 min., with chelation pretreatment and basic additives (standard conditions)

4.6. CHELATION AND ACID WASHING

Table 4.3 below summarizes the metal content of different IP pulps, including one which was chelated, then acid treated, and then washed with distilled, de-ionized water for additional metals removal. These results show how additional removal is achieved for iron and magnesium, which are still appreciable after just chelation treatment. Conditions are also listed in this table. These pulps were then oxygen delignified under the same conditions as discussed earlier. These results in Figure 4.6. show almost the same behavior as Figure 4.5 for the Irving pulp. With the IP pulp, appreciable increases in selectivity were observed for the chelation pretreatment and the gluconate addition, but there was no additive effect. In fact, the selectivity decreased slightly. The acid pretreatment also did not improve the process beyond the chelation.

Sjogren and Hook (2000) had better results from the use of both these pretreatments in combination but the improvements are still modest in comparison with chelation or gluconate addition only.

Table 4.3. Properties of IP pulp A with and without chelation and acid treatment

IP Pulp	Pretreatment Conditions	Kappa #	Visc. cc/g	Mn ppm	Fe ppm	Cu ppm	Mg ppm
Untreated	None	26.7	1133	23.8	30.5	27.4	370
Chelated (Q)	pH 5.0 0.5% DPTA, 70 °C, 30 mins.	26.1	1139	< 1.0	17.2	< 2.0	19.5
Acid treated, then chelated (A - Q)	pH 2.5 (H_2SO_4) 85 to 90 °C for 180 min, then chelated as above	24.2	1118	< 1.0	12.0	2.4	11.0

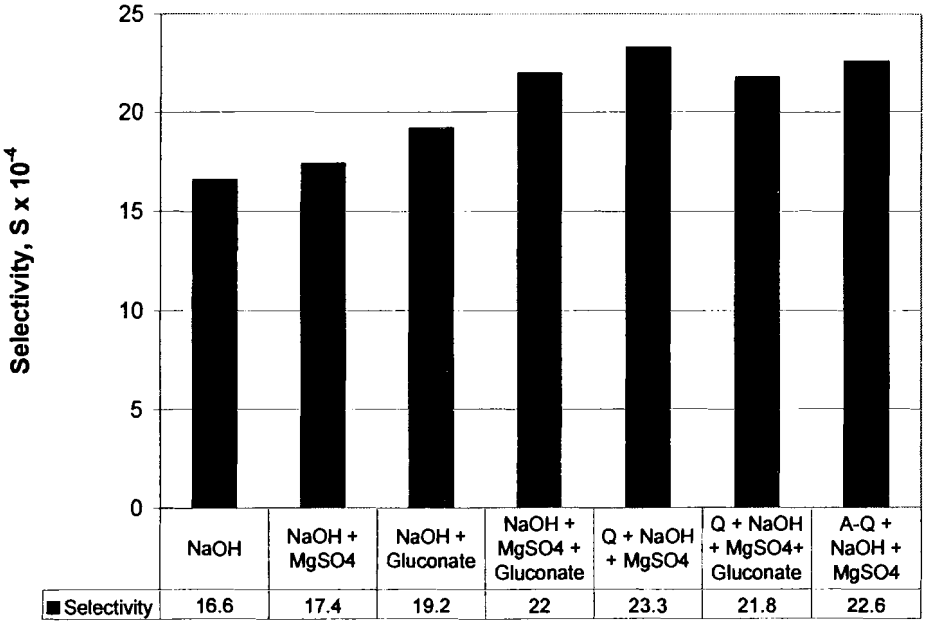

Figure 4.6. Selectivity results on Irving pulp after oxygen delignification for 60 min., with chelation, acid washing, and basic additives (standard conditions)

Table 4.4 summarizes several experiments on IP pulp A which were repeated and reported as the average result to compare treatments tested thus far. Chelation followed by $MgSO_4$ addition had the highest selectivity with this pulp. Sodium gluconate was not very effective and also did not give any improvement when preceded by chelation. Acid washing in combination with chelation also gave no benefit compared to chelation alone. The effect of magnesium sulfate was consistent in most experiments, increasing the selectivity by 1 to 2 (x 10^4) units.

Table 4.4. Summary of basic treatments on IP pulp A (average values)

Description (experiments averaged)	Initial Kappa	Final Kappa	Final η_t	Selectivity S $\cdot 10^{-4}$
Control (0.2 % $MgSO_4$) (5)	26.7	13.11	903	17.4
Control, no $MgSO_4$ (3)	26.7	13.78	903	16.5
2 % Sodium gluconate (2)	26.7	14.24	944	19.2
2 % Sodium gluconate + 0.2 % $MgSO_4$ (3)	26.7	14.56	971	22.0
Q (3)	26.4	14.71	958	21.1
Q + 0.2 % $MgSO_4$ (4)	26.1	12.86	966	23.3
Q + 2 % Gluconate (2)	26.6	14.56	963	20.9
Q + $MgSO_4$ + 2 % Gluconate (2)	26.6	14.56	963	21.8
A – Q (pH = 2.5 to 3) (3)	25.0	12.02	922	21.6
A = Acid washed (2 to 3 pH, 85 to 90 °C, 1 % consistency, 180 minutes) Q = Chelated (5pH, 70 °C, 0.5 % DTPA, 30 min, 3.0 % consistency)				

Table 4.5 summarizes the acid washing pretreatments at different levels of pH. Also contained in these results are experiments in which the A – Q treatment is followed by hydrogen peroxide addition at a charge of 1.5 % on pulp. Some researchers found a very selective oxygen delignification process by combining these treatments (Sjogren and Hook, 1999).

As can be seen in Table 4.5, it was not effective to conduct the acid washing procedure at the lowest pH of 2.0. A significant degree of cellulose hydrolysis occurred, as evidenced by the low viscosity of 972 mL/g after the pretreatment. Not only was the selectivity of the oxygen delignification lower than when the acid wash was performed at a more moderate pH, but the final viscosity was also very low because of the losses in the A stage. The best result was obtained with acid washing at a pH of 2.5.

Table 4.5. Summary of acid washing treatments on IP pulp A

Description	Initial Kappa	Final Kappa	Initial η_0	Final η_t	Selectivity $S \cdot 10^{-4}$
Control	26.7	13.11	1188	903	17.4
1.5% H_2O_2	26.7	13.40	1188	880	15.3
Q	26.1	12.86	1188	966	23.3
Q + 1.5% H2O2	26.5	12.51	1188	934	20.8
A – Q (pH = 3)	26.7	11.39	1140	888	20.8
A – Q (pH = 2.8)	24.8	12.45	1122	941	20.5
A – Q (pH = 2.5) + 1.5% H2O2	24.2	10.63	1118	899	19.2
A – Q (pH = 2.5)	24.2	12.08	1118	931	22.6
A – Q (pH = 2.5) + 1.5% H2O2	24.2	10.63	1118	899	21.0
A – Q (pH = 2.0)	22.5	10.01	972	769	18.3
A = Acid washed (2 to 3 pH, 85 to 90 °C, 1 % consistency, 180 minutes) Q = Chelated (5pH, 70 °C, 0.5 % DTPA, 30 min, 3.0 % consistency)					

4.7. HYDROGEN PEROXIDE ADDITION

Table 4.5 shows that the experiments with hydrogen peroxide addition are not as effective in selectivity enhancement as reported in some studies (Sjogren and Hook, 1999; Parthasarathy, et al., 1989). Recently, Dang (2002) evaluated the use of hydrogen peroxide statistically. A very marginal selectivity improvement was reported when using

a glass reactor, and a negative impact was reported using a steel reactor like the Parr reactor used in this investigation.

4.8. METALS REPLENISHMENT

The pulp was chelated to remove metal ions, and following this, metal sulfates were added back into the pulp to replenish certain metals to test combinations of metals for testing delignification selectivity. The oxidation state of the added iron and manganese ions was 2+. Table 4.6 summarizes the metal content of the pulps after these treatments, showing samples tested before and after they were subsequently oxygen delignified. The metals were added in the dilute pulp suspension at a pH of 2 to 3 at room temperature to reach equilibrium between concentrations in the pulp and liquid before the pulps were drained. Towers and Scalan (2000) have described this method of equilibrating pulp at similar conditions and have been able to predict the resulting metal concentrations.

The results of the oxygen delignification batches are given in Figure 4.7. As before, the conditions used were 4 % NaOH, 90 °C, 100 psig oxygen, 10 % consistency, for 60 minutes. Manganese and magnesium added at these conditions were helpful for the selectivity, but the manganese was more effective in the absence of the magnesium. Iron added at these high levels was very harmful to the selectivity. It is not surprising that the iron added had such a negative impact on radical formation. It is believed that some iron may not be as harmful, for example Fe^{4+} rather than Fe^{2+}, because it will not undergo the Fenton mechanism as readily as dissolved iron that has not been absorbed into the solid pulp. As mentioned, the ions used to replenish the pulp was Fe^{2+}. It

might be beneficial to study the impact of chemically reducing the iron in the pulp, but $NaBH_4$ reduction has not been successful in a few experiments in this investigation (See Appendix B). However, this strategy may be effective on chelated pulp with very low iron and other metals.

Table 4.6. Summary of metals replenishment (by I.C.P.-A.E.S.)

Pulp Sample (IP pulp)	Was pulp delignified?	Mg ppm	Cu ppm	Fe ppm	Mn ppm
Initial	no	320 to 370	12.9 to 27.3	18.4 to 30.5	23.8 to 46.1
Chelated	no	85 to 101	1.2 to 2.3	8.4 to 9.4	< 0.97
NaOH + MgSO4	before	85 to 101	1.2 to 2.3	8.4 to 9.4	< 0.97
	after	389	2.4	19.8	9.74
Mn + NaOH	before	< 10	1.6	6.6	300
	after	< 10	3.1	14.7	161
Mn + NaOH + MgSO4	before	< 10	1.6	6.6	300
	after	201	2.4	18.9	131
Fe + NaOH	before	< 10	1.5	524	< .99
	after	< 10	4.5	338	2.5
Fe + NaOH + MgSO4	before	< 10	1.5	524	< .99
	after	211	4.6	252	< 0.97
Pulp chelation as before; Fe, Mn Replenishment at 2 to 3 pH (H_2SO_4), 1 % consistency, 30 minutes, 100 ppm metal ions in solution, then brought to 33% consistency, for target 200 ppm					

Table 4.7 summarizes the metals replenishment results. As previously described, the Q stage was done at the standard chelation conditions. It is interesting to note that again in this data, the protector $MgSO_4$ was not as effective on manganese and iron replenished pulps as it was on non-chelated and chelated pulps. A reason for this is because in order for the magnesium hydroxide precipitate to effectively ion-exchange

with the manganese, there must be an order of magnitude larger number of magnesium ions as the number of manganese ions.

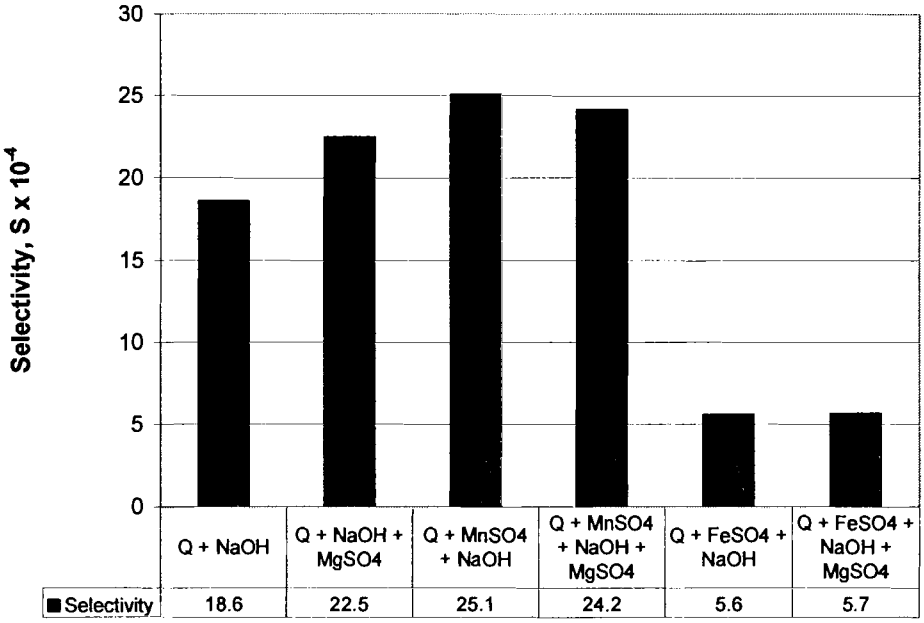

Figure 4.7. Metals replenishment selectivity results, IP pulp.

Table 4.7. Summary of oxygen delignification results after metals replenishment

Description	Initial Kappa	Final Kappa	Initial η_0	Final η_t	Selectivity $S \cdot 10^{-4}$
Q + Mn 25 ppm target	26.7	13.32	1188	961	22.8
Q + Mn 50 ppm target	26.7	13.09	1188	963	23.6
Q + Mn 100 ppm target	26.7	13.84	1188	970	23.1
Q + Mn 200 ppm target	26.7	13.04	1188	977	25.7
Q + Mn 200 ppm target + 0.2 % $MgSO_4$	26.7	13.54	1188	980	25.1
Q + Mn 200 ppm target + 2.0 % gluconate	26.7	12.85	1188	984	27.0
Q + Mn. 200 ppm target	26.7	14.22	1188	989	25.1
Q + Mn 200 ppm target + 0.2 % $MgSO_4$	26.7	14.25	1188	971	24.5
Q + Fe + Mn , 50 ppm target each	26.7	14.43	1188	959	20.8
Q + Fe + Mn , 100 ppm target each	26.7	14.32	1188	964	21.5
Q + Fe 100 ppm target	26.7	14.10	1188	567	4.5
Q + Fe 200 ppm target	26.7	13.85	1188	627	5.6
Q + Fe 200 ppm target + MgSO4	26.7	14.77	1188	648	5.7

Chapter 5

INFLUENCE OF PROCESS VARIABLES ON OXYGEN DELIGNIFICATION

5.1. EFFECT OF REACTOR STIRRING

The experiments presented in this chapter were performed on International Paper softwood pulp A, as described in section 4.2. The data from all experiments are given in Appendix B. As mentioned in the literature review, the mixing of the pulp in oxygen delignification is not nearly as important in the laboratory as it is in the mill (Bennington and Pineault, 1998). This is because there is a large excess of pressurized oxygen and continuous mixing in the laboratory. It also has been previously shown that the liquid phase mass transfer of oxygen is much more significant that other resistances (Hsu and Hsieh, 1985; van Heiningen et al., 2003), and that increasing oxygen pressure beyond 300 kPa has very little effect on delignification rate and selectivity (Zou, 2002; Berry et al., 2002).

In order to determine the mixing conditions whereby the oxygen delignification rate in the Parr reactor became independent of the rate of mixing, a set oxygen delignification experiments were conducted at standard conditions and different mixing speeds. Figure 5.1 shows the effect of reactor stirring rotations per minute (RPM) on the final Kappa number and selectivity of these experiments. It was concluded that speeds greater than 200 RPM provided adequate mixing in the liquid phase. Therefore, the reactor was operated at 250 RPM during all further experiments..

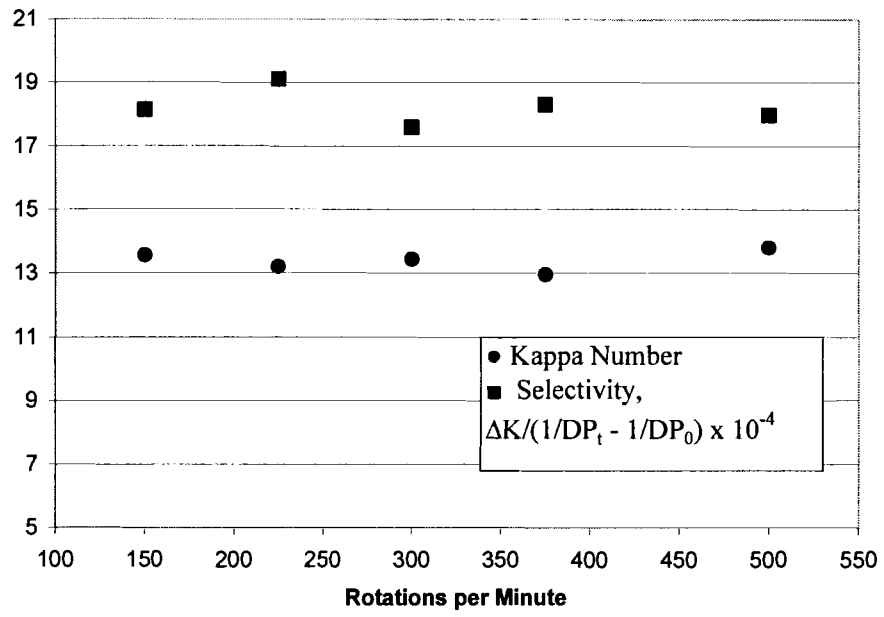

Figure 5.1. Effect of reactor stirring on Kappa number and selectivity during oxygen delignification (60 minutes at standard conditions)

5.2. EFFECT OF TIME AND TEMPERATURE

Experiments were conducted at times of 10, 20, and 60 minutes and temperatures of 90 °C and 120 °C, with a sodium hydroxide charge of 4.0 % on pulp. Results from these experiments are shown in Figures 5.2 and 5.3.

The curves displayed in Figures 5.2 and 5.3 follow a decay-curve shape similar to those obtained in previous studies (Olm and Teder, 1979, Zou, 2002; Berry et al. 2002). Both the lignin removal and cellulose degradation occur rapidly at the beginning of the experiment but proceed more slowly with time. The decrease in the rate of Kappa number reduction appears to be more pronounced at 120 °C when the Kappa number reaches a value of about 10. This is likely because there are certain lignin components contributing to the residual Kappa number, like lignin-carbohydrate complexes (LCC's) and condensed lignin, which are not reactive to oxygen delignification. This level has

been estimated as greater than 30 % of the remaining lignin in softwood Kraft brown stock around 30 Kappa number (Argyropoulos, 2002).

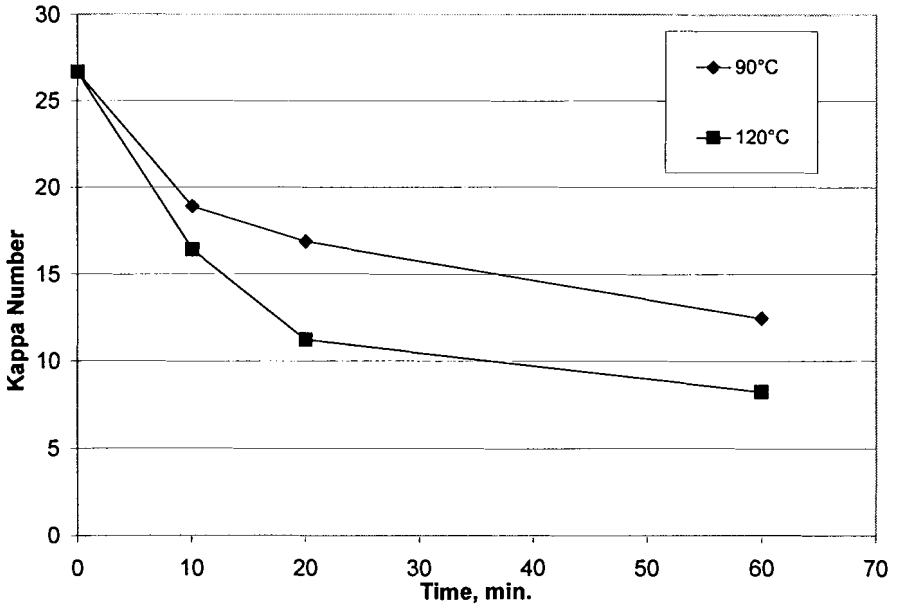

Figure 5.2. Influence of time and temperature on Kappa number during oxygen delignification, 4.0 % NaOH

5.3. SELECTIVITY PLOTS

In pulping and bleaching, it is convenient to view graphs showing a measure of cellulose degradation (e.g. decrease in pulp viscosity) plotted versus the change in Kappa number. These "selectivity plots" show changes in selectivity during the course of the delignification as the curve slope changes. Figure 5.4 is a selectivity plot of data from the same experiments shown in Figures 5.2 and 5.3. These curves display a shape commonly seen in pulping and bleaching reactions, which is more horizontal (better selectivity) near the beginning of the reaction than near the end. Most researchers have shown this general shape for oxygen delignification selectivity plots (Olm and Teder,

1979; Iribarne and Schroeder, 1998), and have also attempted to describe this behavior by postulating the existence of slowly and rapidly removed lignin moieties in their analysis of the reaction kinetics.

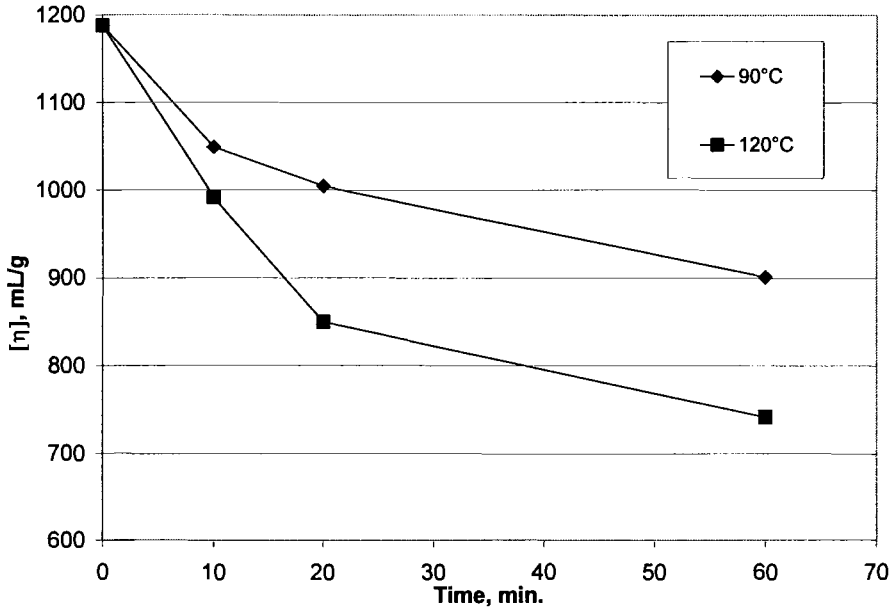

Figure 5.3. Influence of time and temperature on intrinsic viscosity during oxygen delignification, 4.0 % NaOH

The plot in Figure 5.4 also compares the selectivity at two different temperatures. The curves' slopes are essentially the same at a given Kappa number. This shows that the selectivity was not detrimentally affected by raising the temperature from 90 °C to 120 °C, a practice commonly discouraged in mills in fear that raising temperatures has an ill-effect on selectivity. More recent studies have agreed with these findings. Agarwal (1999) and Berry and co-workers (2002) found no significant change in selectivity between 90 °C and 110 °C. This is a significant conclusion because it is relatively easy in practice to raise the temperature and thus the delignification capacity, while the selectivity of the process is not significantly affected.

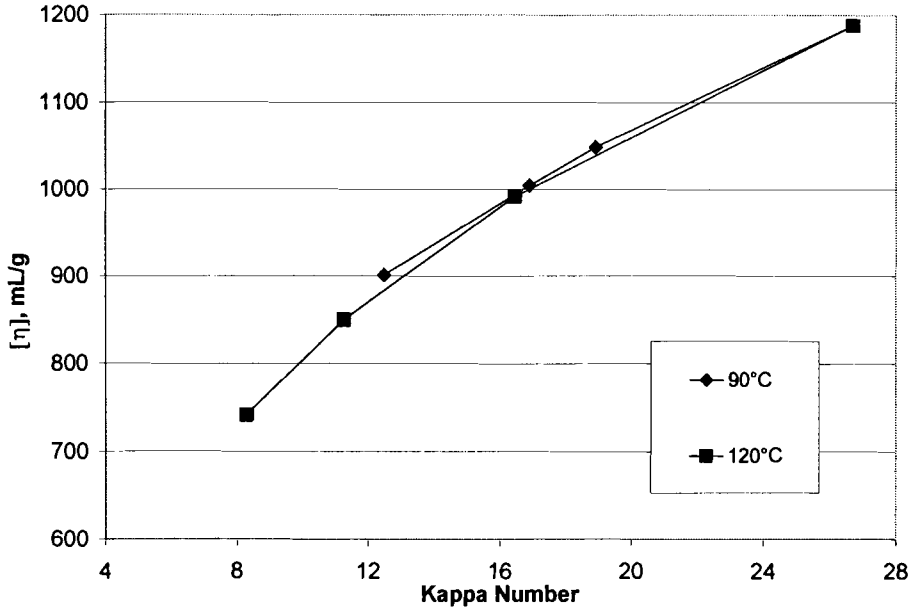

Figure 5.4. Selectivity plot: influence of temperature during oxygen delignification, 4.0 % NaOH

5.4. EFFECT OF ALKALI CHARGE

Experiments were conducted at different charges of sodium hydroxide on pulp at 90 °C and otherwise standard conditions. Figure 5.5 is a selectivity plot showing experiments at the three charges of 1.5 %, 2.5 %, and 4.0 % on NaOH pulp and reaction times of 10 min., 20 min., and 60 min. It is clear from this graph that increasing the sodium hydroxide charge results in a lower viscosity at a given Kappa number, and thus a lower selectivity . This difference is at least 50 mL/g for the charge 1.5 % NaOH compared to 4.0 % NaOH at the higher Kappa numbers, and would be even greater if the reaction at 1.5 % NaOH extended to low Kappa numbers. In a mill it is uncommon to use charges much greater than 3 % NaOH, not only because of selectivity but also because the Kappa number may be reduced quite significantly with less than 3 % NaOH

on pulp. All the kinetic studies mentioned in Chapter 2 found that a sodium hydroxide charge affects selectivity negatively.

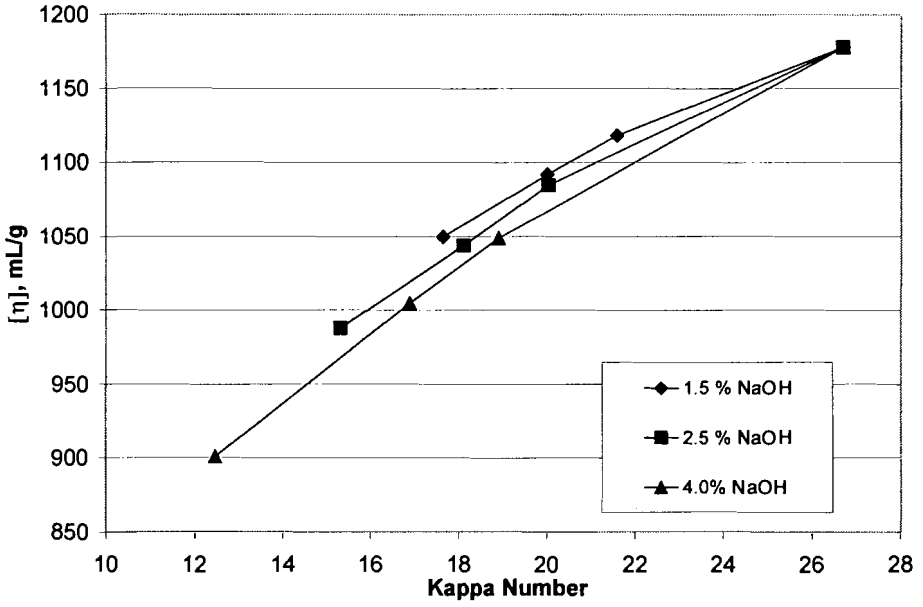

Figure 5.5. Selectivity plot: influence of alkali charge during oxygen delignification, 90 °C

5.5. MODIFIED SELECTIVITY PLOTS

The selectivity plots shown in Figures 5.4 and 5.5 are a practical representation of the development of pulp properties during delignification. However, these graphs do not provide an insight into the fundamentals of cellulose degradation. It is more instructive to express the viscosity loss in terms of the number of cellulose chain scissions. It has been stated previously (in Chapter 3) that the quantity $(1/DP_t - 1/DP_0)$, is the number of chain scissions per glucose unit in cellulose. This quantity was calculated and plotted against the Kappa number change (ΔK) in the modified plot shown in Figure 5.6. This type of plot differs from the selectivity plots in Figures 5.4 and 5.5 not only because it

represents a better measure of cellulose degradation, but also because the initial values of Kappa number and DP were incorporated into the expressions. Therefore, all curves for varying initial properties start at the origin.

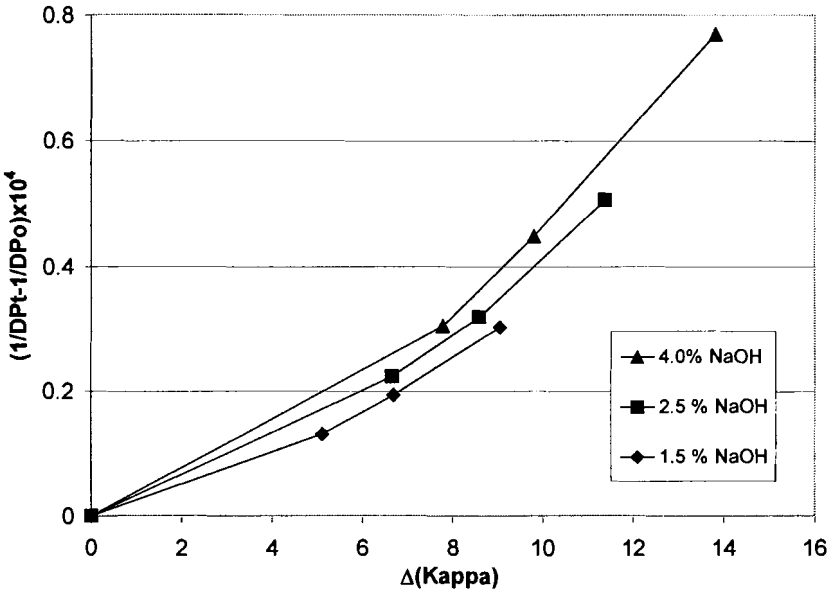

Figure 5.6. Modified selectivity plot: influence of alkali charge during oxygen delignification, 90 °C

5.6. ALKALI EXTRACTION DURING OXYGEN DELIGNIFICATION

The Kappa number decrease shown in Figure 5.6 is the combined result of lignin removal by oxygen-mediated reactions and the dissolution of residual lignin by alkali extraction alone. The Kappa number change by alkali extraction was determined by measuring the Kappa number and viscosity changes resulting from caustic extraction in the absence of oxygen. Table 5.1 summarizes these alkali extraction experiments, which were performed under identical conditions as the oxygen delignification reactions, but pressurized under 100 psig (780 kPa) nitrogen rather than 100 psig oxygen. A second pulp, IP softwood pulp B, is also shown in this table. It was very similar to IP SW pulp

A, but with slightly different initial Kappa number and viscosity. Further details of the properties of pulps A and B are summarized in Chapter 6 (Table 6.7), so that results with these two pulps could be compared. For these nitrogen extraction experiments, it suffices to consider these two pulps essentially the same, and they did behave similarly.

Table 5.1. Summary of experiments conducted under 780 kPa nitrogen

Conditions	Initial Kappa	Final Kappa	η_0 mL/g	η_t mL/g	S (x 10^{-4})	Δ[NaOH] g/L
1.5 % NaOH,10 min, 90 °C	26.7	24.91	1188	1184	217	0.11
1.5 % NaOH, 60 min, 90°C	26.7	24.58	1188	1161	87.3	0.03
1.5 % NaOH, 60 min, 120 °C	26.7	24.02	1188	1180	162	0.27
2.5 % NaOH, 10min, 90 °C	26.7	24.13	1188	1175	95.0	0.18
2.5 % NaOH, 10 min, 90 °C	26.7	24.18	1188	1163	57.9	0.18
2.5 % NaOH, 10 min, 90 °C	26.7	24.38	1188	1180	140	0.28
2.5 % NaOH, 20 min, 90 °C	26.7	24.13	1188	1169	64.7	0.24
2.5 % NaOH, 60 min, 90 °C	26.7	23.99	1188	1177	119	0.31
2.5 % NaOH, 60 min, 120 °C	26.7	23.02	1188	1166	79.5	0.38
4.0 % NaOH, 10 min, 120 °C	26.7	22.73	1188	1165	82.2	0.36
4.0 % NaOH, 60 min, 90 °C	26.7	23.28	1188	1180	206	0.32
4.0 % NaOH, 60 min, 120 °C	26.7	22.11	1188	1144	48.7	0.60
2.5 % NaOH, 10 min, 90 °C	28.0	25.79	1172	1153	74.0	0.25
2.5 % NaOH, 20 min, 90 °C	28.0	25.52	1172	1153	80.6	0.58
2.5 % NaOH, 60 min, 90 °C	28.0	25.29	1172	1149	54.5	0.22

The most important observation from this data is that the Kappa number was reduced much more than the intrinsic viscosity during these experiments. The Kappa number was reduced by as much as 4.6 units, nearly 20 % of the initial Kappa number. However, the biggest intrinsic viscosity loss was 44 mL/g, which is less than 4 % of the viscosity; and many of the viscosity losses were less than a standard deviation (16 ml/g) of the initial value. Therefore, the viscosity loss during the alkali extraction was negligible compared to the Kappa number reduction. This was also reflected in the measured selectivity parameter, which was several times greater during alkali extraction than during oxygen delignification.

Also, it is an important observation that mostly all the delignification during the alkali extraction was complete after 10 minutes reaction time. For these two reasons, it is not difficult to see why previous researchers thought that the oxygen delignification is more selective near the beginning of the process. Figure 5.7. shows the decrease in Kappa number for two pulps, IP softwood pulp A and B, during alkali extraction under 100 psig nitrogen.

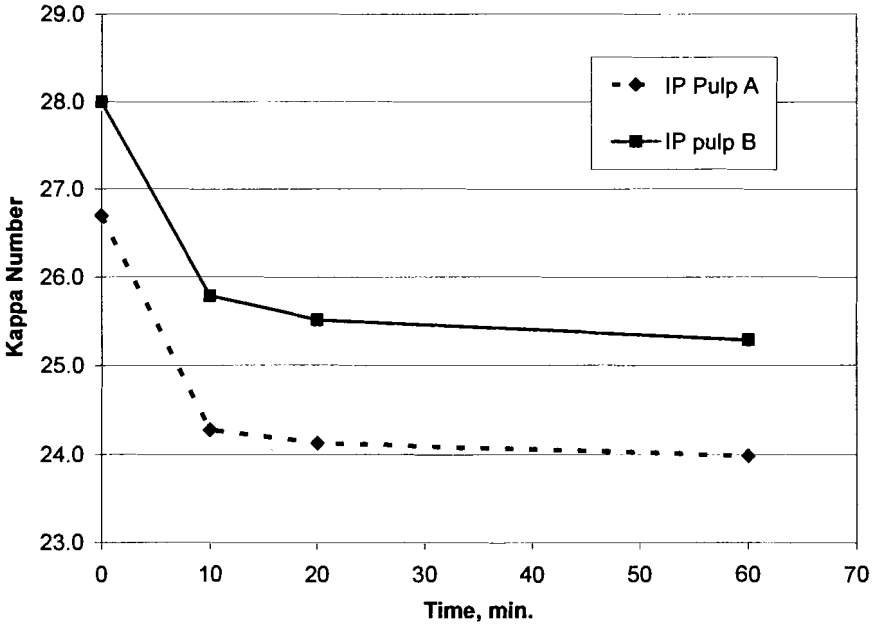

Figure 5.7. Kappa number versus time for experiments conducted under 780 kPa nitrogen pressure, 2.5 % NaOH and 90 °C

5.7. SELECTIVITY OF OXYGEN REACTIONS

The Kappa number and 1/DP changes in Figure 5.6 may be corrected by using the Kappa number and DP values obtained after the alkali extraction experiments as the initial values. By making this adjustment, the changes in Kappa number and 1/DP represent only the effect of the oxygen-mediated reactions on lignin and cellulose, respectively.

The adjusted changes in Kappa number and 1/DP for oxygen delignification experiments at sodium hydroxide charges of 1.5 %, 2.5 %, and 4.0 % NaOH on pulp are plotted in Figure 5.8. The curves contain reaction times of 0, 10, 20, and 60 minutes. The lines with smaller slopes represent more selective delignification.

Data presented in this format show a direct linear relationship between corrected Kappa number change and the number of cellulose chain scissions. This is clearly different from the selectivity plots in Figures 5.4 to 5.6 which show that the selectivity of oxygen delignification was decreasing with increasing delignification. This no longer occurs on the corrected plot, because the correction is most appreciable over the first 10 minutes which previously seemed more selective. The linear shape of the corrected graph indicates that the rate of attack of harmful radicals on cellulose is directly proportional to the rate of delignification. Since the harmful radicals are produced through reactions initiated by the attack of oxygen on phenolic lignin, it also suggests that at each condition the radical yield per lignin unit removed is independent of the degree of delignification, contrary to the general perception that the selectivity decreases with increasing degree of delignification.

Comparison of the lines in Figure 5.8 again shows that the oxygen reactions are more selective at a lower alkali charge, since the slopes of these experiments decrease from 0.071 to 0.052 as alkali charge is varied from 4.0 % to 1.5 %.

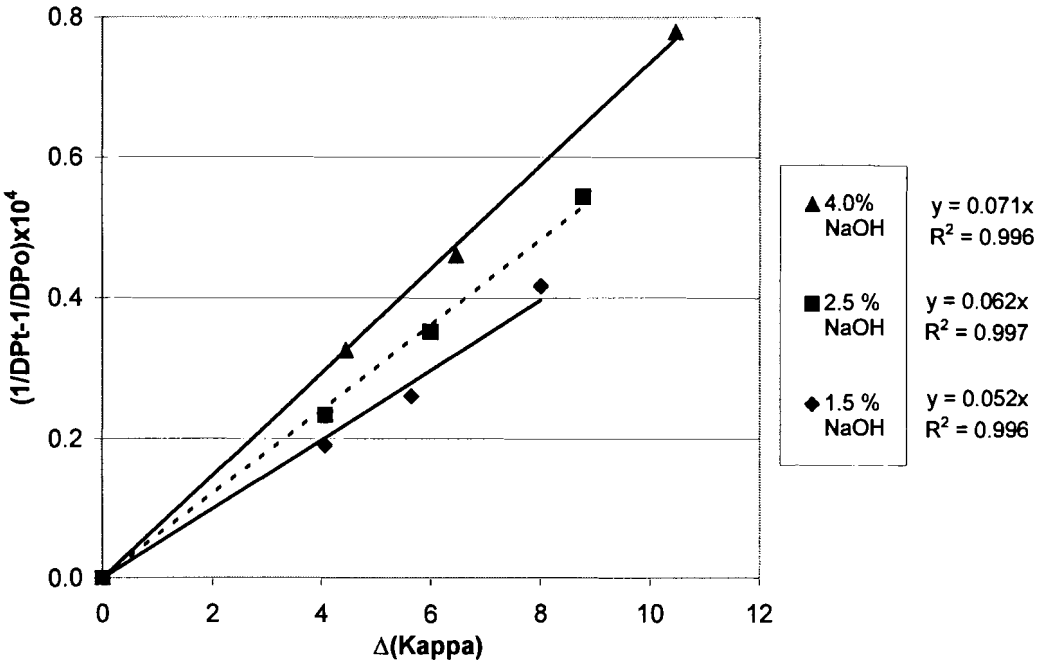

Figure 5.8. Oxygen reaction selectivity: influence of alkali charge, 90 °C

The linear relationships in Figure 5.8 show that the selectivity throughout the delignification process at each condition is constant. Therefore a new selectivity, S_C, the oxygen reaction selectivity parameter, was defined as:

$$S_C = \frac{\Delta K_C}{\left(\frac{1}{DP_t} - \frac{1}{DP_0}\right)} \qquad (5\text{-}1)$$

where ΔKc is the change in Kappa number corrected for alkali extraction, DP_t is the degree of polymerization of cellulose at time t, and DP_0 is the degree of polymerization of cellulose of the alkali-extracted pulp. The selectivity parameter S_C is equal to the inverse of the slopes of the curves in Figure 5.8.

The corrected selectivity based on chain scission number (S_{CSN}, defined in Equation 2-2), is calculated as follows:

$$S_{CSN} = \frac{\Delta K_C}{CSN} = \frac{\Delta K_C}{\left(\frac{1}{DP_t} - \frac{1}{DP_0}\right) \cdot DP_0} \qquad (5\text{-}2)$$

This selectivity is the same as S_C, but are a factor of DP_0 (4550 units/polymer) less.

Results for all three of the selectivity parameters (S, S_C, S_{CSN}) are given in Table 5.3. for experiments at different alkali charges, temperature, and reaction time. The values for S_C are about 70 to 80 % of the magnitude of S because the Kappa number change is decreased more than the change in 1/DP in the correction for alkali extraction. This data shows that the uncorrected selectivity decreases with time, but the corrected selectivity stays relatively constant except for the condition of 120 °C and 60 minutes. This may be because there is no longer any lignin which may be removed under oxygen delignification in the pulp below a Kappa number of 8 (70 % Kappa number reduction). It was shown previously that at the same Kappa number, experiments at 120 °C were equally selective as experiments at 90 °C. Because the experiments at 90 °C do not reach a Kappa number that low, this does not indicate that the higher temperature is less selective.

Table 5.2. Summary of selectivity results

Conditions	Time, Min.	S x 10^{-4}	S_C x 10^{-4}	S_{CSN}
1.5 % NaOH, 90 °C	10	26.5	16.3	35.9
	20	23.6	17.1	37.6
	60	22.3	18.2	40.0
2.5 % NaOH, 90 °C	10	28.4	15.8	34.8
	20	25.2	15.5	34.1
	60	19.2	16.2	35.6
4 % NaOH, 90 °C	10	24.1	13.1	28.8
	20	20.4	14.1	31.0
	60	17.4	14.4	31.7
4 % NaOH, 120 °C	10	24.6	15.5	38.5
	20	17.1	14.3	31.5
	60	14.9	13.3	25.1
5 % NaOH, 90 °C	10	18.1	10.9	24.0
	20	16.4	11.4	25.1
	60	14.9	11.5	25.3

5.8. ALKALI CONSUMPTION DURING OXYGEN DELIGNIFICATION

The sodium hydroxide concentration ([NaOH]) in g/L in the liquor was determined before and after oxygen delignification experiments by titration with acid to neutral pH. It has been observed that the decrease in [NaOH] was proportionate to the decrease in Kappa number. This relationship is seen in Figure 5.9, where a high degree of linearity ($R^2 = 0.95$) is observed when plotting Δ[NaOH] versus ΔK as expected. The slope of this graph (0.139 g/L NaOH per Kappa unit) may be used to determine the amount of alkali needed for a given Kappa number drop or to estimate [NaOH] at a given Kappa number without taking measurements. This slope is also equivalent to 0.125 % NaOH on pulp/Kappa unit. This equation may be given as:

$$\Delta[NaOH] = 0.139 \text{ g/L} \cdot \Delta K \qquad (5\text{-}3)$$

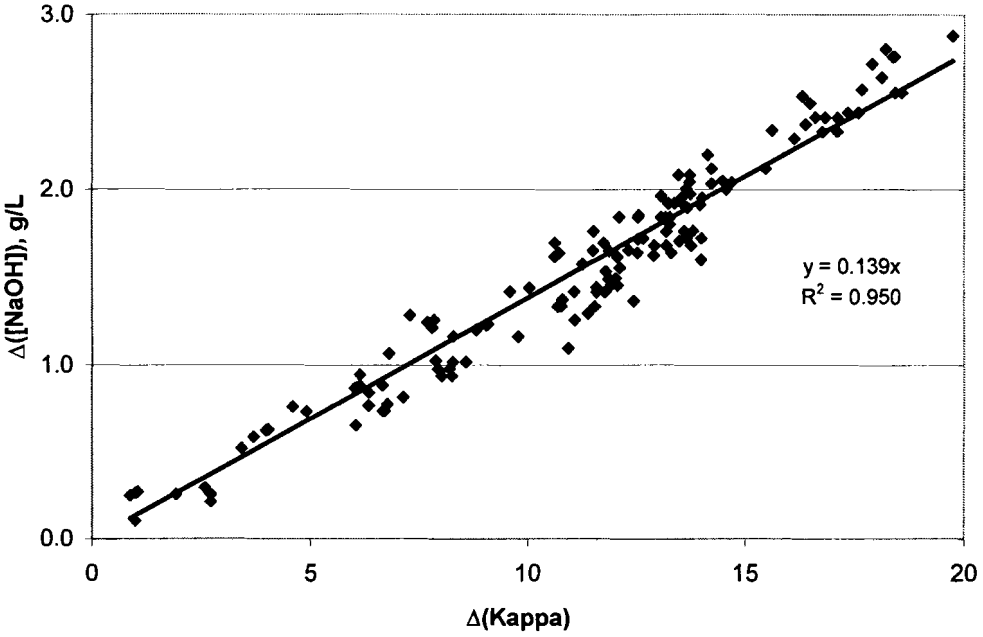

Figure 5.9. Alkali charge consumption versus Kappa number decrease during oxygen delignification

The same plot was constructed to correlate Δ[NaOH] to the corrected Kappa number change, ΔK_C. This graph is not shown, but the plot had the same linear shape ($R^2 = 0.95$) with a slightly larger slope and a more significant intercept. The equation for this trend line was determined as:

$$\Delta[NaOH] = 0.168 \text{ g/L} \cdot \Delta K_C + 0.2 \text{ g/L} \qquad (5\text{-}4)$$

The small y-intercept in this equation signifies the alkali consumed in extracting some of the Kappa number components. The data during nitrogen extraction experiments were excluded thus far, but generally the values were somewhat lower than

for during oxygen delignification. These data are also given in Appendix B with the compiled data. The average Δ[NaOH] for all extraction experiments was 0.28 g/L. This is not much different from the 0.2 g/L estimated in equation 5-4.

Chapter 6

EFFECT OF ADSORBED POLYMER ADDITIVES ON OXYGEN DELIGNIFICATION

As outlined in the hypothesis, the objective is to improve the selectivity of oxygen delignification with adsorbed polymer additives. Specifically, carbohydrate polymers were assessed due to their abundance, familiarity in papermaking, and results of experiments with the monomer radical scavenger sodium gluconate (Kang, et al, 1998). Among these polymers are starch, carboxymethylcellulose (CMC), galactomannan (galactomannan), glucomannan, and xylan.

6.1. STARCH

6.1.1. Oxygen Delignification with Starch

Oxygen delignification experiments were conducted under standard conditions and with different starches charged at 5 % on pulp, as shown in shown in Table 6.1. High charges were chosen for the initial testing, to make any differences in results more discernible, but it is doubtful that such high charges would ever be employed in a mill process. Two of these starches were cationic starches which should possess increased affinity and thereby adsorb more effectively on pulp's negatively charged fiber surfaces in an alkaline environment. Starch 3 is a food starch thinned by mild hydrolysis Even at this very high charge, there was very little improvement in selectivity; and a decrease in lignin removal was observed, compared to the control reaction. Other starches were evaluated similarly under these conditions, but no improvement in selectivity was found than those listed in Table 6.1.

Starch may be ineffective as a cellulose protector because amylopectin is a very large and highly branched molecule, so it may not be able to penetrate within the fiber wall. Also, it is unlikely that amylopectin will adsorb to pulp as well as amylose due to its high degree of branching. The starch (starch 3) with the lowest molecular weight and highest amylose content had the best selectivity, perhaps because it has more linear amylose units that will adsorb on cellulose and a much lower molecular weigh enabling some starch to penetrate into the fiber. It is a fair estimation that a polysaccharide with a molecular weight well under 100,000 Daltons has the best chance to fit into the micro-pores in pulp, but definitely nothing may penetrate that is over 1 million Daltons and highly branched.

Table 6.1. Effect of starch on oxygen reaction selectivity

	Component and Molecular Weight (MW) Estimation, Daltons	Functional Group content	% Kappa Number Reduction	Corrected Selectivity, S_C x10-4
Control	No additive	No additive	49.8	14.4
5 % Starch 1	Amylose (17 %): MW 500,000 Amylopectin (83%): MW > 5 M	4° amine, 0.32% Nitrogen	38.3	14.1
5 % Starch 2	Amylose (17 %): MW < 100,000 Amylopectin (83 %): MW > 1 M	4° amine, 0.18% Nitrogen	41.9	15.8
5 % Starch 3	Amylose (21 %): MW 8000 to 12,000 Amylopectin (79 %): MW 100,000 to 500,000	None	45.8	16.4
Conditions: IP softwood pulp A, 4.0 % NaOH, 90 °C, 100 psig oxygen, 0.2 % $MgSO_4$, 60 minutes.				

6.1.2. Adsorption of Starch on Pulp

The adsorption of starch on pulp was measured gravimetrically as described in Section 3.12.1, when the pulps were equilibrated at 60°C under neutral and alkaline conditions. These results are shown in Figure 6.1. In these experiments, the liquor

solids were measured of 10% consistency pulp suspensions, with and without the polymer addition. These isotherms show that only at addition levels up to 0.5 % and at neutral pH did the majority of the starch (starch 1) added adsorb on the pulp. Very little adsorbs at an alkali level similar to that which exists during oxygen delignification.

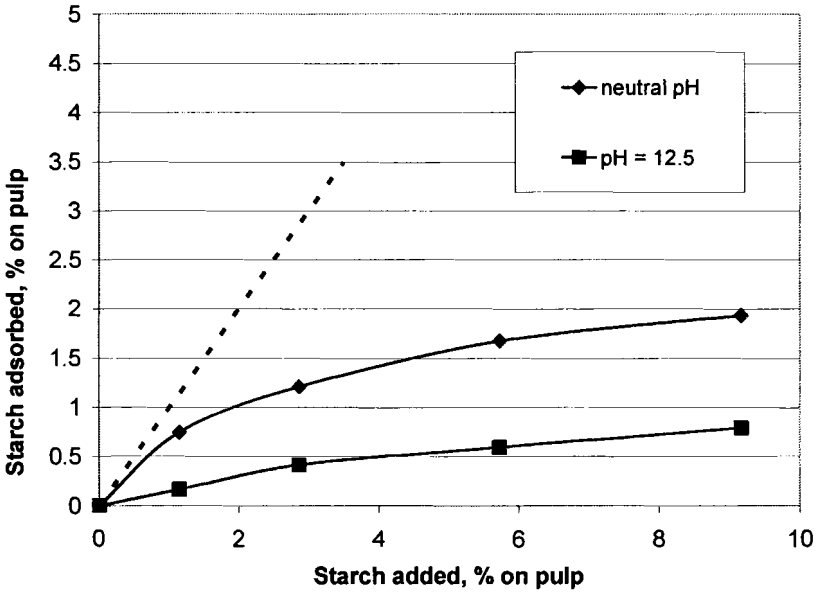

Figure 6.1. Adsorption of starch (1) on pulp, at neutral and alkaline pH, determined gravimetrically at 60 °C

6.2. CARBOXYMETHYLCELLULOSE (CMC)

6.2.1. Oxygen Delignification with CMC

Table 6.2 shows oxygen delignification experiments conducted under standard conditions and with three different CMC's varying in molecular weight and degree of substitution (DS) of the carboxymethyl group. As with the three starch additives shown in Table 6.1, only very modest selectivity improvements were observed at this very high addition charge. The degree of delignification was also inhibited by the addition of the CMC.

6.2.2. Adsorption of CMC on Pulp

Figure 6.2 shows the adsorption of CMC 1 on pulp, which was also determined gravimetrically. CMC adsorbed even less than starch at a high pH. This may be due to the high solubility of CMC's at high alkali concentration levels. At a 5 % addition charge, only 0.4 % CMC was adsorbed on pulp. CMC 2 had the highest adsorption among the CMC's tested, because of its low DS and high molecular weight.

Table 6.2. Effect of CMC on oxygen reaction selectivity

	Molecular Weight Estimation, Daltons	Degree of Substitution (DS)	% Kappa Number Reduction	Corrected Selectivity, S_C x10^{-4}
Control	No additive	No additive	49.8	14.4
5% CMC 1	90,000	0.80	45.0	16.7
5% CMC 2	300,000 to 570,000	0.22 – 0.25	44.9	15.9
5% CMC 3	43,000	0.22	46.0	15.8
Conditions: IP softwood pulp A, 4.0 % NaOH, 90 °C, 100 psig oxygen, 0.2 % $MgSO_4$, 60 minutes.				

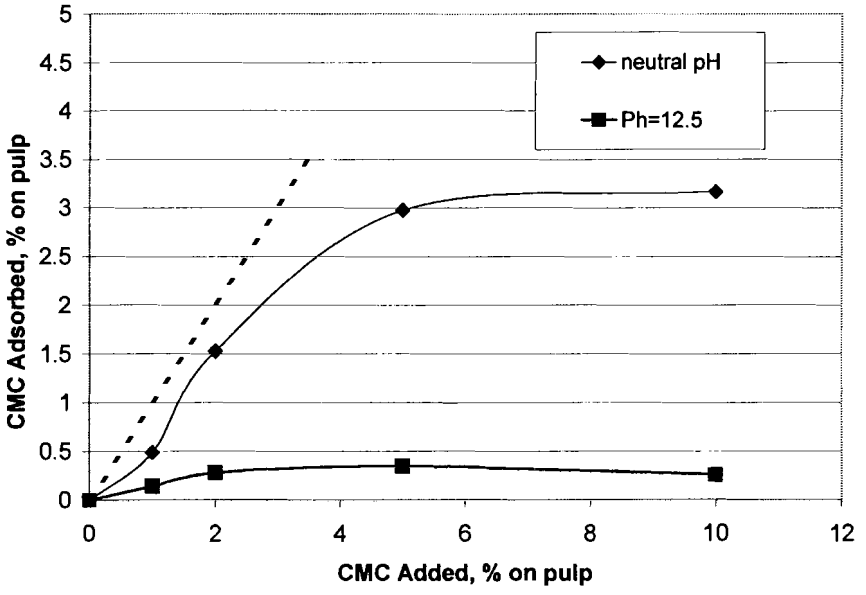

Figure 6.2. Adsorption of CMC (2) on pulp, at neutral and alkaline pH, determined gravimetrically at 60 °C

6.3. GUAR GALACTOMANNAN

6.3.1. Effect of Galactomannan Charge

Galactomannan is a thickener and dry strength additive used in the papermaking industry which is extracted from the Guar bean. Guar galactomannan is similar to the hemicellulose glucomannan, but has a much higher molecular weight of 200,000 to 1 million and has a galactan to mannan ratio of about one half. Galactomannan was added at different charges and compared to control oxygen delignification experiments at the standard conditions. Table 6.3 shows that improvements in selectivity were observed for charges much lower than 5 % on pulp, and the selectivity was improved significantly with only 0.3 % Galactomannan charge on pulp, going form 14.4 to 18.2 or a 26 % increase. At a higher charge of 2.0 % galactomannan, the selectivity is improved 46 % up to 21.0. Three or more experiments were averaged for these results.

Table 6.3. Effect of galactomannan on oxygen reaction selectivity

	Molecular Weight Estimation, Daltons	% Kappa Number Reduction	Selectivity, S_C x10-4
Control	No additive	49.8	14.4
5% Galactomannan	720,000	46.4	22.9
2% Galactomannan	720,000	48.1	21.0
0.75% Galactomannan	720,000	48.9	20.1
0.3% Galactomannan	720,000	49.5	18.2
Conditions: IP softwood pulp A, 4.0 % NaOH, 90 °C, 100 psig oxygen, 0.2 % $MgSO_4$, 60 minutes.			

The selectivity plot in Figure 6.3 shows the results of oxygen delignification experiments with different charges of galactomannan added, at an alkali charge of 2.5 % NaOH at 90 °C, and reaction times of 10, 20, and 60 minutes. Without significantly

affecting the Kappa number, increasing charges of galactomannan gave higher intrinsic viscosities. The largest improvement, about 50 mL/g, occurred at the highest galactomannan charge tested, 2.0 % on pulp. The improvements increased with increasing reaction times or degree of delignification, and with increasing galactomannan charge.

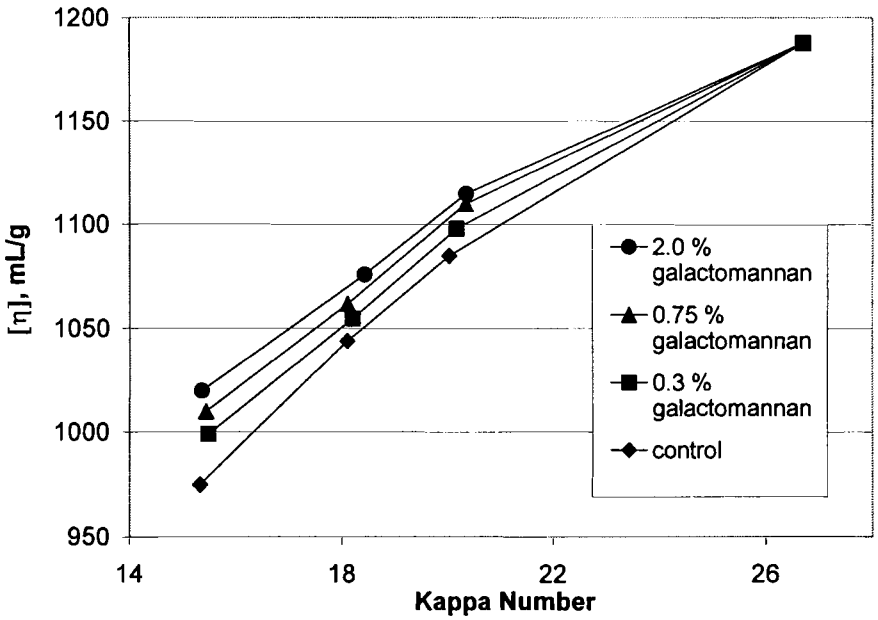

Figure 6.3. Effect of galactomannan charge on oxygen delignification selectivity, 2.5 % NaOH and 90 °C (t = 0, 10, 20, and 60 min.)

6.3.2. Effect of Galactomannan and Temperature

Figure 6.4 shows the effect of temperature on the oxygen delignification selectivity of the control experiments and with 2.0 % galactomannan addition. The temperature increase from 90 °C to 120 °C had no significant impact on the viscosity at a given Kappa number, or on the selectivity improvement with 2.0 % galactomannan.

Although a higher temperature achieved more lignin removal at a fixed reaction time, the intrinsic viscosity at a given Kappa number was not affected by temperature.

Agarwal (1999) and Berry and co-workers (2002) also found that the temperature did not affect the selectivity, although earlier kinetic studies by Olm and Teder (1979) and Iribarne and Schroeder (1997) determined higher activation energies for cellulose degradation than for delignification. The lack of a significant temperature effect is an important result, because in a mill it is easier to increase the temperature than the reaction time to extend delignification.

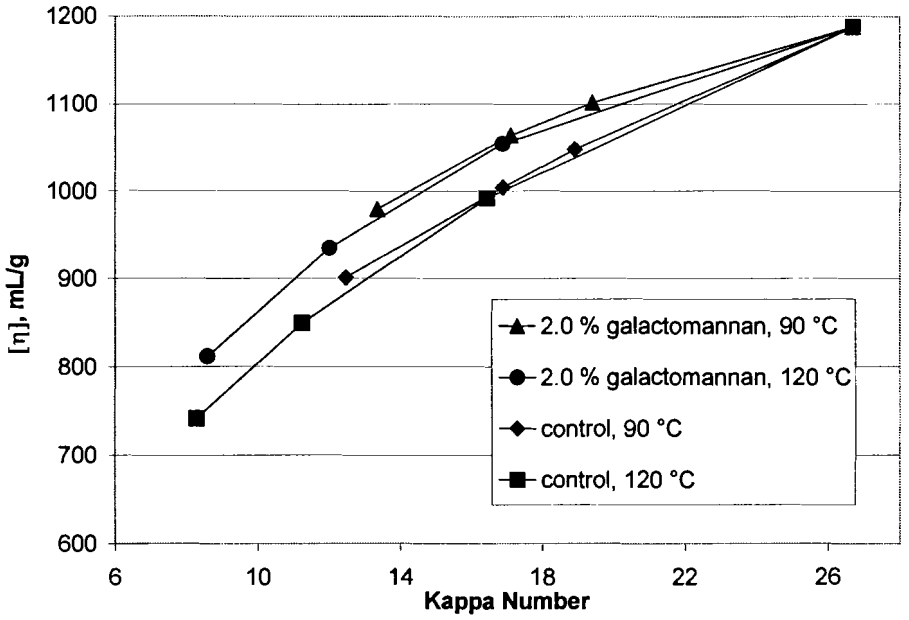

Figure 6.4. Effect of temperature and 2.0 % galactomannan charge on oxygen delignification selectivity (t = 0, 10, 20, and 60 min.)

6.3.3. Effect of Galactomannan and Alkali Charge

Figure 6.5 shows the effect of varying the alkali charge from 1.5 % NaOH to 4.0 % NaOH. Higher alkali charges gave a larger decrease in viscosity at the same Kappa number. This indicates that increasing alkali charge decreases oxygen delignification selectivity. Most evidence from other studies supports this finding. Berry and co-workers (2002) and Agarwal (1999) observed a lower selectivity at higher alkali charges,

and the aforementioned studies by Olm and Teder (1979) and Iribarne and Schroeder (1997) listed a higher dependence on the hydroxyl ion concentration for cellulose degradation than for delignification (Table 2.1). The positive effect of galactomannan on the selectivity was observed at both alkali charges.

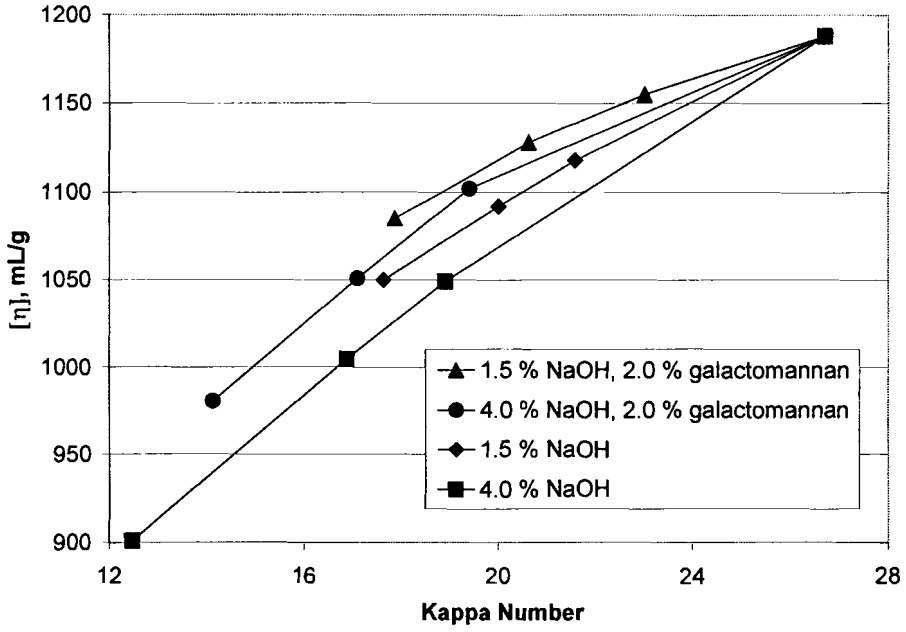

Figure 6.5. Effect of alkali charge and 2.0 % galactomannan addition on oxygen delignification selectivity (t = 0, 10, 20, and 60 min.)

6.3.4. Effect of Galactomannan on Kappa Number and Viscosity Tests

Experiments were conducted to determine the effect of galactomannan on the pulp Kappa number and viscosity tests. This was done in order to determine how much the test results were impacted by the presence of galactomannan rather than due to the reactions occurring during the delignification process. Table 6.4 gives the average of duplicate test results with galactomannan added at 1.0 %, 2.0 %, and 3.0 % of the total mass of the pulp mixture. The presence of galactomannan had a larger effect on the intrinsic viscosity than it did on the Kappa number, since the viscosity decreased by

about 2.5 %, while the Kappa number only decreased by about 1.0 % at the maximum galactomannan addition level of 3.0 %. This means that the viscosity and selectivity improvements observed after oxygen delignification with the addition of galactomannan are slightly reduced due to the presence of adsorbed galactomannan, which mostly acts as a diluent in the viscosity test.

Table 6.4. Effect of galactomannan on pulp intrinsic viscosity and Kappa number tests

Galactomannan Added:	0 %	1.0 %	2.0 %	3.0 %
Intrinsic Viscosity, mL/g	1172	1156	1151	1143
Kappa Number	26.04	25.93	25.83	25.77

6.3.5. Effect of Galactomannan on Oxygen Reaction Selectivity

Figure 6.6 is the modified selectivity plot showing the number of cellulose chain scissions versus the change in Kappa number during oxygen delignification at 90°C. The selectivity improvements by adding 0.3 %, 0.75 %, and 2.0 % galactomannan on pulp are shown by the lower-sloped lines.

As discussed in Section 5.6, the Kappa number decreases shown in Figure 5.6 (and now Figure 6.6) are the combined result of lignin removal by oxygen-mediated reactions and the dissolution of residual lignin by alkali extraction as well. As before, we have conducted alkali extraction reactions to separate these effects. Table 6.5 summarizes the alkali extraction experiments for samples containing galactomannan. Neither the Kappa number nor the intrinsic viscosity during alkali extraction experiments were significantly affected by these charges of galactomannan; but the viscosity was decreased slightly, similarly to the results shown in Table 6.4.

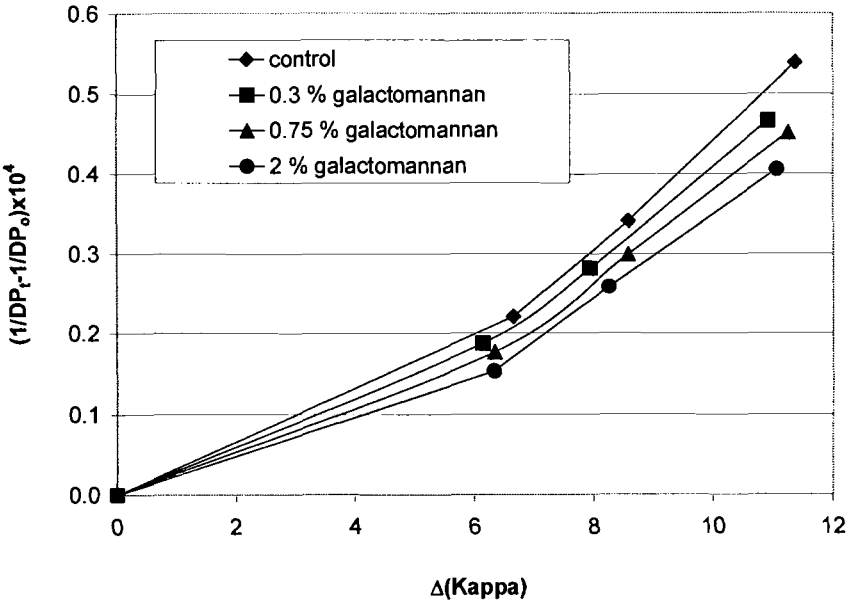

Figure 6.6. Effect of galactomannan charge on oxygen delignification selectivity, 2.5 % NaOH (t = 0, 10, 20, and 60 min.)

Table 6.5. Summary of alkali extraction experiments with galactomannan, conducted under 100 psig nitrogen and 90 °C

Conditions:	Kappa Number	Intrinsic Viscosity, mL/g
1.5 % NaOH, 60 min	25.58	1161
1.5 % NaOH, 60 min, 0.3 % galactomannan	25.71	1165
1.5 % NaOH, 60 min, 0.75 % galactomannan	25.66	1152
1.5 % NaOH, 60 min, 2.0 % galactomannan	25.84	1148
Original pulp: viscosity = 1188 mL/g, Kappa number = 26.7		

As before, the initial Kappa number and initial intrinsic viscosity were corrected to the corresponding values obtained by alkali extraction experiments. The adjusted changes in Kappa number and 1/DP for oxygen delignification experiments at alkali charges of 1.5 %, 2.5 %, and 4.0 % are plotted in Figures 6.7, 6.8, and 6.9, respectively. The plots contain reaction times of 0, 10, 20, and 60 minutes, and galactomannan charges of 0 %, 0.30 %, 0.75 %, and 2.0 % on pulp. The lines with smaller slopes represent more selective delignification.

The data presented in this format again show a direct linear relationship between the adjusted Kappa number change and the number of cellulose chain scissions for experiments conducted with and without galactomannan addition. As with the uncorrected selectivity plots presented in Chapter 5, Figures 6.3 to 6.6 had lower slopes at the beginning of the delignification, then became steeper with time, giving the appearance that the selectivity was decreasing. Again, the corrected selectivity plots no longer display this perceived change in selectivity. The linear shape of the corrected graphs indicates that the rate of attack of harmful radicals on cellulose is directly proportional to the rate of delignification as shown in Chapter 5.

The reduction in cellulose degradation with increasing galactomannan charge can be explained by the shielding effect of the adsorbed galactomannan, which decreases the attack on cellulose by the radicals. Comparison of the results in Figures 6.7 to 6.9 also shows that the oxygen reactions are more selective at a lower alkali charge, since the slopes of the control experiments decrease from 0.071 to 0.052 (x 10^4) as alkali charge is varied from 4.0 % to 1.5 %. The galactomannan addition leads to an improvement in selectivity for all the conditions of alkali tested. For example, the slope in Figures 6.7 to 6.9 decreases about 30 % relative to the control for all three levels of alkali at a galactomannan charge of 2.0 %. The galactomannan addition is most effective up to addition levels of about 0.75 % on pulp. The incremental selectivity improvement by increasing the charge from 0.75 % to 2.0 % is significantly smaller.

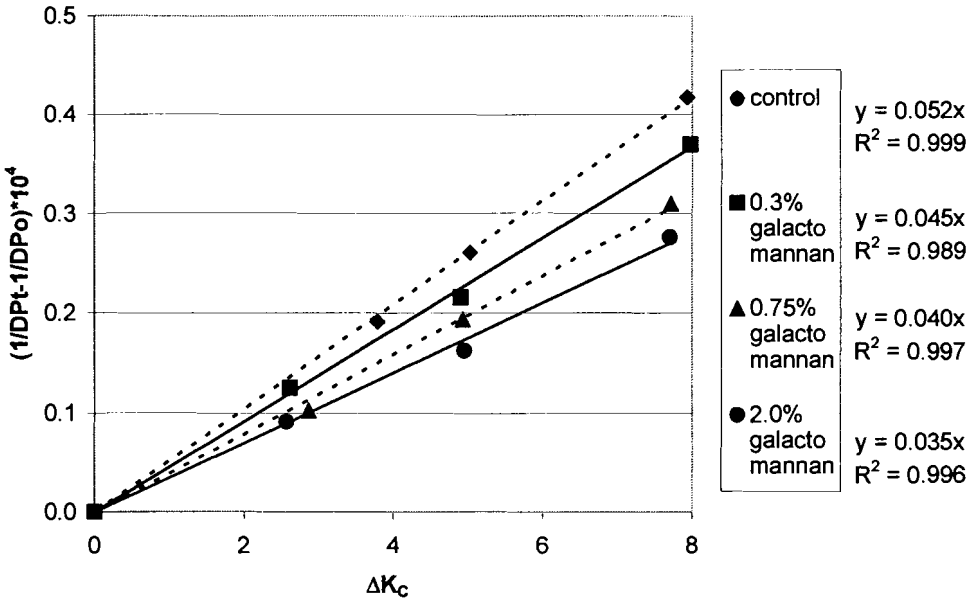

Figure 6.7. Effect of galactomannan charge on oxygen reaction selectivity during delignification, corrected for alkali extraction, 1.5 % NaOH and 90 °C

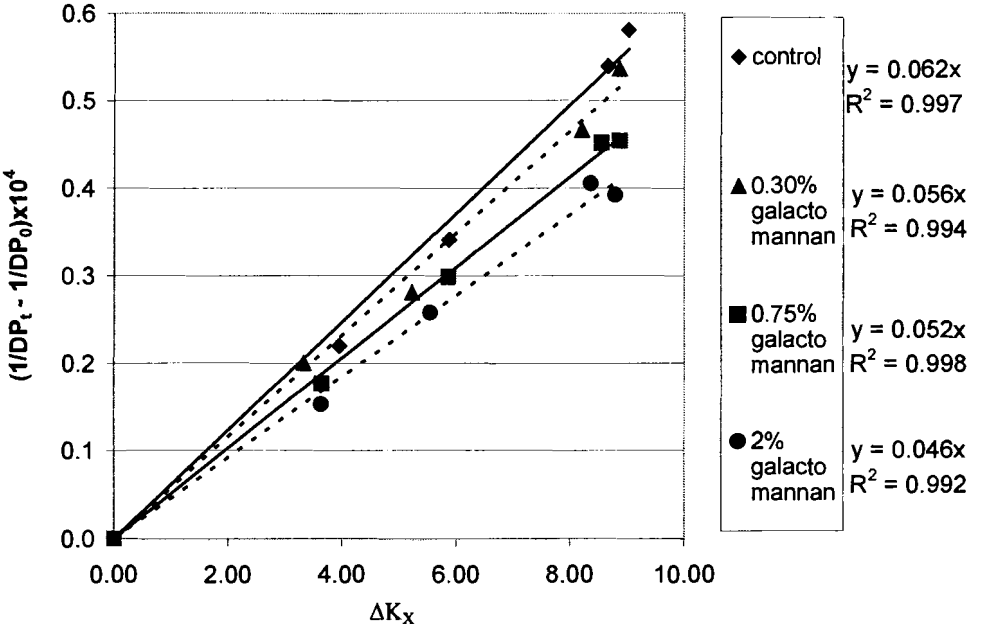

Figure 6.8. Effect of galactomannan charge on oxygen reaction selectivity during delignification, corrected for alkali extraction, 2.5 % NaOH and 90 °C

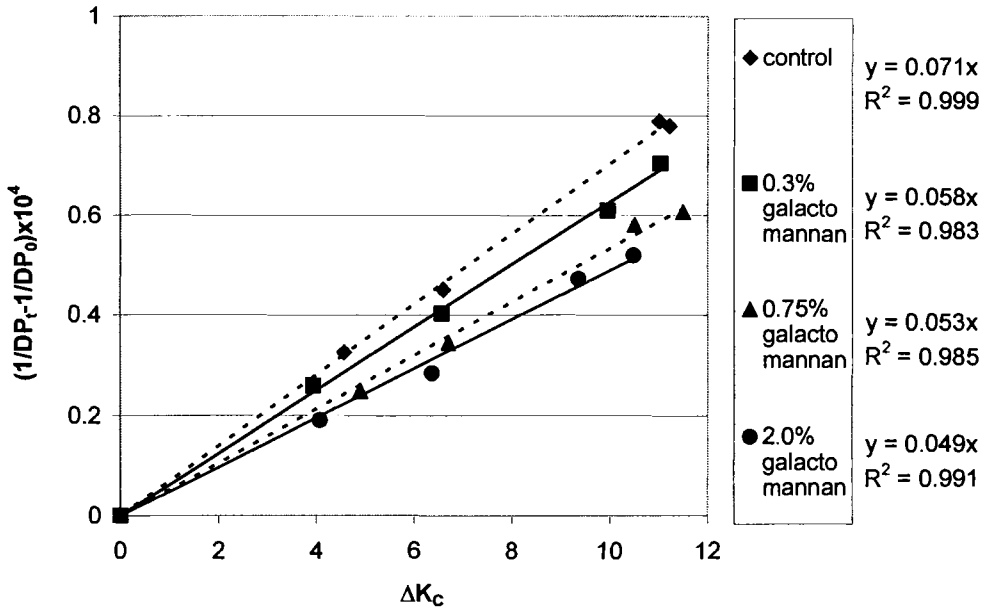

Figure 6.9. Effect of galactomannan charge on oxygen reaction selectivity during delignification, corrected for alkali extraction, 4.0 % NaOH and 90 °C

Figure 6.10 shows the corrected selectivity plot showing the effect of temperature as well as galactomannan charge on the experiments shown in Figure 6.4. This corrected plot also shows a linear relationship between cellulose degradation and lignin removal regardless of temperature or galactomannan addition. The addition of 2.0 % galactomannan also had the same effect on the selectivity at both temperatures, a selectivity parameter increase of 44 % to 46 %.

The corrected selectivity parameter for experiments conducted for 60 minutes at alkali charges from 1.5 % to 5.0 % with galactomannan charges varying from 0 % to 2.0 % are given in Figure 6.11. As previously, this selectivity parameter is the reciprocal of the slope from the oxygen reaction selectivity plots. This graph illustrates more

clearly that galactomannan is more effective as a cellulose protector at low addition levels, and that the selectivity increases substantially at lower alkali charges.

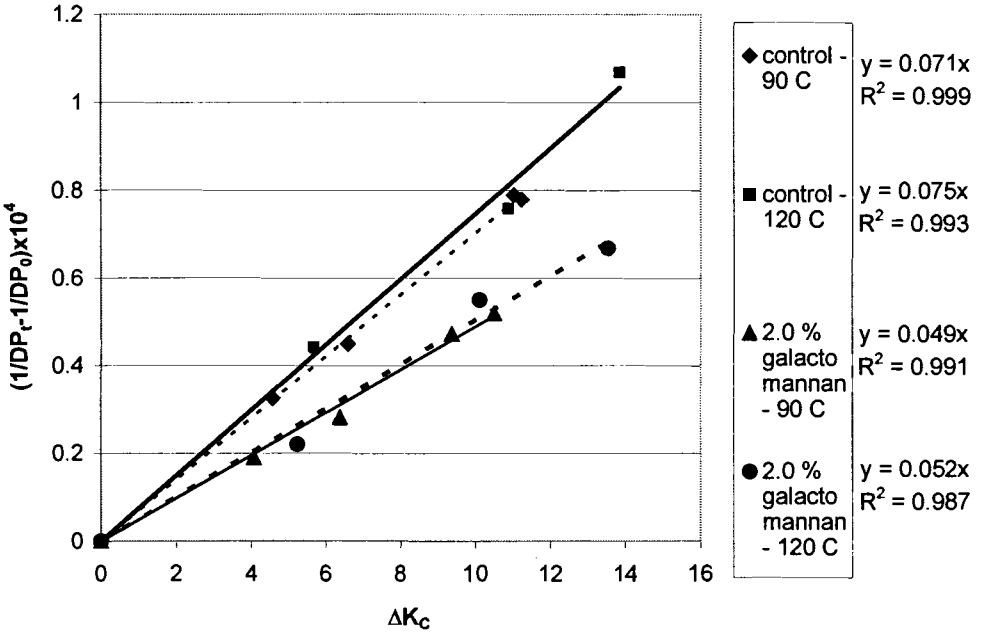

Figure 6.10. Effect of temperature and 2 % galactomannan on oxygen reaction selectivity, 4 % NaOH

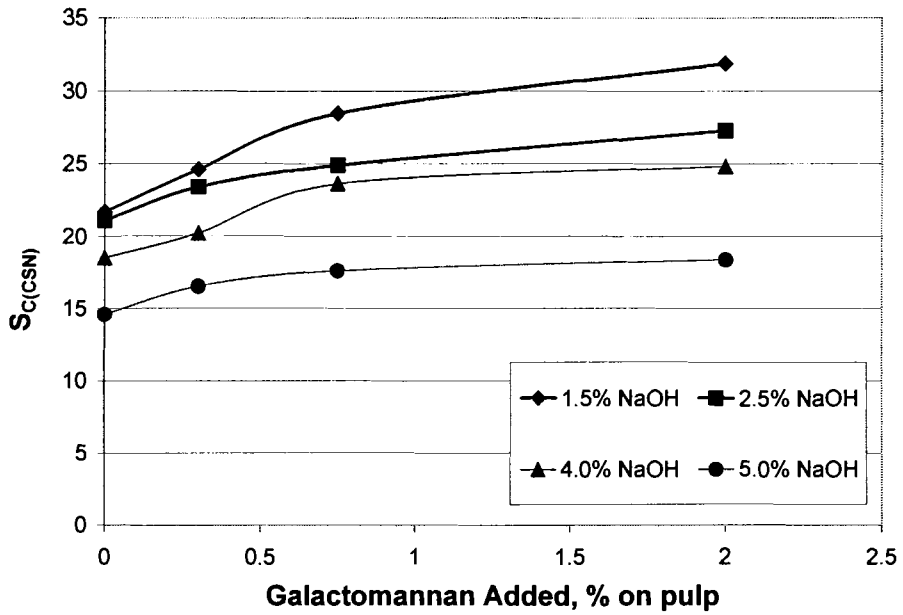

Figure 6.11. Effect of galactomannan charge on the oxygen reaction selectivity parameter (5.0 % NaOH results based on data obtained for only 60 minute reaction times)

6.3.6. Adsorption of Galactomannan on Pulp

The hypothesis of this investigation is that a polymeric radical scavenger will be most effective if it adsorbs on pulp at oxygen delignification conditions. Adsorption amounts of galactomannan on pulp at varying addition concentrations were measured gravimetrically. Figure 6.12 gives the results of these measurements when the pulp was equilibrated at 60°C under neutral and alkaline conditions. In these experiments, the dissolved liquor solids were measured for samples of pulp with and without galactomannan addition. While this method is useful for additive prescreening on adsorption, the method has disadvantages. The adsorption is performed at a lower temperature than during oxygen delignification, and the samples have not undergone actual delignification. Also, it is difficult to obtain accurate data at alkaline conditions because of dissolution of solid material from the pulp.

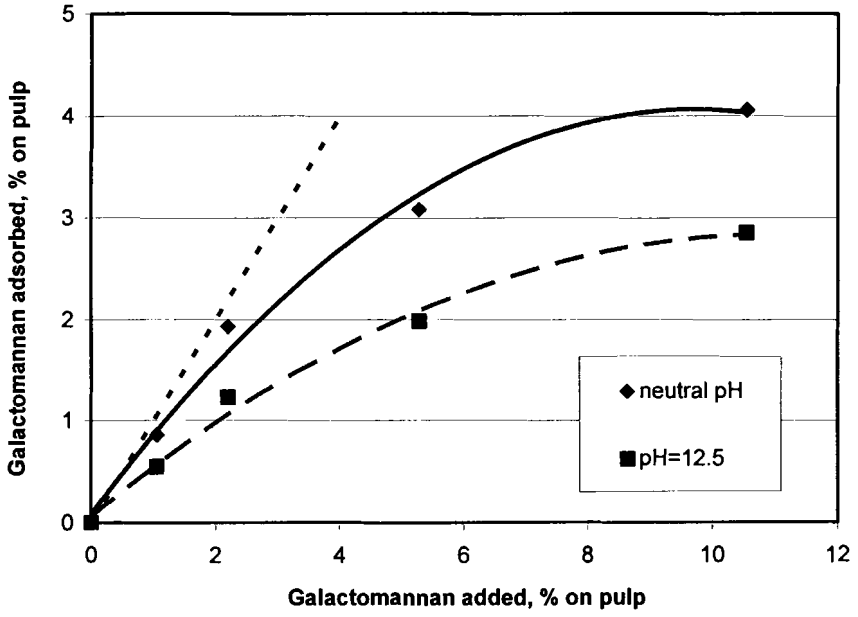

Figure 6.12. Adsorption of galactomannan on pulp, at neutral and alkaline pH, determined gravimetrically

The results in Figure 6.12. show almost complete adsorption of galactomannan at low addition levels and neutral pH, while at high charges a plateau level is approached. The adsorption of galactomannan at a high pH is much more appreciable than that of the starches and CMC's previously tested. The level of galactomannan adsorption at 12.5 pH increases to 2 % at charges of 5 % and approaches a plateau around 3.0 % on pulp at about 10 % charge; whereas even at 10 % addition rates, neither starch nor CMC reached an adsorbed charge of one percent.

6.3.7. Adsorption of Galactomannan on Pulp by H.P.A.E.C.

The adsorption of galactomannan on pulp samples that have actually undergone oxygen delignification were determined by H.P.A.E.C. First, the monosugar masses of the hydrolyzed pulp samples were measured by H.P.A.E.C., then the adsorbed amounts of galactomannan were calculated from the mannan and galactan mass fractions. The mass fractions in sugar analysis are based on the weight of the polysaccharides only, not the whole pulp weight. The procedures for the preparing and running the chromatography samples are detailed in Section 3.12.2 and Appendix A. Appendix D contains some of the H.P.A.E.C. data, sample calibrations, sugar analysis calculations, and adsorption calculations. The areas of the chromatography peaks are related to the mass fractions of the different mono-sugars by the determined calibration curves shown in Appendix D (Figures D.1 to D.5). Then the mass fractions of polysaccharides are determined, and from these values the adsorbed additive charge is calculated. For a pulp sample with an adsorbed polysaccharide consisting of two mono-sugars such as galactomannan, the percentage of adsorbed additive is given as:

$$A_a = \frac{x_m - x_p + y_m - y_p}{1 - x_m - y_m} \cdot (\%\ \text{Polysaccharides}) \qquad (6\text{-}1)$$

where x_m and y_m are the mass fractions of the measured components in the sample containing adsorbed polymer, and x_p and y_p are the mass fractions in the control sample with no polymer adsorbed. If there is only one monosugar increasing in the adsorbed sample, then the y terms are eliminated in the expression. The % polysaccharides is the weight percentage of polysaccharides of the total pulp weight. A derivation of this equation is given in Appendix D.

Table 6.6 summarizes the sugar profiles of the IP pulp A described previously in Table 4.1., showing duplicate sugar profiles for the brown stock pulp and delignified samples containing no additive and galactomannan charges of 0.30, 0.75, and 2.0 % on pulp. The column on the right is the percentage of polysaccharides in the pulp, which is the total pulp mass minus the mass of lignin, extractives and ash content. These calculations are shown in Appendix D.

The mass fractions of galactan and mannan shown in Table 6.6 increase with increased galactomannan addition. This indicates that the galactomannan was permanently absorbed on the pulp, because it is still present after oxygen delignification and two subsequent washings at 1 % consistency.

The sugar profiles also increase in glucose mass fraction and decrease in hemicellulose mass fractions after oxygen delignification (compare IP pulp A with control in Table 6.6), which indicates that hemicelluloses are removed more easily than

cellulose. This may be because of the difference in molecular weight of the cellulose and hemicellulose as well as their difference in chemical reactivity.

Table 6.6. Summary of H.P.A.E.C. monosugar profiles and galactomannan adsorption (IP pulp A, 2.5 % NaOH, 60 minutes, 90 °C)

	Mass fractions (of polysaccharides):					% Poly-Saccharides
	Arabinan	Galactan	Glucan	Xylan	Mannan	
IP pulp A	0.00561	0.00432	0.851	0.0576	0.0812	
IP pulp A	0.00556	0.00518	0.853	0.0588	0.0797	96.1
Control	0.00529	0.00315	0.858	0.0548	0.0787	
Control	0.00516	0.00318	0.861	0.0524	0.0779	97.4
0.3 % Galactomannan	0.00540	0.00406	0.851	0.0578	0.0801	
0.3 % Galactomannan	0.00525	0.00452	0.855	0.0551	0.0794	97.6
0.75 % Galactomannan	0.00538	0.00598	0.849	0.0560	0.0816	
0.75 % Galactomannan	0.00551	0.00545	0.850	0.0556	0.0853	97.3
2.0 % Galactomannan	0.00540	0.00683	0.845	0.0555	0.0883	
2.0 % Galactomannan	0.00511	0.00643	0.844	0.0545	0.0848	97.5

Adsorption Calculation:

Charge Added, % on Pulp	Avg. % increase in galactan	Avg. % increase in mannan	% increase in mannan and galactan, based on polysaccharide fraction	% increase, based on pulp weight (Adsorbed %)
0 (control)	0	0	0	0
0.3	0.121	0.147	0.296	0.287
0.75	0.260	0.444	0.704	0.688
2	0.343	0.880	1.329	1.298

At the bottom of the table is an example calculation of adsorbed galactomannan charges from the average values of the mass fractions as calculated with equation 6-1. After the percent increases in mannan and galactan are calculated, they are corrected for the non-polysaccharide mass fraction The charge of adsorbed additive ([Aa]) then is given in the last column. The results of adsorption determined gravimetrically at pH 12.5 was lower than these results at 2.5 % NaOH (pH = 12.2), comparing charges of about 1.0 % to 1.3 % on pulp at the addition level of 2.0 % galactomannan on pulp.

Figure 6.13 shows isotherm curves for galactomannan adsorbed on pulp determined by H.P.A.E.C. on pulp samples that were oxygen delignified at 1.5 %, 2.5 % and 4.0 % NaOH. These isotherms have the same shape as the one determined gravimetrically in Figure 6.12, since the curves show almost complete adsorption of galactomannan at low addition levels and gradually decreasing adsorption efficiency at higher charges. These results also show that the adsorption decreases slightly with increasing alkali charge.

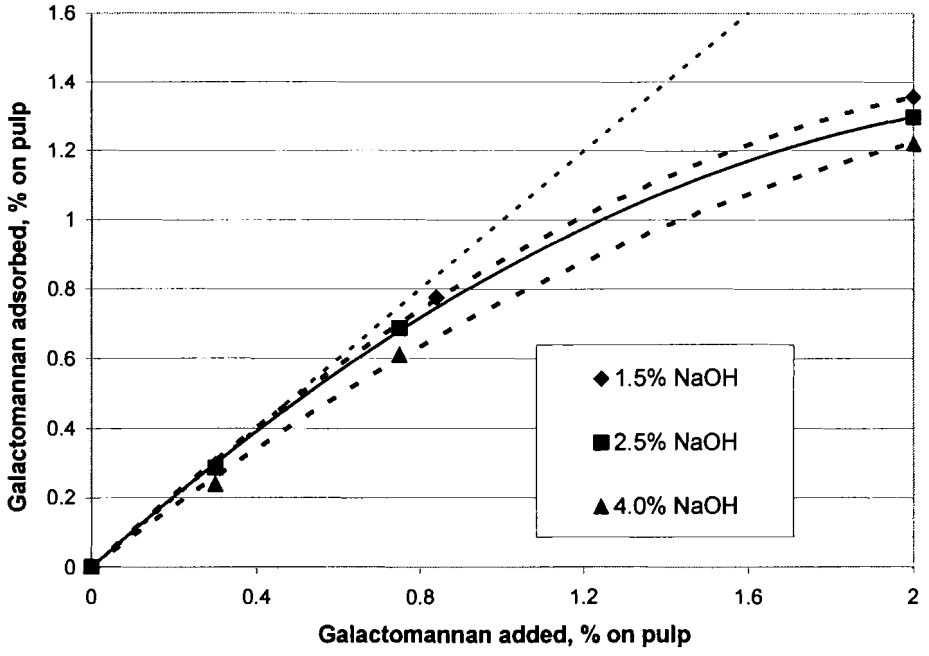

Figure 6.13. Adsorption on galactomannan on pulp at different alkali charges, determined by H.P.A.E.C.

Figure 6.14 shows a comparison of results obtained by the gravimetric and H.P.A.E.C. measurement methods, at two different alkali addition levels. Although the measurements were slightly higher by the H.P.A.E.C. method, all the points are close to the line Y=X, which would indicate perfect agreement. Since there are many differences

in these two procedures, including temperature and washing conditions, this degree of agreement is quite satisfactory.

6.3.8. Effect of Adsorbed Galactomannan

Figure 6.15 shows the relationship between lignin-free yield and the amount of galactomannan adsorbed on pulp determined by H.P.A.E.C. The lignin-free pulp yield is determined by subtracting the lignin mass from that of the pulp before and after delignification. The lignin mass percentage was taken as 0.15 times the Kappa number. It can be seen that the slope of the trend lines are close to 1, meaning that adsorption of galactomannan directly translates to a yield increase. The trend lines also suggest that increasing the alkali charge reduces the carbohydrate yield slightly, from 99.4 % to 98.9 % in the control experiments.

The adsorption curves in Figures 6.12 and 6.13 are similar in shape compared to the selectivity parameter curves in Figure 6.11. This suggests that improvements in selectivity are more dependent on the amount of galactomannan adsorbed on pulp than galactomannan added to the pulp. Figure 6.16 shows the oxygen reaction selectivity parameter plotted versus percentage of adsorbed galactomannan. Since the selectivity increases fairly linearly with galactomannan adsorption, this supports the present hypothesis that adsorption on pulp is beneficial for effective cellulose protection.

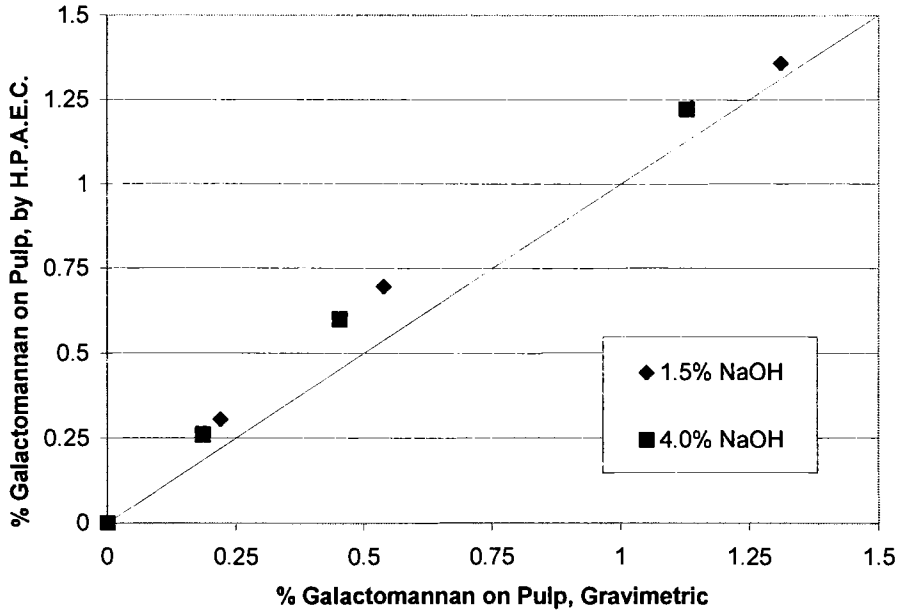

Figure 6.14. Comparison of galactomannan adsorption methods, gravimetric and H.P.A.E.C.

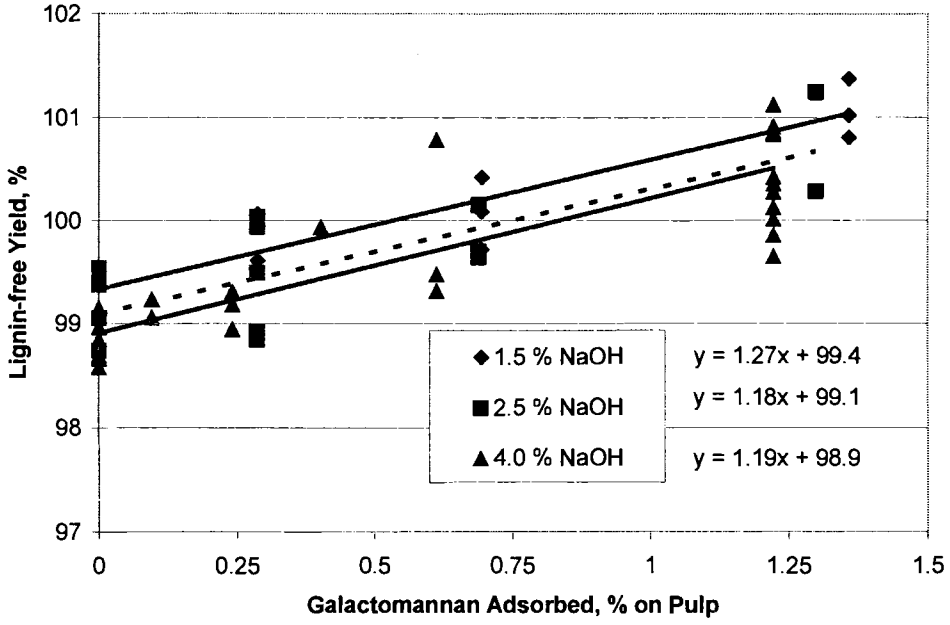

Figure 6.15. Effect of galactomannan adsorption on pulp yield (60 minutes and 90 °C)

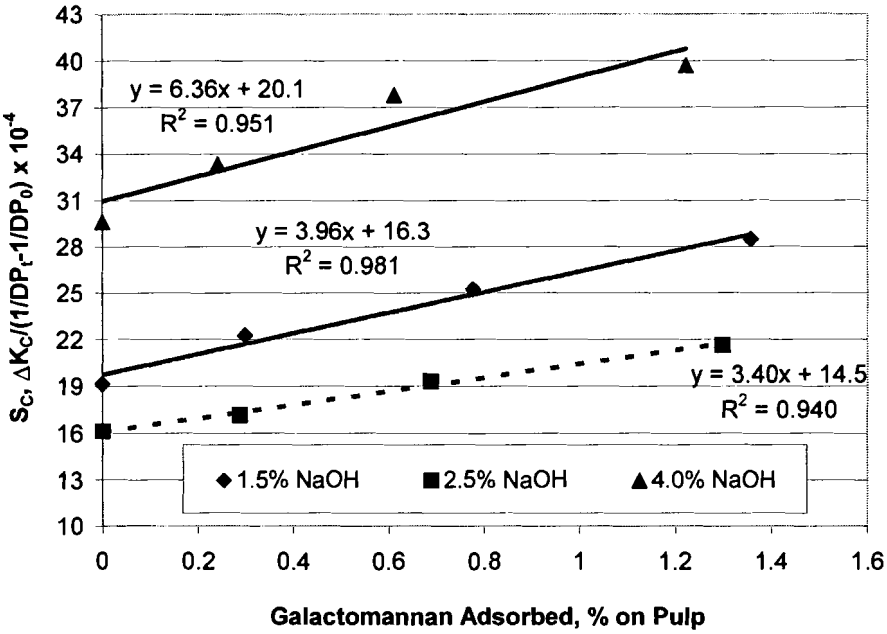

Figure 6.16. Effect of adsorbed galactomannan on the oxygen reaction selectivity parameter

6.3.9. Wet Zero Span Tensile Strength

Figure 6.17 shows the improvement in intrinsic fiber strength achieved with galactomannan at three charges of alkali and a reaction time of 60 minutes. The original pulp has a wet tensile breaking length of 15.3 km, which decreases to about 13.0 km or 13.5 km during the control experiments, depending on the alkali charge. At the highest level of galactomannan addition, the breaking length is improved to 13.8 km or 14.0 km respectively, a reduction in wet tensile strength loss of slightly less than 30 %.

Figure 6.18 shows the results of wet zero span tensile breaking length plotted versus the percentage of adsorbed galactomannan. Contrary to the linear behavior of the oxygen reaction selectivity parameter in Figure 6.16, the results in Figure 6.18 suggest that there is a level of galactomannan addition at which a maximum improvement in wet zero span tensile strength is obtained. This is caused by the effect that the wet zero span

of a pulp decreases with increasing galactomannan addition because on a weight basis the load is carried by a reduced number of fibers. The dotted line in the graph shows how the breaking length decreases for the original pulp with increasing galactomannan content.

Figure 6.19 shows the relationship between DP and wet zero span breaking length for pulp samples that were tested for wet zero span. This graph shows a nearly linear relationship. The degree of polymerization changes more appreciably than the wet zero span strength. While DP ranges from 3300 to 4700 units/polymer (40 %), the zero span ranges only from 13 to 14.2 (17 %).

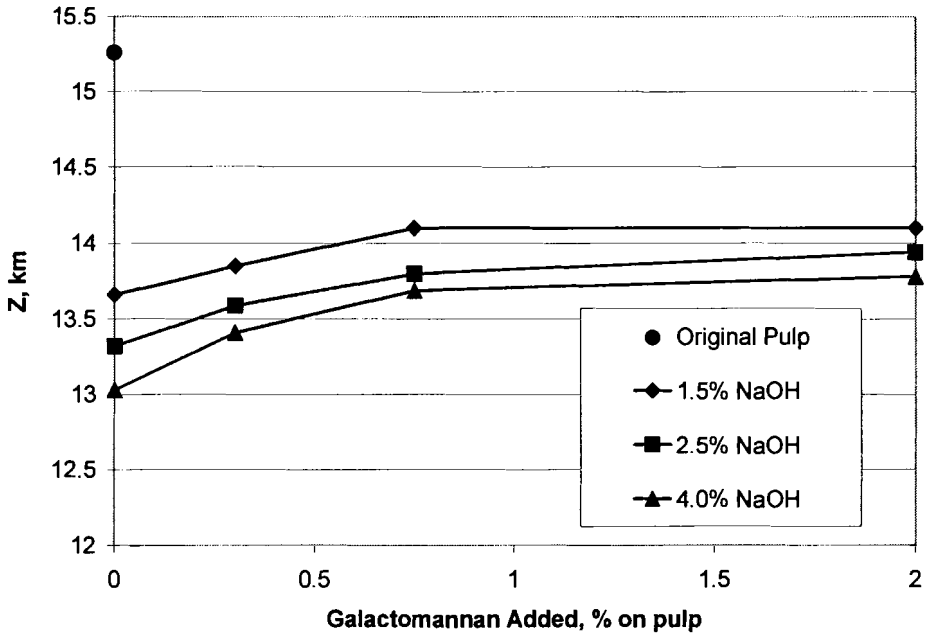

Figure 6.17. Effect of galactomannan charge on the wet zero span breaking length of oxygen delignified pulp, 60 minute experiments

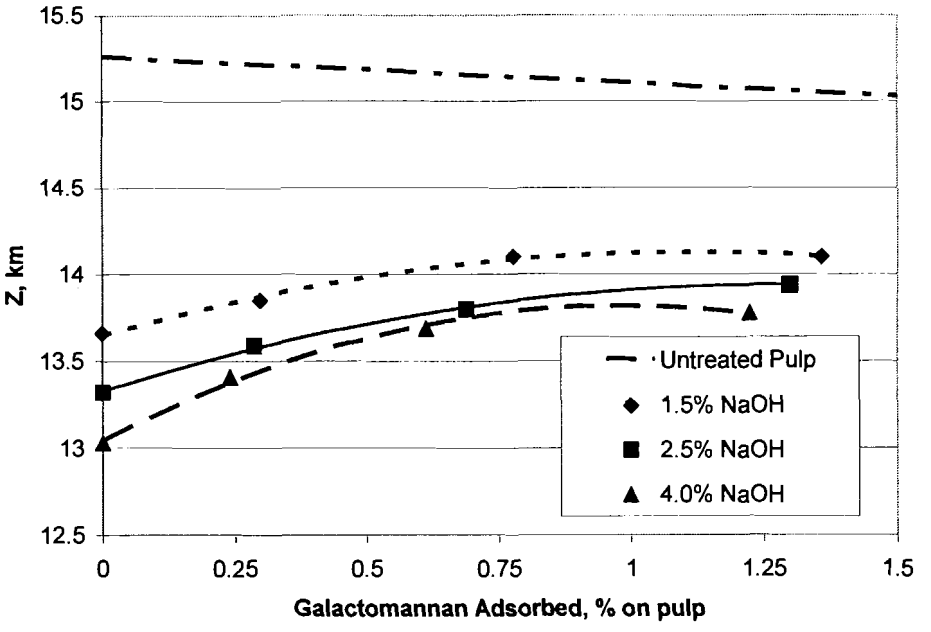

Figure 6.18. Effect of adsorbed galactomannan on the wet zero span breaking length, 60 minute experiments

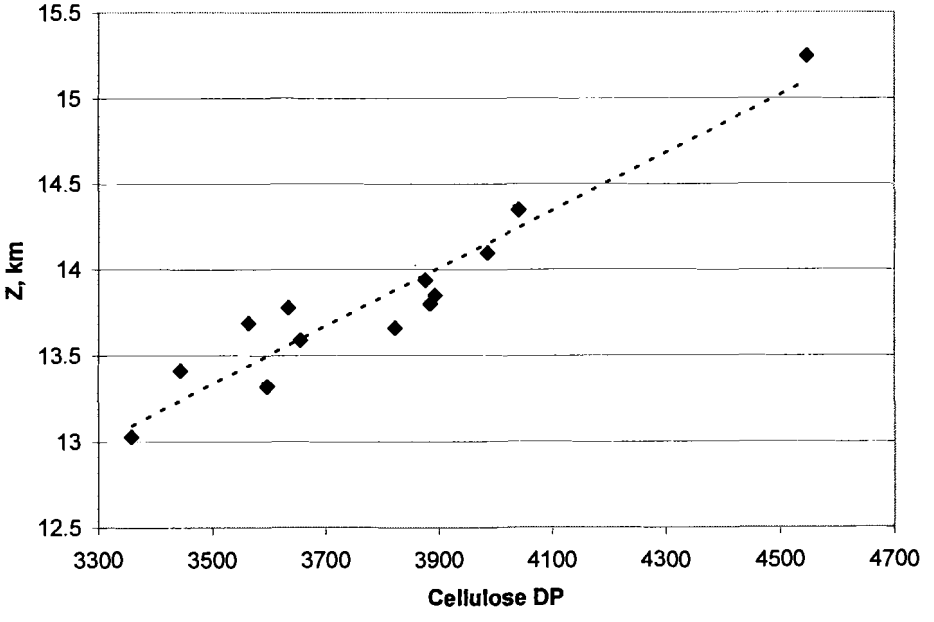

Figure 6.19. Wet zero span tensile strength (Z) versus cellulose degree of polymerization (DP)

6.4. GLUCOMANNAN AND XYLAN

6.4.1. Oxygen Delignification with Glucomannan and Xylan

Increases in oxygen delignification selectivity were obtained from experiments with galactomannan, as described in the preceding sections. Also, it has also been shown that pulps with higher hemicellulose content (Zou, 2002) resulted in higher oxygen delignification selectivity. Therefore, the remainder of this chapter focuses on two other hemicellulose-type polymers, glucomannan and xylan. Glucomannan is a major hemicellulose found in softwoods; and xylan, the major hardwood hemicellulose, was extracted from birch wood.

Experiments were conducted with glucomannan and xylan added to oxygen delignification. For these experiments a new IP pulp (IP pulp B) was used. The properties of Pulp B are compared to pulp A in Table 6.7. Pulp B has very similar properties to pulp A when comparing Kappa number, intrinsic viscosity, and total metals content, although Pulp B was lower in iron content. The sugar profiles were similar, with a 1 percent difference in glucan content.

Table 6.7. Properties of two Kraft softwood pulps (IP pulps A and B)

	Kappa #	Viscosity, mL/g	Fe ppm	Mn ppm	Mg ppm	Cu ppm
Pulp A	26.7	1188	30.5	23.8	370	27.4
Pulp B	28.0	1172	8.24	53.1	380	17.6

Sugar Analysis on Polysaccharides, % monosugar	Arabinan	Galactan	Glucan	Xylan	Mannan
Pulp A	0.559	0.475	85.1	5.82	8.05
Pulp B	0.680	0.695	83.5	6.75	8.38

For the experiments with glucomannan and xylan, the same conditions of 100 psig oxygen pressure and 90 °C as before were applied, and an alkali charge of 2.5 % NaOH on pulp. Figure 6.20 shows the results of these experiments for the control, and 2.0 % xylan, and 2.0 % glucomannan, at reaction times of 0, 10, 20, and 60 minutes. Similarly to the largest increase observed by the addition of galactomannan noted in Section 6.3.1, the most significant improvement in intrinsic viscosity was about 60 mL/g, at a 2.0 % glucomannan charge and 60 minutes reaction time. The addition of xylan did not give as much viscosity or selectivity improvement in these experiments.

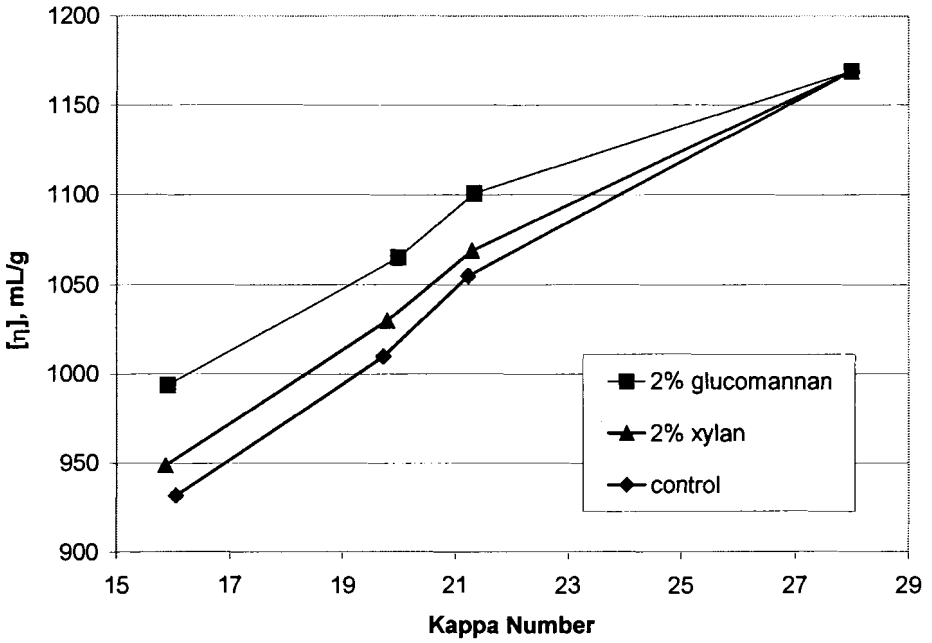

Figure 6.20. Effect of xylan and glucomannan addition on oxygen delignification, IP softwood pulp B (2.5 % NaOH and 90 °C)

Figure 6.21 shows the oxygen reaction selectivity for the data shown in Figure 6.20, corrected for alkali extraction. As before, the selectivity curves are linear, supporting the idea that the production of cellulose-degrading radicals is proportional to the number of lignin reactions taking place throughout the delignification. This graph

also shows the similar performance of glucomannan and galactomannan, as the charge of 2.0% additive gives close to a thirty percent decrease in slope, going from 0.064 to 0.046 (x 10^4) compared to 0.063 to 0.046 (x 10^4) in the corresponding galactomannan experiments.

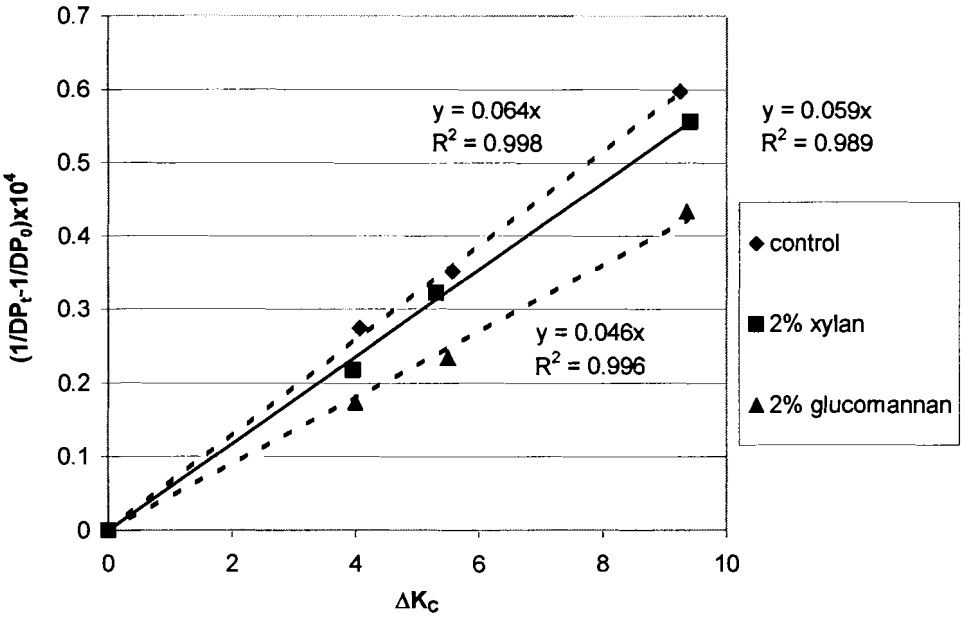

Figure 6.21. Effect of xylan and glucomannan adsorption on oxygen reaction selectivity, 2.5 % NaOH and 90 °C

The results of the delignification experiments with glucomannan and xylan on pulp B at a charge 2.5% NaOH are summarized in Table 6.8. This table also lists the results obtained with galactomannan on pulp A for comparison. The data shows a similar performance for glucomannan as an additive compared to galactomannan, because the selectivity parameter increased from about 16 to 22 in both cases. As expected, the results with xylan, however, did not exhibit a significant selectivity improvement. This

table also shows that pulps A and B have very similar oxygen reaction selectivity parameters.

Table 6.8. Summary of experiments with galactomannan, xylan, and glucomannan, 2.5 % NaOH and 90 °C

Initial Pulp	Experiment	Final Kappa #	% Kappa # Reduction	Final Intrinsic Viscosity, mL/g	Selectivity, $S_C \times 10^{-4}$
Pulp A Kappa# = 26.7 [η]=1188 mL/g	Control	15.3	42.7	962	16.2
	0.3 % galactomannan	15.6	41.5	990	17.3
	0.75 % galactomannan	15.5	42.0	1011	19.2
	2.0 % galactomannan	15.6	41.5	1024	21.7
Pulp B Kappa# = 28.0 [η]=1172 mL/g	Control	16.0	42.9	932	15.7
	0.3 % xylan	16.2	42.1	941	16.0
	0.75 % xylan	16.2	42.1	945	16.6
	2.0 % xylan	15.9	43.2	949	17.0
	0.3 % glucomannan	16.0	42.9	962	16.9
	0.75 % glucomannan	16.1	42.5	989	19.1
	2.0 % glucomannan	15.9	43.2	994	21.6

6.4.2. Adsorption of Glucomannan and Xylan on Pulp

Adsorption amounts of glucomannan and xylan on pulp at varying addition concentrations were measured gravimetrically, as previously when the pulps were equilibrated at 60°C under neutral and alkaline conditions and 10% consistency. Figure 6.22 shows the adsorption curves for xylan and glucomannan at an alkaline pH of 12.5.

At the lower addition rate (up to 0.75%), nearly all the glucomannan was adsorbed on the pulp, whereas a significantly smaller amount of xylan adsorbs on the pulp at all levels of addition.

As done with galactomannan, the adsorption of glucomannan and xylan was also measured by H.P.A.E.C. The sugar profiles and adsorption results are given in Table 6.9.

Following the sugar profiles in the top half of the table, a comparison of methods of determination is included with the adsorption results for both glucomannan and xylan.

For glucomannan, it was very difficult to measure the mass fraction increase in glucan because of the predominance of this component in pulp. The denominator in the equation used to calculate adsorbed charges by mass fraction differences (equation 6-1) becomes very small when the majority of mass fraction is subtracted from one.

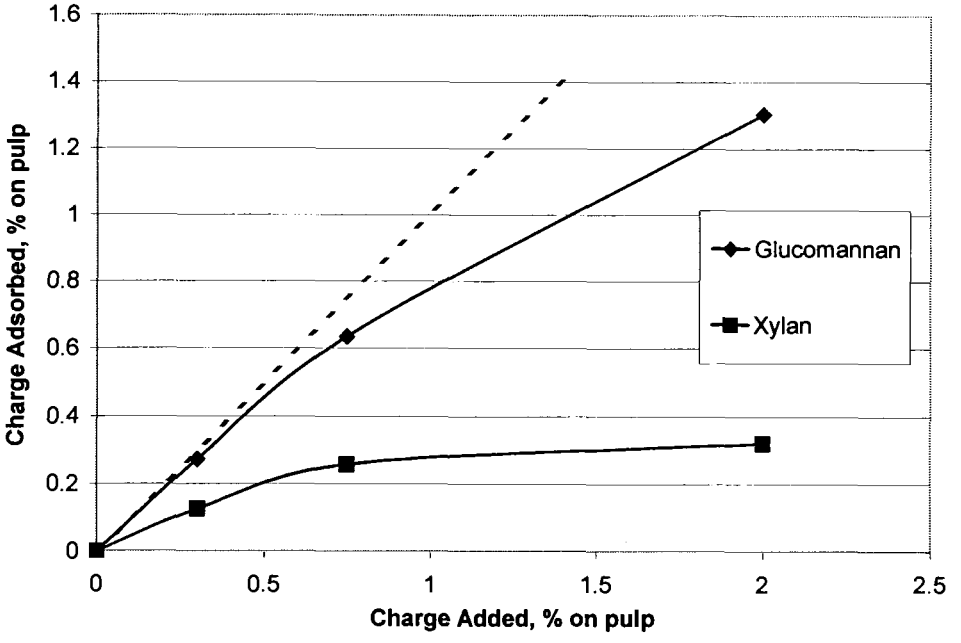

Figure 6.22. Adsorption on glucomannan and xylan on pulp at pH = 12.5, determined gravimetrically

Table 6.9. Summary of H.P.A.E.C. monosugar profiles and adsorption of glucomannan (GM) and xylan (X), (IP pulp B, 2.5 % NaOH, 60 minutes, 90 °C)

	Mass fractions (of polysaccharides):					% Poly-Saccharides
	Arabinan	Galactan	Glucan	Xylan	Mannan	
Pulp A avg.	0.00559	0.00475	0.851	0.0582	0.0805	96.1
Pulp B avg.	0.00680	0.00695	0.835	0.0675	0.0838	95.8
Control	0.00662	0.00877	0.832	0.0652	0.0877	97.3
Control	0.00848	0.00972	0.829	0.0648	0.0879	
0.3 % GM	0.00665	0.00834	0.829	0.0651	0.0910	97.4
0.3 % GM	0.00698	0.00821	0.831	0.0649	0.0886	
0.75 % GM	0.00713	0.00891	0.834	0.0603	0.0918	97.2
0.75 % GM	0.00536	0.00752	0.831	0.0647	0.0914	
2.0 % GM	0.00674	0.00760	0.832	0.0586	0.0947	97.8
2.0 % GM	0.00566	0.00504	0.833	0.0594	0.0974	
0.3 % X	0.00794	0.00895	0.830	0.0656	0.0879	97.5
0.3 % X	0.00792	0.00911	0.826	0.0627	0.0941	
0.75 % X	0.00707	0.00973	0.826	0.0684	0.0892	97.9
0.75 % X	0.00656	0.00850	0.832	0.0651	0.0878	
2.0 % X	0.00583	0.00499	0.829	0.0717	0.0881	97.6
2.0 % X	0.00739	0.00931	0.830	0.0694	0.0841	

Adsorption Calculations for Glucomannan:

Charge Added, % on Pulp	Avg. increase in glucan fraction	Avg. increase in mannan fraction	% increases by glucan and mannan, based on pulp weight (Adsorbed %)	% increases by mannan, based on pulp weight (Adsorbed %)	% increase, gravimetrically based on pulp (Adsorbed %)
0 (control)	0	0	0	0	0
0.3	0.00000	0.00203	0.217	0.325	0.273
0.75	0.00204	0.00378	1.57	0.604	0.636
2	0.00197	0.00827	2.01	1.312	1.304

Adsorption Calculations for Xylan:

Charge Added, % on Pulp	Avg. increase in xylan fraction	% increase by xylan, based on pulp weight (Adsorbed %)	% increase, gravimetrically, based on pulp (Adsorbed %)
0 (control)	0	0	0
0.3	0.00000	0	0.126
0.75	0.00175	0.186	0.258
2	0.00556	0.591	0.361

In order to measure a small increase in glucan such as 0.005 mass fraction on pulp (or 0.5 %), it is necessary to detect mass fraction differences less than 0.001 mass fraction. It is impossible to do this accurately since it requires a fourth significant decimal in mass fraction. The results for calculation of glucomannan adsorption by mannan and glucan fractions are included in Table 6.9 and then compared to the results by mannan fraction alone and taking a mannan fraction of 0.61 in the glucomannan as determined by H.P.A.E.C. Also shown are the results determined gravimetrically. The agreement between the H.P.A.E.C. results by mannan and gravimetrically was much better than when the glucan content was used. The use of glucan resulted in some estimations even higher than the additive charge.

The results H.P.A.E.C. adsorption results for xylan are shown in Table 6.9 at the bottom then compared to the gravimetric results as well. The results show a poor agreement between the two methods, particularly at the lowest charge of 0.3 % added on pulp, where no adsorption was detected. Since the gravimetric determination proved more reliable in this case, further results containing the adsorption of xylan will be based on this method rather than by H.P.A.E.C.

6.4.3. Effect of Adsorbed Glucomannan and Xylan

Figure 6.23 displays the selectivity data from Table 6.8 plotted against the adsorbed amount of galactomannan, glucomannan, and xylan. These three plots are all essentially linear, much like the selectivity parameter versus galactomannan plotted in Figure 6.16. The two lines for glucomannan and galactomannan nearly overlap with slopes of 4.0 and 4.3. Although the curve for xylan is much shorter than the other two

curves due to the relatively small amounts of xylan adsorbed, it exhibits the same slope as the curves for galactomannan and glucomannan. The y-intercepts of the two lines are slightly different because the selectivity parameters of the control experiments are 16.2 for pulp A and 15.7 for pulp B. Based on the chemical similarity of these three polymers, it is to be expected that their ability to scavenge radicals will be the same. Therefore, the equivalent slopes in Figure 6.23 confirm that the cellulose protection will be the same amongst these hemicellulose-type polymers provided they are adsorbed.

These results also suggest that it may be beneficial to maximize the hemicellulose retention during pulping for improved oxygen delignification selectivity. Finally, they indicate the potential of more economical additives if they are made to adsorb on pulp at oxygen delignification conditions.

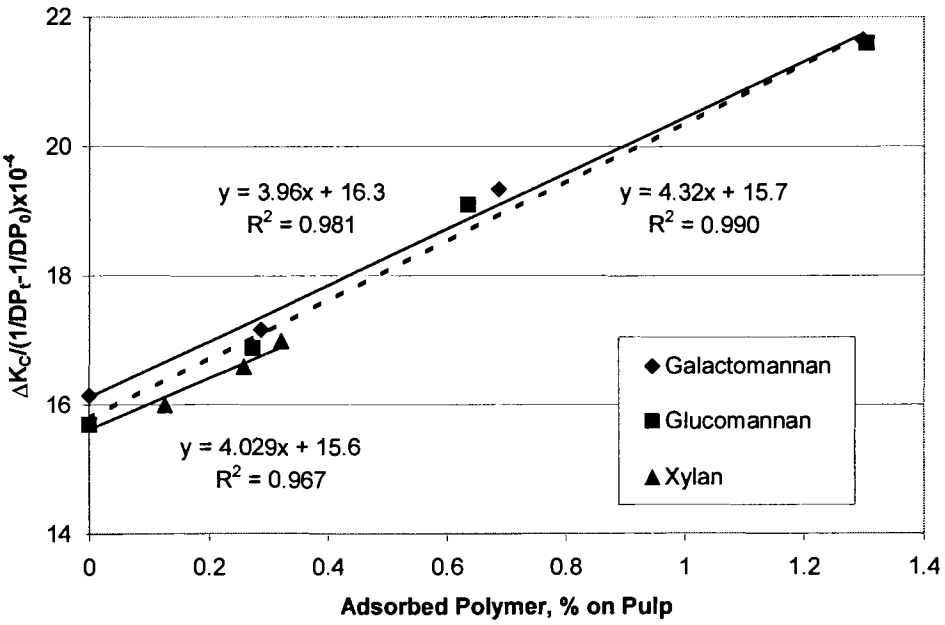

Figure 6.23. Effect of adsorbed polymers on oxygen reaction selectivity (pulp A used for galactomannan, pulp B used for xylan and glucomannan)

Chapter 7

MATHEMATICAL MODELING OF EXPERIMENTAL RESULTS

7.1. INTRODUCTION TO MODELING AND STATISTICS

The objective in this chapter is to find the best mathematical expressions to describe the experimental results. The general solution in determining an appropriate model is to postulate a function for the dependence of Y on the independent variables x_p, ($Y = f(x_1,x_2,x_3\ldots)$), by determining the parameters (b_1, b_2, $b_3\ldots$) for that model that minimize the sum of the squared deviations, S:

$$S = \sum (Y_i - f(x_1, x_2, x_3, \ldots)_i)^2 \qquad (7\text{-}1)$$

between the predicted values, f, and the actual experimental values, (Y_1 to Y_n). The expression in equation 7.1 is known as a regression function because it gives a measure of how much the predicted values differ from the actual data. In the present study, this is done by iterative methods using computer software in Microsoft Excel 2002 and MathCad version 2001i. The agreement between the prediction function and the experimental data may be evaluated by statistical measurements. These statistical measurements are R-squared (the coefficient of determination), Residuals, % errors, F-ratio, and the p-values. Definitions of statistical terms are given in Table 7.1.

The built-in statistical programs in Excel are used to minimize the function S to determine the parameters (b_1, b_2, $b_3\ldots$) and to calculate the key statistics. A basic understanding of the statistics is required to interpret the results.

Table 7.1. Definitions and significance of statistical measurements
(Hogg and Ledolter, 1987; Kiemele, et al., 1997)

Measurement	Definition and Significance
n	Number of observations of Y
p	Number of non-constant terms in linear regression analysis (or dependencies). These are the variables, or factors.
j	Number of values in a variable or factor. These are the levels, or average levels in a random population
Y	Values of dependent variable or measurement (subscripted i =1 to n)
Y_{avg}	Mean value of Y = $\Sigma Y_i/n$. Analysis of variance uses the deviations from the mean to correlate influences, much like partial derivatives.
σ	Standard deviation of Y: $\sigma^2 = \Sigma (Y_i\text{-}Yavg)^2/(n\text{-}1)$
Y'	Predicted value of Y (also subscripted i = 1 to n)
SSTO (sum of squares total)	SSTO = $\Sigma (Y_i\text{-}Y_{avg})^2$. The values' deviation from mean
SSR (sum of squares due to regression)	SSR = $\Sigma (Y'_i\text{-}Y_{avg})^2$. Predictions' deviation from mean
SSE (sum of squared errors)	SSE = Σe_i^2 = SSTO – SSR. Sum of differences between predictions and values
MSR (mean square due to regression)	MSR = (SSR)/p
MSE (mean square due to error)	MSE = (SSE)/(n-p-1). Estimates σ^2
R-squared (coefficient of determination)	R^2 = SSR/SSTO = 1 – SSE/SSTO. The fraction of the total variation from the mean accounted for by regression.
Adjusted R-squared	R^2 = 1 – (SSE/(n-p-1))/(SSTO/(n-1)), which is adjusted for degrees of freedom. This represents the *proportionate* reduction in variation from regression.
Residuals	$E_i = Y_i - Y'_i$. Difference between prediction and actual experimental value.
% error	% relative error = ($\|E_i\| / Y_i$)*100, the percent relative error from the actual experimental values.
F ratio	$F = R^2/(1\text{-}R^2)$ = MSR/MSE. Larger value represents greater significance of dependencies, follows F distribution, so compare to F(α=0.05,p,n-p-1), [p is df for the regression, n-p-1 is df for the variance], in hypothesis test to reject Ho: $b_i = 0$ over i.
p value	p value = P[F(p,n-p-1) > calculated F]. Probability that $b_i = 0$ for the parameter corresponding to x_i. A rule of thumb is that the p-value is a good number below α = 0.05 (1 minus confidence level) (Kiemele, et al, 1997)

The appropriateness of fit is often evaluated using the coefficient of determination R^2, or the adjusted R^2 value. If the R^2 value of the model is just a few hundredths lower than one, the errors for which the model does not account are well within reasonable experimental error. When the R^2 value is lower than 0.90, the model is only accounting for most of the variation. The R^2 value alone should not determine the appropriateness of a model, but only the overall fit of the regression to the trends resulting from the independent variables. Residuals and relative errors are more important criteria when evaluating a model, because they may be assessed according to a desired tolerance.

The F-ratio gives the likelihood that there is a dependence of the data on the chosen independent variables. The F-significance test is a test of the hypothesis that all the determined parameters are actually zero, so it does not give the accuracy of the model's parameters. The p-value is similar, as (1-p) represents the probability that an individual parameter, b_p, is non-zero. It is more useful in denying a possible dependence or eliminating extraneous independent variables than it is for measuring accuracy. The confidence intervals give a better measure of certainty of the determined parameters. For each model, the determined 95 % confidence intervals were examined, generally with the criteria that they should be an order of magnitude lower than the parameter.

Several key measurements in the investigation were modeled and presented in this chapter: sodium hydroxide consumption (Δ[NaOH]), corrected Kappa number (K_C), the initial Kappa number correction ($K_O - K_{CO}$), Kappa number through nitrogen extraction experiments (K_N), Kappa number (K), charge of the additive ([Aa]) galactomannan adsorbed on pulp, chain scission number (CSN), and the selectivity parameter based on chain scission number (S_{CSN}).

The statistical treatment was performed on data from experiments conducted with IP pulp A, described in Table 4.1. Experimental conditions were temperatures of 90°C and 120°C; reaction times of 0 min., 10 min., 20 min., and 60 min.; initial sodium hydroxide charges 1.5 % on pulp (1.67 g/L), 2.5 % on pulp (2.78 g/L), and 4.0 % on pulp (4.44 g/L); and galactomannan charges of 0 %, 0.3 %, 0.75 %, and 2.0 % on pulp. The oxygen or nitrogen pressure was fixed at 780 kPa. For the modeling of alkali consumption only, all the appropriate experiments from the collected data in Appendix B were used. For the other key measurements, the data used is shown in Appendix C.

7.2. CORRECTION OF KAPPA NUMBER

In studying the changes in Kappa number during oxygen delignification, we have focused primarily on ΔK_C, which has been defined as the change in Kappa number by oxygen reaction only. To find this value, the initial Kappa number, K_O, has been corrected to K_{CO}, based on experiments conducted under nitrogen rather than oxygen. As mentioned in section 5.6, the viscosity was not affected nearly as significantly as Kappa number during extraction experiments. Although the resulting viscosity corrections were used to calculate changes in DP previously, it is not necessary to develop mathematical models for these corrections, as they are too small to model accurately. However, it is necessary to develop models for Kappa number corrections.

At reaction times beyond the initial part of the delignification (10 minutes), the values of K and K_C have been considered essentially equal. This is based on the finding that nearly all the Kappa number change by alkali extraction alone is complete beyond 10 minutes (see section 5.6). The Kappa number obtained by extraction only has been

denoted K_N. The Kappa number decrease by oxygen reaction has been determined as ΔK_C. The Kappa number development due to the combined effects of both mechanisms is the measured Kappa number, K, during the experiments. Estimations of these three curves are plotted alongside each other in Figure 7.1 for some of the experimental conditions. This graphic was constructed to illustrate the concepts of Kappa number correction employed in this investigation.

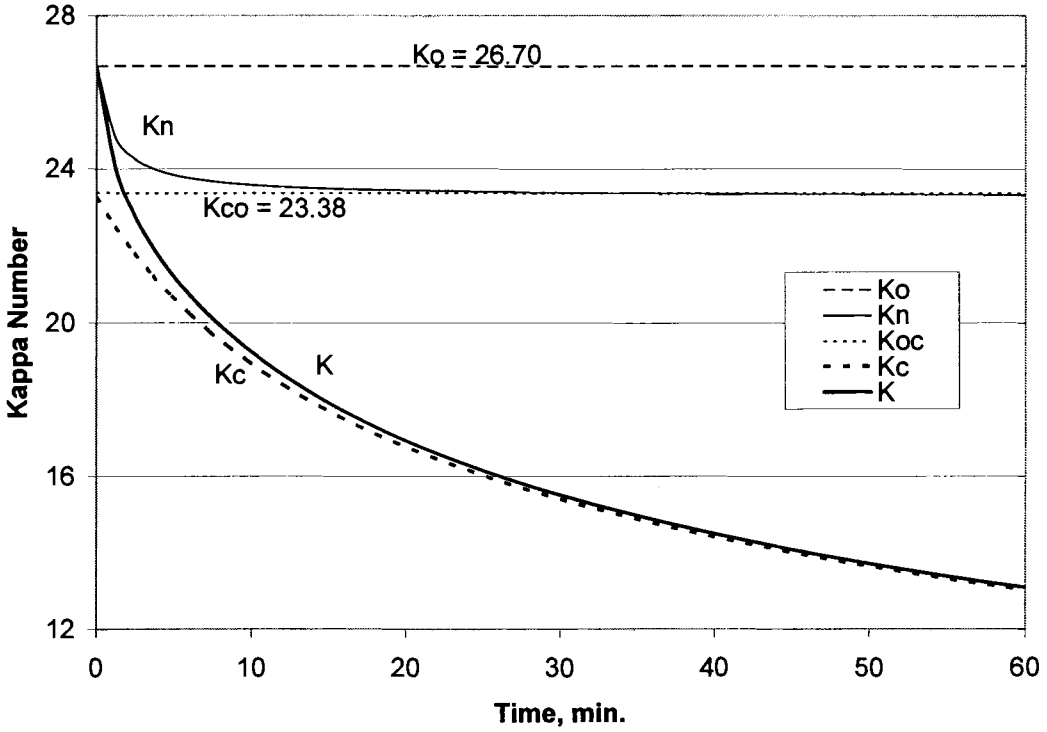

Figure 7.1. Illustration of Kappa number versus time during reactions under 780 kPa nitrogen (K_N), 780 kPa oxygen (K), and the corrected value for oxygen-mediated reactions (K_C), 90 °C and 4.0 % NaOH

As mentioned previously, K and K_C are very close together except in the beginning of the reaction. The curves K and K_N have been shown previously, in Figures 5.1 and 5.8. The values for these curves were calculated with the modeling results. The

total decrease in Kappa number by alkali extraction at infinite time is $K_O - K_{CO}$, or $K_O - K_{N\ (at\ t = 60\ min.)}$. The value $K_O - K_{CO}$ is the correction used for the initial Kappa number, and it is dependent on the initial conditions of the extraction. As the curves K_N and K_C decrease over time, the sum of their changes is the total decrease in K. Thus the value of K is related to K_C and K_N as follows:

$$K = K_O - \Delta K_N - \Delta K_C = K_O - (K_O - K_N) - (K_{CO} - K_C)$$

$$\text{or} \quad K = K_C + (K_N - K_{CO}) \qquad (7\text{-}2)$$

In the following sections, models are developed for Δ[NaOH], K_C, K_N, $(K_O - K_{CO})$, and K. The model for alkali consumption is developed before these other models because the alkali concentration must be known at all times to employ the models for the other variables. Then models are developed for the chain scission number (CSN), the selectivity parameter (S_{CSN}), and for additive adsorption on pulp [Aa].

7.3. ALKALI CONSUMPTION

The alkali concentration in the liquor was measured by titration to neutral pH in samples taken before and after oxygen delignification experiments. From this data, the decrease in sodium hydroxide concentration (Δ[NaOH]), in g/L was calculated. This data is given in the tables in Appendix B. As discussed in Chapter 5 (section 5.6), the decrease in caustic charge was found to be proportional to Kappa number change (ΔK) throughout the delignification process. Other possible variables influencing the alkali

charge change were temperature (T), initial alkali charge ($[NaOH]_o$), charge of the adsorbed additive galactomannan ([Aa]), and time (t). In Figure 5.8, the decrease in alkali concentration in g/L is plotted against the change in Kappa number, for all oxygen delignification experiments and all pulps used in the investigation. Since this figure shows data from various experiments with conditions other than those listed in section 7.1, it indicates that alkali consumption is mostly determined by Kappa number change. Experiments conducted under nitrogen pressure in the absence of oxygen were excluded for the alkali consumption model, because it is more practical to calculate the alkali consumption which would be typically seen in a mill. As mentioned in Chapter 5, the alkali consumption for the nitrogen extraction experiments was much lower than for the oxygen delignification experiments. The average consumption was 0.28 g/L, compared to decreases of 1 to 3 g/L during oxygen delignification experiments.

The appropriate model for alkali consumption to test initially was the linear model, designated model A1, in the form $y = m \Delta K + b$. Table 7.2 summarizes all the models tested for alkali consumption and the regression statistics. The constants determined were the y-intercept, b_0, and the slope, b_1. In the first columns are the overall regression coefficients (R and R^2), the adjusted R, and the F-ratio, then the other columns contain the determined constants, showing confidence intervals and p-stats.

Table 7.2. Alkali consumption models

Model A1: $\Delta[NaOH] = b_0 + b_1 \Delta K$					
R	0.969		± 95% confidence interval	p-stats:	
R^2	0.940	b_0	-.0757 ± .051	int.	.062
R-adj.	0.941	b_1	0.147 ± .006	x_1	7e-88
F-ratio	2198				
Model A2: $\Delta[NaOH] = b_1 \Delta K$					
R	0.968		± 95% confidence interval	p-stats:	
R^2	0.937	b_1	0.139 ± 0.005	x_1	5e-145
R-adj.	0.950				
F-ratio	2110				
Model A3: $\Delta[NaOH] = b_0 + b_1 \Delta K + b_2 T$					
R	0.970		± 95% confidence interval	p-stats:	
R^2	0.941	b_0	-0.086 ± 0.045	int.	0.046
R-adj.	0.946	b_1	0.145 ± 0.007	x_1	8e-45
F-ratio	1108	b_2	1.1e-6 ± 1.3e-6	x_2	0.149
Model A4: $\Delta[NaOH] = b_0 + b_1 \Delta K + b_2 t$					
R	0.969		± 95% confidence interval	p-stats:	
R^2	0.940	b_0	-0.102 ± 0.070	int.	0.069
R-adj.	0.942	b_1	0.143 ± .009	x_1	5e-67
F-ratio	1104	b_2	9.8e-4 ± 1.5e-3	x_2	0.206
Model A5: $\Delta[NaOH] = b_0 + b_1 \Delta K + b_2[Aa]$					
R	0.970		± 95% confidence interval	p-stats:	
R^2	0.941	b_0	-0.083 ± 0.079	int.	0.073
R-adj.	0.936	b_1	0.147 ± 0.007	x_1	7e-88
F-ratio	1115	b_2	-0.017 ± 0.019	x_2	0.089
Model A6: $\Delta[NaOH] = b_0 + b_1 \Delta K + b_2 [NaOH]_0$					
R	0.969		± 95% confidence interval	p-stats:	
R^2	0.940	b_0	-0.068 ± 0.01	int.	0.18
R-adj.	0.939	b_1	0.146 ± .006	x_1	6e-87
F-ratio	1097	b_2	-0.013 ± 0.03	x_2	0.394
Model A7: $\Delta[NaOH] = b_0 + b_1 \Delta K_C$					
R	0.960		± 95% confidence interval	p-stats:	
R^2	0.922	b_1	0.204 ± .06	x_1	5e-4
R-adj.	0.921	b_2	0.169 ± 0.0007	x_2	4e-27
F-ratio	986				
[NaOH] in g/L, T in Kelvin, t in minutes, Aa in % adsorbed on pulp, K in Kappa units					

In Table 7.2, the statistics for model A1 show that the suspected linear correlation between ΔK and Δ[NaOH] is very strong. The R value of 0.969 means that close to 97% of the variation in Δ[NaOH] is accounted for by this regression model. The slope 0.147 is close to the one indicated in Figure 5.7 (0.14). The determined y-intercept is -0.076 ± 0.051, which has a very small value and a wide range of uncertainty. Also, the p-value of the intercept is large and there is no scientific basis for a negative intercept. In the measurement of sodium hydroxide concentration, the minimum resolution of the measurement is 0.002 N, which is 0.08 g/L in NaOH charge, with a standard deviation of about 0.15 g/L NaOH. Therefore, this intercept is essentially insignificant because it is as close to zero as our ability to determine this measurement. Model A2, without intercept, is a more appropriate equation than model A1. The other models in Table 7.2 test the influence of other variables besides Kappa number decrease. As can be seen by the statistics, the inclusion of temperature, time, additive charge, and initial alkali charge as independent variables did not significantly improve the model's regression statistics.

Model A7 is the same model as A1, only Δ[NaOH] is regressed against the corrected Kappa number K_C, rather than K. This models differs from A1 because the y-intercept is more significant, having a value of 0.2 g/L and a standard error of 0.06 g/L, which is much better than a value of -0.07 g/L and a standard error of 0.05 g/L. Also, we expect this because the curve of Δ[NaOH] versus ΔK_C contains an intercept corresponding to the NaOH consumption during alkali extraction. As mentioned previously in this section, this value was averaged 0.28 g/L, which is closely approximated by the intercept determined here as 0.20 g/L.

Model A2 best describes the alkali consumption versus Kappa number during the oxygen delignification of this pulp. The model then takes on the form:

$$\Delta[NaOH] = 0.139 \cdot \Delta K \qquad (7\text{-}3)$$

where Δ[NaOH] is in g/L and ΔK is Kappa number. The other appropriate model of interest is model A7:

$$\Delta[NaOH] = 0.169 \cdot \Delta K_C + 0.20 \text{ g/L} \qquad (7\text{-}4)$$

Figure 7.2 shows the residuals ($E_i = |Y_i - Y'_i|$) from model A2 calculated for each data point plotted against the experimental Δ[NaOH]. The diagonal line y = x is included to compare the residuals to the experimental values. This figure shows that the residuals are all lower than 0.5 g/L and increase slightly as the values of Δ[NaOH] increase.

Figure 7.3 shows the relative percent errors from model A2, calculated by dividing the absolute value of the residuals Ei by the experimental values Y_i. This bar graph shows additionally that the relative errors decrease as the Δ[NaOH] values become larger. This is because the sum of the squared deviations, or residuals, are minimized when determining the regression coefficients, not the relative errors. The vast majority of the relative errors shown in Figure 7.3 are less than 20 %, and many are around 10% and less. High relative errors above 20% are only evident for very small values of Δ[NaOH]. This is accounted for by the fact that when Δ[NaOH] is less than 1.0 g/L, the accuracy in measurement is a significant portion of the difference Δ[NaOH]. As mentioned previously, the uncertainty of this measurement is much greater than 0.08 g/L.

Recall it is a rule of thumb statistically that 95 % of normally distributed data lies within 2 standard deviations (0.15 g/L) of the mean, so we would expect to see measurements that are occasionally off by as much as 0.3 g/L.

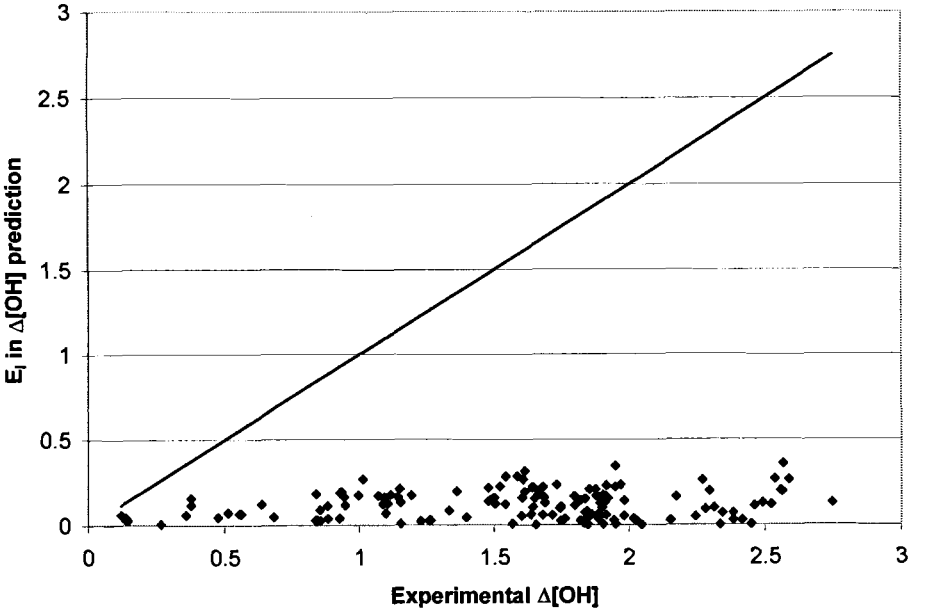

Figure 7.2. Residual deviations in predicting alkali consumption

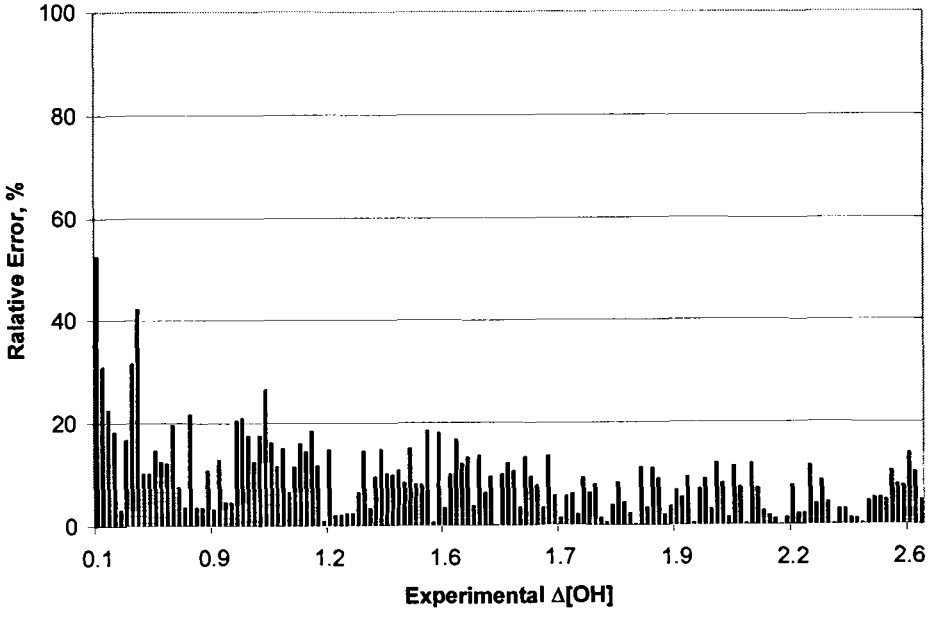

Figure 7.3. Relative errors in predicting alkali consumption

Figure 7.4 shows another way of evaluating models. It plots the predicted values of Δ[NaOH] versus the actual experimental values. This type of plot is expected to follow the line y = x for a perfect model, and will be used to illustrate the appropriateness of fit for our best model prediction in each section of this chapter. Models A2 (equation 7.3) will be used to calculate expected NaOH consumption per Kappa number in oxygen delignification. Model A7 (equation 7.4) will be used to calculate the NaOH consumption corresponding to changes in corrected Kappa number.

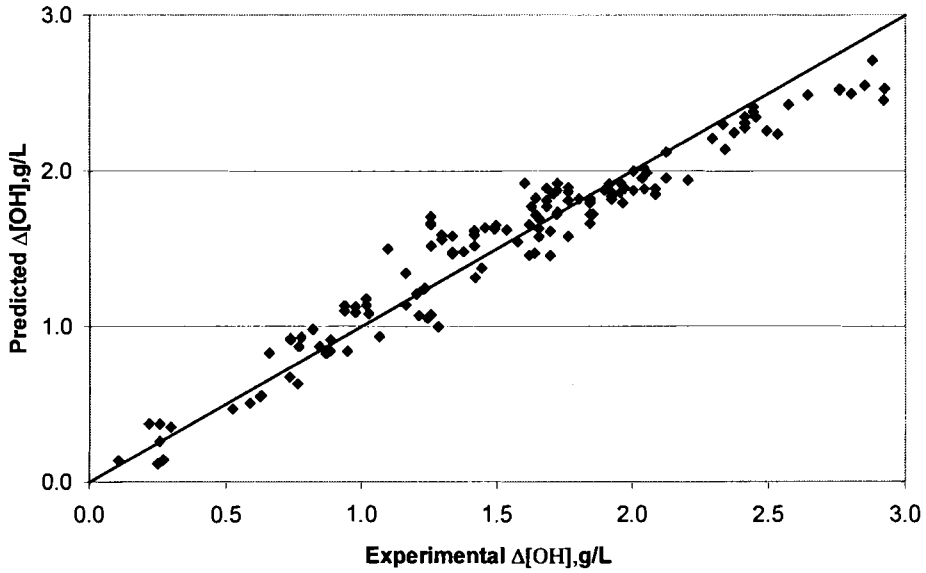

Figure 7.4. Predicted versus experimental alkali consumption

7.4. KAPPA NUMBER MODELS

7.4.1. Corrected Kappa Number

The alkali-extraction corrected Kappa number of the pulp, K_C, is the primary value on which the progress of the lignin reactions with oxygen will be based. It is also one of two primary aspects of the selectivity. Previously, we have shown that the initial Kappa number should be corrected according to the results obtained from caustic extraction experiments under a nitrogen atmosphere. Because the extraction is essentially complete after the first 10 minutes reaction time, the initial corrected Kappa number used for the correlation of the K_C data will be taken to be constant as K_{CO}. The rate of change of Kc, - dKc/dt, may be dependent on corrected Kappa number (K_C), temperature (T), alkali concentration ([NaOH]), and charge of the adsorbed additive galactomannan ([Aa]).

Previous kinetic studies were summarized in Chapter 2. The formulae in Figure 2.5 show the generic differential equations for lignin concentration and cellulose molecular weight as functions of temperature, time, hydroxyl ion concentration, oxygen pressure, and either lignin concentration or cellulose molecular weight, respectively. The previous investigators used different nomenclature, units, and variables, but the equations all have a similar power-model form. Some simple models, as well as power models, were tested for the corrected Kappa number change in this section. For the lignin concentration, Kc was used instead of [L], and the sodium hydroxide charge ([NaOH]) in g/L was used instead of hydroxyl ion molar concentration. Oxygen pressure was also omitted from the equation as the pressure was held constant at 100 psig (780 kPa).

Appendix C contains the data used in this section and subsequent sections in this chapter. From this data, the values for $-dK_C/dt$ at time t were determined from the curve of Kc versus t for each set of data. The values of $-dK_C/dt$ were regressed in a multiple linear regression, as done previously, against the corresponding instantaneous measurements of temperature, alkali charge, Kappa number, and adsorbed additive charge using the multiple linear regression model. The three linear models tested are shown in Table 7.3, models B1 to B3. Power models tested are shown in this table as models B4 to B5.

Model B1 included temperature, alkali charge, and additive charge as independent variables, and contains a y-intercept. This model displays rather poor statistics, as the regression coefficient of 0.60 shows that the model accounts for less than two-thirds of the variation. This is a clear indication that some influence is missing. Model B2 is the same as model B1, except now includes the Kappa number as an influence. As with model B1, model B2 has a significant intercept, and one unnecessary variable, the adsorbed additive charge, [Aa]. The confidence intervals, p-value, and lack of detriment by eliminating this variable show that this variable is unimportant. This finding is consistent with the discussion in section 6.2. Model B3 is the best linear model, and this indicates that –dKc/dt is a function of Kappa number, alkali charge, and temperature primarily.

Although model B3 accounts for most of the variation in $-dK_C/dt$, a better basis for our equation must be considered. Other researchers have previously determined an exponential rate dependence on temperature for these reactions (Iribarne and Schroeder, 1997; Olm and Teder, 1979; Hsu and Hsieh, 1988; Perng and Oloman, 1994; Agarwal, et

al., 1996). Therefore, a general Arrhenius expression was incorporated with a power model equation to provide different orders with respect to the influencing factors. Then the model takes the following form:

$$-dK_C/dt = b_0 \exp(-b_1/T)\,[NaOH]^{b2}\,K_C^{b4}\,[Aa]^{b3}. \qquad (7\text{-}5)$$

This equation is no longer linear, but a logarithmic transform may be carried out so that we may apply the linear regression model. Equation 7-3 becomes

$$\ln(-dK_C/dt) = \ln b_0 - (b_1/T) + b_2 \ln[NaOH] + b_3 \ln K_C + b_4 \ln[Aa]. \qquad (7\text{-}6)$$

Regressing the left hand side against 1/T and these logarithms should show linear influences if the power model is effective in describing the data. The coefficients b_0 and b_1 represent the frequency factor constant and activation energy constant (E_A/R).

Model B4 in Table 7.3 shows this power law model, evaluated with the influences shown in equation 7-5. As can be seen in Table 7.3, the statistics are significantly improved for this model, as the coefficient of determination is 0.99 compared to 0.88. Also the confidence intervals around the determined constants are smaller than in the previous models, by an order of magnitude lower, with the exception of the additive. Again the statistics favor elimination of this influence.

Table 7.3. Corrected Kappa number (K_C) models

Model B1: $-dK_C/dt = b_0 + b_1 T + b_2 [NaOH] + b_3 [Aa]$					
R	0.601		± 95% confidence interval	p-stats:	
R^2	0.361	b_0	-2.36 ± 1.4	int.	0.004
R-adj.	0.389	b_1	0.0064 ± .005	x_1	0.004
F-ratio	8.28	b_2	0.0654 ± 0.048	x_2	0.016
		b_3	0.0034 ± .038	x_3	0.92
Model B2: $-dK_C/dt = b_0 + b_1 T + b_2 [NaOH] + b_3 K_C + b_4 [Aa]$					
R	0.882		± 95% confidence interval	p-stats:	
R^2	0.778	b_0	-6.59 ± 1.3	int.	8e-13
R-adj.	0.751	b_1	0.0155 ± .0025	x_1	3e-12
F-ratio	37.7	b_2	0.0831 ± 0.031	x_2	4e-6
		b_3	0.0485 ± .0011	x_3	2e-11
		b_4	-0.00544 ± .041	x_4	0.78
Model B3: $-dK_C/dt = b_0 + b_1 T + b_2 [NaOH] + b_3 K_C$					
R	0.882		± 95% confidence interval	p-stats:	
R^2	0.777	b_0	-6.59 ± 1.3	int.	8e-13
R-adj.	0.756	b_1	0.0155 ± .0028	x_1	2e-12
F-ratio	51.3	b_2	0.0828 ± 0.030	x_2	3e-6
		b_3	0.0484 ± .0011	x_3	1e-11
Model B4: $-dK_C/dt = b_0 \exp(-b_1/T) [NaOH]^{b2} K_C^{b3} [Aa]^{b4}$					
R	0.990		± 95% confidence interval	p-stats:	
R^2	0.982	b_0	12.9 ± 1.5	int.	3e-17
R-adj.	0.981	b_1	-9870 ± 700	x_1	5e-24
F-ratio	422	b_2	0.827 ± 0.042	x_2	5e-19
		b_3	3.90 ± 0.22	x_3	5e-26
		b_4	-0.026 ± 0.028	x_4	0.45
Model B5: $-dK_C/dt = b_0 \exp(-b_1/T) [NaOH]^{b2} K_C^{b3}$					
R	0.989		± 95% confidence interval	p-stats:	
R^2	0.979	b_0	12.9 ± 1.3	int.	2e-23
R-adj.	0.977	b_1	-9770 ± 600	x_1	9e-33
F-ratio	735	b_2	0.819 ± 0.036	x_2	6e-26
		b_3	3.90 ± 0.099	x_3	2e-35
[NaOH] in g/L, T in Kelvin, t in minutes, Aa in % adsorbed on pulp, K in Kappa units					

For each of the models B1 to B5 above, residuals deviations and percent errors were calculated and compared, and model B5 had the lowest errors and best fit overall. The model for $-dK_C/dt$ then becomes:

$$-dKc/dt = 4.0 \times 10^5 \exp(-9770/T) [NaOH]^{0.819} K_C^{3.81} \qquad (7\text{-}7)$$

where t is in minutes, T is in Kelvin, and [NaOH] is in g/L..

This prediction is very similar to those listed from the literature in Chapter 2 (Table 2.1). The Kappa number dependence is about the same order as determined by two of the studies listed (Hsu and Hsieh, 1988; Perng and Oloman, 1994). Higher orders have been observed, as high as 7 or 8 (Agarwal, et al., 1996; Zou, 2002), but these studies were conducted on hardwood pulp which contains more hexeneuronic acids, a constituent which is unreactive in oxygen delignification, but is counted as part of the Kappa number (Li and Gellerstedt, 1998). As previously mentioned, the high reaction orders have been attributed to parallel reactions between different species. The wider range of reactivity, the higher the reaction order would be. Two other studies (Olm and Teder, 1979; Iribarne and Schroeder, 1997) had listed this exponent as 1.0, but these were first-order assumptions and not determined values. The models which list two-region models (Olm and Teder, 1979; Hsu and Hsieh, 1988; Iribarne and Schroeder, 1997) introduced these two separate phases in order to be able to describe the slow lignin removal during the latter part of the delignification. As discussed in section 5.6, this behavior is also caused by the rapid initial extraction of lignin without the occurrence of any oxygen

delignification reactions. Our data for Kc eliminated this Kappa number reduction as a result of the extraction.

The values of –dKc/dt at times of 0, 10, 20, and 60 minutes were calculated at each condition using equation 7-7, and then were plotted versus the experimental values of $-dK_C/dt$, as shown in Figure 7.5. This plot shows a good proximity to the unity line for most of the data points, but with some larger deviation at the high reaction rates corresponding to experiments at 120°C. Figure 7.6 shows that data at 90°C only. The data is distributed around the unity line quite well, but the scatter for some points in the lower region leads to the few significant relative errors (25-35 %) of the prediction.

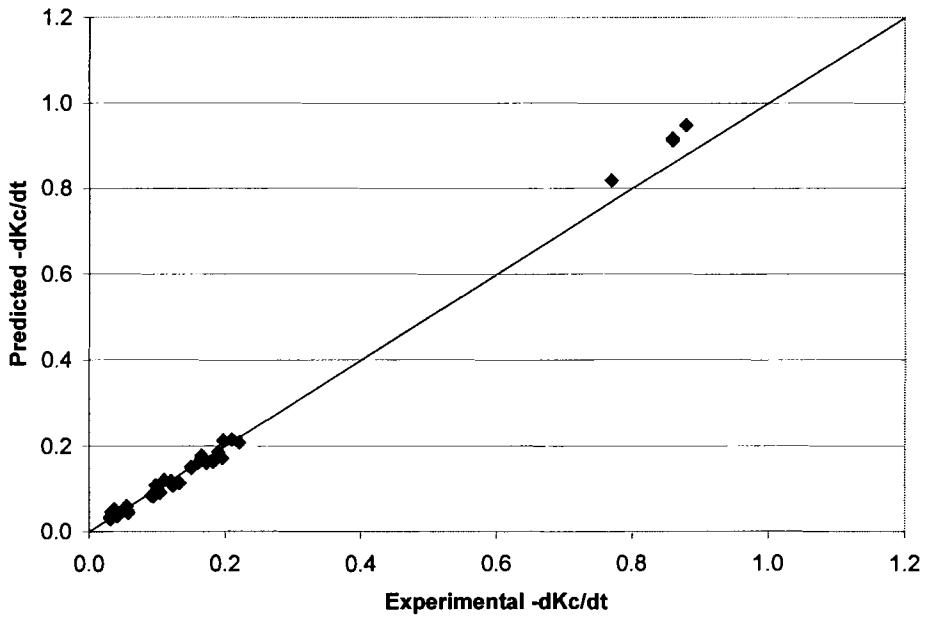

Figure 7.5. Predicted versus experimental $-dK_C/dt$

It is useful to be able to evaluate the differential equation $-dK_C/dt$ in this model to generate predicted data for the corrected Kappa number, given sets of initial conditions for oxygen delignification experiments. A program was written in MathCad 2001i to solve the differential equation using the Runge-Kutta method as described by Rice and

Do (1995). This program is given in Appendix C. For each set of initial conditions of the oxygen delignification experiments, the corrected Kappa number was determined over the time duration using this program. Figure 7.7 plots the predicted corrected Kappa number versus experimental corrected Kappa number. Although most of the points in this plot are right around the unity line, some deviations are high (up to 1.2 Kappa units) for Kappa numbers less than 10. The reason for this is that the value –dKc/dt is over-estimated for some higher temperature reactions, so the resulting Kappa number prediction is lower than the experimental value. Nevertheless, equation 7-7 provides a fairly accurate and reliable estimation of the delignification rate at the given conditions.

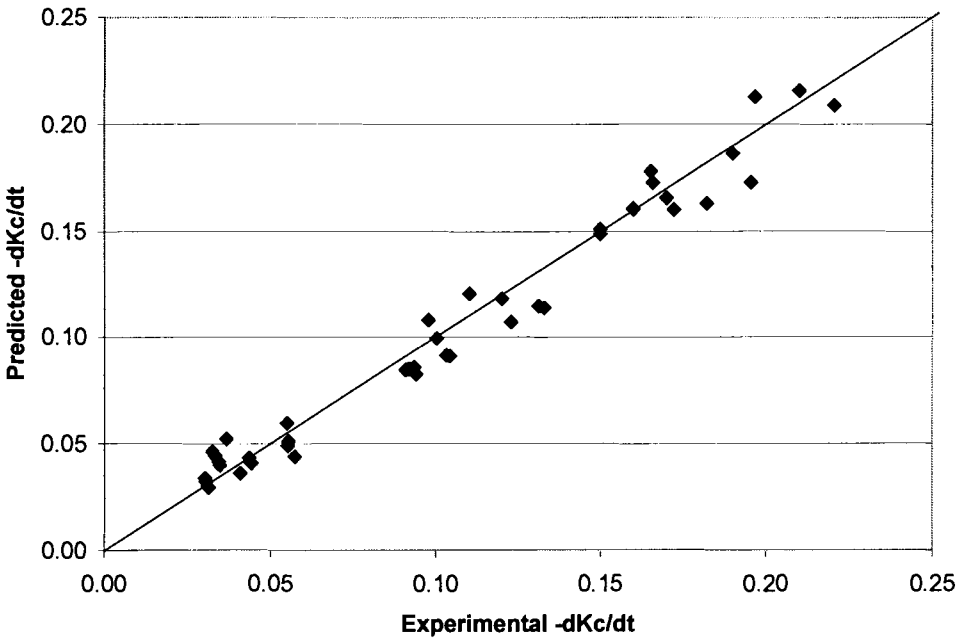

Figure 7.6. Predicted versus experimental $-dK_C/dt$, 90 °C only

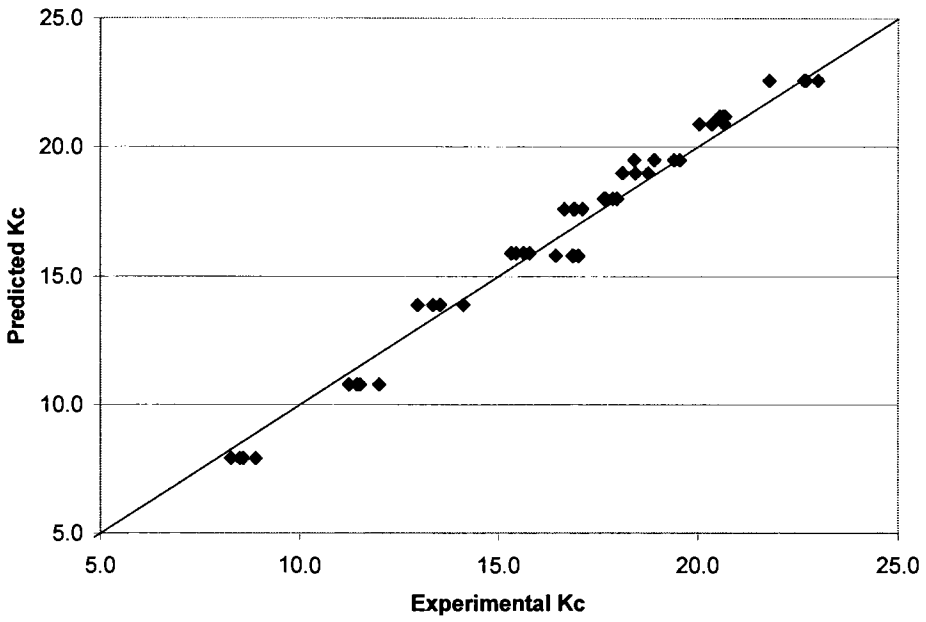

Figure 7.7. Predicted versus experimental corrected Kappa number (K_C)

7.4.2. Kappa Number

The Kappa number (K) was modeled exactly as the corrected Kappa number (K_C) with the same potential influences. Table 7.4 gives the best model tested, model B6.

Table 7.4. Kappa number (K) model

Model B5: $-dK/dt = b_0 \exp(-b_1/T)\,[NaOH]^{b2}\,K^{b3}$					
R	0.945		± 95% confidence interval	p-stats:	
R^2	0.919	b_0	8.38 ± 2.4	int.	9e-8
R-adj.	0.909	b_1	-7140 ± 600	x_1	2e-15
F-ratio	522	b_2	0.588 ± 0.11	x_2	8e-13
		b_3	3.12 ± 0.40	x_3	2e-19
[NaOH] in g/L, T in Kelvin, t in minutes, Aa in % adsorbed on pulp, K in Kappa units					

The final form of the equation is given as equation 7-8.

$$-dK/dt = 4.4 \times 10^3 \exp(-7140/T)\,[NaOH]^{0.588}\,K^{3.12} \qquad (7\text{-}8)$$

where T is in Kelvin, t is in minutes, and [NaOH] is in g/L. Again, for each set of initial conditions of the oxygen delignification experiments, the Kappa number was determined over time using the differential solver program and now equation 7-8, as done in the previous section with K_C. Figure 7.8 plots the predicted Kappa number versus experimental Kappa number. The predictions of this model deviate more than the model shown Figure 7.7.

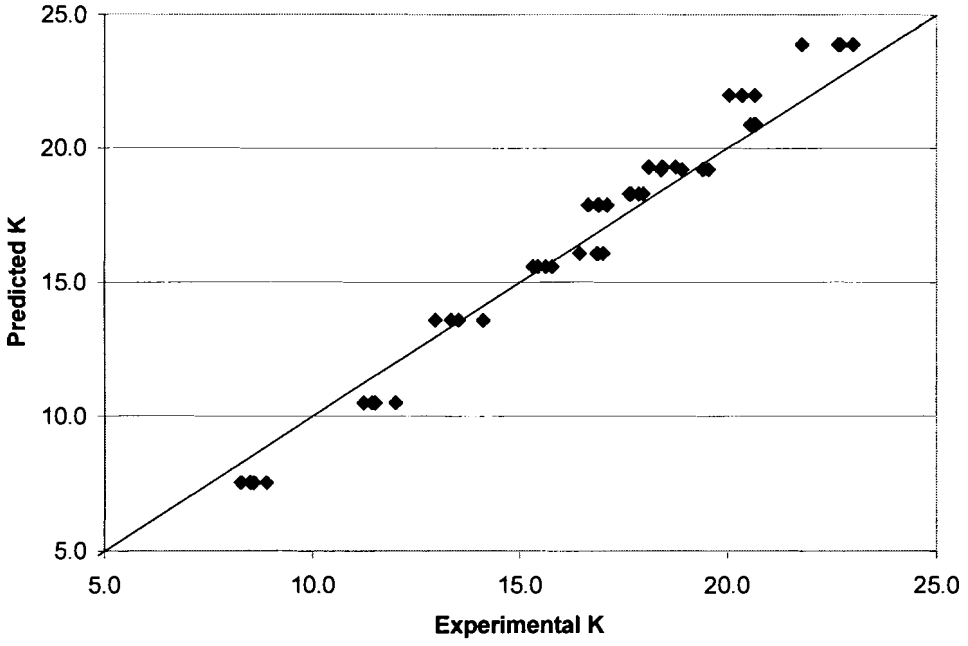

Figure 7.8. Predicted versus experimental Kappa number (K), using equation 7-8

In Figure 7.8, higher Kappa numbers are overestimated and lower Kappa numbers are underestimated. The activation energy is lower in this model than model B5, thus it is more temperature sensitive. This leads to a higher rate at the high temperature, making the Kappa number to go lower than the experimental data. Also, because the Kappa

number exponent is lower and the original Kappa number is higher, this model does not fully account for the rapid Kappa number decrease due to the initial extraction of lignin.

7.4.3. Kappa Number Correction

Since the model for Kappa number did not work as sufficiently as the model for corrected Kappa number, we will attempt to model the Kappa number changes with two separate models. We have formulated the oxygen reactions with lignin in our model for $-dK_C/dt$, and now we will develop a model suitable for K_N. Since K_C may be obtained from equation 7-7, K may be calculated from equation 7-2 if K_N and K_{C0} are known. First the value of K_{CO} is modeled by obtaining a correlation for the maximum fractional decrease in Kappa number $(1-K_{CO}/K_O)$ for the different extraction experiments, over 60 minutes time. Thus $(1-K_{CO}/K_O)$ is related to the initial conditions of temperature, alkali charge, and additive charge. The data used for the analysis on extraction experiments is in the small table on the last page of Appendix C. In Table 7.5, models are shown for the Kappa number correction models. Model C2 was the best fit for estimating the maximum Kappa number change, given by:

$$(1- K_{CO}/K_O) = 0.35 + 0.0011\ T + 0.020\ [NaOH] \qquad (7\text{-}9)$$

Where T is in Kelvin and [NaOH] is in g/L. This equation is used to obtain values for K_{CO} given initial conditions for temperature, K_O, and [NaOH].

Table 7.5. Kappa number correction models

Model C1: $(1- K_{CO}/K_O) = b_0 + b_1 T + b_2 [NaOH] + b_3 [Aa]$					
R	0.987		± 95% confidence interval	p-stats:	
R^2	0.975	b_0	-0.367 ± 0.11	int.	0.0005
R-adj.	0.963	b_1	0.00112 ± 0.0002	x_1	0.0002
F-ratio	79.2	b_2	0.0210 ± 0.0020	x_2	4e-2
		b_3	0.0054 ± 0.005	x_3	0.32
Model C2: $(1- K_{CO}/K_O) = b_0 + b_1 T + b_2 [NaOH]$					
R	0.985		± 95% confidence interval	p-stats:	
R^2	0.971	b_0	-0.347 ± 0.052	int.	0.0003
R-adj.	0.962	b_1	0.00112 ± 0.0001	x_1	0.0001
F-ratio	116	b_2	0.0202 ± 0.002	x_2	1e-5
Model C3: $(1- K_{CO}/K_O) = b_0 \exp(-b_1/T) [NaOH]^{b2}$					
R	0.948		± 95% confidence interval	p-stats:	
R^2	0.899	b_0	1.50 ± 1.4	int.	0.038
R-adj.	0.886	b_1	-1560 ± 470	x_1	8e-6
F-ratio	67	b_2	0.430 ± 0.12	x_2	2e-6
Model C4: time dependence only $[(K_N-K_{CO})/(K_O-K_{CO})] = b_0 + b_1 [(0.9 \cdot t +1)^{-1}]$					
R	0.998		± 95% confidence interval	p-stats:	
R^2	0.997	b_0	0.0021 ± 0.070	int.	0.75
R-adj.	0.996	b_1	0.999 ± 0.012	x_1	3e-32
F-ratio	7238				
[NaOH] in g/L, T in Kelvin, t in minutes, Aa in % adsorbed on pulp, K in Kappa units					

Results for the prediction of $(1-K_{CO}/K_O)$ versus the experimental values are presented in Figure 7.9. The model given by equation 7-9 allows us to formulate the maximum decrease in Kappa number, $K_O - K_{CO}$, which is equal to $K_O - K_{N(t = 60\ min.)}$. Also needed is a model for the time dependence of K_N. Since $(K_N - K_{CO})/(K_O - K_{CO})$ varies from 1.0 to 0 when the time changes from zero to infinity, the value of $(K_N - K_{CO})$ in equation 7-2 is modeled as:

$$[(K_N - K_{CO})/(K_O - K_{CO})] = 1/(b \cdot t + 1) \qquad (7\text{-}10)$$

where K_N is the Kappa number observed in nitrogen extraction experiments, and b is a constant which describes the slope of changes in K_N. Once K_{CO} is determined from Equation 7-9, this equation is used to determine K_N at specific values of time.

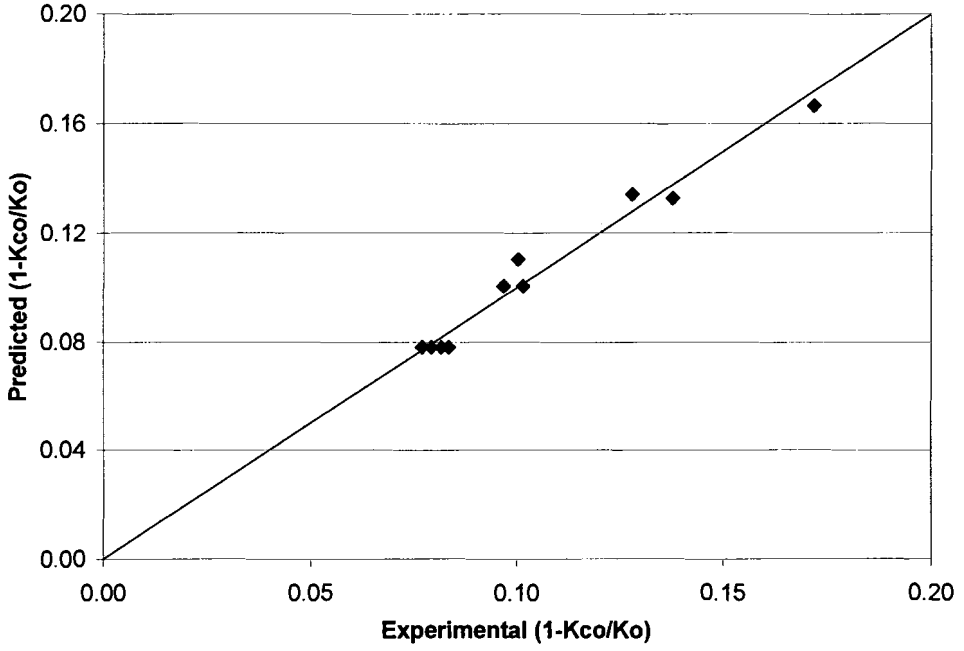

Figure 7.9. Predicted and experimental $(1- K_{CO}/K_O)$, 60 minute experiments

The constant b in equation 7-10 was determined by trial and error by varying its value in the right hand side expression, until the linear regression against the left hand side gave the optimal result (slope = 1, y-intercept = 0). The graph in Figure C.1 in appendix C shows the optimization of this parameter. The value b was found to be 0.90 min^{-1}. The regression results of modeling equation 7-8 is shown as Model C4 in Table 7.5. The slope was 0.999 and the y-intercept was 0.002, with an R^2 value of 0.998 for the regression. The prediction based on this result is plotted in Figure 7.10. This correlation for the time dependence of the Kappa number correction does not contain many points, but it describes the trend over time very well.

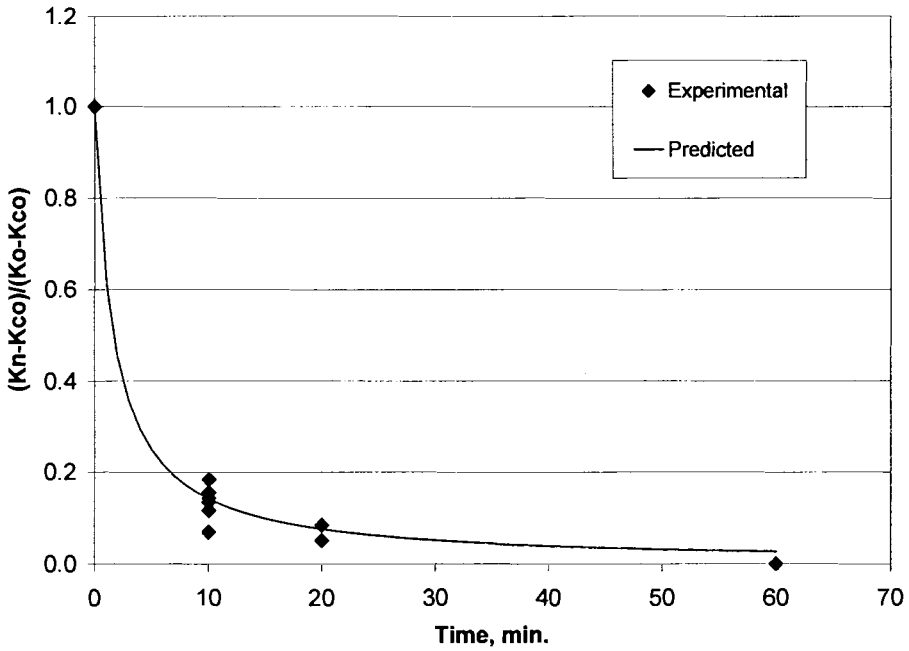

Figure 7.10. Predicted and experimental curves of $[(K_N-K_{CO})/(K_O-K_{CO})]$ versus time

Therefore, the best fit models for the Kappa number correction are:

$$(K_O - K_{CO}) = K_O [-0.35 + 0.0011\ T + 0.020\ [NaOH]\ ] \qquad (7\text{-}11)$$

$$(K_N - K_{CO}) = K_O [-0.35 + 0.0011\ T + 0.020\ [NaOH]\ ]/ (0.90\ t + 1) \qquad (7\text{-}12)$$

where equation 7-11 is for determining the maximum nitrogen-extracted Kappa number change, and equations 7-12 and 7-2 are used for the calculation of K from K_C.

7.5. GALACTOMANNAN ADSORPTION MODELS

The galactomannan adsorption was modeled according to the modified Langmuir equation, given in Hiemenz and Rajagopalan (1997). Adsorption of polymers can be described by the Langmuir equation although they do not strictly follow the thermodynamics. The surface coverage of the polymer on the substrate may be expressed by the following equation:

$$\Phi = [Aa]/ [A_{max}] = k \cdot a / (k \cdot a + 1) \qquad (7\text{-}13)$$

where Φ is the fractional coverage of adsorbed additive, a is the charge of the polymer (% on pulp), and k is an empirical constant which determines the steepness of the curve. The models tested in this section are listed in Table 7.6. Model D1 is for 1.5 % NaOH, model D2 is for 2.5 % NaOH, and model D3 is for 4.0 % NaOH. The value of k was determined by trial and error until the intercept approached zero and the R^2 value approached 1.0 in the regressions analysis. This was found to be 0.35 for all 3 alkali charges. The value Amax, which is the maximum adsorbable concentration, was determined between 3.3 % to 3.0 % on pulp as the sodium hydroxide charge goes from 1.5 % to 4.0 % on pulp. Equation 7-13 then becomes:

$$\Phi = [Aa]/ [A_{max}] = 0.35 \cdot a / (0.35 \cdot a + 1) \qquad (7\text{-}14)$$

Figure 7.11 plots the three adsorption curve predictions, showing the actual experimental observations for adsorbed charges as well, as determined by H.P.A.E.C..

Table 7.6. Galactomannan adsorption models ($Aa/A_{max}= k \cdot a / (k \cdot a +1)$)

Model D1: [Aa] = [A_{max}](k·a / (k·a +1), NaOH % = 1.5 % (k=0.35)					
R	1.000		± 95% confidence interval	p-stats:	
R^2	0.999	b_0	-0.0019 ± .032	int.	.92
R-adj.	0.999	b_1 (A_{max})	3.32 ± 0.14	x_1	0.0005
F-ratio	2162				
Model D2: [Aa] = [A_{max}](k·a / (k·a +1), NaOH % = 2.5 % (k=0.35)					
R	0.999		± 95% confidence interval	p-stats:	
R^2	0.999	b_0	-0.00085 ± 0.034	int.	.97
R-adj.	0.998	b_1 (A_{max})	3.17 ± 0.15	x_1	0.0006
F-ratio	1786				
Model D3: [Aa] = [A_{max}](k·a / (k·a +1), NaOH % = 4.0 % (k=0.35)					
R	0.999		± 95% confidence interval	p-stats:	
R^2	0.999	b_0	-.018 ± 0.036	int.	.42
R-adj.	0.998	b_1 (A_{max})	3.00 ± 0.14	x_1	0.0006
F-ratio	1574				
Aa in % adsorbed on pulp, a is in % added on pulp					

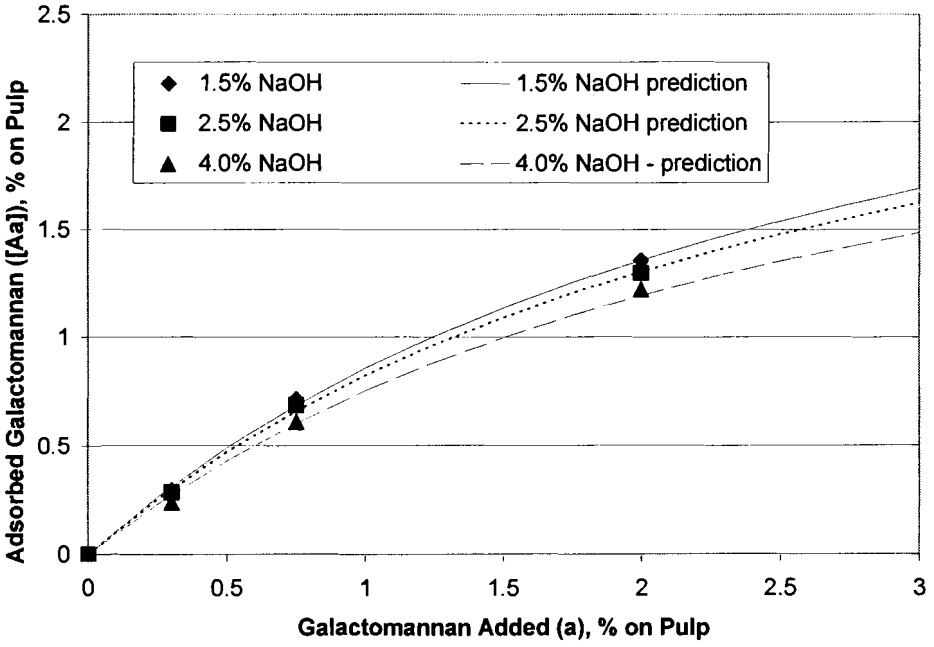

Figure 7.11. Predicted and experimental galactomannan adsorption

7.6. CHAIN SCISSION NUMBER MODELS

The quantity ($1/DP_t - 1/DP_0$) represents the chain scissions per glucose unit in cellulose. The chain scission number (CSN) is taken by multiplying this quantity by DP_0:

$$CSN = (1/DP_t - 1/DP_0) \cdot DP_0 \qquad (7\text{-}15)$$

Thus the CSN is the number of scissions per cellulose molecule, or the fraction of the chains cleaved. A model was developed to predict the value of d(CSN)/dt, the differential increase in chain scission number over time. A similar treatment for the data of d(CSN)/dt was used as was done for $-dK_C/dt$. The models are shown in Table 7.7.

The linear models gave reasonable predictions contrary to the data for $-dK_C/dt$ The influence of adsorbed additive on d(CSN)/dt could not be disregarded, nor could be the dependence on K_C. Power law models were also tested as they were for the Kappa number models, listed as models E3 and E4 . In chapter 4, it was shown that the cellulose degradation was directly proportional to Kappa number change. Therefore, model E4 tests the value $-dK_C/dt$ as an influence instead of K_C. Here we would expect the reaction order with respect to $-dK_C/dt$ to be close to 1. Indeed, a reaction order of 0.83 is obtained, which is not much different from 1.0. From model E3, we also would expect the reaction order with respect to Kappa number to be close to that of the $-dK_C/dt$ correlation's order with respect to Kappa number, which was 3.81. Now an order of 3.3 was obtained. Overall, E3 gave a better fit than model E4.

Table 7.7. Chain scission number models

Model E1: $d(CSN)/dt = b_0 + b_1 T + b_2 [NaOH] + b_3 [Aa]$					
R	0.787		± 95% confidence interval	p-stats:	
R^2	0.619	b_0	-0.102 ± 0.034	int.	6e-7
R-adj.	0.593	b_1	0.000279 ± 5e-5	x_1	8e-7
F-ratio	23.8	b_2	0.00196 ± 0.0011	x_2	0.0019
		b_3	-0.00142 ± 0.0024	x_3	0.246
Model E2: $d(CSN)/dt = b_0 + b_1T + b_2 [NaOH] + b_3 K_C + b_4 [Aa]$					
R	0.929		± 95% confidence interval	p-stats:	
R^2	0.863	b_0	-0.1957 ± 0.030	int.	2e-16
R-adj.	0.850	b_1	0.00485 ± 7e-50	x_1	2e-16
F-ratio	67.8	b_2	0.00234 ± 0.00072	x_2	8e-8
		b_3	0.00110 ± 0.0002	x_3	4e-11
		b_4	-0.00187 ± 0.0014	x_4	0.0144
Model E3: $d(CSN)/dt = b_0 \exp(-b_1/T) [NaOH]^{b2} K_C^{b3} [Aa]^{b4}$					
R	0.989		± 95% confidence interval	p-stats:	
R^2	0.980	b_0	10.29 ± 1.8	int.	4e-12
R-adj.	0.977	b_1	-9837 ± 880	x_1	3e-21
F-ratio	379	b_2	1.27 ± 0.10	x_2	9-22
		b_3	3.33 ± 0.28	x_3	3e-21
		b_4	-0.184 ± 0.081	x_4	0.0001
Model E4: $d(CSN)/dt = b_0 \exp(-b_1/T) [NaOH]^{b2} [-dK_C/dt]^{b3} [Aa]^{b}$					
R	0.985		± 95% confidence interval	p-stats:	
R^2	0.971	b_0	-0.412 ± 2.08	int.	0.71
R-adj.	0.967	b_1	-1544 ± 805	x_1	0.0006
F-ratio	258	b_2	0.570 ± 0.13	x_2	2e-9
		b_3	0.830 ± 0.083	x_3	1e-18
		b_4	-0.151 ± 0.010	x_4	0.005
Model E5: $d(CSN)/dt = b_0 \exp(-b_1/T) [NaOH]^{b2} K_C^{b3} (1-[Aa]/3.1)$					
R	0.989		± 95% confidence interval	p-stats:	
R^2	0.977	b_0	10.98 ± 1.2	int.	6e-27
R-adj.	0.975	b_1	-9980 ± 760	x_1	1e-29
F-ratio	459	b_2	1.22 ± 0.085	x_2	8e-31
		b_3	3.38 ± 0.22	x_3	1e-33
		b_4	0.998 ± 0.23	x_4	3e-12
[NaOH] in g/L, T in Kelvin, t in minutes, Aa in % adsorbed on pulp, K in Kappa units					

Clearly the power law model improves the regression, but its disadvantage is that these models could not be analyzed for the zero values of [Aa], because the logarithm is taken to evaluate the transform. It seemed most appropriate to include the effect of additive as the fractional coverage, $[Aa]/[A_{MAX}]$.

$$d(CSN)/dt = b_0 \exp(-b_1/T) [NaOH]^{b2} [K_C]^{b3} (1-[Aa]/[A_{max}]) \quad (7\text{-}16)$$

where the value [Aa]/[Amax] increases from zero to one as [Aa] approaches [Amax], the um adsorbed amount of additive.

Model E5 (also in Table 7.7) follows equation 7-16, and was the best model tested for d(CSN)/dt. Not only does it allow the analysis of data without additive, but the statistics are also better than the previous models. Model E5 has the smallest confidence intervals and p-values. The constant A_{max} was determined by trial and error to be around 3.1 when the regression gave the best statistics and a slope of 1 (0.998), so this value was given in model E5. This value also corresponds to the A_{max} determined in the previous section, which ranged from 3.0 to 3.3. The equation for cellulose degradation is then:

$$d(CSN)/dt = 6.0 \times 10^4 \exp(-9980/T) [NaOH]^{1.22}[K_C]^{3.38} (1/(1-[Aa]/3.1)) \quad (7\text{-}17)$$

Values of [Aa] used in 7-17 should be no greater than those observed in the experiments modeled (0 to 1.4 %). Although it is possible to adsorb higher levels of galactomannan, the changes in CSN will not approach zero, which is probably due to multi-layer adsorption. The following graphs were constructed from the prediction given in equation 7-17. Figure 7.12 contains all the points of d(CSN)/dt measured, and Figure 7.13 is for experiments at 90 °C only. Figure 7.14 compares experimentally determined intrinsic

viscosity with values calculated from CSN values generated by the differential solver in Appendix C using equation 7-17, as done similarly with K_C.

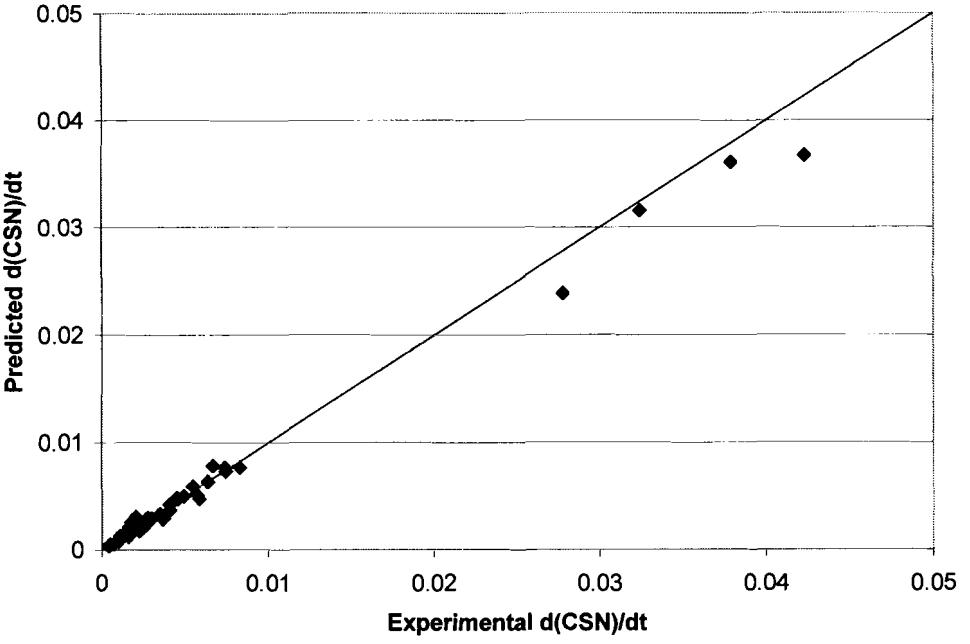

Figure 7.12. Predicted versus experimental d(CSN)/dt

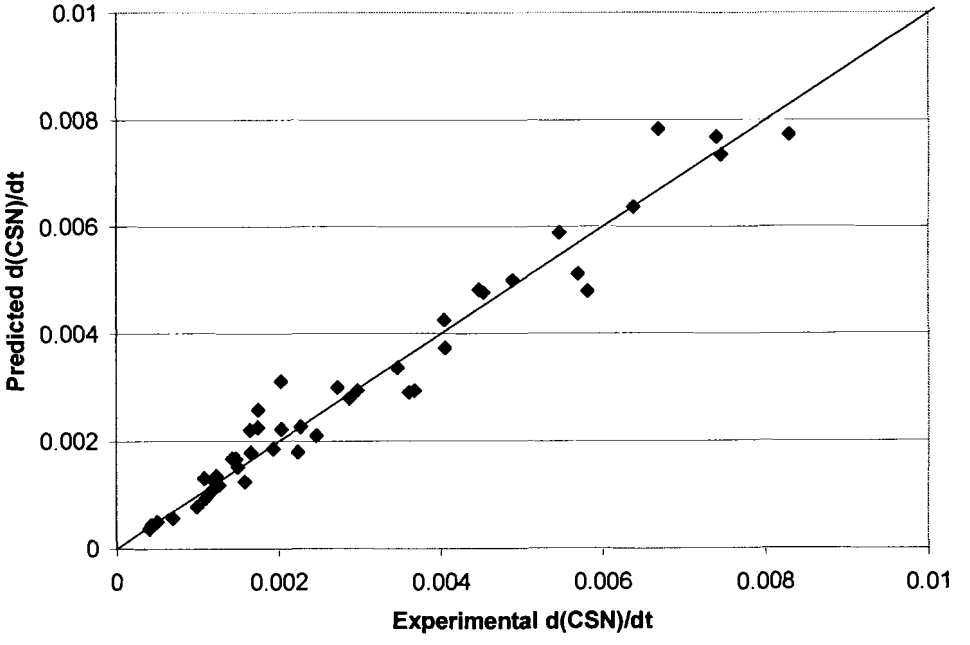

Figure 7.13. Predicted versus experimental d(CSN)/dt, 90 °C only

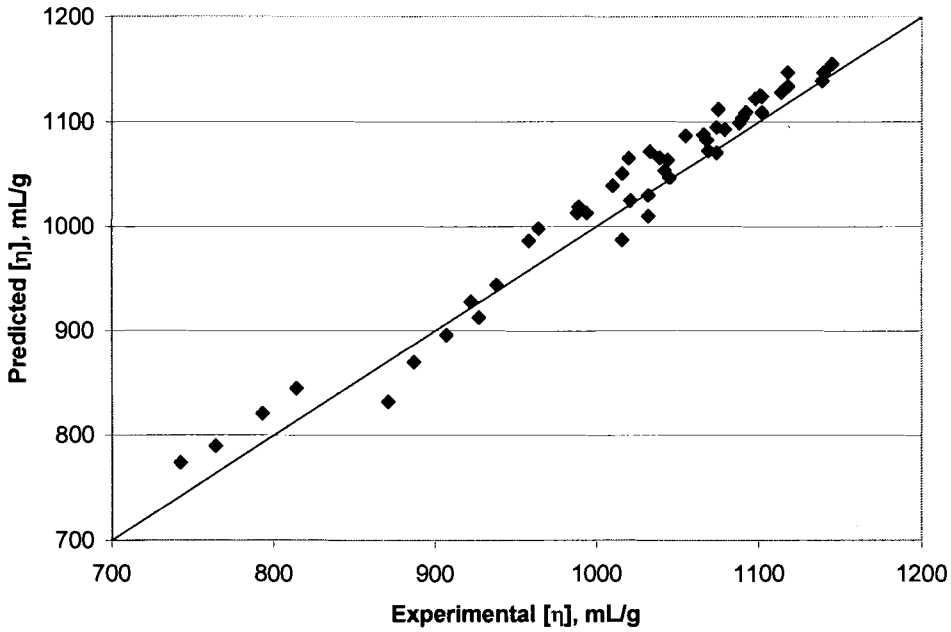

Figure 7.14. Predicted versus experimental intrinsic viscosity

7.7. SELECTIVITY PARAMETER MODELS

Several models were tested for the selectivity based on chain scission number. These models are shown in Table 7.8 The differential $(-dK_C/dt)/(d(CSN)/dt)$ did not have a favorable regression against the same variables as were tested for the numerator and denominator. Linear and power models for S_{CSN} ($\Delta K_C/CSN$) were tested as well. The best fit was model F4, as none of the R^2 values were better than 0.88. This model is given as:

$$S_{CSN} = \Delta K_C/CSN = 9.6\,[NaOH]^{-0.17}\,K_C^{0.52}\,(1-[Aa]/3.1)^{-0.66} \qquad (7\text{-}18)$$

Table 7.8. Selectivity parameter models

Model F1: $(-dK_C/dt)/(d(CSN)/dt) = b_0 \exp(-b_1/T)\,[NaOH]^{b2}\,K_C^{b3}\,(1-[Aa]/3.1)$					
R	0.870		± 95% confidence interval	p-stats:	
R^2	0.756	b_0	1.98 ± 2.1	int.	0.07
R-adj.	0.733	b_1	189 ± 566	x_1	.699
F-ratio	33.3	b_2	-.41 ± 0.06	x_2	2e-8
		b_3	0.44 ± 0.16	x_3	0.01
		b_4	-0.82 ± 0.15	x_4	3e-6
Model F2: $\Delta K_C/CSN = b_0 + b_1T + b_2\,[NaOH] + b_3\,K_C + (1-[Aa]/3.1)$					
R	0.928		± 95% confidence interval	p-stats:	
R^2	0.861	b_0	65.0 ± 28	int.	0.02
R-adj.	0.848	b_1	-0.076 ± 0.07	x_1	0.27
F-ratio	66.6	b_2	-4.24 ± 0.74	x_2	8e-7
		b_3	0.888 ± 0.26	x_3	0.001
		b_4	-28.0 ± 3.2	x_4	4e-11
Model F3: $\Delta K_C/CSN = b_0 \exp(-b_1/T)\,[NaOH]^{b2}\,K_C^{b3}\,(1-[Aa]/3.1)$					
R	0.924		± 95% confidence interval	p-stats:	
R^2	0.883	b_0	1.53 ± 0.5	int.	0.002
R-adj.	0.873	b_1	347 ± 220	x_1	0.111
F-ratio	81.4	b_2	-0.156 ± 0.03	x_2	3e-7
		b_3	0.446 ± 0.07	x_3	2e-7
		b_4	-0.666 ± 0.07	x_4	1e-12
Model F4: $\Delta K_C/CSN = b_0\,[NaOH]^{b1}\,K_C^{b2}\,(1-[Aa]/3.1)$					
R	0.936		± 95% confidence interval	p-stats:	
R^2	0.876	b_0	2.26 ± 0.16	int.	1e-17
R-adj.	0.868	b_1	-0.166 ± 0.03	x_1	8e-8
F-ratio	103	b_2	0.523 ± 0.06	x_2	5e-12
		b_3	-0.663 ± 0.07	x_3	2e-12
[NaOH] in g/L, T in Kelvin, t in minutes, Aa in % adsorbed on pulp, K in Kappa units					

Although equation 7-18 reports the model for the selectivity parameter, the best prediction of S_{CSN} is obtained by using the separate equations for $-dK_C/dt$ and d(CSN)/dt. In the differential solver in Appendix E, these models (B5 and E5, or equations 7.7 and 7.17) are already used to calculate final Kappa number and CSN. In Figures 7.15 and 7.16, the two methods of predictions are compared. Clearly, better results were obtained using equation 7.7 and 7.17 and calculating the selectivity than the selectivity correlation given in equation 7.18.

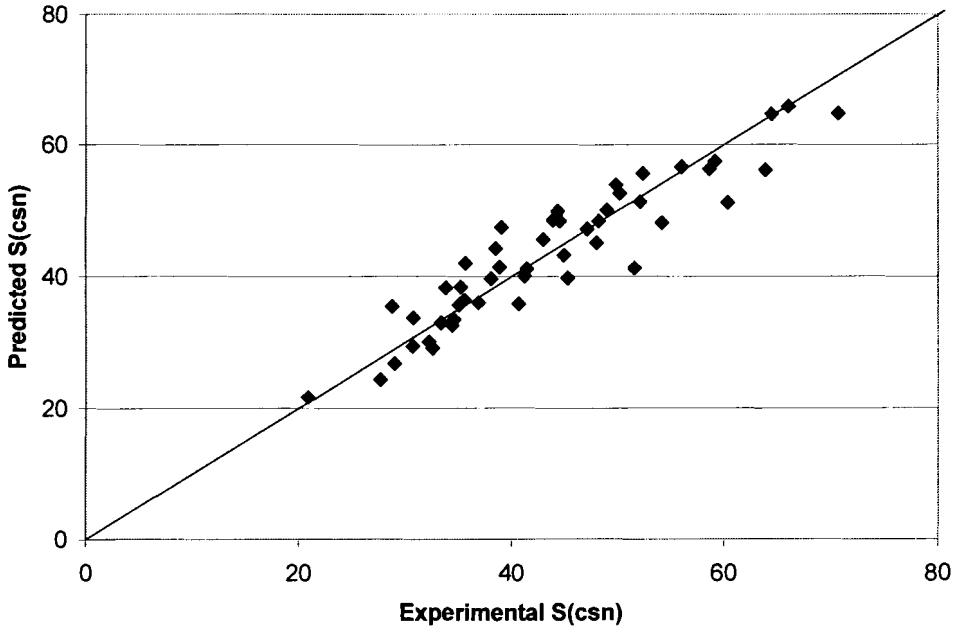

Figure 7.15. Predicted versus experimental selectivity parameter, equation 7-18

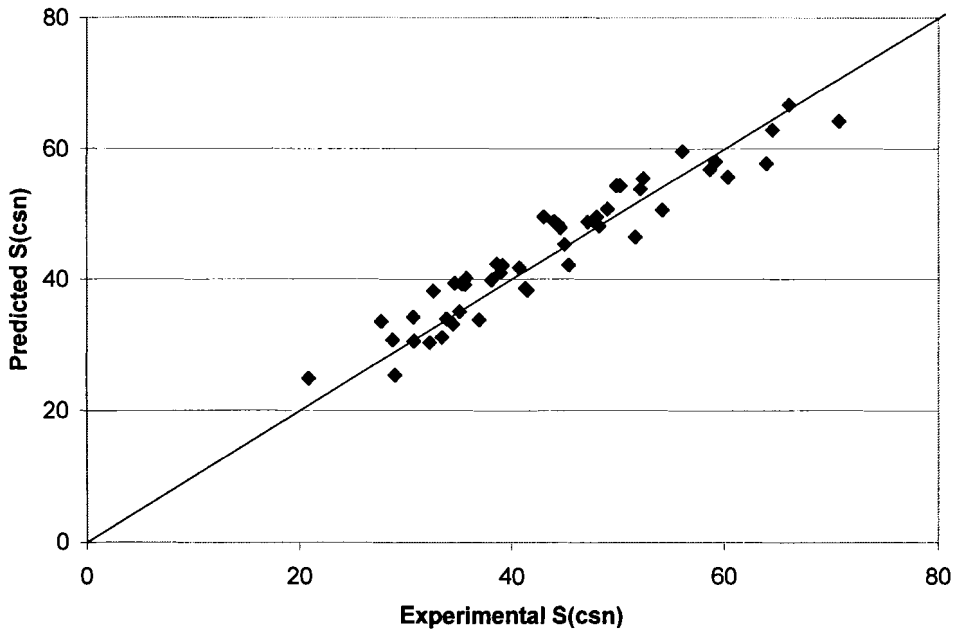

Figure 7.16. Predicted versus experimental selectivity parameter, equations 7-7 and 7-17

7.8. SUMMARY OF MODELS AND THEIR USE

Table 7.9 summarizes each of the best models determined in this chapter. In order to use these models to predict oxygen delignification behavior, the following instructions should be followed:

1. Specify initial conditions of Temperature, Oxygen Pressure (100 psig), [NaOH], Kappa number, Additive Charge, Intrinsic viscosity. Calculate DP_0
2. Calculate K_{CO} *by equation 7-11.*
3. Calculate [Aa] by equation 7-14.
4. Using Equation 7-7 and 7-4, K_C *and [NaOH] may be determined over time with use of differential solver.*
5. Using Equation 7-17, CSN may be determined over time similarly ($CSN_0 = 0$) *with the use of differential solver.*
6. Using equations 7-2 and 7-12, Kappa number may be calculated for each value of K_C *and* K_N.
7. Calculate viscosities and S_{CSN} *using the other useful equations.*

Table 7.9. Summary of best prediction models

Model	Equation
Corrected Kappa Number $-dK_C/dt = 4.0 \times 10^5 \exp(-9770/T) [NaOH]^{0.819} K_C^{3.81}$	(7-7)
Chain Scission Number $d(CSN)/dt = 6.0 \times 10^4 \exp(-9980/T) [NaOH]^{1.22} K_C^{3.38} (1/(1-[Aa]/3.1))$	(7-17)
[NaOH] consumption $\Delta[NaOH] = 0.169 \cdot \Delta K_C + 0.20$ g/L or $\Delta[NaOH] = 0.139 \cdot \Delta K$	(7-4) or (7-3)
K_O Correction $(K_O - K_{CO}) = K_O [-0.35 + 0.0011\ T + 0.020\ [NaOH]\ ]$	(7-11)
Kappa Number (via K_C and K_N) $(K_N - K_{CO}) = K_O [-0.35 + 0.0011\ T + 0.020\ [NaOH]\ ]/ (0.90\ t + 1)$ $K = K_C + (K_N - K_{CO})$	(7-12) (7-2)
Galactomannan Adsorption $\Phi = [Aa]/[A_{max}] = 0.35 \cdot a / (0.35 \cdot a + 1)$ A_{max}=3.0 (at 4.44 g/L NaOH), 3.2 (at 2.78 g/L NaOH), 3.3 (at 1.67 g/L NaOH)	(7-14)
Selectivity Parameter (model) $S_{CSN} = 9.6 [NaOH]^{-0.17} K_C^{0.52} (1-[Aa]/3.1)^{-0.66}$	(7-18)
Kappa Number (model) $-dK/dt = 4.4 \times 10^3 \exp(-7140/T) [NaOH]^{0.588} K^{3.12}$	(7-8)
Other Useful Equations $CSN = (1/DP_t - 1/DP_0) \cdot DP_0$ $\lvert\eta\rvert = 848 \log (\text{Tappi cp/cp}) - 265$ (in mL/g) $\lvert\eta\rvert = 0.6061 DP^{0.90}$ (Evans and Wallis, 1989) $S_{CSN} = \Delta K_C/CSN$	(7-15) (3-1)
[NaOH] in g/L, T in Kelvin, t in minutes, Aa in % adsorbed on pulp, a is in % adsorbed on pulp, K in Kappa units	

7.9. PREDICTION OF SELECTIVITY CURVES

Using the models and directions presented in the previous section, predicted data sets were generated for some initial conditions used in this investigation. Figures 7.17 to 7.19 show the predictions and the experimentally determined points, showing the effects of sodium hydroxide charge, galactomannan additive charge, and temperature on selectivity plots of Tappi viscosity versus Kappa number. The curves generated from our models accurately describe the experimental behavior. They contain an inflection point because the initial period is the most selective due to nitrogen extraction. The curves decrease rapidly when the alkali extraction has a lesser effect. Then at lower Kappa numbers, the curve becomes more selective. Although this is different from the selectivity curves we have seen previously, this is an expected result because the caustic concentration decreases with the Kappa number.

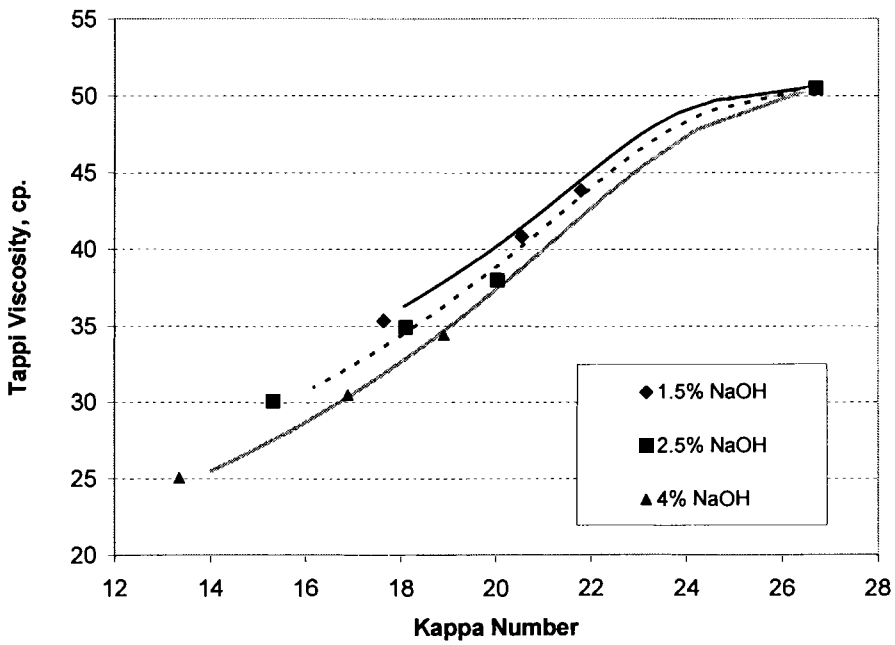

Figure 7.17. Predicted and experimental selectivity curves, Tappi viscosity versus Kappa number (effect of alkali charge)

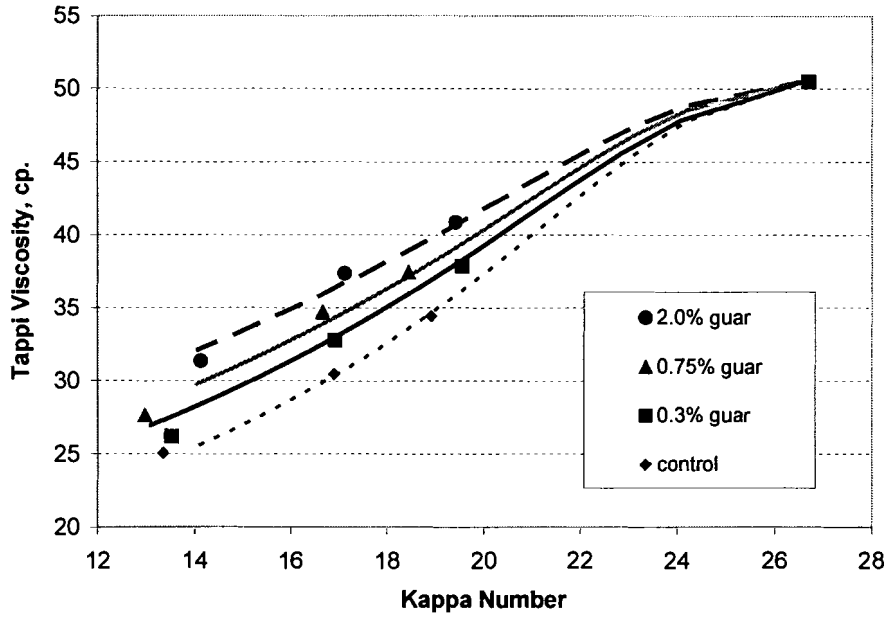

Figure 7.18. Predicted and experimental selectivity curves, Tappi viscosity versus Kappa number (effect of galactomannan charge, 4.0% NaOH and 90 °C)

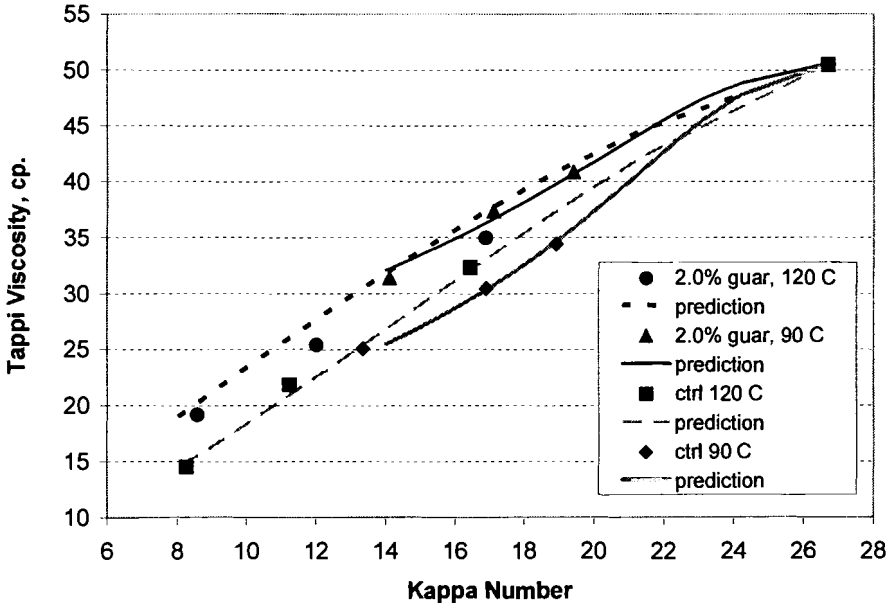

Figure 7.19. Predicted and experimental selectivity curves, Tappi viscosity versus Kappa number (effect of temperature and galactomannan charge, 4.0% NaOH)

Chapter 8

EXTENDED OXYGEN DELIGNIFICATION

The objective of this chapter is to extend oxygen delignification beyond 50 % Kappa number reduction, and possibly attain 70 % Kappa number reduction while minimizing excessive cellulose degradation. It has been previously shown that the selectivity decreased significantly by increasing alkali charge, but was unchanged by increasing the temperature above 90 °C (Section 5.4). Therefore, the strategy of increasing temperature and reaction times rather than alkali charge to achieve higher levels of delignification will be tested. Also, it has been shown that a constant alkali profile was beneficial for kinetic selectivity in pulping (Gullichsen and Paulapuro, 1999). This has led to the addition of caustic at multiple locations in extended cooking rather than all at the beginning of the pulping process. The present study will also test the impact of a more uniform sodium hydroxide charge profile on oxygen delignification selectivity by inter-stage addition.

The following sections will give results from extended delignification experiments employing the strategies of high temperature, greater reaction times, control of NaOH profile by split caustic addition, and the combination of multi-stage extended delignification with other additives tested previously in the investigation.

8.1. TWO STAGE DELIGNIFICATION

The results of some two stage delignification experiments are shown in Table 8.1. The experiments presented in this section were performed on IP pulp B as described in Table 6.7. The first experiment (A) in Table 8.1 shows the one stage control experiment

during which the time of delignification was 80 minutes at 3 % NaOH and 90 °C. This experiment was followed by a two stage experiment (B) at the same temperature but with the 3 % NaOH split evenly before each stage. The selectivity improvement from 17.7 to 22.7 (x 10^4) was similar to improvements when lowering caustic charge with IP pulp A, as seen in Table 5.2 where the selectivity was about 23 (x 10^4) at 1.5 % NaOH and 17 (x 10^4) at 4 % NaOH after 60 minutes. Clearly, the split caustic addition is a good strategy because the selectivity increased over 20 % and the Kappa number reduction was only 6 % lower at 45 % compared to 51 %.

In order to increase the degree of delignification, higher temperatures were employed in the second stage. This resulted in more delignification without much loss in selectivity, as the degree of Kappa number reduction reaches 58 % with a second stage temperature of 120 °C. At the intermediate second stage temperature of 110 °C, most of the increase in degree of delignification at 120 °C (58 %) was realized (55 %), and the selectivity was still favorable, only decreasing from 22.8 to 22.1 (x 10^4).

Table 8.1. Two stage extended oxygen delignification results

	Stage	Temp. °C	NaOH % on pulp	time min.	Kappa # (ΔK %)	[η] mL/g	S (x10^{-4})	Yield, %
A	1	90	3.0	80	13.52 (51 %)	916	17.7	97.1
B	1 2	90 90	1.5 1.5	20 60	14.25 (45 %)	979	23.4	97.3
C	1 2	90 110	1.5 1.5	20 60	11.62 (55 %)	952	22.1	96.2
D	1 2	90 120	1.5 1.5	20 60	10.89 (58 %)	919	21.8	96.1
Original pulp: Kappa = 28.0, [η] = 1172 mL/g								

The results shown in Table 8.1 are plotted in Figure 8.1 as well, with the conditions of each stage shown above the Figure caption. This plot clearly shows that the second stage higher temperature did not affect the selectivity significantly but extended the Kappa number reduction. This graphic also clearly shows that with split caustic addition a lower Kappa number may be reached at the same level of cellulose degradation. At the same maximum value of $(1/DP_t - 1/DP_0)$ of about 0.7 (x 10^4), the split caustic addition in combination with a higher temperature resulted in a Kappa number reduction of 17 units, compared to 14 units for the one stage experiment.

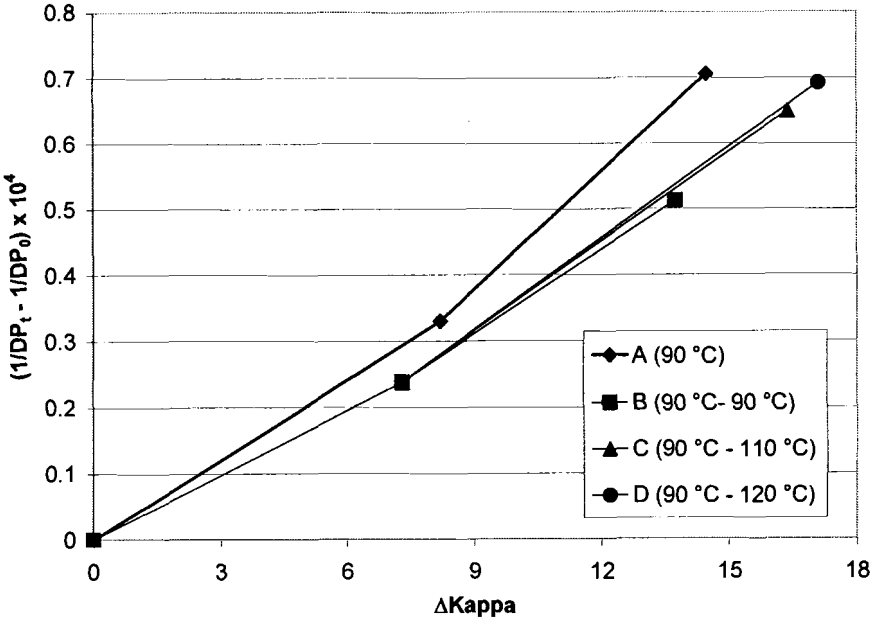

A = One stage, 3.0 % NaOH, 90 °C, t = 20 min. and 80 min.
B, C, D = Two Stage, 3.0 % NaOH split evenly before each stage:
First Stage: 20 min. at T = 90 °C
Second Stage: 60 min. at T = 90 °C (B), 110 °C (C), 120 °C (D)

Figure 8.1. Two stage oxygen delignification selectivity plot

In the experiments described above, a low temperature was used in the first stage. This was done because some previous researchers found that the cellulose degradation

was more temperature sensitive in the beginning of delignification (Olm and Teder, 1979; Hsu and Hsieh, 1988), and more recently Brewster and Justason (1999) reported a two stage process with a low temperature followed by a high temperature which has been patented (Section 2.7). However, in the present study, no major influence on selectivity was found at higher temperatures, particularly at the onset of oxygen delignification. It was only at very low Kappa numbers (below 8) when experiments at 120 °C became less selective (see Table 5.2), so this should not make any difference in the first stage of a two stage process. Table 8.2 compares the selectivity of two different first stage temperatures, 90 °C and 105 °C. As expected, a higher temperature did not decrease the selectivity significantly. Therefore, in subsequent multi-stage experiments the temperature of the first stage was raised as well.

Table 8.2. Comparison of first stage temperatures

Temp. °C	NaOH % on pulp	time min.	Kappa # (ΔK %)	[η] mL/g	S (x 10^{-4})
90	1.5	20	22.03 (21)	1062	23.4
105	1.5	20	21.36 (23)	1053	22.7
Original pulp: Kappa = 28.0, [η] = 1172 mL/g					

8.2. MULTI-STAGE DELIGNIFICATION

Table 8.3 summarizes some experiments in which three and four stages were used to achieve an even more uniform alkali concentration and a higher degree of lignin removal. The experiments E and H are the one stage controls without split caustic addition for the three and four stage experiments, respectively. The difference between F

and G is that in experiment G the time of the first stage is shortened to 20 minutes and the time of the third stage is increased to 40 minutes, because more NaOH should be consumed at the beginning than at the end of the reaction. As can be seen from the Kappa number reduction and the selectivity, there is not much difference between experiments F, G , and J. A high degree of delignification was reached, and the selectivity was significantly higher than that of the control reactions.

Table 8.3. Multi-stage extended oxygen delignification results

	Stage	Temp. °C	NaOH % on pulp	time min.	Kappa # (ΔK %)	[η] mL/g	S (x 10^{-4})
Three Stages							
E	1	105	3.0	90	9.63 (65 %)	739	14.6
F	1 2 3	105 105 105	1.5 1.5	30 30 30	10.54 (62 %)	910	24.3
G	1 2 3	105 105 105	1.5 1.5	20 30 40	10.11 (64 %)	920	25.0
Four Stages							
H	1	105	4.5	120	8.26 (70.5)	692	11.1
J	1 2 3 4	105 105 105 105	1.125 1.125 1.125 1.125	30 30 30 30	9.59 (65.8)	885	22.5
Original pulp: Kappa = 28.0, [η] = 1172 mL/g							

The four stage process (J) contained the lowest initial NaOH charge, 1.125 % on pulp, and the longest total reaction time of 120 minutes. Although this strategy does improve the degree of delignification some, the slightly lower selectivity and added

process equipment would prohibit the fourth stage in practice. The most promising options therefore are the three stage process G and the two stage process C.

The three stage delignification selectivity plot is shown in Figure 8.2, comparing these two options (F and G) to the one stage control experiment (E) with all the caustic added beforehand. In order to show the progress of these experiments, intermediate reaction times were also tested for Kappa number, viscosity, and alkali charge. There was little difference between the curves F and G. Figure 8.3 shows the alkali profile differences between three stage experiments F and G and the control one stage experiment E, which illustrates how the NaOH charge remains low with split addition.

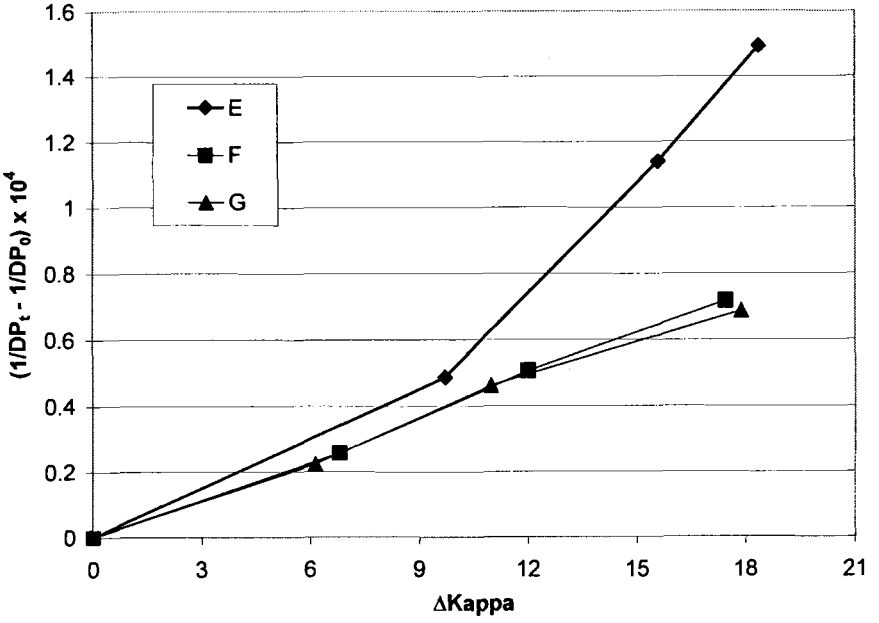

E = One stage, 105 °C, 4.5 % NaOH, 30, 60, 90 minutes shown.
F, G = Three Stage, 105 °C, 4.5 % NaOH split evenly each stage:
F: t = 30 min., then 30 min., then 30 min.
G: t = 20 min., then 30 min., then 40 min.

Figure 8.2. Three stage oxygen delignification selectivity plot

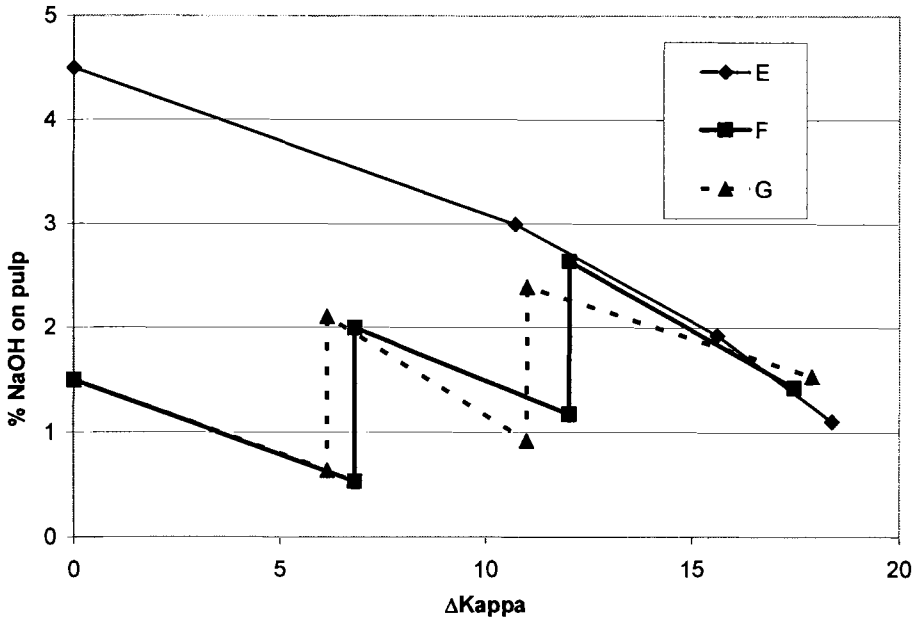

Figure 8.3. Alkali charge profile during three stage delignification

8.3. EXTENDED OXYGEN DELIGNIFICATION WITH ADDITIVES

The additives sodium gluconate, galactomannan , and glucomannan have thus far been the most promising chemical additives to the oxygen delignification process. These additives were then tested in combination with an extended two stage delignification process, and the results are shown in Table 8.4. Again, these results show that the split caustic addition is more selective than all caustic added beforehand, as indicated by comparison of experiments K and L in the first two rows of the table.

Charges of 0.75 % galactomannan (M) and glucomannan (N) were added, and the results were again similar, with glucomannan leading to a slightly higher selectivity. The same comparison resulted previously, as summarized in Table 6.8. Sodium gluconate, at a higher charge of 1 % (O), gave slightly better selectivity results than 0.75 glucomannan or galactomannan. Previously, a sodium gluconate charge of 2 % improved

the selectivity of IP pulp A from 17.4 to 22.2 (x 10^4) (See Figure 4.4), which is lower than the increase observed in Table 8.4 where the selectivity parameter increased from 25.3 to 32.6 (x 10^4). Sodium gluconate did not improve the selectivity of IP pulp B as much as it improved the selectivity of the other pulps shown in Figure 4.4; but this experiment was conducted at a lower alkali level (split 1.5 % + 1.5 % compared to 4 % NaOH). IP pulp B contained less iron but the same overall metals content as IP pulp A, and displayed about the same selectivity (Table 6.8). Lastly, the combination 0.75 % galactomannan and 1 % sodium gluconate (P) was tested in the two stage process. The resulting selectivity shown of 34.7 (x 10^4) was the greatest obtained thus far for such a high degree of Kappa number reduction (59 %). Although this is the highest selectivity yet attained, the observed increase from the two additives combined was not as great as the sum of the increases when adding them individually.

Table 8.4. Two stage extended oxygen delignification with additives

	Stage	Temp. °C	NaOH % on pulp	time min.	Kappa # (ΔK %)	[η] mL/g	S (x10^{-4})
K – one stage control	1	105	3.0	80	10.33 (63 %)	849	18.3
L – two stage	1 2	105 105	1.5 1.5	20 60	10.88 (61 %)	924	25.3
M – two stage + 0.75 % galactomannan	1 2	105 105	1.5 1.5	20 60	11.17 (60 %)	951	28.8
N – two stage + 0.75 % glucomannan	1 2	105 105	1.5 1.5	20 60	11.80 (58 %)	967	30.4
O – two stage + 1 % gluconate	1 2	105 105	1.5 1.5	20 60	11.23 (60 %)	973	32.6
P – two stage + 0.75 % galactomannan + 1 % gluconate	1 2	105 105	1.5 1.5	20 60	11.52 (59 %)	992	34.7
Original pulp: Kappa = 28.0, [η] = 1172 mL/g							

Figure 8.4. shows these experiments on the same graph. The comparative improvement in selectivity of split caustic addition (L) over the control experiment is larger than the improvement of the additives (M to P) over the split caustic addition (L). Also, as previously mentioned, these additives in combination do not improve the selectivity as much as the combined improvements from adding them individually. This may be due to the simple fact that a selective process is not as easily improved as a non-selective process.

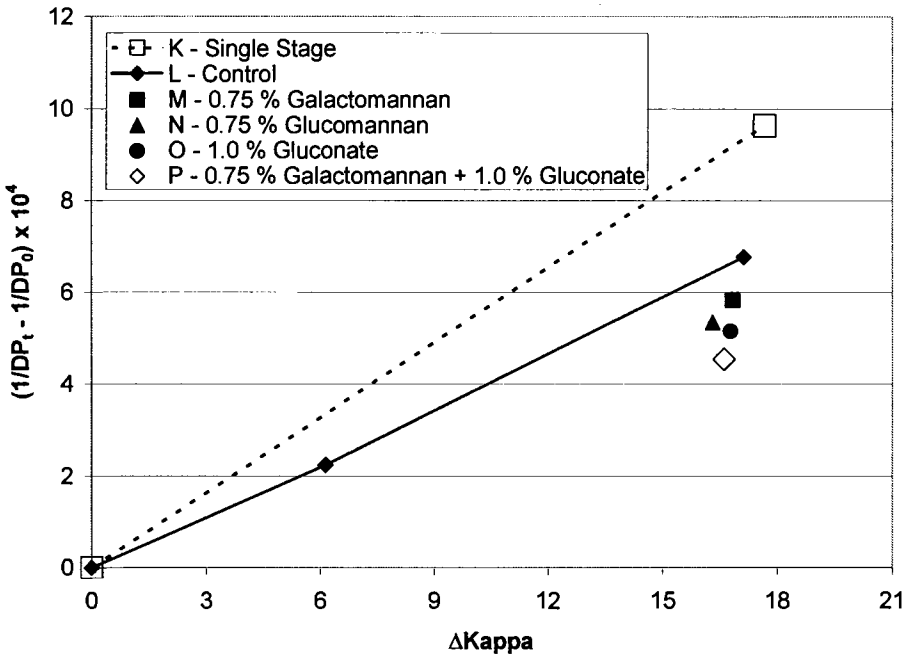

K = One stage, 105 °C, 3.0 % NaOH, 80 minutes
L = Control: Two Stages, 105 °C, 3.0 % NaOH even split, 20 min., 60 min.:
M = Two Stage + 0.75 % Gaur Galactomannan
N = Two Stage + 0.75 % Glucomannan
O = Two Stage + 1.0 % Sodium Gluconate
P = Two Stage + 0.75 % Gaur Galactomannan + 1.0 % Sodium Gluconate

Figure 8.4. Two stage oxygen delignification with additives

Chapter 9

CONCLUSIONS AND RECOMMENDATIONS

9.1. CONCLUSIONS

The objective of this research was to increase the selectivity of oxygen delignification, which may be achieved by decreasing the extent of cellulose degradation and/or by increasing the extent of lignin removal. The major hypothesis of our investigation was that polymer additives which adsorb on the pulp surfaces may scavenge harmful oxygen radicals and act as barriers protecting the cellulose from chain cleavage. The carbohydrate polymers starch, CMC, galactomannan, xylan, and glucomannan were tested. Although the focus here was primarily on inhibiting cellulose degradation, many of our findings deal with extending the degree of lignin removal as well.

9.1.1. Kinetics of Oxygen Delignification

Alkali charge was found to have a larger negative effect on oxygen delignification selectivity while the selectivity is not much affected by temperature. The temperature can be raised from 90 °C to 120 °C, increasing lignin removal by 36 % with almost no impact on selectivity. However, about the same increase in lignin removal (38 %) achieved by increasing the alkali charge from 1.5 % to 4 % resulted in a 36 % decrease in selectivity.

The selectivity of the oxygen-mediated reactions on lignin and cellulose during oxygen delignification can be determined by correcting the delignification and cellulose degradation by the changes solely due to alkali extraction. This newly calculated selectivity parameter is independent of the degree of delignification, supporting that

radicals generated by the lignin reactions are responsible for cellulose degradation. Previously it was believed that oxygen delignification was more selective at its onset, but the findings from the extraction experiments under nitrogen pressure showed that this is caused by extra lignin dissolution by caustic rather than oxygen reactions.

Extended delignification (55-65 % lignin removal) was successfully achieved by two- and multiple-stage oxygen delignification experiments, while not sacrificing selectivity. By using high temperatures, extended reaction time, and split NaOH addition to keep the alkali concentration low, the degree of delignification may be increased beyond that of conventional methods by almost a factor of two (from 33 % to 63 %) at just about the same selectivity ($S = 23 \times 10^4$).

9.1.2. Polymer Additives

Addition of galactomannan as an adsorbable radical scavenger gave significant improvements in oxygen delignification selectivity. The improvements in selectivity increased almost linearly with galactomannan charge at addition levels less than 0.75 % on pulp, after which the improvements become smaller. At the highest charge of 2.0 %, the improvement in lignin-cellulose selectivity was about 30 %, independent of alkali charge. Galactomannan adsorption on pulp was accurately measured using H.P.A.E.C. The improvements in selectivity were related to the adsorbed amount of galactomannan.

Other polymers tested in the investigation included starch, CMC, glucomannan, and xylan. Among these, glucomannan behaved similarly to galactomannan, but none of the other additives gave results as favorable. The differences can also be explained by the adsorption behavior of the polymers under alkaline conditions.

The selectivity parameter was found to increase linearly with the amount of adsorbed galactomannan, glucomannan, and xylan. Considering the chemical similarity of these three polymers, this confirms the hypothesis that adsorption of these polymers on pulp provides a protective shield against the radical attack on the cellulose.

9.1.3. Mathematical Modeling

By statistical analysis of the data, equations have been developed for modeling the experimental results and to predict oxygen delignification behavior. The models for the rate of Kappa number change by oxygen mediated reactions ($-dK_C/dt$), chain scission number ($d(CSN)/dt$), alkali consumption ($\Delta[NaOH]$), galactomannan adsorption ([Aa]), and the correction between K and K_C were determined as follows:

$$-dK_C/dt = 4.00 \times 10^5 \cdot \exp(-9770/T)\,[NaOH]^{0.819}\,K_C^{3.81} \qquad (7\text{-}7)$$

$$d(CSN)/dt = 5.99 \times 10^4 \cdot \exp(-9980/T)\,[NaOH]^{1.22} K_C^{3.38}\,(1/(1-[Aa]/3.1)) \qquad (7\text{-}17)$$

$$\Delta[NaOH] = 0.169 \cdot \Delta K_C + 0.20 \text{ g/L} \qquad (7\text{-}4)$$

$$(K_N - K_{CO}) = K_O\,[-0.35 + 0.0011\,T + 0.020\,[NaOH]\,]/\,(0.90\,t + 1) \qquad (7\text{-}12)$$

$$\Phi = [Aa]/\,[A_{max}] = 0.35 \cdot a\,/\,(0.35 \cdot a + 1) \qquad (7\text{-}14)$$

$$K = K_C + (K_N - K_{CO}) \qquad (7\text{-}2)$$

where K_C is the corrected Kappa number, K is the Kappa number, t is time in minutes, T is temperature in Kelvin, [NaOH] is the sodium hydroxide charge in g/L, CSN is the chain scission number, [Aa] is the adsorbed charge in % on pulp, and A_{max} is the maximum adsorbable charge of galactomannan in % on pulp (3.1 to 3.3 % as given in Section 7.9), and a is the galactomannan charge added in % on pulp.

9.2. RECOMMENDATIONS

Further evaluation of glucomannan as an additive to oxygen delignification should be conducted, since this additive was comparable or slightly more effective than galactomannan. In particular it should be studied how the increase in glucomannan content in pulp, for example by modifying the pulping process as in polysulfide and polysulfide-anthraquinone, will affect the oxygen delignification selectivity.

The use of the linear starch component amylose should be evaluated as an additive, but must be separated from amylopectin. Because of the molecular weight and structure of amylose, it should be much more capable of penetrating into the fiber and adsorbing on cellulose.

The kinetic models developed may be improved by adding data at one or two other temperatures, and by adding more conditions and reaction times for the alkali extraction experiments. It may also be beneficial to include oxygen pressure, pulp type, and initial Kappa number as influences to be studied.

More work should be conducted on extended oxygen delignification with even higher temperatures and a low alkali profile. This includes experiments with a different design of the oxygen reactor to achieve a uniform, low NaOH concentration throughout the process, for example by using a flow of liquor through the pulp suspension.

LIST OF TERMS

C	consistency, % solids
K	Kappa number, (milli-equivalents $KMnO_4$ consumed/10 g pulp)
K_C	Kappa number corrected to reflect changes only from oxygen reactions
K_O	Initial Kappa number
K_{CO}	Initial K_C value
K_N	The Kappa number resulting from extraction in the presence of nitrogen
NaOH %	Sodium Hydroxide charge, in % on Pulp
[NaOH]	Sodium Hydroxide charge in g/L
$[NaOH]_O$	Initial Sodium Hydroxide charge in g/L
DP	Degree of polymerization, monomer units per molecule
DP_t	Degree of polymerization at time t
DP_0	Degree of polymerization at time zero
CSN	Chain Scission Number $CSN = (1/DP_t - 1/DP_o)\cdot DP_0$
$[\eta]$	Intrinsic viscosity, mL/g
V	Tappi viscosity, centipoise
S	Selectivity, $S = \Delta K(1/DP_t - 1/DP_o)$
S_c	Corrected selectivity, $S = \Delta K_C(1/DP_t - 1/DP_o)$
S_{csn}	Corrected Selectivity based on chain-scission, $S = \Delta K_C / CSN$
[Aa]	Adsorbed additive, % on pulp
$[A_{max}]$	Maximum adsorbable additive, % on pulp
a	Charge added, % on pulp
T	Temperature, K or °C
t	Time, minutes
P	Pressure, kPa or psig
Φ	Fractional coverage of adsorbent (in Langmuir equation)
k	constant (slope) used in Langmuir equation
Y	The independent variable Y (used in models)
Y_i	Values of Y from 1 to i
Y'_i	Values of the prediction of Y from 1 to i
$x_1, x_2, \ldots$	Independent variables x from 1 to j
$b_0, b_1, b_2,$	Coefficients determined from regression
Y_{avg}	Mean value of all Y
b	Constant used in numerical models
E_A/R	Activation energy divided by the gas constant, in K^{-1}

WORKS CITED

Abrahamsson, K. and Samuelson, O., Oxygen-alkali Cooking of Wood Meal (5) Influence of Metal Compounds and Soaking in Acid, *Svensk Papperstid.* v. 78, no. 4, 1975, p. 135-140.

Agarwal, N. and Gustafson, R., Effect of Carbohydrate Degradation on Zero-span Tensile Strength, *Tappi Journal,* v. 78, no. 1, January 1995, p. 97-100.

Agarwal, S. B., Genco, J. M., Cole, B. J. W., and Miller, W., Kinetics of Oxygen Delignification, *Journal of Pulp and Paper Science,* v. 25, no. 10, October 1999, p. 361.

Argyropoulos, D. and Liu, Y., The Role and Fate of Lignin's Condensed Structures During Oxygen Delignification, *Journal of Pulp and Paper Science,* v. 26, no. 3, March 2000, p. 107-113.

Argyropoulos, D., Akim, L., and Ahazi, B., Salient Reactions in Lignin During Pulping and Bleaching, *88th Annual PAPTAC Meeting,* 2002, p. A165-A170.

Bennington, C.P.J. and Pineault, I., Mass Transfer in Oxygen Delignification Systems: Mill Survey Results, Analysis, and Interpretation, *Pulp and Paper Canada,* v. 100, no. 12, 1999, p. 123-131.

Berry, R., Zhi-Hua, J., van Lierop, B., and Sacciadis, G., Recommendations from Computer Modeling for Improving Single Stage Oxygen Delignification systems, *PAPTAC 88th Annual Meeting*, Montreal, Canada, January 2002, p. B151-B161.

Bouchard, J., Nugent, H. M., and Berry, R. M., A Comparison Between Acid Treatment and Chelation Prior to Hydrogen Peroxide Bleaching of Kraft Pulps, *Journal of Pulp and Paper Science*, v. 21, no. 6, 1995, p. J203-J208.

Brewster, J. and Justason, A., Extended Oxygen Delignification at Irving Pulp and Paper, Ltd., *1999 Tappi Pulping Conference*, 1999, p. 161-168.

Brown, G. and Dawe, R., Effects of Metal Ions on Oxygen Delignification of Kraft Pulp, *1996 International Pulp Bleaching Conference*, 1996, p. 383-390.

Colodette, J. L. and Santos de Campos, A. S. , Improvements in a Process for Delignifying Lignocellulosic Pulp by Means of Oxygen, *European Patent 0524127A2*, 1993.

Dang, Z., Pulp pretreatments for improved selectivity and extended oxygen delignification, M.S. Thesis, University of Maine, 2002.

Dence, C. W. and Reeve, D. W., Pulp Bleaching Principles and Practices, Tappi Press, Atlanta, GA, 1996, p. 215.

Evans, R. and Wallis, A.F., Cellulose Molecular Weights Determined by Viscometry, *Journal of Applied Polymer Science,* v. 37, 1989, p. 2331.

Fenton, H. J. H., Oxidation of Tartaric Acid in the Presence of Iron, *Journal of the Chemical Society,* v. 65, 1894, p. 899.

Gelman, R. A., Novel Salts of Carboxymethylcellulose, *U. S. Patent no. 4,650,716,* March 1987, p. 1.

Gendron, S., Bouchard, J., and Berry, R., Optimal Selection of Operating Conditions for an Oxygen Delignification Tower, *2002 International Pulp Bleaching Conference*, Portland, OR, May 2002, p. 121-137.

Gevert, B. S., Lohmander, S. F., and Samuelson, O. H., Interactions Between Metal Compounds During Oxygen Bleaching of Kraft Pulp in Virtually Closed Recovery Systems, *Tappi Journal,* v. 80, no. 7, 1997, p. 177-185.

Gierer, J., Ek, M., Jansbo, K., and Reitberger, T., A Study on the Selectivity of Bleaching with Oxygen-Containing Species, *Holzforschung,* v. 43, no. 6, 1989, p. 391-396.

Gratzl, J. S., The Chemical Basis of Pulp Bleaching with Oxygen, Hydrogen Peroxide, and Ozone - a Short Review, *Papier,*v. 10A, Oct. 1992, p. V1-V8.

Guay, D., Cole, B. W., Fort Jr., R. C., Genco, J. M., and Hausman, M. C., Mechanisms of Oxidative Degradation of Carbohydrates during Oxygen Delignification, *I.S.W.P.C.*, 1999.

Gullichsen, J., Jakara, J., Koljonen, J., and Soini, P., Effect of Transition Metals on Oxygen Delignification and Peroxide Bleaching, *Paperi ja Puu*, v. 80, no. 2, 1997, p. 116-121.

Gullichsen, J. and Paulapuro, H., Papermaking Science and Technology Volume 6A: Chemical Pulping, Gummerus Printing, Finland, 1999, p. A556.

Hausman, M. C., A Mechanistic Study of the Degradation of Lignin Model Compounds with Oxygen Species, Ph.D. Thesis, University of Maine, 1999.

Hiemenz, P.C. and Rajagopalan, R., Principles of Colloid and Surface Chemistry, Marcel Dekker, Inc., New York, 1997, p. 333-335.

Hogg, J. and Ledolter, J. Engineering Statistics, MacMillan Publishing, New York, 1987, p. 304-307.

Hsu, C. L. and Hsieh, J. S., Reaction Kinetics in Oxygen Bleaching, *AICHE Journal,* v. 34, no. 1, 1988, p. 116-132.

Iribarne, J. and Schroeder, L., High Pressure Delignification of Kraft Pulps: Kinetics. *Tappi Journal,* v. 80, no. 10, October 1997, p. 241.

Kang, G. J., Ni, Y., and van Heiningen, A. R. P., Effect of Selected Chemicals in Recycled Filtrate on the Selectivity During O_2 Delignification, *1998 Tappi Pulping Conference,* 1998, p. 7-12.

Kiemele, M., Schmidt, S., and Berdine, R. Basic Statistics, 4th ed., Air Academy Press, Colorado Springs, CO, 1997, p. 7-28 – 7-33.

Li, J. and Gellerstedt, G., On the structural significance of the kappa number measurement, *Nordic Pulp & Paper Research Journal*, v. 13, no. 2, June 1998, p. 153-158.

Li, Z., Ni, Y., and van Heiningen, A. R. P., Acid Washing and Chelation in a Displacement System: A Comparative Study, *Journal of Pulp and Paper Science*, v. 26, no. 10, 2000, p. 341-345.

Li, Z., van Heiningen, A. R. P., and Ni, Y., Removal of Manganese from Pulp Fibers with MgSO4 in a Displacement System, *1999 Tappi Pulping Conference,* 1999, p. 197-205.

Liden, J. and Ohman, L. O., Redox Stabilization of Iron and Manganese in the +II Oxidation State by Magnesium Precipitates and Some Anionic Polymers, *Journal of Pulp and Paper Science,* v. 23, no. 5, 1997, p. J193-J199.

Manouchehri, M. and Samuelson, O., Oxygen Bleaching in the Presence of Manganese and Iron Compounds, *Svensk Papperstd,* v. 80, no. 12, 1977, p. 381.

McDonough, T. J., Mechanism of Nitrogen Dioxide Pretreatment for Oxygen Bleaching of Kraft Pulp. *Journal Jpn. Wood Res. Soc.,* v. 38, no. 6, June 1992, p. 570-578.

McDonough, T. J., Oxygen Bleaching Processes, *Tappi Journal*, v. 69, no. 6, June 1986, p. 46.

Miller, W., Sullivan, D. P., Genco, J. M., Zou, H., Johnson, D., and Kwon H. B., Medium Consistency Oxygen Delignification Design Using a Two Phase Concept. Part 2. High Solids Carry-over. *1998 Tappi Pulping Conference*, 1998.

Olm, L. and Teder, A., The Kinetics of Oxygen Bleaching, *Tappi Journal,* v. 62, no. 12, 1979, p. 43-46.

Olm, L. and Teder, A., Extended Delignification by Combination of Modified Kraft Pulping and Oxygen Bleaching, *Paperi ja Puu.,* v. 4a, 1981, p. 315-326.

Pageau, G.L., Optimization and Control of a Two-stage Oxygen Delignification System, *1996 International Pulp Bleaching Conference*, 1996, p. 123-128.

Parthasarathy, V.R. et al. Hydrogen Peroxide Reinforced Delignification of Southern Pine Kraft Pulp and Short Sequence Bleaching, *1989 Tappi Pulping Conference,* 1989, p. 539-545.

Payton, J. H. and Canaris, N. M., Bleaching Compositions Comprising Sulfamates and Borates or Gluconates and Processes, *US Patent no. 5,639,348*, 1997.

Perng, Y. and Oloman, C. W., Kinetics of Oxygen Bleaching Mediated by Electrochemically Generated Ferricyanide, *Tappi Journal,* v. 77, no. 7, 1994, p. 115-124.

Presley, J., Hill, R., and Chauveheid, E., New Metals-Control Technique Improves Bleaching Performance, *Pulp and Paper,* v. 71, no. 10, October 1997, p. 125-131.

Rice, R. G. and Do, D. D., Applied Mathematics and Modeling for Chemical Engineers, John Wiley and Sons, Inc., New York, 1995, p. 253-258.

Robert, A., Traynard, P., and Martin-Borrett, O., Delignification and Bleaching of Chemical and Semichemical Cellulose Pulps with Oxygen and Catalyst, *US Patent no. 3,384,533*, 1968.

Rojas, O. J. and Neuman, R. D., Adsorption of Polysaccharide Wet-end Additives in Papermaking Systems, *Colloids and Surfaces A: Physiochem. Eng. Aspects,* v. 155, 1999, p. 419-432.

Samuelson, O. and Ojteg, U., Behavior of Calcium, Magnesium and Manganese Compounds During Oxygen Bleaching of Kraft Pulps, *Journal of Wood Chemistry and Technology,* v. 15, no. 3, 1995, p. 303-328.

Samuelson, O. and Ojteg, U. Optimized Oxygen Bleaching of Kraft Pulp Treated with Nitrogen Dioxide, *Tappi Journal,* v. 77, no. 11, 1994, p. 127-134.

Sawyer, D. T., Metal-Gluconate Complexes, *Journal of Chemical Abstracts,* 1964, p. 633-645.

Schoon, N.H., Interpretation of rate equations from kinetic studies of wood pulping and bleaching, *Svensk Papperstid*, v. 85, no. 18, December 1982, p. R185.

Seth, R.S., Zero-span Tensile Strength of Papermaking Fibres, *85th Annual Paptac Meeting,* 1999, p. A161.

Sihtola, H. et al, Comparisons and Conversion of Viscosity and DP – Values by Different Methods. *Paperi ja Puu*, v. 4a, 1963, p. 225.

Sjogren, B. and Hook, J., Extended Oxygen Delignification – the Effect of Pretreatments and Process Conditions, *2000 International Pulp Bleaching Conference*, p. 242.

Solinas, M. and Proust, A. M., Oxygen Bleaching Process for Cellulosic Pulps with a Polyhydric Alcohol Cellulose Protector, *US Patent no. 5,609,723*, 1997.

Steffes, F., Bokstrom, M. and Norden, S., Pulp Yield Improvement using Two-Stage, Extended Oxygen Delignification, *1998 TAPPI Proceedings: Breaking the Pulp Yield Barrier Symposium*, 1998, p. 183-195.

Swan, B. and Gustavsson, R., Bleaching Cellulose Pulp in the Presence of Formaldehyde, *US Patent 4,004,967*, 1977.

Swinkels, J. J. M., Compositions and Properties of Commercial Native Starches, *Starke*, v. 37, no. 1, 1985, p. 1-5.

Towers, M. and Scalan, A. M., Predicting the Ion Exchange of Kraft Pulps Using Donnan Theory, *Nonwovens Report International*, v. 76, no. 281, August 1994, p. 50.

Ullmann, F., Cellulose Ethers. Ullmann's Encyclopedia of Industrial Chemistry 5th Ed., v. B2, Weinheim Publishers, New York, 1989, p. 461.

Yethon A.E., Nitrogen Dioxide-Oxygen Delignification, *Canadian Patent no. 1070909*, 1980.

Young, J. H., Peroxide Bleaching Compositions and Their Use, *US Patent no. 2,927,082*, 1960.

Zou, H., Effect of Kraft Pulping on Oxygen Delignification Kinetics, Ph.D. Thesis, University of Maine, 2002.

Zou, H. and Genco, J. M., Influence of Kraft Pulping on the Kinetics of Oxygen Delignification. *TAPPI Journal*, v. 83, no. 2, 2000, p. 65-71.

APPENDICES

APPENDIX A

Detailed Experimental Methods

Experimental Method for Carbohydrate Analysis using H.P.A.E.C.

by Dr. Denilson Da Silva Parez, Dr. Yang Gao, and revised by Steven Violette

A.1. PURPOSE OF SUGAR ANALYSIS:

To quantitatively determine carbohydrate compositions in pulp or wood sample, using High Performance Liquid Chromatograph (HPLC), by analyze the hydrolysate.

A.2. PREPARATION OF STANDARD SOLUTIONS

A.2.1. Preparation of the internal standard solutions

Prepare 100 ml solution containing approximately 50 mg/ml of fucose. The final concentration must be exactly determined by both the weight and the purity of fucose. If using fructose as internal standard, the concentration should be prepared in 5.0 g/L or 2.5 g/L (2.5 mg/mL).

A.2.2. Preparation of the external standard solutions (calibration solutions)

Authentic sugar samples must be purchased from Supelco, Aldrich or other suppliers. Arabinose, Galactose, Glucose, Xylose and Mannose are compositions used for the determinations. Rhamnose and other minor sugars may also present in some wood species though in very little concentration, therefore they will be neglected. A stock solution is prepared and diluted into six different concentrations. Those calibration solution will be used as external standards No.1 though No.6.

Stock Solution

Prepare 100 ml of tock solution, which contains all of 5 sugars in the following approximate concentrations:

- Arabinose: 1 mg/ml 0.10 g/100ml volumetric flask
- Galactose: 1 mg/ml 0.10 g/100ml volumetric flask
- Glucose: 4 mg/ml 0.40 g/100ml volumetric flask
- Xylose: 2 mg/ml 0.20 g/100ml volumetric flask
- Mannose: 2 mg/ml 0.20 g/100ml volumetric flask

Before weighing monosugars for preparing stock solution, the sugars should be dried in a vacuum oven at 40°C. The final concentration must be exactly determined by weighing. Purity of the compounds must be taken into account when calculate the final concentration of the stock solution.

External Standard Solution (Calibration No.1 to No.6)

To prepare the standard solution, dilute the stock solution as following procedure:

1. Take exactly and quantitatively 1 ml, 2 ml, 4 ml, 8 ml, 16 ml and 32 ml of stock solution, transfer into 6 numbered 50-ml volumetric flasks. Fill separately the six volumetric flasks with 40, 39, 37, 33 25 and 9 ml of de-ionized water.
2. Add into each flask with 1.5 ml 72% H_2SO_4 and 1ml internal standard solution (fucose).
3. Cover the volumetric flasks with a piece of aluminum foil.
4. Hydrolyze the solution in an autoclave at 121°C for 1 hour.
5. Fill the volumetric flasks with de-ionized water to 50 ml volume.
6. Filter the solution through a 0.45 μm membrane.
7. Transfer about 8 ml of filtrate into a 10 ml testing vial, which is used for HPLC analysis.

Keep the standard solution frozen for preventing negative effect by microorganism, oxygen, light and temperature.

A3. PREPARATION OF PULP SAMPLES

Before hydrolysis, pulp or wood must be ground. Prepare about 1.5 g of the sample for all of the determination. For the quantitatively determination of carbohydrates, moisture content of sample must be determined.

For wood samples, extraction step is required before hydrolysis. For pulp, if this step is neglected, the extractive content should be known for the carbohydrates calculation, and as well as ash content. For the purpose of protecting of the column system, all samples should be the extractive-free.

1. Weigh 100 mg (o.d.) of sample in a test tube, add exactly 1.5 ml of 72 % H_2SO_4 for 1 hr of primary hydrolysis at 30°C. During the period of primary hydrolysis, the slurry must be manually stirred using a stirring rod every 10-15 min.
2. Using 41 ml of de-ionized water to transfer quantitatively the slurry into a 50-ml volumetric flask. Add 1 ml of the internal standard solution (fucose or fructose) in advance of transferring.
3. Cover the volumetric flasks with a piece of aluminum foil.
4. Put the volumetric flasks inside an autoclave, to hydrolyze the solution for 1 hr. at 121°C.
5. Fill the volumetric flask with de-ionized water to the final volume of 50 ml.
6. Filter the hydrolysate through a 0.45-μm membrane, or using a "Fine" porosity filter (for quantitative purposes only).
7. Transfer about 8 ml of filtrate into a 10 ml testing vial, which is used for HPLC analysis.

After completed sample preparation, HPLC analysis should be run as soon as possible. Before running HPLC analysis, keep the specimens in a freezer for preventing negative effect by microorganism, oxygen, light and temperature.

A4. OPERATION OF ION CHROMATOGRAPH

A.4.1. Preparation of the solutions to be used in the IC

***General recommendations*:**

- Freshly de-ionized water should be used to prepare the solutions.
- De-ionized water stored in the reservoir contains too much dissolved carbon dioxide what leads to instability in the retention time of the sugars.
- Before preparing the solutions, water must be filtered through a 0.45 μm membrane and then de-aired with helium for at least 10 minutes.
- A line adapter is needed for de-aerating the bottles, otherwise you will throw the liquid out of the bottle.
- Sodium hydroxide solutions MUST be prepared from 50 % weight solution.
- Pellets should not be used because they are covered with a layer of sodium carbonate.
- Sodium hydroxide solutions should not be filtered after prepared, because it will absorb CO_2 from the air.
- Sodium hydroxide solutions should not be de-aired because bubbles are generated, and bubbles are one of the major problems in the liquid chromatography.
- Run the chromatography with 0.3 M NaOH solution in the column for 24 hours before each batch.

NaOH solutions

(1) 0.3 M NaOH (used as eluent C and for post-column addition)
- 15.84 ml of 50 % NaOH solution for 1 L of solution, or 31.68ml for 2 L.

(2) 1.0 M NaOH (used for reconditioning the column)
- 52.80 ml of 50 % NaOH solution for 1 L of solution.

0.17 M Sodium Acetate in 0.20 M Sodium Hydroxide solution (used as eluent B)

(3) - 23.14 g of $NaCH_3COO$ for 1 L, or 46.68 g for 2 L.
- 10.56 ml of 50 % NaOH solution for 1 L of solution, or 21.12 ml for 2 L.

- Dissolve the sodium acetate in 100 ml of filtered, de-aired, and de-ionized water. Filter again and wash the filter system with 50 ml of water. Transfer the solution quantitatively to a 1-L volumetric flask and add the sodium hydroxide. Finally, complete to the 1-L mark with water. Before starting pumping into the column, if you newly prepared new solution, you MUST purge the system to remove bubbles !!!

A.4.2. Preparation of the Chromatograph

Before running samples:

- Fill up the bottles with the eluent solutions:
  - A – water
  - B – 0.17 M $NaCH_3COO$ in 0.2 NaOH solution
  - C – 0.3 NaOH solution
- Pressurize both nitrogen and helium lines.
  - Pressurize the bottles (1 main valve and 1 valve for each bottle) and the post-column addition system (1 switcher).
  - Turn the auto-sampler, the pump and the detector ON.
  - Purge the lines containing new solutions by doing the following:
  - Open the valve that allows the bypass of the column (if you don't know which valve is, CHECK THE PUMP MANUAL FIRST).
  - Set up the composition of eluent mixture in 100 % of the line that you want to be purged and pressing PURGE on the pump panel.
  - Allow the line to be purged until all bubbles are eliminated (at least 4 minutes, but it can take longer if you see bubbles in the outlet line).
  - Change the composition to 100 % of the next line to be purged and repeat the purge procedure.
  - Stop the purging by pressing PURGE in the pump panel. Do not close the valve before stopping the purge because it leads to an excessive pressure in the system and this can damage in the column !
  - Close the by-pass valve.
- Run the chromatography with 0.3 M NaOH solution in the column for 24 hours before each batch.
- Set the composition of the eluent to 94 % A – 6 % C and turn the pump ON.
- Observe if pressure increases and if it remains stable. If the pressure oscillates between two values, there probably is a bubble in one of the heads of the pump. You need to check the pump manual in order to remove it.

A.4.3. Using the PeakNet software to control the IC

When you turn the computer on, the PeakNet Software will automatically be loaded. You will have the main menu on the screen. A selection of the most important functions of the software, presented in the PeakNet Software User's Guide is reproduced here. If you need further information, see the Manual.

Configuration

This program allows you to specify the connection between the computer and the modules of the ion chromatograph. Unless you have a problem of communication, you do not need to run this program.

Method

The analytical method used for sugar analysis is based on the paper published by M. Davis from the Forest Products Laboratory (*M. W. Davis, J. Wood Chem. Technol., 18(2), 235-252 (1998)*) with some minor modifications. All the information related to the method is stored in the file *UMaine Sugar Analysis Method.* Each operator must have a copy of the method in its personal folder. If the file is destroyed or re-written by mistake, a copy of the file can be found in the folder C:\Operators\Copy of UMaine Method. The method is also described in the appendix A. If you need to create a new method, see the PeakNet Software User's Guide, section 5.

Creating or up-dating calibration curve concentration data

One important operation to be performed here is the input of calibration curves parameters. When you **prepare** new solutions of the calibration curve standards, you need to up-date the information about the real concentrations of the sugars to be analyzed. **If you are not using new calibration standard solutions, go to the next topic.** Once the parameters are entered once, you do not need to change until the next time you prepare the solutions. However, you need to up-date the response factors every time you run calibration curve standards (see *3.5.1. Up-dating calibration curve response factors* topic). You can use the following sequence:

- Load the *UMaine Sugar Analysis Method* file from your personal folder.
- Highlight the ED-40 ELECTROCHEMICAL DETECTOR box. Data Click on the edit calibration parameters icon one and be sure to use the following parameters:
    - Under General menu:
        - Standardization: INTERNAL;
        - Replicates: Although the calibration curves obtained with only 1 injection are very good, better correlation coefficients can be obtained with 3 or 4 replicates.
        - Update date: REPLACE RETENTION TIME AND UPDATE RESPONSE (replace) should be marked.
    - Under Defaults menu:

    Enter the Internal Standard Amount in Samples in mg

Click on component table icon. A table containing the information about the calibration standards will appear.

- Check (and adjust if necessary) the sugars retention time if you have run one chromatogram (if not, this operation can be performed later).
- Click on CALIBRATION STANDARDS on the top of the table.
- Up-date the concentrations of the Levels 1 to 6, according to the concentration calculations for the new solutions.
- Click on APPLY when you have done.
- Click on OK to finish this operation and do not forget to SAVE the method.

Schedule

The Schedule Editor is used to create, edit, and save Schedules, which consist of a series of analysis to be automatically performed. A typical schedule is composed of calibration standards, samples, column storage preparations, and system shutoff. An example is given here:

Each line of the schedule represents one injection. If you are going to build up a new schedule file, go to FILE, and then NEW and chose AS50 SCHEDULE. Otherwise, you can use an old schedule file, but first of all, SAVE it with different file name. You can then make the modifications you need and have a new schedule without much trouble.

The following information fields are to be completed for each sample:

- Vial #: The position of the sample on the auto-sampler samples compartment.
- Ink/Vial: Number of injections of the same sample to be performed
- Volume (to be injected): Use 2 to 5 μL. 3 μL is the usual volume.
- Inj. Type: Chose PARTIAL LS among the options.
- Cut. Vol.: Use 0 for the volume to be discarded for each injection.
- Syr. Spd: Use 3 for the syringe speed.
- Sample: Type the sample identification - Sample type: You have the choice between calibration std., calibration chk., or sample, depending or your sample.
- Level: Used only for calibration standard injections. The number of the concentration level here MUST match with those entered in the *component table* of method (*see Creating or up-dating calibration curve concentration data* topic).
- Method: Double-click on the cell and open the method file from you personal folder.
- Sample prep.: Leave blank.
- Data file: Double-click on the cell and enter a name for saving the file to be generated for this sample. You can use the same name for all the samples of a batch, and the system will add a number at the end of the name, starting with A001, A002, etc.
- Dilution, Weight, Int. std: Use 1 for these fields. By adding the last two lines shown in the example, you will be sure that the column will be stored with the correct NaOH concentration solution and the system will be turned OFF. This is very important when you perform the analysis overnight. Do not forget to place the sample in the same order described in the schedule file. SAVE the file when you have done.

Run

Run program is used to conduct the analyses specified in Schedule and Method programs. Besides this main function, it also provides real-time information about the equipment and direct control of all the installed modules, among others.

Direct control

Use the icon shown in the picture above or click on RUN and then DIRECT CONTROL to have access to full control of all the modules of the equipment. You can make changes on the operating variables of the pump, auto-sampler, or electrochemical detector. The most useful parameters for the operation of each one of the modules are listed here:

a) AS-50 auto sampler:

Flush and Prime (removal of bubbles and cleaning up both syringe and injection port).

b) GP-50 pump

On/Off, Flow, Pressure Limits, Eluent Composition, Open/Close Pneumatic Valves.

c) Electrochemical detector

On/Off, Offset (auto zero).

Running a Schedule

With the Schedule program, you prepare a list of the analyses to be performed. The 'GO AHEAD' is done through the Run program. To load a Schedule file, click on the Load Schedule icon in the toolbar (see picture in the previous page) or click on FILE and then LOAD SCHEDULE. When the schedule is loaded and the connection with all the modules of the equipment is tested, you can start the analyses. Click on the Start icon toolbar (see picture in the previous page), or go to RUN and then START. All the analyses listed in the schedule file that you have loaded will be sequentially performed, unless a problem occurs during the data acquisition.

Optimization

Optimize program is used to manipulate chromatograms after their acquisition. Two important operations are described here: a) up-dating the calibration curve response factors; b) re-treatment of chromatograms.

Up-dating calibration standard response factors

Load the chromatogram related to the Calibration # 1. Depending upon the acquisition conditions, some variations in the retention time compared to the values stored in the method file can occur. You need to up-date the values for the new retention time. To do that, click on the NAME PICKS icon (or click on Operations and then Name Picks). Retention calipers, representing the retention time values and tolerance data stored in the method file will appear on the top of the chromatogram. You must match the retention calipers with the peaks in the chromatogram. Maximize the peaks using the upper arrow in the toolbar at the right of the screen and use the cursor to move the retention calipers in order to match them with the six sugars peaks.

You must now up-date the calibration curve response factors. Click on CALIBRATE icon or go to Operations menu and then Calibration. You will see the Calibrate dialog box. By using the arrow at the right of Level and Replicate fields, enter the correct information about the calibration standard. Once again, do not forget that the level of concentration must correspond to those specified in the method file.

Make sure that *Replace Retention Times* and *Update Response* fields are marked. You will be asked about the replacement of new values for the response factor calculations. You can answer individually, by clicking on *Accept* or for all the sugars by clicking on *Accept All.*

When you have finish with all sugars, you MUST SAVE BOTH CHROMATOGRAM AND METHOD FILES, otherwise, the replacement work is lost.

Repeat all the procedure for the next calibration standard. When you have done all the standards, you may check your calibration curves. Save both chromatogram and method files and before closing the file, click on the *Component Table* icon. A table containing information about the retention time of the sugars will appear. Click on *Detail.* You will see the up-dated area surface data for the response factors calculations. You can check the calibration curve for each sugar, under the Component field. An example for galactose is provided below:

Recalculations of chromatograms.

When you have finished the up-dating of the calibration standards, you need to retreat the chromatograms once the response factors have been probably changed.

Open the file containing the chromatogram to be retreated. Depending upon the acquisition conditions, some variations in the retention time compared to the values stored in the method file can occur. Retention calipers, representing the retention time values and tolerance data stored in the method file will appear on the top of the chromatogram. You must match the retention calipers with the peaks in the chromatogram. Maximize the peaks using the upper arrow in the toolbar at the right of the screen and use the cursor to move the retention calipers in order to match them with the six sugars peaks.

Click on the *print preview* icon to see the new chromatogram report. If all the six sugars are shown with retention time and concentration in mg, print out the chromatogram.

APPENDIX B

Compiled Data

Table B.1. Compiled data

IP Softwood (IP SW A before 7/01)		
Batch #	Description	Date
990705	Control - 375 RPM	7/28/1999
990706	Control - 500 RPM	7/28/1999
990801	Control - 225 RPM	8/4/1999
990802	Control - 300 RPM	8/4/1999
990807	Control - 150 RPM	8/12/1999
991001	Control (6)	10/5/1999
000702	Control 10min	7/27/2000
000703	Control 20min	7/27/2000
000704	Control 60min	7/27/2000
000801	Control 60min	7/27/2000
000802	Control 20min	7/27/2000
000803	Control 10min	7/27/2000
000813	Control 60min	8/21/2000
000907	Control 5% NaOH	9/18/2000
000908	Control 2.5% NaOH	9/18/2000
010205	2.5% NaOH, 60 min	2/26/2001
010301	2.5% NaOH, 10 min	3/3/2001
010302	2.5% NaOH, 20 min	3/3/2001
010401	2.5% NaOH, 60 min	4/2/2001
010405	3.0% NaOH, 90 C, 20 min	4/9/2001
010406	4.0 % NaOH ctrl, 60 min	4/17/2001
010501	2.5 % NaOH ctrl, 60 min	5/1/2001
010506	ctrl, 60 mins, 1.5 % NaOH	5/7/2001
010507	ctrl, 20 mins, 1.5 % NaOH	5/8/2001
010508	ctrl, 10 mins, 1.5 % NaOH	5/8/2001
010901	ctrl, 2.5% NaOH, 60 min, 90C	9/30/2001
010903	ctrl, 2.5% NaOH, 60 min, 90C	9/30/2001
011007	ctrl, 2.5% NaOH, 20 min, 90C	10/27/2001
011008	ctrl, 2.5% NaOH, 10 min, 90C	10/27/2001
020302	Control. 2.5% NaOH 90 C, 60 min	3/5/2002
000608	Control (1)	6/30/1999
990805	Control (5)	8/9/1999
000101	Control (2)	1/5/2000
000201	Control (3)	2/23/2000
010203	Control (4)	2/23/2001
990708	Chelated Pulp, no MgSO4	7/29/1999
990707	2% Sodium gluconate	7/29/1999
990709	Chelated Pulp + 2% Gluconate, no MgSO4	7/30/1999
990803	Control, no MgSO4	8/4/1999
990811	Chelated Pulp - no additives	8/18/1999
990901	Chelated Pulp, no additives	9/3/1999
991002	2 % Gluconate, 0.2% MgSO4	10/5/1999
991004	Chelated pulp, 0.2% MgSO4	10/7/1999
991005	Chelated pulp, 2% gluconate, 0.2% MgSO4	10/10/1999
991006	NaOH only - (no MgSO4)	10/10/1999

Table B.1. Compiled data (continued)

Batch #	Temp. °C	% NaOH Charge total	Time, Minutes	Additive charge %	Initial Kappa #	Final Kappa number
990705	90	4	60	0	26.7	12.96
990706	90	4	60	0	26.7	13.81
990801	90	4	60	0	26.7	13.20
990802	90	4	60	0	26.7	13.46
990807	90	4	60	0	26.7	13.56
991001	90	4	60	0	26.7	15.13
000702	90	4	10	0	26.7	18.91
000703	90	4	20	0	26.7	16.89
000704	90	4	60	0	26.7	12.47
000801	120	4	60	0	26.7	7.27
000802	120	4	20	0	26.7	11.24
000803	120	4	10	0	26.7	16.44
000813	90	4	60	0	26.7	12.94
000907	90	5	60	0	26.7	12.47
000908	90	2.5	60	0	26.7	14.05
010205	90	2.5	60	0	26.7	15.32
010301	90	2.5	10	0	26.7	20.04
010302	90	2.5	20	0	26.7	18.11
010401	90	2.5	60	0	26.7	15.62
010405	90	3	20	0	26.7	18.89
010406	90	4	60	0	26.7	12.26
010501	90	2.5	60	0	26.7	14.95
010506	90	1.5	60	0	26.7	17.65
010507	90	1.5	20	0	26.7	20.55
010508	90	1.5	10	0	26.7	21.79
010901	90	2.5	60	0	28.0	16.14
010903	90	2.5	60	0	28.0	15.94
011007	90	2.5	20	0	28.0	19.72
011008	90	2.5	10	0	28.0	21.22
020302	90	2.5	60	0	28.0	16.11
000608	90	4	60	0	26.7	13.85
990805	90	4	60	0	26.7	13.47
000101	90	4	60	0	26.7	12.47
000201	90	4	60	0	26.7	13.20
010203	90	4	60	0	26.7	12.56
990708	90	4	60	0	26.6	14.71
990707	90	4	60	2	26.7	14.24
990709	90	4	60	2	26.6	14.56
990803	90	4	60	0	26.7	13.78
990811	90	4	60	0	26.7	14.19
990901	90	4	60	0	26.7	12.96
991002	90	4	60	0	26.7	13.81
991004	90	4	60	0	26.7	13.20
991005	90	4	60	0	26.7	13.46
991006	90	4	60	0	26.7	13.56

Table B.1. Compiled data (continued)

Batch #	η_0, mL/g	η_t, mL/g	Total Yield, %	[NaOH] after, N
990705	1188	913	95.6	***
990706	1188	909	95.8	***
990801	1188	925	96.4	***
990802	1188	912	95.8	***
990807	1188	920	96.2	***
991001	1188	926	97.7	***
000702	1188	1039	98.5	0.094
000703	1188	994	97.6	0.090
000704	1188	900	96.9	0.058
000801	1188	742	93.5	0.013
000802	1188	871	96.0	0.033
000803	1188	1016	98.4	0.058
000813	1188	915	97.4	0.069
000907	1188	859	97.1	0.088
000908	1188	953	97.5	0.038
010205	1188	975	97.3	0.037
010301	1188	1090	98.5	0.054
010302	1189	1044	97.8	0.004
010401	1188	966	97.1	0.038
010405	1172	1022	98.7	0.053
010406	1188	898	97.0	***
010501	1188	962	97.3	0.027
010506	1188	1016	98.5	0.038
010507	1188	1074	98.8	0.039
010508	1188	1102	99.4	0.040
010901	1172	937	98.6	0.039
010903	1172	928	98.5	0.040
011007	1172	1010	98.8	0.044
011008	1172	1069	99.2	0.05
020302	1172	932	98.4	0.036
000608	1188	915	96.6	***
990805	1188	921	96.7	***
000101	1188	896	97.2	***
000201	1188	913	96.6	***
010203	1188	871	96.6	0.081
990708	1188	958	96.3	***
990707	1188	961	96.4	***
990709	1188	963	96.3	***
990803	1188	903	96.4	***
990811	1188	934	95.7	***
990901	1188	910	98.0	***
991002	1188	971	97.5	***
991004	1188	980	98.1	***
991005	1188	974	97.9	***
991006	1188	921	99.9	***

Table B.1. Compiled data (continued)

Batch #	Description	Date
991007	NaOH + 2% gluconate(no MgSO4)	10/18/1999
991008	Chelated pulp + NaOH (no MgSO4)	10/18/1999
991009	chel + NaOH + 2% gluconate (no MgSO4)	10/19/1999
991101	QR - Chelated, then NaBH4 reduced	11/4/1999
991102	QR - Chelated, then NaBH4 reduced, plus Mn	11/4/1999
001102	Chelated pulp	11/13/2000
990104	A - Q4 (pH=3)	11/5/1999
991103	A - Q4 (pH=3) + 2.0% guar	11/5/1999
010104	A - Q4(pH=2.5), ctrl	1/11/2001
010105	A - Q4 (pH=2.5) + 1.5% H2O2	1/11/2001
010106	A - Q4(pH=2.5) + 0.3% guar	1/16/2001
010107	A - Q2 (pH=2) + 2.0% guar	1/17/2001
010201	A - Q3 (pH = 2.8)	1/22/2001
010108	A - Q2 (pH=2)	1/22/2001
990810	Mn Replen Chel pulp#001 100 ppm	8/17/1999
990813	Mn Replen Chel pulp#11 50 ppm	8/28/1999
990814	Mn Replen Chel pulp#22 100 ppm	8/28/1999
990815	Mn Replen. Ch. pulp#23 100 + gluconate	8/29/1999
990816	Mn Replen Chel pulp#31 200ppm	8/29/1999
990902	Mn Replen. Ch. pulp#9025 25 ppm	9/3/1999
990903	Acid treated Chelated pulp#9-002, 2.5 pH 0.5 hr	9/4/1999
990904	Fe + Mn replen chel IP pulp, 100 ppm	9/13/1999
990905	Fe + Mn replen chel IP pulp, 50 ppm	9/13/1999
991003	Fe replen chel IP pulp - 100 ppm Fe	10/10/1999
991010	Mn repl. IP chel plp#10Mn200, no MgSO4	10/21/1999
991011	Mn repl. IP chel plp#10Mn200 + MgSO4	10/21/1999
991012	Fe repl. IP chel plp#10Fe200	10/22/1999
991013	Fe repl. IP chel plp#10Fe200 + MgSO4	10/22/1999
990804	5% Sta-lok 310 starch addition - 4% NaOH	8/5/1999
991105	5 % SL 310	11/15/1999
991106	5 % Lok-siz 30	11/15/1999
000102	10% PEG (1000 MW)	1/5/2000
000103	10% 7L CMC (90,000 MW, DS 0.8)	1/12/2000
000202	10.3% CMC-B (alkali cellulose gum)	2/23/2000
000203	5.4% CMC-B	2/24/2000
000310	5.0% CMC A dissolved in water	3/1/2000
000302	5.0% CMC A dissolved in NaOH (~1N)	3/1/2000
000303	2.0% CMC A (.25DS) in 1N NaOH into .37N pulp	3/13/2000
000304	5.0% CMC A (.25DS) in 1.4N NaOH into .37N pulp	3/13/2000
000305	2.0% CMC A (.25DS) in 30 mLs 1.0N NaOH	3/21/2000
000306	5% Flojel 65 starch	3/21/2000
000307	5.0% CMC A in 30 mLs 1.0N NaOH	3/26/2000
000308	2.0% CMC A in 30 mLs 1.0N NaOH	3/26/2000
000603	G0221 depolymerized CMC (5mL/g CMC) - charge 10%	6/13/2000
000604	G0221-2 depolymerized CMC (2% enzyme)9.2 %	6/14/2000

Table B.1. Compiled data (continued)

Batch #	Temp. °C	% NaOH Charge total	Time, Minutes	Additive charge %	Initial Kappa #	Final Kappa number
991007	90	4	60	2	26.7	15.11
991008	90	4	60	0	26.7	15.36
991009	90	4	60	2	26.7	15.65
991101	90	4	60	0	26.7	14.46
991102	90	4	60	0	26.7	13.32
001102	90	4	60	0	26.1	12.86
990104	90	4	60	0	26.7	11.39
991103	90	4	60	0	26.7	11.86
010104	90	4	60	0	24.2	12.08
010105	90	4	60	1.5	24.2	10.63
010106	90	4	60	0.3	24.2	11.70
010107	90	4	60	2	22.5	10.70
010201	90	4	60	0	22.8	12.45
010108	90	4	60	0	22.5	10.01
990810	90	4	60	0	26.7	13.54
990813	90	4	60	0	26.7	13.09
990814	90	4	60	0	26.7	13.84
990815	90	4	60	2	26.7	12.85
990816	90	4	60	0	26.7	13.04
990902	90	4	60	0	26.7	13.32
990903	90	4	60	0	26.7	13.80
990904	90	4	60	0	26.7	14.32
990905	90	4	60	0	26.7	14.43
991003	90	4	60	0	26.7	14.10
991010	90	4	60	0	26.7	14.22
991011	90	4	60	0	26.7	14.25
991012	90	4	60	0	26.7	13.85
991013	90	4	60	0	26.7	14.77
990804	90	4	60	5	26.7	13.93
991105	90	4	60	5	26.7	15.37
991106	90	4	60	5	26.7	13.96
000102	90	4	60	10	26.7	12.70
000103	90	4	60	0	26.7	13.76
000202	90	4	60	10.3	26.7	12.69
000203	90	4	60	5.4	26.7	12.33
000310	90	4	60	5	26.7	12.45
000302	90	4	60	5	26.7	13.72
000303	90	4	60	2	26.7	14.08
000304	90	4	60	5	26.7	13.71
000305	90	4	60	2	26.7	14.98
000306	90	4	60	5	26.7	14.62
000307	90	4	60	5	26.7	13.33
000308	90	4	60	2	26.7	14.03
000603	90	4	60	10	26.7	22.81
000604	90	4	60	3.2	26.7	18.19

Table B.1. Compiled data (continued)

Batch #	η_0, mL/g	η_t, mL/g	Total Yield, %	[NaOH] after, N
991007	1188	913	97.8	***
991008	1188	981	96.9	***
991009	1188	980	97.4	***
991101	1188	955	98.5	***
991102	1188	936	95.4	***
001102	1188	966	97.1	0.063
990104	1140	888	96.9	***
991103	1140	914	96.7	***
010104	1118	931	96.8	0.065
010105	1118	899	96.0	0.063
010106	1118	949	97.1	0.050
010107	972	799	98.0	0.052
010201	1122	941	97.1	0.055
010108	972	769	96.0	0.051
990810	1188	980	98.0	***
990813	1188	963	98.9	***
990814	1188	970	97.2	***
990815	1188	984	97.9	***
990816	1188	977	97.1	***
990902	1188	961	98.7	***
990903	1140	962	97.1	***
990904	1188	964	96.7	***
990905	1188	959	98.7	***
991003	1188	567	97.3	***
991010	1188	989	96.8	***
991011	1188	971	97.0	***
991012	1188	627	95.7	***
991013	1188	648	96.3	***
990804	1188	920	95.5	***
991105	1188	944	98.5	***
991106	1188	937	96.8	***
000102	1188	905	97.7	***
000103	1188	924	97.4	***
000202	1188	920	98.9	***
000203	1188	903	97.7	***
000310	1188	912	98.8	***
000302	1188	940	99.0	***
000303	1188	895	99.2	***
000304	1188	910	96.9	***
000305	1188	925	98.4	***
000306	1188	939	97.7	***
000307	1188	940	97.7	***
000308	1188	947	97.9	***
000603	1188	1099	99.7	***
000604	1188	1001	99.7	***

Table B.1. Compiled data (continued)

Batch #	Description	Date
000605	G0221-3 (0.02%enzyme), 5%	6/23/2000
000606	G0221(initial CMC), 5%	6/28/2000
000607	g0221-4 (0.002% enzyme), 5%	6/29/2000
000701	5% G0221-4B purified enzyme treated CMC	7/10/2000
001009	2.0 % Emdex MTW low MW starch	10/19/2000
001010	0.3 % Emdex MTW low MW starch	10/19/2000
000402	5.0% carboxymethyl,2-hydroxyethyl Guar Gum	4/2/2000
000401	5.0% Guar Gum	4/26/2000
000501	Control (4)	5/2/2000
000502	5.0% Guar Gum	5/2/2000
000503	5.0% Guar Gum	5/4/2000
000504	2.0% guar - 60 min	5/4/2000
000505	2.0% guar - 60 min	5/8/2000
000507	5.0% NaClO2 oxidized Guar Gum	5/8/2000
000508	3.12% SWD Hemicellulose	5/15/2000
000509	1.0% Guar Gum	5/16/2000
000510	10.0% Guar Gum	5/16/2000
000511	10.0% Guar Gum	5/31/2000
000601	1.0% Guar Gum	6/1/2000
000602	0.5% Guar Gum	6/6/2000
000705	0.3% guar - 10 min	7/28/2000
000706	0.3% guar - 20 min	7/28/2000
000805	0.3% guar - 20 min	7/28/2000
000806	0.3% guar - 10 min	7/28/2000
000707	0.3% guar - 60 min	7/31/2000
000708	0.75% guar - 10 min	7/31/2000
000709	0.75% guar - 20 min	7/31/2000
000710	0.75% guar - 60 min	7/31/2000
000804	0.3% guar - 60 min	7/31/2000
000807	0.75% guar - 60 min	7/31/2000
000808	0.75% guar - 20 min	7/31/2000
000809	0.75% guar - 10 min	7/31/2000
000711	2.0% guar - 10 min	8/1/2000
000712	2.0% guar - 20 min	8/1/2000
000713	2.0% guar - 60 min	8/1/2000
000714	2.0% guar - 60 min	8/1/2000
000810	2.0% guar - 60 min	8/1/2000
000811	2.0% guar - 20 min	8/1/2000
000812	2.0% guar - 10 min	8/1/2000
000814	0.3% guar - 60 min	8/21/2000
000815	0.75% guar - 10 min	8/22/2000
000901	2.0 % guar in H2O	9/1/2000
000902	2.0 % guar in 1N NaOH	9/1/2000
000903	0.3% guar gum	9/3/2000
000906	0.3% guar, 5% NaOH	9/18/2000

Table B.1. Compiled data (continued)

Batch #	Temp. °C	% NaOH Charge total	Time, Minutes	Additive charge %	Initial Kappa #	Final Kappa number
000605	90	4	60	5	26.7	13.85
000606	90	4	60	5	26.7	13.47
000607	90	4	60	5	26.7	13.63
000701	90	4	60	5	26.7	13.66
001009	90	4	60	2	26.7	14.16
001010	90	4	60	0.3	26.7	13.33
000402	90	4	60	5	26.7	14.62
000401	90	4	60	5	26.7	14.12
000501	90	4	60	0	26.7	13.88
000502	90	4	60	5	26.7	14.45
000503	90	4	60	5	26.7	13.99
000504	90	4	60	2	26.7	13.80
000505	90	4	60	2	26.7	14.05
000507	90	4	60	5	26.7	13.79
000508	90	4	60	3.12	26.7	14.23
000509	90	4	60	1	26.7	12.62
000510	90	4	60	10	26.7	15.30
000511	90	4	60	10	26.7	14.42
000601	90	4	60	1	26.7	12.89
000602	90	4	60	0.5	26.7	13.15
000705	90	4	10	0.3	26.7	19.55
000706	90	4	20	0.3	26.7	16.92
000805	120	4	20	0.3	26.7	11.44
000806	120	4	10	0.3	26.7	16.86
000707	90	4	60	0.3	26.7	13.53
000708	90	4	10	0.75	26.7	18.41
000709	90	4	20	0.75	26.7	16.66
000710	90	4	60	0.75	26.7	12.97
000804	120	4	60	0.75	26.7	8.49
000807	120	4	60	0.75	26.7	8.89
000808	120	4	20	0.75	26.7	11.52
000809	120	4	10	0.75	26.7	17.01
000711	90	4	10	2	26.7	19.41
000712	90	4	20	2	26.7	17.11
000713	90	4	60	2	26.7	14.12
000714	90	4	60	2	26.7	14.12
000810	120	4	60	2	26.7	8.58
000811	120	4	20	2	26.7	12.01
000812	120	4	10	2	26.7	16.88
000814	90	4	60	0.3	26.7	12.71
000815	90	4	10	0.75	26.7	19.01
000901	90	4	60	2	26.7	13.59
000902	90	4	60	2	26.7	14.14
000903	90	4	60	0.3	26.7	13.35
000906	90	5	60	0.3	26.7	12.69

Table B.1. Compiled data (continued)

Batch #	η_0, mL/g	η_t, mL/g	Total Yield, %	[NaOH] after, N
000605	1188	920	98.5	***
000606	1188	901	98.9	***
000607	1188	919	98.7	***
000701	1188	916	97.2	***
001009	1188	948	96.7	0.065
001010	1188	924	96.7	0.063
000402	1188	965	97.5	***
000401	1188	1012	97.8	***
000501	1188	913	97.0	***
000502	1188	1009	99.2	***
000503	1188	1005	100.2	***
000504	1188	981	99.1	***
000505	1188	994	99.0	***
000507	1188	969	99.3	***
000508	1188	919	99.7	***
000509	1188	968	98.4	***
000510	1188	1007	99.7	***
000511	1188	1005	100.0	***
000601	1188	951	98.5	***
000602	1188	936	97.7	***
000705	1188	1074	99.2	0.100
000706	1188	1021	98.0	0.082
000805	1188	887	96.2	***
000806	1188	1032	99.0	***
000707	1188	938	96.9	0.065
000708	1188	1088	99.5	0.082
000709	1188	1042	98.7	0.075
000710	1188	958	97.2	0.049
000804	1188	750	93.8	0.016
000807	1188	793	94.2	***
000808	1188	907	96.3	***
000809	1188	1032	99.1	***
000711	1188	1102	100.0	0.079
000712	1188	1069	98.6	0.066
000713	1188	992	98.5	0.058
000714	1188	986	98.5	0.058
000810	1188	814	95.0	0.020
000811	1188	927	96.0	0.035
000812	1188	1045	97.0	0.060
000814	1188	948	98.2	0.068
000815	1188	1077	99.6	0.080
000901	1188	984	98.1	***
000902	1188	974	97.9	***
000903	1188	943	97.5	***
000906	1188	891	97.3	0.090

Table B.1. Compiled data (continued)

Batch #	Description	Date
000911	0.3% guar, 2.5% NaOH	9/18/2000
000904	2.0 % guar, 5% NaOH	9/19/2000
000905	0.75% guar, 5% NaOH	9/19/2000
000909	2.0 % guar, 2.5% NaOH	9/19/2000
000910	0.75% guar, 2.5% NaOH	9/19/2000
001001	0.1% guar gum (4.0%NaOH)	10/3/2000
001002	0.1% guar gum (4.0%NaOH)	10/3/2000
001003	2.0% G100 depolymerized guar gum	10/5/2000
001008	2.0% Depoly- guar gum (G101) w/ 10% EtOH	10/10/2000
001011	2.0 % g102 depoly- guar gum	10/20/2000
001012	0.3 % g102 depoly- guar gum	10/20/2000
001103	Chelated pulp + 0.3 % guar gum	11/13/2000
001104	Chelated pulp + 2.0 % guar gum	11/14/2000
001105	0.3 % g103 depoly- guar gum	11/15/2000
001106	2.0 % g103 depoly- guar gum	11/15/2000
010102	0.3% g104 guar gum	1/6/2001
010103	2.0% g104 guar gum	1/6/2001
010204	2% guar, 4% NaOH	2/23/2001
010206	2% guar, 2.5% NaOH	2/26/2001
010207	2% guar, 2.5% NaOH, 60 min	2/26/2001
010304	2% guar, 2.5% NaOH, 20 min	3/5/2001
010305	2% guar, 2.5% NaOH, 10 min	3/5/2001
010306	0.75% guar, 2.5% NaOH, 60 min	3/8/2001
010307	0.75% guar, 2.5% NaOH, 20 min	3/9/2001
010308	0.75% guar, 2.5% NaOH, 10 min	3/9/2001
010309	0.30% guar, 2.5% NaOH, 60 min	3/26/2001
010310	0.30% guar, 2.5% NaOH, 20 min	3/26/2001
010311	0.30% guar, 2.5% NaOH, 10 min	3/27/2001
010402	2.5% NaOH, 60 min, 0.3% guar	4/2/2001
010403	2.5% NaOH, 60 min, 0.75% guar	4/2/2001
010404	2.5% NaOH, 60 min, 2.0% guar	4/3/2001
010406	4.0 % NaOH 0.3 % guar, 60 min	4/18/2001
010407	4.0 % NaOH 0.75 % guar, 60 min	4/19/2001
010408	4.0 % NaOH 2.0 % guar, 60 min	4/20/2001
010502	2.5 % NaOH 0.3 % guar, 60 min	5/1/2001
010503	2.5 % NaOH 0.75 % guar, 60 min	5/2/2001
010504	2.5 % NaOH 2.0 % guar, 60 min	5/2/2001
010509	0.3% guar, 60 mins	5/9/2001
010510	0.3% guar, 20 mins	5/10/2001
010511	0.3% guar, 10 mins	5/10/2001
010512	0.75% guar, 60 mins	5/12/2001
010513	0.75% guar, 20 mins	5/12/2001
010514	0.75% guar, 10 mins	5/13/2001
010515	2.0% guar, 60 mins	5/18/2001
010516	2.0% guar, 20 mins	5/18/2001

Table B.1. Compiled data (continued)

Batch #	Temp. °C	% NaOH Charge total	Time, Minutes	Additive charge %	Initial Kappa #	Final Kappa number
000911	90	2.5	60	0.3	26.7	14.15
000904	90	5	60	2	26.7	13.15
000905	90	5	60	0.75	26.7	12.74
000909	90	2.5	60	2	26.7	14.26
000910	90	2.5	60	0.75	26.7	14.16
001001	90	4	60	1	26.7	12.98
001002	90	4	60	1	26.7	13.05
001003	90	4	60	2	26.7	13.23
001008	90	4	60	2	26.7	14.18
001011	90	4	60	2	26.7	13.80
001012	90	4	60	0.3	26.7	13.44
001103	90	4	60	0.3	26.1	13.03
001104	90	4	60	2	26.1	13.03
001105	90	4	60	0.3	26.7	13.51
001106	90	4	60	2	26.7	13.79
010102	90	4	60	0.3	26.7	13.11
010103	90	4	60	2	26.7	13.04
010204	90	4	60	2	26.7	13.21
010206	90	2.5	60	2	26.7	15.63
010207	90	2.5	60	2	26.7	15.63
010304	90	2.5	20	2	26.7	18.44
010305	90	2.5	10	2	26.7	20.36
010306	90	2.5	60	0.75	26.7	15.44
010307	90	2.5	20	0.75	26.7	18.12
010308	90	2.5	10	0.75	26.7	20.35
010309	90	2.5	60	0.3	26.7	15.78
010310	90	2.5	20	0.3	26.7	18.76
010311	90	2.5	10	0.3	26.7	20.66
010402	90	2.5	60	0.3	26.7	15.93
010403	90	2.5	60	0.75	26.7	15.9
010404	90	2.5	60	2	26.7	16.01
010406	90	4	60	0.3	26.7	12.45
010407	90	4	60	0.75	26.7	12.36
010408	90	4	60	2	26.7	12.99
010502	90	2.5	60	0.3	26.7	15.12
010503	90	2.5	60	0.75	26.7	15.12
010504	90	2.5	60	2	26.7	15.2
010509	90	1.5	60	0.3	26.7	17.61
010510	90	1.5	20	0.3	26.7	20.68
010511	90	1.5	10	0.3	26.7	22.66
010512	90	1.5	60	0.75	26.7	17.87
010513	90	1.5	0	0.75	26.7	20.65
010514	90	1.5	10	0.75	26.7	22.71
010515	90	1.5	60	2	26.7	17.88
010516	90	1.5	20	2	26.7	20.63

Table B.1. Compiled data (continued)

Batch #	η_0, mL/g	η_t, mL/g	Total Yield, %	[NaOH] after, N
000911	1188	978	98.0	0.037
000904	1188	921	98.1	0.090
000905	1188	905	97.7	0.091
000909	1188	994	99.3	0.038
000910	1188	979	98.2	0.038
001001	1188	928	97.2	0.060
001002	1188	931	97.0	0.061
001003	1188	939	98.3	0.059
001008	1188	1036	98.0	0.070
001011	1188	972	98.3	0.070
001012	1188	946	97.3	0.066
001103	1188	979	97.2	0.062
001104	1188	994	98.0	0.065
001105	1188	950	96.9	0.069
001106	1188	968	97.7	0.069
010102	1188	933	97.6	0.067
010103	1188	947	98.8	0.068
010204	1188	932	98.8	0.074
010206	1188	1009	98.6	0.034
010207	1188	1020	98.6	0.034
010304	1189	1075	99.2	0.046
010305	1190	1118	100.1	0.054
010306	1188	1010	98.0	0.03
010307	1188	1079	98.5	0.044
010308	1188	1118	99.7	0.055
010309	1188	989	98.4	0.042
010310	1188	1066	98.8	0.045
010311	1188	1098	99.1	0.053
010402	1188	995	97.2	0.036
010403	1188	1017	98.0	0.035
010404	1188	1033	98.6	0.036
010406	1188	925	96.8	***
010407	1188	954	97.3	***
010408	1188	971	98.8	***
010502	1188	976	97.8	0.037
010503	1188	1031	98.0	0.034
010504	1188	1029	99.6	0.065
010509	1188	1033	98.6	0.038
010510	1188	1092	99.1	0.039
010511	1188	1139	99.5	0.040
010512	1188	1055	98.7	0.038
010513	1188	1101	99.6	0.039
010514	1188	1140	99.8	0.040
010515	1188	1068	99.4	0.038
010516	1188	1114	99.8	0.039

Table B.1. Compiled data (continued)

Batch #	Description	Date
010517	2.0% guar, 10 mins	5/18/2001
020604	2.0% guar gum, 2.5% NaOH, 90 C, single stage	6/17/2002
020404	2% cationic guar,1% tannic acid, 2.5% NaOH	4/27/2002
020507	2% cationic guar, 3.83% tannic acid, 2.5 % NaOH	5/16/2002
020601	2% cationic guar (3215) 60 min, 90 C, 2.5% NaOH	6/1/2002
990806	Alkali Source = 4% Na_2CO_3	8/9/1999
990812	5% Sta-lok 310 starch addition - 4% Na2CO3	8/18/1999
001101	10% EtOH	11/3/2000
001201	Chelated pulp + Mn (200 ppm)	12/6/2000
001202	Chel + Mn (200 ppm) + 1.5% H2O2	12/6/2000
001203	Chelated pulp + 1.5% H2O2	12/13/2000
001204	1.5% H2O2	12/13/2000
001205	Chelated pulp + 2.0% guar +1.5% H2O2	12/14/2000
010101	(nonChelated)pulp + 2.0% guar +1.5% H2O2	1/5/2001
011103	100 psig N2, 1.5% NaOH, 10 min, 90 C	11/15/2001
010505	100 psig N2, 60 min., 1.5% NaOH	5/7/2001
010520	0.3% guar 100 psig N2, 60 min., 1.5% NaOH	5/14/2001
010518	2.0% guar 100 psig N2, 60 min., 1.5% NaOH	5/15/2001
010519	0.75% guar 100 psig N2, 60 min., 1.5% NaOH	5/15/2001
020601	100 psig N2, 1.5% NaOH, 60 min, 120C	6/15/2002
010303	100 psig N2, 2.5% NaOH, 10min, 90 C	3/4/2001
011102	100 psig N2, 2.5% NaOH, 10 min, 90 C	11/15/2001
011102	100 psig N2, 2.5% NaOH, 10 min, 90 C	11/15/2001
020604	100 psig N2, 2.5% NaOH, 20 min, 90 C	6/16/2002
010207	100 psig N2, 2.5% NaOH, 60 min, 90 C	2/27/2001
020602	100 psig N2, 2.5% NaOH, 60 min, 120C	6/15/2002
020603	100 psig N2, 4.0% NaOH, 10 min, 120C	6/15/2002
010202	100 psig N2, 4% NaOH, 60 min	1/20/2001
011104	100 psig N2, 4.0% NaOH, 60 min, 120 C	11/26/2001
011101	100 psig N2, 2.5% NaOH, 10 min, 90 C	11/1/2001
020605	100 psig N2, 2.5% NaOH, 20 min, 90C	6/17/2002
011006	100 psig N2, 2.5% NaOH, 60 min, 90C	10/15/2001
010902	2.0% glucomannan, 2.5% NaOH	9/30/2001
011001	2.0% xylan, 2.5% NaOH	10/1/2001
011002	0.75% glucomannan, 2.5% NaOH	10/12/2001
011003	0.75% xylan, 2.5% NaOH	10/12/2001
011004	0.30% glucomannan, 2.5% NaOH	10/13/2001
011005	0.30% xylan, 2.5% NaOH	10/13/2001
011009	2.0% glucomannan, 20 min	10/28/2001
011010	2.0% glucomannan, 10 min	10/28/2001
011011	2.0% xylan, 20 min.	10/31/2001
011012	2.0% xylan, 10 min.	10/31/2001
020301	10.1 grams extracted wood (2.5% NaOH), 90 C, 60 min	3/4/2002
020405	100 g extracted wood solution	4/27/2002
020506	100 g extracted wood sol. (well washed), 2.5%NaOH	5/13/2002

Table B.1. Compiled data (continued)

Batch #	Temp. °C	% NaOH Charge total	Time, Minutes	Additive charge %	Initial Kappa #	Final Kappa number
010517	90	1.5	10	2	26.7	23.01
020604	90	2.5	60	2	28.0	16.12
020404	90	2.5	60	3	28.0	20.15
020507	90	2.5	60	2	28.0	21.96
020601	90	2.5	60	2	28.0	16.46
990806	90	4	60	0	26.7	18.25
990812	90	0	60	5	27.3	20.39
001101	90	4	60	10	26.7	13.43
001201	90	4	60	0	26.5	14.98
001202	90	4	60	1.5	26.5	13.31
001203	90	4	60	1.5	26.5	12.51
001204	90	4	60	1.5	26.7	13.40
001205	90	4	60	3.5	26.5	12.70
010101	90	4	60	3.5	26.7	12.14
011103	90	1.5	10	0	26.7	24.91
010505	90	1.5	60	0	26.7	24.58
010520	90	1.5	60	0.3	26.7	25.71
010518	90	1.5	60	2	26.7	25.84
010519	90	1.5	60	0.75	26.7	25.66
020601	120	1.5	60	0	26.7	24.02
010303	90	2.5	10	0	26.7	24.13
011102	90	2.5	10	0	26.7	24.18
011102	90	2.5	10	0	26.7	24.38
020604	90	2.5	20	0	26.7	24.13
010207	90	2.5	60	0	26.7	23.99
020602	120	2.5	60	0	26.7	23.02
020603	120	4	10	0	26.7	22.73
010202	90	4	60	0	26.7	23.28
011104	120	4	60	0	26.7	22.11
011101	90	2.5	10	0	28.0	25.79
020605	90	2.5	20	0	28.0	25.52
011006	90	2.5	60	0	28.0	25.29
010902	90	2.5	60	2	28.0	15.93
011001	90	2.5	60	2	28.0	15.88
011002	90	2.5	60	0.75	28.0	16.08
011003	90	2.5	60	0.75	28.0	16.22
011004	90	2.5	60	0.3	28.0	15.97
011005	90	2.5	60	0.3	28.0	16.2
011009	90	2.5	20	2	28.0	19.79
011010	90	2.5	10	2	28.0	21.29
011011	90	2.5	20	2	28.0	19.98
011012	90	2.5	10	2	28.0	21.33
020301	90	2.5	60	1.53	28.0	17.38
020405	90	2.5	60	10	28.0	14.33
020506	90	2.5	60	3.1	28.0	15.68

Table B.1. Compiled data (continued)

Batch #	η_0, mL/g	η_t, mL/g	Total Yield, %	[NaOH] after, N
010517	1188	1145	99.8	0.040
020604	1172	991	99.8	0.038
020404	1172	991	100.1	0.038
020507	1172	1022	99.7	0.030
020601	1172	970	99.4	0.036
990806	1188	1033	96.0	***
990812	1188	1047	97.0	***
001101	1188	1055	96.6	0.065
001201	1188	980	97.7	0.067
001202	1188	941	97.4	0.067
001203	1188	934	97.4	0.071
001204	1188	880	96.9	0.070
001205	1188	931	98.4	0.067
010101	1188	881	98.5	0.061
011103	1188	1184	99.5	0.037
010505	1188	1161	99.7	0.036
010520	1188	1152	99.9	0.037
010518	1188	1148	100.9	0.035
010519	1188	1165	100.3	0.037
020601	1188	1180	98.9	0.032
010303	1188	1175	99.0	0.062
011102	1188	1163	99.2	0.065
011102	1188	1180	99.2	0.065
020604	1188	1169	99.0	0.063
010207	1188	1177	99.0	0.063
020602	1188	1166	99.5	0.060
020603	1188	1165	99.0	0.102
010202	1188	1180	98.3	0.098
011104	1188	1144	98.7	0.096
011101	1172	1153	99.2	0.063
020605	1172	1153	98.9	0.055
011006	1172	1149	99.3	0.064
010902	1172	994	99.3	0.038
011001	1172	958	99.0	0.038
011002	1172	989	98.9	0.033
011003	1172	945	99.0	0.034
011004	1172	962	98.7	0.032
011005	1172	941	98.0	0.031
011009	1172	1059	99.7	0.045
011010	1172	1101	100.2	0.051
011011	1172	1020	99.5	0.046
011012	1172	1065	100.0	0.051
020301	1172	947	97.2	0.027
020405	1172	930	98.9	0.056
020506	1172	954	96.9	0.028

Table B.1. Compiled data (continued)

Batch #	Description	Date
011201	extended (80 MIN) - 90 C, 3.0% NaOH, 90 C	12/1/2001
011202	2 stage (20,60 MIN) - 90 C, (1)1.5% (2)+1.5% NaOH	12/1/2001
011203	2 stage (20,60 MIN) - 90 C, 1.5% +1.5% NaOH, 110 C	12/7/2001
011204	2 st (20,60 min) - 90 C,1.5%+1.5% NaOH,110 C,0.75% guar	12/12/2001
011205	2 stage (20,60 MIN) - 90 C, 1.5% +1.5% NaOH, 120 C	12/15/2001
020101	1.5% NaOH, 20 mins 90 C, ctrl	1/3/2002
020406	2 stages(of 4)1.125% NaOH each, 15 min, 25 min, 105 C	1/5/2002
020102	2 st (20,60 MIN) - 90 C,1.5%+1.5% NaOH,110 C, 0.75% guar	1/6/2002
020201	3 stage 3x (1.5% NaOH, 30 mins, 105 C)	2/23/2002
020202	3 stage (1.5% NaOH each, 20, 30, 40 mins, 105 C)	2/28/2002
020203	90 minutes, 4.5% NaOH, 105 C	2/28/2002
020303	2 stage: 3% NaOH 20 min @ 90C then 60 min @ 120C	3/12/2002
020304	1st stage (105C) 1.5% NaOH 30 min	3/13/2002
020305	1st stage and 2nd stage (105C) 30 min, 1.5% NaOH each	3/14/2002
020306	3 satges, 30 min (105C), 1.5% NaOH each (REPEAT)	3/14/2002
020307	1st stage (105C) 1.5% NaOH 20 min	3/16/2002
020308	1st stage and 2nd stage (105C), 1.5% each, 20 then 30 min	3/16/2002
020310	1 stage, 120 min, 105C, 4.5% NaOH	3/20/2002
020311	4 stage, 1.125% NaOH each, 105C (15, 25, 35, 45 min)	3/21/2002
020401	1 stage (for 3 stage ctrl) - 30 min 105C, 4.5% NaOH	4/8/2002
020402	2 stage (for 3 stage ctrl) - 60 min 105C, 4.5% NaOH	4/8/2002
020407	4 stage, 1.125% NaOH each, 105C (15, 25 , 35 , 45 min)	4/30/2002
020501	2 stage, 20 min then 60 min, 1.5% NaOH each, 105 C	5/5/2002
020502	2 st, 20, 60 min, 1.5% NaOH each, 105 C, 0.75% guar gum	5/5/2002
020503	3 stage, 20, 60 min, 1.5% NaOH each, 105 C, 0.75% GM	5/6/2002
020503	2 stage, 20, 60 min, 1.5% NaOH each, 105 C, 1% gluconate	5/6/2002
020504	2 stage, (as above) 0.75% guar, 1% gluconate	5/12/2002
020505	Control, 3.0% NaOH, 80 min @ 105 C	5/12/2002
020602	repeat 020504 0.75% guar, 1% gluconate, premixed	6/1/2002
020603	repeat 020602, split gluconate add'n (0.5 + 0.5) %	6/2/2002

Table B.1. Compiled data (continued)

Batch #	Temp. °C	% NaOH Charge total	Time, Minutes	Additive charge %	Initial Kappa #	Final Kappa number
011201	90	3	80	0	28.0	13.52
011202	90	3	80	0	28.0	14.25
011203	90,110	3	80	0	28.0	11.62
011204	90,110	3	80	0.75	28.0	11.88
011205	90,120	3	80	0	28.0	10.89
020101	90	1.5	20	0	28.0	22.03
020406	105	2.25	40	0	28.0	17.38
020102	90,110	3	80	0.75	28.0	11.88
020201	105	4.5	90	0	28.0	10.65
020202	105	4.5	90	0	28.0	10.11
020203	90,105	4.5	90	0	28.0	9.63
020303	90,120	3	80	0	28.0	9.42
020304	105	1.5	30	0	28.0	21.19
020305	105	3	60	0	28.0	15.98
020306	105	4.5	90	0	28.0	10.41
020307	105	1.5	20	0	28.0	21.66
020308	105	3	50	0	28.0	17.01
020310	105	4.5	120	0	28.0	8.26
020311	105	4.5	120	0	28.0	9.59
020401	105	4.5	30	0	28.0	17.28
020402	105	4.5	60	0	28.0	12.39
020407	105	4.5	120	0	28.0	10.11
020501	105	3	80	0	28.0	10.88
020502	105	3	80	0.75	28.0	11.17
020503	105	3	80	0.75	29.0	11.81
020503	105	3	80	1	28.0	11.23
020504	105	3	80	1.75	28.0	11.39
020505	105	3	80	0	28.0	10.33
020602	105	3	80	0.75	28.0	11.69
020603	105	3	80	0.75	28.0	11.52

Table B.1. Compiled data (continued)

Batch #	η_0, mL/g	η_t, mL/g	Total Yield, %	[NaOH] after, N
011201	1172	915	97.1	0.032
011202	1172	979	97.3	0.034
011203	1172	931	96.2	0.024
011204	1172	952	96.8	0.026
011205	1172	919	96.1	0.022
020101	1172	1062	98.8	0.016
020406	1172	1011	***	0.022
020102	1172	955	96.9	0.026
020201	1172	868	95.2	0.040
020202	1172	920	94.5	0.052
020203	1172	739	94.5	0.031
020303	1172	781	95.1	0.012
020304	1172	1062	***	0.015
020305	1172	975	***	0.033
020306	1172	910	***	0.040
020307	1172	1053	***	0.018
020308	1172	989	***	0.026
020310	1172	692	94.0	0.028
020311	1172	885	94.7	0.031
020401	1172	965	***	0.084
020402	1172	809	***	0.054
020407	1172	902	***	0.052
020501	1172	924	96.1	0.023
020502	1172	951	97.4	0.023
020503	1172	967	97.0	0.021
020503	1172	973	96.6	0.025
020504	1172	977	97.3	0.023
020505	1172	849	96.0	0.019
020602	1172	969	96.9	0.020
020603	1172	992	96.7	0.021

Table B.2. Compiled data, Irving pulp only

Irving Softwood		
Batch #	Description	Date
UNB1	Miramachi SW @ UNB	2/12/1999
UNB2	Miramachi SW @ UNB, w/ gluconate	2/12/1999
990501	control	5/1/1999
990502	w/ gluconate	5/1/1999
990601	control, no MgSO4	6/7/1999
990602	no MgSO4, 2% gluconate	6/8/1999
990603	Chelated pulp	6/10/1999
990604	Chelated pulp - w/ gluconate	6/10/1999
990609	control	6/21/1999
990610	chelated pulp	6/22/1999
990701	control	6/23/1999
990703	w/ gluconate	7/7/1999
990702	chelated pulp	7/7/1999
990704	Chelated pulp + 2% gluconate	7/7/1999
990615	375 RPM stirring	6/30/1999
990614	2% ethylene glycol	6/25/1999
990613	10% ethylene glycol	6/24/1999
990611	2% succinic acid	6/23/1999
990612	2% maleic acid	6/23/1999
990608	2% Sta-lok 400 starch	6/15/1999
990606	5% Sta-lok 400 starch	6/14/1999
990605	10% Sta-lok 400 starch	6/14/1999
990607	20% Sta-lok 400 starch	6/15/1999
990808	New Blades - 225 RPM - Mn added	8/12/1999
990809	New Blades - 375 RPM - Mn added	8/12/1999

Table B.2. Compiled data, Irving pulp only (continued)

Batch #	Temp. °C	% NaOH Charge total	Time, Minutes	Additive charge %	Initial Kappa #	Final Kappa number
UNB1	90	4	60	0	32.5	14.43
UNB2	90	4	60	2	32.5	15.07
990501	90	4	60	0	25.8	12.16
990502	90	4	60	2	25.8	12.67
990601	90	4	60	0	24.9	11.70
990602	90	4	60	2	24.9	12.05
990603	90	4	60	0	24.9	13.37
990604	90	4	60	2	24.9	13.75
990609	90	4	60	0	24.6	10.70
990610	90	4	60	0	23.0	12.37
990701	90	4	60	0	24.6	12.02
990703	90	4	60	2	24.6	11.91
990702	90	4	60	0	23.0	11.44
990704	90	4	60	2	23.0	12.22
990615	90	4	60	0	24.6	11.35
990614	90	4	60	2	24.6	11.01
990613	90	4	60	10	24.6	11.11
990611	90	4	60	2	24.6	11.68
990612	90	4	60	2	24.6	12.33
990608	90	4	60	2	24.9	12.69
990606	90	4	60	5	24.9	13.34
990605	90	4	60	10	24.9	13.87
990607	90	4	60	20	24.9	14.98
990808	90	4	60	0	24.9	11.48
990809	90	4	60	0	24.9	11.87

Table B.2. Compiled data, Irving pulp only (continued)

Batch #	η_0, mL/g	η_t, mL/g	Total Yield, %
UNB1	32.5	14.43	94.7
UNB2	32.5	15.07	95.7
990501	25.8	12.16	95.7
990502	25.8	12.67	96.4
990601	24.9	11.70	95.7
990602	24.9	12.05	96.5
990603	24.9	13.37	97.5
990604	24.9	13.75	97.7
990609	24.6	10.70	96.8
990610	23.0	12.37	96.9
990701	24.6	12.02	96.2
990703	24.6	11.91	96.1
990702	23.0	11.44	97.0
990704	23.0	12.22	96.0
990615	24.6	11.35	95.9
990614	24.6	11.01	97.3
990613	24.6	11.11	97.5
990611	24.6	11.68	97.1
990612	24.6	12.33	97.1
990608	24.9	12.69	93.5
990606	24.9	13.34	96.0
990605	24.9	13.87	97.6
990607	24.9	14.98	97.8
990808	24.9	11.48	96.8
990809	24.9	11.87	95.9

APPENDIX C

Mathematical Modeling Data and Software

Table C.1. Modeling data

Modeling Data						
n	time, min.	$[NaOH]_0$	Temp., °C	[additive], % on pup	[Aa] Adsorbed	K_{CO}
1	10	4	90	0	0	23.28
2	20	4	90	0	0	23.28
3	60	4	90	0	0	23.28
4	10	4	120	0	0	22.11
5	20	4	120	0	0	22.11
6	60	4	120	0	0	22.11
7	10	2.5	90	0	0	23.99
8	20	2.5	90	0	0	23.99
9	60	2.5	90	0	0	23.99
10	10	1.5	90	0	0	25.58
11	20	1.5	90	0	0	25.58
12	60	1.5	90	0	0	25.58
13	10	4	90	0.3	0.241	23.28
14	20	4	90	0.3	0.241	23.28
15	60	4	90	0.3	0.241	23.28
16	10	4	120	0.3	0.241	22.11
17	20	4	120	0.3	0.241	22.11
18	60	4	120	0.3	0.241	22.11
19	10	2.5	90	0.3	0.287	23.99
20	20	2.5	90	0.3	0.287	23.99
21	60	2.5	90	0.3	0.287	23.99
22	10	1.5	90	0.3	0.296	25.58
23	20	1.5	90	0.3	0.296	25.58
24	60	1.5	90	0.3	0.296	25.58
25	10	4	90	0.75	0.612	23.28
26	20	4	90	0.75	0.612	23.28
27	60	4	90	0.75	0.612	23.28
28	10	4	120	0.75	0.612	22.11
29	20	4	120	0.75	0.612	22.11
30	60	4	120	0.75	0.612	22.11
31	10	2.5	90	0.75	0.688	23.99
32	20	2.5	90	0.75	0.688	23.99
33	60	2.5	90	0.75	0.688	23.99
34	10	1.5	90	0.75	0.746	25.58
35	20	1.5	90	0.75	0.746	25.58
36	60	1.5	90	0.75	0.746	25.58
37	10	4	90	2	1.222	23.28
38	20	4	90	2	1.222	23.28
39	60	4	90	2	1.222	23.28
40	10	4	120	2	1.222	22.11
41	20	4	120	2	1.222	22.11
42	60	4	120	2	1.222	22.11
43	10	2.5	90	2	1.298	23.99
44	20	2.5	90	2	1.298	23.99
45	60	2.5	90	2	1.298	23.99
46	10	1.5	90	2	1.357	25.58
47	20	1.5	90	2	1.357	25.58
48	60	1.5	90	2	1.357	25.58

Table C.1. Modeling data (continued)

n	K_t	ΔK_C	dK_C/dt Calculated	$[NaOH]_0$	$[NaOH]_t$	η_{oc}	η_t
1	18.91	4.37	-0.190	4.44	3.83	1180	1039
2	16.89	6.39	-0.133	4.44	3.55	1178	994
3	13.35	9.93	-0.044	4.44	3.05	1174	900
4	16.44	5.67	-0.770	4.44	3.65	1170	1016
5	11.24	10.87	-0.172	4.44	2.92	1160	871
6	8.27	13.84	-0.057	4.44	2.51	1140	742
7	20.04	3.95	-0.150	2.78	2.22	1183	1090
8	18.11	5.88	-0.104	2.78	1.95	1177	1044
9	15.32	8.67	-0.035	2.78	1.56	1175	964
10	21.79	3.79	-0.120	1.67	1.14	1186	1102
11	20.55	5.03	-0.094	1.67	0.96	1184	1074
12	17.65	7.93	-0.031	1.67	0.56	1178	1016
13	19.55	3.73	-0.210	4.44	3.92	1180	1074
14	16.92	6.36	-0.131	4.44	3.55	1178	1021
15	13.53	9.75	-0.044	4.44	3.08	1174	938
16	16.86	5.25	-0.860	4.44	3.71	1170	1032
17	11.44	10.67	-0.166	4.44	2.95	1160	887
18	8.49	13.62	-0.055	4.44	2.54	1140	764
19	20.66	3.33	-0.196	2.78	2.31	1183	1098
20	18.76	5.23	-0.098	2.78	2.05	1177	1066
21	15.78	8.21	-0.033	2.78	1.63	1175	989
22	22.66	2.92	-0.150	1.67	1.26	1186	1139
23	20.68	4.9	-0.094	1.67	0.98	1184	1092
24	17.69	7.89	-0.031	1.67	0.56	1178	1033
25	18.41	4.87	-0.170	4.44	3.76	1180	1088
26	16.66	6.62	-0.123	4.44	3.52	1178	1042
27	12.97	10.31	-0.041	4.44	3.00	1174	958
28	17.01	5.1	-0.880	4.44	3.73	1170	1032
29	11.52	10.59	-0.165	4.44	2.96	1160	907
30	8.89	13.22	-0.055	4.44	2.59	1140	793
31	20.35	3.64	-0.160	2.78	2.27	1183	1118
32	18.12	5.87	-0.103	2.78	1.96	1177	1079
33	15.44	8.55	-0.034	2.78	1.58	1175	1010
34	22.71	2.87	-0.150	1.67	1.26	1186	1140
35	20.65	4.93	-0.092	1.67	0.98	1184	1101
36	17.87	7.71	-0.031	1.67	0.59	1178	1055
37	19.41	3.87	-0.221	4.44	3.90	1180	1102
38	17.11	6.17	-0.110	4.44	3.58	1178	1069
39	14.12	9.16	-0.037	4.44	3.16	1174	988
40	16.88	5.23	-0.860	4.44	3.71	1170	1045
41	12.01	10.1	-0.197	4.44	3.03	1160	927
42	8.58	13.53	-0.056	4.44	2.55	1140	814
43	20.36	3.63	-0.160	2.78	2.27	1183	1118
44	18.44	5.55	-0.100	2.78	2.00	1177	1075
45	15.63	8.36	-0.033	2.78	1.61	1175	1020
46	23.01	2.57	-0.182	1.67	1.31	1186	1145
47	20.63	4.95	-0.091	1.67	0.97	1184	1114
48	17.98	7.6	-0.030	1.67	0.60	1178	1068

Table C.1. Modeling data (continued)

n	DP_{OC}	DP_t	CSN Uncorrected	CSN Corrected	dCSN/dt	$S_{C(CSN)}$
1	4.51E+03	3.92E+03	0.152	0.160	7.40E-03	28.8
2	4.50E+03	3.73E+03	0.208	0.218	4.53E-03	30.8
3	4.49E+03	3.34E+03	0.308	0.357	1.66E-03	32.2
4	4.47E+03	3.82E+03	0.170	0.187	4.23E-02	33.4
5	4.43E+03	3.22E+03	0.375	0.402	8.29E-03	29.0
6	4.34E+03	2.70E+03	0.664	0.657	2.27E-03	20.9
7	4.53E+03	4.13E+03	0.095	0.101	5.82E-03	41.5
8	4.50E+03	3.94E+03	0.143	0.153	3.61E-03	41.3
9	4.49E+03	3.61E+03	0.246	0.259	1.58E-03	35.3
10	4.54E+03	4.18E+03	0.085	0.088	2.87E-03	44.6
11	4.53E+03	4.07E+03	0.114	0.119	1.93E-03	44.0
12	4.50E+03	3.82E+03	0.179	0.189	6.95E-04	44.4
13	4.51E+03	4.07E+03	0.110	0.118	6.68E-03	33.8
14	4.50E+03	3.84E+03	0.172	0.182	4.05E-03	36.9
15	4.49E+03	3.50E+03	0.283	0.297	1.47E-03	34.4
16	4.47E+03	3.89E+03	0.150	0.167	3.79E-02	35.1
17	4.43E+03	3.29E+03	0.347	0.374	7.46E-03	30.7
18	4.34E+03	2.78E+03	0.621	0.605	2.03E-03	21.9
19	4.53E+03	4.17E+03	0.086	0.092	4.48E-03	38.6
20	4.50E+03	4.03E+03	0.116	0.127	2.72E-03	45.0
21	4.49E+03	3.71E+03	0.211	0.224	1.21E-03	38.9
22	4.54E+03	4.34E+03	0.046	0.048	2.03E-03	63.5
23	4.53E+03	4.14E+03	0.094	0.098	1.42E-03	52.1
24	4.50E+03	3.89E+03	0.157	0.167	5.06E-04	50.2
25	4.51E+03	4.12E+03	0.094	0.102	5.71E-03	51.6
26	4.50E+03	3.93E+03	0.146	0.156	3.46E-03	45.3
27	4.49E+03	3.58E+03	0.253	0.267	1.26E-03	40.7
28	4.47E+03	3.89E+03	0.150	0.167	3.24E-02	34.1
29	4.43E+03	3.37E+03	0.314	0.341	6.38E-03	33.7
30	4.34E+03	2.90E+03	0.497	0.542	1.74E-03	26.6
31	4.53E+03	4.25E+03	0.075	0.070	4.06E-03	48.2
32	4.50E+03	4.09E+03	0.125	0.112	2.47E-03	47.1
33	4.49E+03	3.80E+03	0.199	0.196	1.09E-03	43.0
34	4.54E+03	4.34E+03	0.045	0.047	1.75E-03	63.9
35	4.53E+03	4.18E+03	0.084	0.088	1.23E-03	58.6
36	4.50E+03	3.99E+03	0.130	0.140	4.36E-04	59.2
37	4.51E+03	4.18E+03	0.079	0.087	4.89E-03	49.0
38	4.50E+03	4.04E+03	0.114	0.124	2.97E-03	54.2
39	4.49E+03	3.71E+03	0.221	0.225	1.08E-03	41.5
40	4.47E+03	3.94E+03	0.134	0.151	2.78E-02	39.1
41	4.43E+03	3.45E+03	0.283	0.310	5.47E-03	35.7
42	4.34E+03	2.99E+03	0.529	0.499	1.49E-03	25.6
43	4.53E+03	4.25E+03	0.065	0.070	3.68E-03	56.0
44	4.50E+03	4.07E+03	0.106	0.117	2.24E-03	52.4
45	4.49E+03	3.84E+03	0.210	0.183	9.91E-04	49.9
46	4.54E+03	4.36E+03	0.040	0.042	1.64E-03	64.5
47	4.53E+03	4.23E+03	0.070	0.074	1.16E-03	70.7
48	4.50E+03	4.04E+03	0.115	0.125	4.11E-04	66.1

Table C.1. Modeling data (continued)

Modeling Data – Nitrogen Extraction Experiments only							
Time, minutes	$[NaOH]_0$ g/L	Temp., °C	[Aa]	K_0	K_N	K_{C0}	$1 - K_{C0}/K_0$
60	4.444	363	0	26.7	23.28	23.28	0.128
60	2.778	363	0	26.7	23.99	23.99	0.101
60	1.667	363	0	26.7	24.58	24.58	0.079
60	1.667	363	0.30	28.0	25.71	25.71	0.082
60	1.667	363	0.75	28.0	25.84	25.84	0.077
60	1.667	363	1.36	28.0	25.66	25.66	0.084
60	1.667	393	0	26.7	24.02	24.02	0.100
60	4.444	393	0	26.7	22.11	22.11	0.172
60	2.778	393	0	26.7	23.02	23.02	0.138
60	2.778	363	0	28.0	25.29	25.29	0.097
20	2.778	363	0	26.7	24.13	23.99	0.096
20	2.778	363	0	28.0	25.52	25.29	0.089
10	4.444	363	0	26.7	23.68	23.28	0.113
10	2.778	363	0	26.7	24.18	23.99	0.096
10	2.778	363	0	26.7	24.38	23.99	0.094
10	1.667	363	0	26.7	24.91	24.58	0.067
10	4.444	393	0	26.7	22.73	22.11	0.149
10	2.778	363	0	28.0	25.79	25.29	0.068
0	4.444	363	0	26.7	26.70	23.28	0
0	2.778	363	0	26.7	26.70	23.99	0
0	2.778	363	0	26.7	26.70	23.99	0
0	1.667	393	0	26.7	26.70	25.71	0
0	4.444	393	0	26.7	26.70	22.11	0
0	2.778	363	0	28.0	28.00	25.29	0
0	1.667	363	0.30	28.0	28.00	25.71	0
0	1.667	363	0.75	28.0	28.00	25.84	0
0	1.667	363	1.36	28.0	28.00	25.66	0

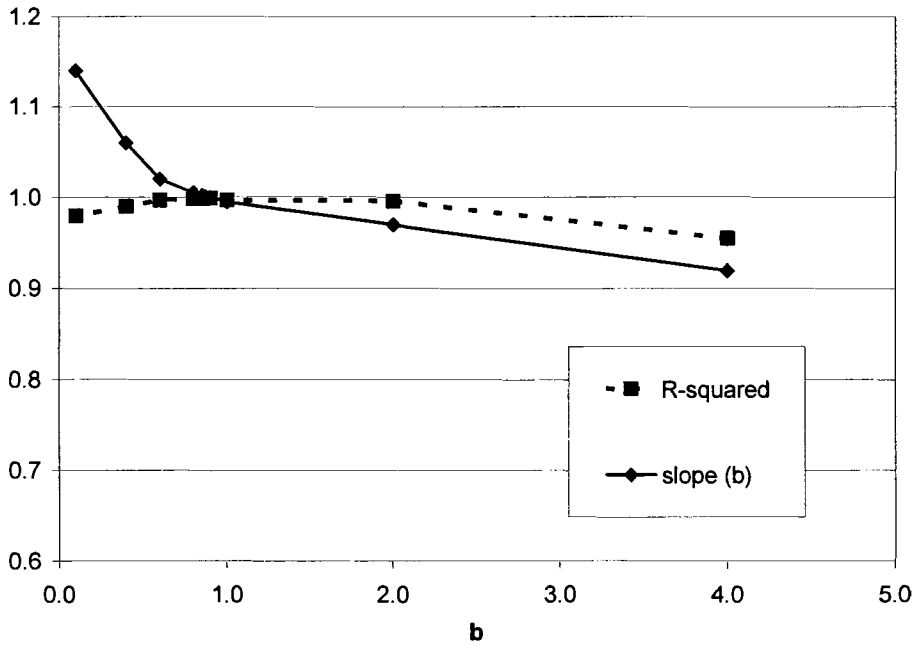

Figure C.1. The regression coefficient R^2 and b_1 for model C4

Kinetic Model Evaluation Program for Oxygen Delignification Reactions

This program, written in Mathcad 2001i, solves differential equations which describ the oxygen delignification reactions according to the models given as differential equations. The differential solver uses the Runge-Kutta adaptive step-size method, described by Rice and Do (Rice and Do, 1995). Inputs to this program are the initia values for corrected Kappa number (K), intrinsic viscosity (η) in mL/g initial NaOH charge in g/L, temperature (T) in K, and adsorbed additive charge (Aa). The solver returns a matrix containing 4 columns: time, K, NaOH charge, and Chain Scission Number(CSN).

Input Initial Conditions:

Initial Intrinsic viscosity

$I_0 := 1180$

Initial Kappa Number (corrected)

$Kco := 23.3$

initial chain scission number

$CSN_0 := 0$

Initial Alkali charge

$initialOH := 0.5$

Functions for converting between intrinsic viscosity and DP :

$DP(I) := (1.65 \cdot I)^{1.1111}$

$I(DP) := \dfrac{\left[(DP)^{\frac{1}{1.111}}\right]}{1.65}$

initial DP:

$DP_0 := DP(I_0)$ $DP_0 = 4516.63$

Rate Constants and Arrhenius' Expression :

Temperature $T_C := 110$ $T := 273.15 + T_C$ $T = 383.15$

lignin: $b0 := 12.9$ $A_L := \exp(b0)$ $E_{AL} := 9770$

$k_L := A_L \cdot \exp\left(\dfrac{-E_{AL}}{T}\right)$ $k_L = 3.375 \times 10^{-6}$

cellulose: $c0 := 11.0$ $A_M := \exp(c0)$ $E_{AM} := 9980$

$k_M := A_M \cdot \exp\left(\dfrac{-E_{AM}}{T}\right)$ $k_M = 2.918 \times 10^{-7}$

Figure C.2. Software used to solve models

Alkali Consumption : Kappa Number Decrease ratio: $\alpha := .169$

Adsorbed Additive Concentration, % by wgt.on pulp : $Aa := 0$ $Amax := 3.1$

Kinetic Model differential Equations:

$$D(t,F) := \begin{bmatrix} -k_L \cdot (F_1)^{0.819} \cdot (F_0)^{3.81} \\ \alpha \cdot \left[k_L \cdot (F_1)^{0.819} \cdot (F_0)^{3.81} \right] \\ k_M \cdot \left[(F_1)^{1.22} \cdot (F_0)^{3.38} \cdot \left(1 - \frac{Aa}{Amax} \right) \right] \end{bmatrix}$$

Lignin=0

Alkali=1

CSN=2

Arguments for Runge-Kutta Adaptive Step-size method :

$N := 50$ $t0 := 0$ $t1 := 90$ $Y0 := \begin{pmatrix} Kco \\ initialOH \\ CSN_0 \end{pmatrix}$ $Y0 = \begin{pmatrix} 23.3 \\ 0.5 \\ 0 \end{pmatrix}$

Solution matrix $S := Rkadapt(Y0, t0, t1, N, D)$

$S =$

	0	1	2	3
0	0	23.3	0.5	0
1	1.8	22.727	0.597	0.01
2	3.6	22.131	0.698	0.021
3	5.4	21.526	0.8	0.034
4	7.2	20.922	0.902	0.047
5	9	20.328	1.002	0.061
6	10.8	19.751	1.1	0.075
7	12.6	19.195	1.194	0.089
8	14.4	18.664	1.283	0.103

Figure C.2. Software used to solve models (continued)

Calculation of Viscosity from CSN: $i := 0..50$ $CSN := S^{\langle 3 \rangle}$ $t := S^{\langle 0 \rangle}$ $Kappa := S^{\langle 1 \rangle}$

$$DP_i := \left(\frac{CSN_i}{DP_0} + \frac{1}{DP_0} \right)^{-1} \qquad I_i := \frac{\left[\left(DP_i \right)^{\frac{1}{1.111}} \right]}{1.65}$$

intrinsic visc.:

$I_{50} = 853.2$

$Kappa_{50} = 9.742$

$I =$

	0
0	$1.181 \cdot 10^3$
1	$1.17 \cdot 10^3$
2	$1.158 \cdot 10^3$
3	$1.146 \cdot 10^3$
4	$1.133 \cdot 10^3$
5	$1.12 \cdot 10^3$
6	$1.107 \cdot 10^3$

Calculation of corrected chain-scission-number Selectivity:

$\Delta Kc := Kco - Kappa_{50}$ $\Delta Kc = 13.558$

selectivity: $CSN_{50} = 0.4347$ $S_{CSN} := \frac{\Delta Kc}{CSN_{50}}$ $S_{CSN} = 31.187$

Tappi Visc. $V_i := 10^{\left(\frac{I_i + 264.64}{848.12} \right)}$

Matrix containing Kc and Tappi Visc.

$PlotX_{i,1} := V_i$ $PlotX_{i,0} := Kappa_i$

$V =$

	0
0	50.617
1	49.174
2	47.635
3	46.048
4	44.454

$V_{50} = 20.801$

$PlotX =$

	0	1
0	23.3	50.617
1	22.727	49.174
2	22.131	47.635
3	21.526	46.048

Figure C.2. Software used to solve models (continued)

APPENDIX D

H.P.A.E.C. Data and Adsorption Calculations

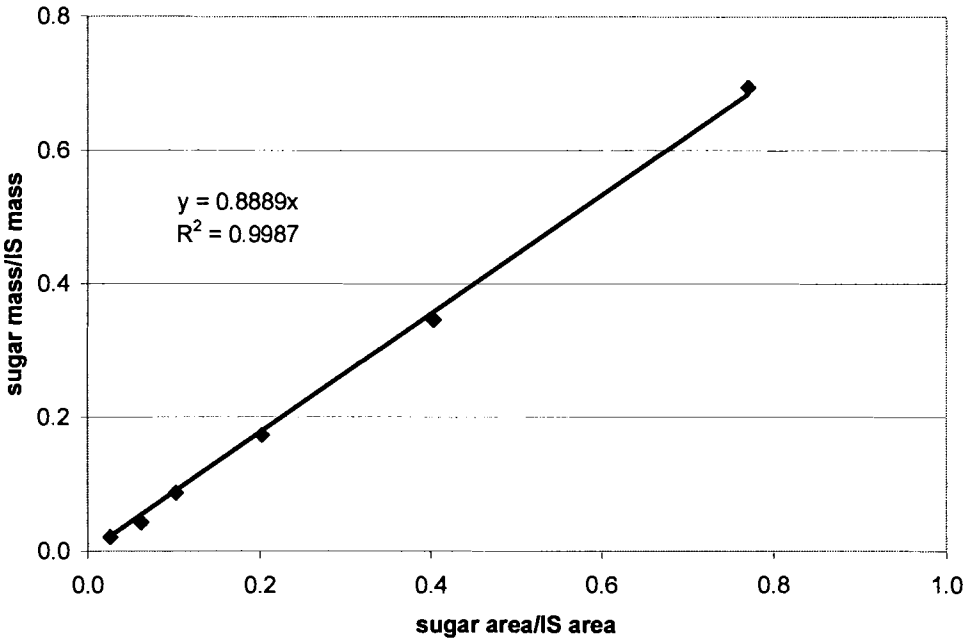

Figure D.1. Arabinose calibration

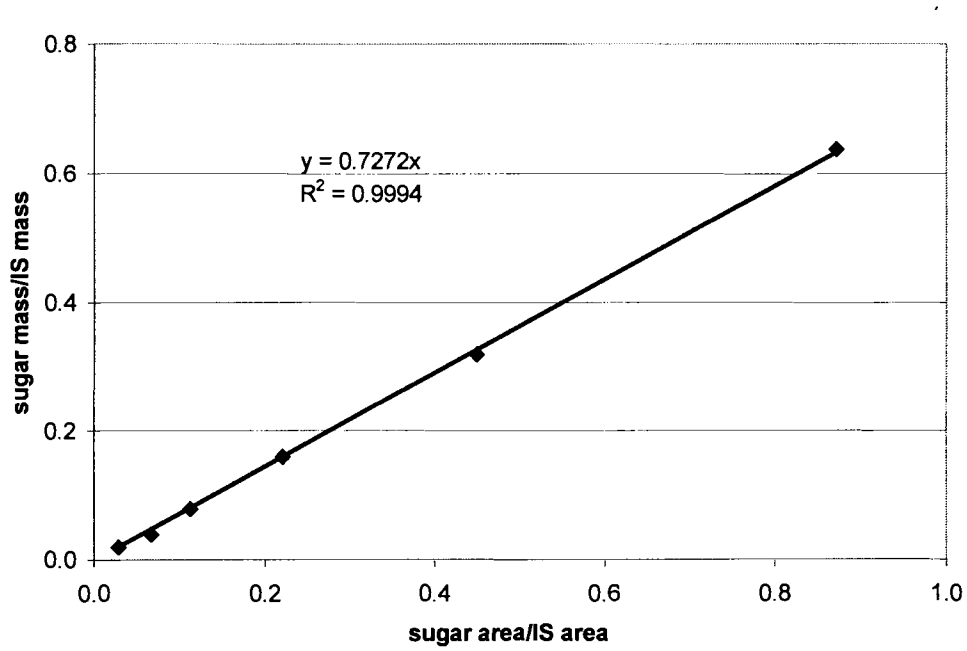

Figure D.2. Galactose calibration

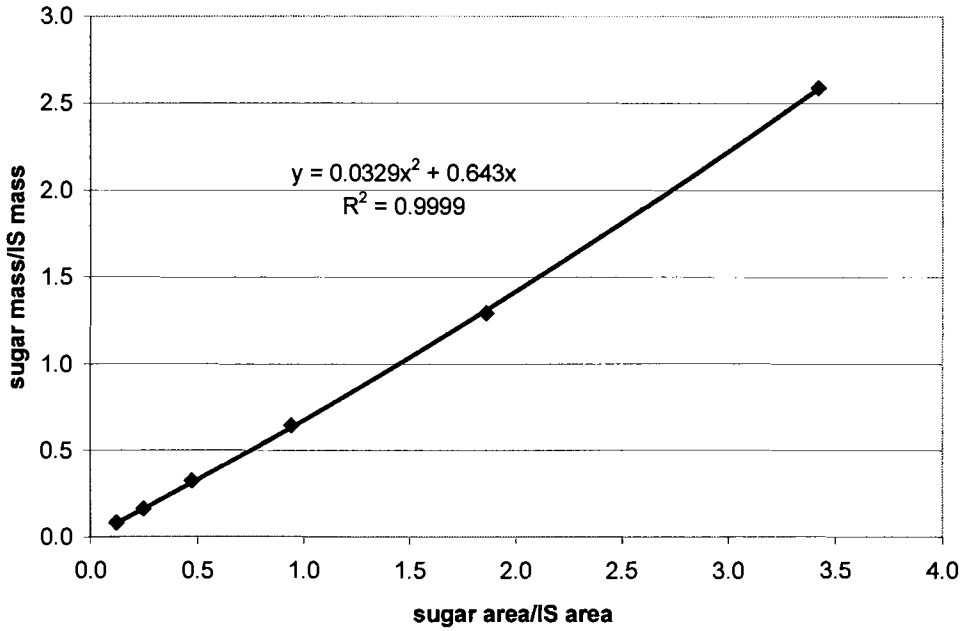

Figure D.3. Glucose calibration

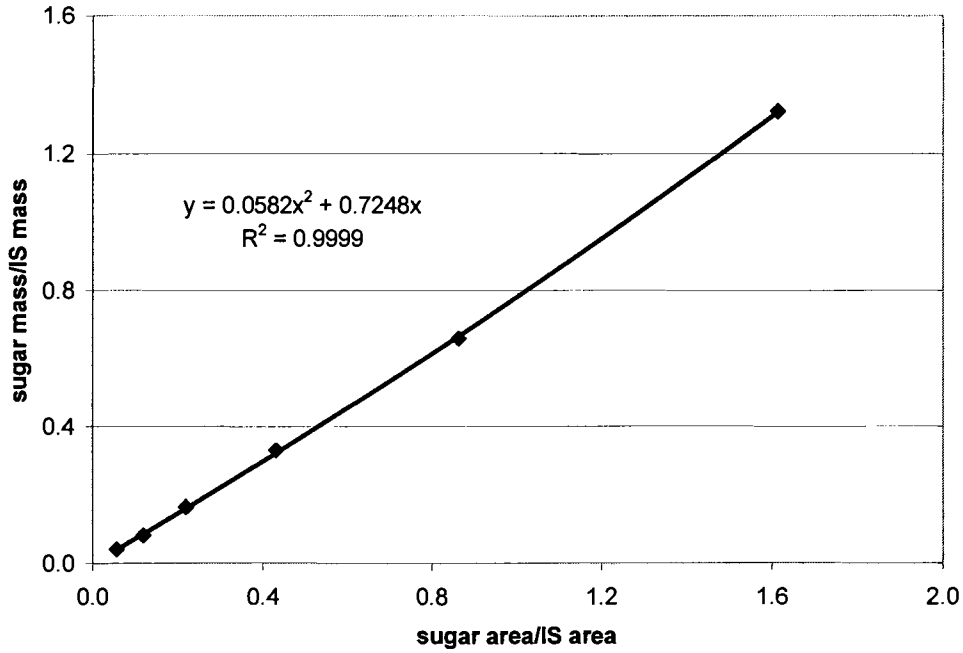

Figure D.4. Xylose calibration

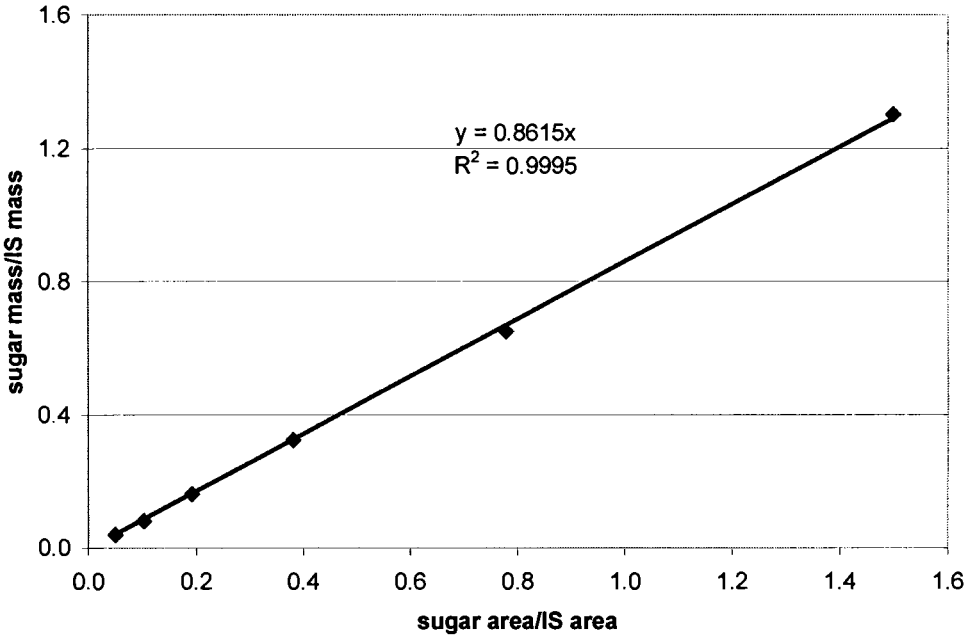

Figure D.5. Mannose calibration

Derivation of Equation (6-1)

Derivation for equation 6-1: calculation of adsorbed polysaccharide mass fractions from measured samples with adsorbed polysaccharides, (x_M, y_M and z_M) and control sample (x_P, y_P, z_P) which contained the pulp only. The mass fractions x and y are the mass fractions of sugars in the adsorbing polymer, and z represents the sum of all the other mass fractions of sugars.

In the control sample: $x_P + y_P + z_P = 1$ (A)

In the measured sample: $x_m + y_m + z_m = 1$ (B)

For the basis 1 mass unit of pulp, x_P, y_P, z_P are also the masses of each sugar Therefore, the new pulp weight is greater than this unit by the increases in x (Δx) and y (Δy):

$$x_M = (x_P + \Delta x)/(1 + \alpha) \quad \text{(C)}$$

$$y_M = (y_P + \Delta y)/(1 + \alpha) \quad \text{(D)}$$

$$z_M = z_P/(1 + \alpha)$$

where $\alpha = \Delta x + \Delta y$, or the extra mass which was adsorbed. The L.H.S. are mass fractions, whereas the R.H.S. contains masses. Adding together equations (C) and (D):

$$x_M + y_M = (x_P + y_P + \Delta x + \Delta y)/(1 + \alpha)$$

Solving for α, then multiplying by the percentage of polysaccharides in the pulp:

$$A_a = \frac{x_m - x_p + y_m - y_p}{1 - x_m - y_m} \cdot (\%\ \text{Polysaccharides}) \qquad (6\text{-}1)$$

Table D.1. Sugar analysis sample calculations

Sugar Analysis Calculations

Sample 1 - 010401 - 1 control, 2.5% NaOH, 60 min

	Fucose	Arabinose	Galactose	Glucose	Xylose
peak area	35962684	459956	327903	89489465	5779110
area ratio		0.01279	0.00912	2.48840	0.16070
mass monosugar, mg	49.56	0.563	0.329	89.39	5.85
mass polysaccharide, mg		0.49578	0.29572	80.44754	5.14481
mass fraction		0.00529	0.00315	0.85802	0.05487
corrected mass, mg		0.51561	0.30755	83.66444	5.35054

Sample 1 - 010401 - 2 control, 2.5% NaOH, 60 min

	Fucose	Arabinose	Galactose	Glucose	Xylose
peak area	28768564	369202	271341	73596021	4539543
area ratio		0.01283	0.00943	2.55821	0.15780
mass monosugar, mg	49.56	0.565	0.340	92.19	5.74
mass polysaccharide, mg		0.49748	0.30590	82.96655	5.05073
mass fraction		0.00516	0.00318	0.86130	0.05243
corrected mass, mg		0.50534	0.31074	84.27731	5.13053

Sample 2 - 010402 - 1 0.3% guar, 2.5% NaOH, 60 min

	Fucose	Arabinose	Galactose	Glucose	Xylose
peak area	47754494	606556	639063	115188207	7869740
area ratio		0.01270	0.01338	2.41209	0.16480
mass monosugar, mg	49.56	0.560	0.482	86.35	6.00
mass polysaccharide, mg		0.49236	0.43403	77.71055	5.27773
mass fraction		0.00540	0.00476	0.85187	0.05785
corrected mass, mg		0.52977	0.46700	83.61463	5.67871

Sample 2 - 010402 - 2 0.3% guar, 2.5% NaOH, 60 min

	Fucose	Arabinose	Galactose	Glucose	Xylose
peak area	42160274	534762	550445	104604702	6808080
area ratio		0.01268	0.01306	2.48112	0.16148
mass monosugar, mg	49.56	0.559	0.470	89.10	5.88
mass polysaccharide, mg		0.49168	0.42345	80.18576	5.17021
mass fraction		0.00525	0.00452	0.85562	0.05517
corrected mass, mg		0.50792	0.43743	82.83353	5.34094

Table D.1. Sugar analysis sample calculations (continued)

Sugar Analysis Calculations

Sample 1 - 010401 - 1

	Mannose	Total
peak area	6903139	
area ratio	0.1920	
mass monosugar, mg	8.1949	104.32
mass polysaccharide, mg	7.3754	93.76
mass fraction	0.0787	1.00
corrected mass, mg	7.6703	97.51

pulp mass used, mg	100.09

Kappa#	15.62
% Extractives	0.1995
% ash	0.08
calculated mass of polysaccharides, mg	polysaccharide recovery, %
97.51	96.15
cellulose%	80.07
hemicellulose %	17.36
sum	97.42

Sample 1 - 010401 - 2

	Mannose	Total
peak area	5620771	
area ratio	0.1954	
mass monosugar, mg	8.3411	107.17
mass polysaccharide, mg	7.5070	96.33
mass fraction	0.0779	1.00
corrected mass, mg	7.6256	97.85

pulp mass used, mg	100.44

Kappa#	15.62
% Extractives	0.1995
% ash	0.08
calculated mass of polysaccharides, mg	polysaccharide recovery, %
97.85	98.44
cellulose%	80.45
hemicellulose %	16.97
sum	97.42

Sample 2 - 010402 - 1

	Mannose	Total
peak area	9084353	
area ratio	0.1902	
mass monosugar, mg	8.1213	101.51
mass polysaccharide, mg	7.3092	91.22
mass fraction	0.0801	1.00
corrected mass, mg	7.8645	98.15

pulp mass used, mg	100.84

Kappa#	15.93
% Extractives	0.238
% ash	0.08
calculated mass of polysaccharides, mg	polysaccharide recovery, %
98.15	92.94
cellulose%	79.30
hemicellulose %	18.04
sum	97.34

Sample 2 - 010402 - 2

	Mannose	Total
peak area	8169309	
area ratio	0.1938	
mass monosugar, mg	8.2723	104.27
mass polysaccharide, mg	7.4451	93.72
mass fraction	0.0794	1.00
corrected mass, mg	7.6909	96.81

pulp mass used, mg	99.46

Kappa#	15.93
% Extractives	0.238
% ash	0.08
calculated mass of polysaccharides, mg	polysaccharide recovery, %
96.81	96.80
cellulose%	79.73
hemicellulose %	17.61
sum	97.34

Table D.1. Sugar analysis sample calculations (continued)

Sugar Analysis Calculations

Sample 3 - 010403 - 1	0.75% guar, 2.5% NaOH, 60 min				
	Fucose	Arabinose	Galactose	Glucose	Xylose
peak area	43364456	526011	664114	100379889	6639276
area ratio		0.01213	0.01531	2.31480	0.15310
mass monosugar, mg	49.56	0.534	0.552	82.50	5.57
mass polysaccharide, mg		0.47021	0.49670	74.24552	4.89875
mass fraction		0.00538	0.00568	0.84930	0.05604
corrected mass, mg		0.51526	0.54429	81.35946	5.36814

Sample 3 - 010403 - 2	0.75% guar, 2.5% NaOH, 60 min				
	Fucose	Arabinose	Galactose	Glucose	Xylose
peak area	37376781	538287	683079	98998284	6580737
area ratio		0.01440	0.01828	2.64866	0.17606
mass monosugar, mg	49.56	0.634	0.659	95.83	6.41
mass polysaccharide, mg		0.55826	0.59273	86.25142	5.64367
mass fraction		0.00551	0.00585	0.85072	0.05566
corrected mass, mg		0.54410	0.57769	84.06352	5.50051

Sample 4 - 010404 - 1	2.0% guar, 2.5% NaOH, 60 min				
	Fucose	Arabinose	Galactose	Glucose	Xylose
peak area	51610451	646141	1120481	122142086	8059249
area ratio		0.01252	0.02171	2.36662	0.15616
mass monosugar, mg	49.56	0.551	0.782	84.54	5.68
mass polysaccharide, mg		0.48531	0.70413	76.08752	4.99759
mass fraction		0.00540	0.00783	0.84593	0.05556
corrected mass, mg		0.53412	0.77496	83.74075	5.50027

Sample 4 - 010404 - 2	2.0% guar, 2.5% NaOH, 60 min				
	Fucose	Arabinose	Galactose	Glucose	Xylose
peak area	40707029	540297	953191	106342325	6969082
area ratio		0.01327	0.02342	2.61238	0.17120
mass monosugar, mg	49.56	0.585	0.844	94.37	6.23
mass polysaccharide, mg		0.51451	0.75945	84.93110	5.48565
mass fraction		0.00511	0.00755	0.84400	0.05451
corrected mass, mg		0.51737	0.76368	85.40472	5.51624

Table D.1. Sugar analysis sample calculations (continued)

Sugar Analysis Calculations

Sample 3 - 010403 - 1

	Mannose	Total
peak area	8248933	
area ratio	0.1902	
mass monosugar, mg	8.1210	97.27
mass polysaccharide, mg	7.3089	87.42
mass fraction	0.0836	1.00
corrected mass, mg	8.0092	95.80

pulp mass used, mg: 98.49

Kappa#	15.9
% Extractives	0.322
% ash	0.08
calculated mass of polysaccharides, mg	polysaccharide recovery, %
95.80	91.26
cellulose%	78.90
hemicellulose %	18.36
sum	97.26

Sample 3 - 010403 - 2

	Mannose	Total
peak area	8113372	
area ratio	0.2171	
mass monosugar, mg	9.2671	112.81
mass polysaccharide, mg	8.3404	101.39
mass fraction	0.0823	1.00
corrected mass, mg	8.1289	98.81

pulp mass used, mg: 101.60

Kappa#	15.9
% Extractives	0.322
% ash	0.08
calculated mass of polysaccharides, mg	polysaccharide recovery, %
98.81	102.60
cellulose%	79.09
hemicellulose %	18.17
sum	97.26

Sample 4 - 010404 - 1

	Mannose	Total
peak area	10303786	
area ratio	0.1996	
mass monosugar, mg	8.5233	100.08
mass polysaccharide, mg	7.6709	89.95
mass fraction	0.0853	1.00
corrected mass, mg	8.4425	98.99

pulp mass used, mg: 101.54

Kappa#	16.01
% Extractives	0.0725
% ash	0.08
calculated mass of polysaccharides, mg	polysaccharide recovery, %
98.99	90.86
cellulose%	78.72
hemicellulose %	18.78
sum	97.49

Sample 4 - 010404 - 2

	Mannose	Total
peak area	9469912	
area ratio	0.2326	
mass monosugar, mg	9.9317	111.96
mass polysaccharide, mg	8.9385	100.63
mass fraction	0.0888	1.00
corrected mass, mg	8.9884	101.19

pulp mass used, mg: 103.79

Kappa#	16.01
% Extractives	0.0725
% ash	0.08
calculated mass of polysaccharides, mg	polysaccharide recovery, %
101.19	99.45
cellulose%	78.43
hemicellulose %	19.06
sum	97.49

Table D.2. Adsorption sample calculations

Adsorption Calculations 2.5% NaOH trials

	Batch #	% galactan	% mannan	% galactan increase	% mannan increase	sum
control	010401	0.315	7.866	-0.001	0.037	0.035
control	010401	0.318	7.793	0.001	-0.037	-0.035
ctrl avg		0.316	7.830	0.000	0.000	0.000
0.3% 60 min	010402	0.476	8.012	0.159	0.183	0.342
0.3% 60 min	010402	0.452	7.944	0.135	0.115	0.250
0.75% 60 min	010403	0.568	8.361	0.252	0.531	0.783
0.75% 60 min	010403	0.585	8.226	0.268	0.397	0.665
2.0% 60 min	010404	0.783	8.528	0.466	0.699	1.165
2.0% 60 min	010404	0.758	8.883	0.441	1.053	1.494

% increase polysaccharides	% increase on pulp	Charge 0	adsorbed 0
0.296	0.28704	0.3	0.2865
0.724	0.70199	0.75	0.6876
1.329	1.28961	2	1.2984

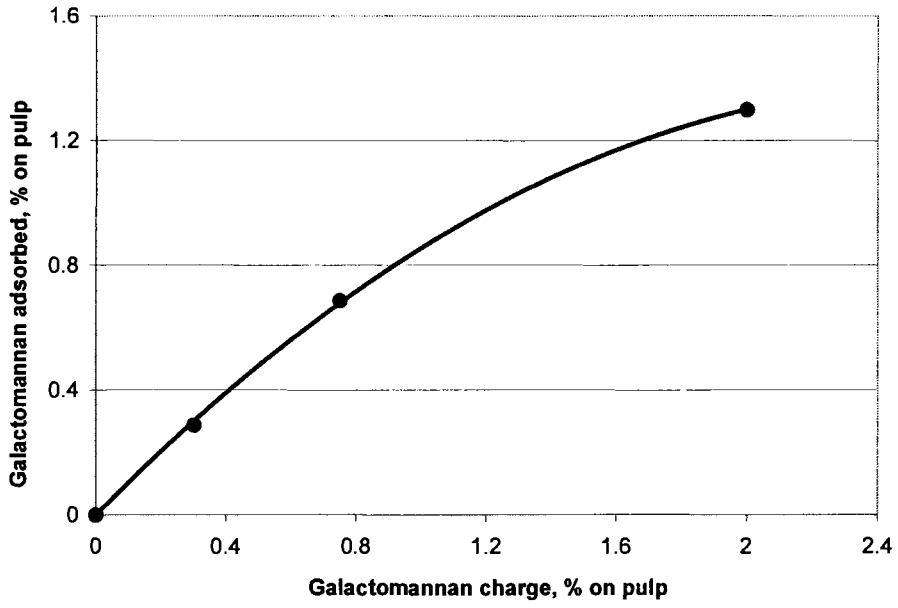

Figure D.6. Adsorption of galactomannan on pulp by sugar analysis using H.P.A.E.C., 2.5 % NaOH, 60 minutes

BIOGRAPHY OF THE AUTHOR

Steven Violette was born in Lewiston, Maine on April 8, 1967. He resided with his parents in Poland Springs, Maine, and graduated from Edward Little High School in Auburn, Maine, in 1985. Steven attended the University of Maine from 1990 to 1994, where he received a Bachelors degree in Chemical Engineering in August 1994. He then attended the Institute of Pulp and Paper Science at Georgia Tech in Atlanta, Georgia for one year of pulp and paper studies. Following his undergraduate education, Steven worked in industry for three years, serving as a process engineer for S. D. Warren Company and Georgia Pacific Corporation.

In the fall of 1998, Steven entered the graduate program in Chemical Engineering at the University of Maine. During his tenure at the University of Maine, he has conducted research in oxygen delignification, taught courses, and completed the doctoral requirements. Steven is a candidate for the Doctor of Philosophy degree in Chemical Engineering from the University of Maine in May, 2003.